PROTEOMICS

# Supporting Information for Proteomics

DOI 10.1002/pmic.200600987

Lars Wöhlbrand, Birte Kallerhoff, Daniela Lange, Peter Hufnagel, Jürgen Thiermann, Richard Reinhardt and Ralf Rabus

## Functional proteomic view of metabolic regulation in "*Aromatoleum aromaticum*" strain EbN1

# Content

**4. Central and other metabolic features***



**5. Biosynthesis***

## 6. References

* Numbering as used in supplementary material for genome sequence of strain EbN1 (Rabus *et al.*, 2005; http://www.micro-genomes.mpg.de/ebn1/)

# 1. General proteome features

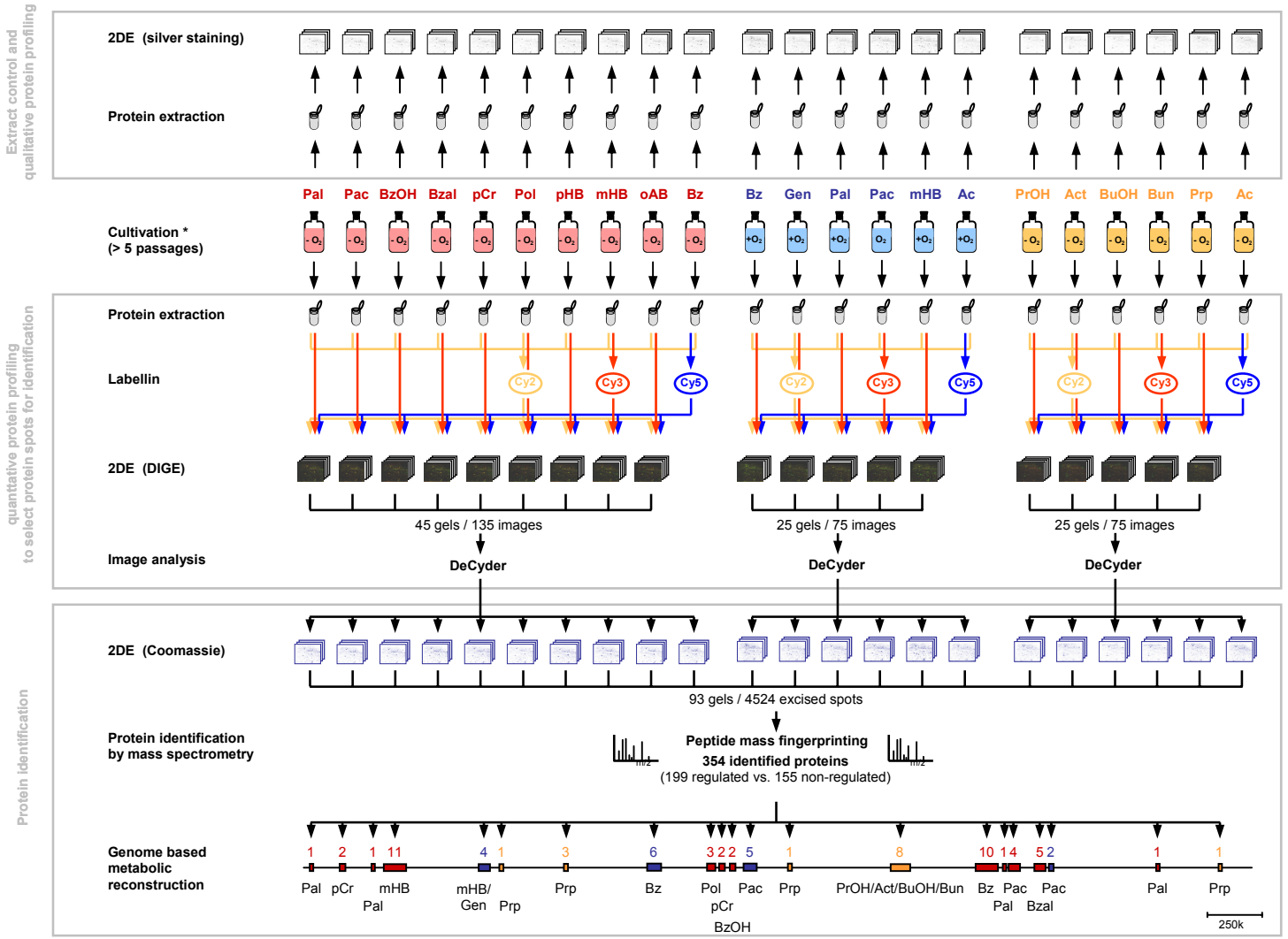


**Fig. 1.1.** Experimental outline of the presented study with "Aromatoleum aromaticum" strain EbN1. Prior to proteomic analysis, cells were adapted for at least 5 passages to aerobic (blue) or anaerobic (red and orange) growth with the respective substrate. Names of indicated substrates are as follows: Pal, phenylalanine; Pac, phenylacetate; BzOH, benzyl alcohol; Bzal, benzaldehyde; pCr, *p*-cresol; Pol, phenol; pHB, *p*-hydroxybenzoate; mHB, *m*-hydroxybenzoate; oAB, *o*-aminobenzoate; Bz, benzoate; Gen, gentisate; Ac, acetate; PrOH, 2-propanol; Act, acetone; BuOH, 2-butanol; Bun, butanone, Prp; propionate. Quality control of the prepared protein extracts as well as qualitative protein profiling was done with silver-stained gels (top). Applying the 2D DIGE technique allowed quantitative protein profiling of independent protein extracts (center). The project was divided into three principle physiological groups: (i) anaerobic growth with aromatic compounds, (ii) aerobic growth with aromatic compounds and (iii) anaerobic growth with carboxylic acids, ketones and alcohols. Image analysis using the DeCyder software confirmed regulated spots as assigned by silver staining. In addition, more proteins could be identified as specifically regulated. Coomassie stained gels were used for protein identification (indicated). Selected regulated as well as non-regulated spots were excised and identified via mapping of peptide mass fingerprints.

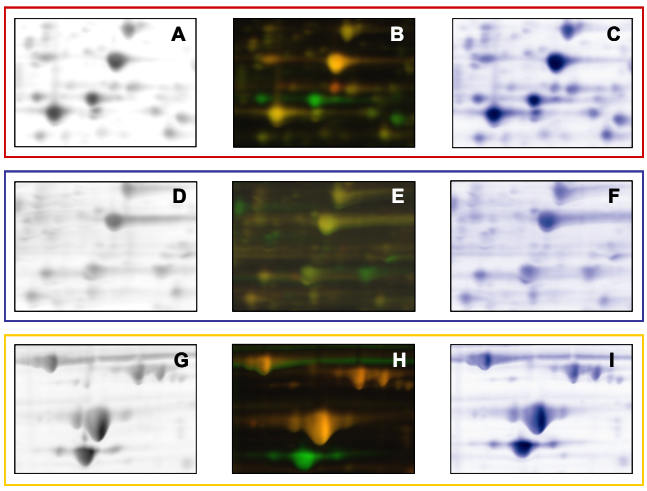


**Fig. 1.2.** Spot pattern comparison of differently visualized 2DE gels. (A, D and G) silver stained gels, (B, E and H) false color images of 2D DIGE gels, (C, F and I) Coomassie Brilliant Blue staining. Independent protein extracts from cells adapted to anaerobic growth with *m*-hydroxybenzoate (red box), aerobic growth with phenylalanine (blue box) or anaerobic growth with 2-propanol (orange box) are shown exemplarily.

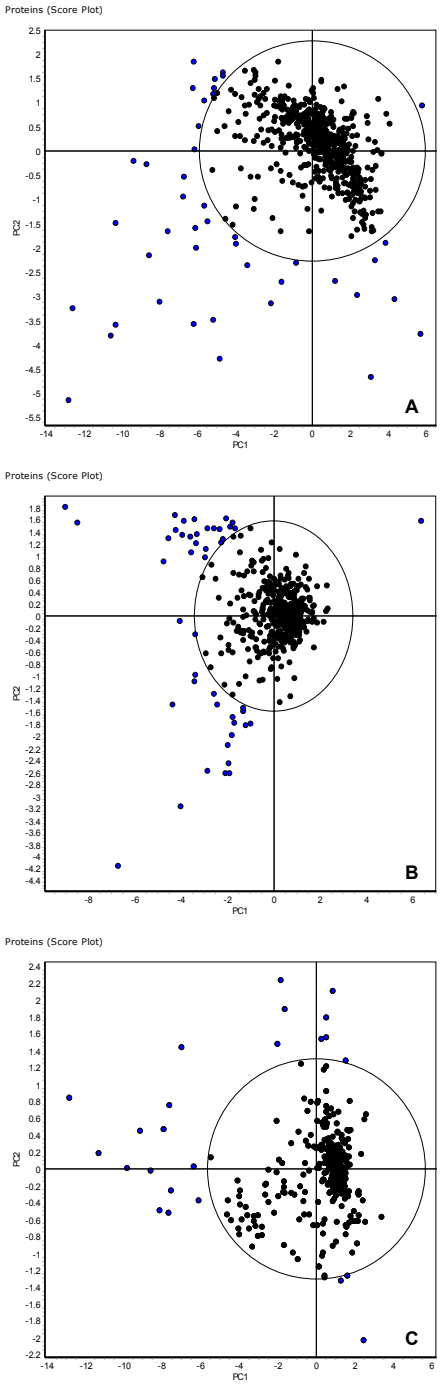


**Fig. 1.3.** Principal component analysis of the proteins for each analyzed 2D DIGE gel of all main physiological groups. Protein spots fulfilling the 95 % analytical significance criterion (ellipse) defined by the principal components analysis in all three main physiological groups ranged between 540 and 305 (out of 603 to 329 total matched spots). The overwhelming majority (90.7 % to 86.9 %) of these "outliers" (highlighted in blue) represent specifically and strongly regulated proteins, rather than analytical artifacts (data not shown). (A) anaerobic growth with aromatic compounds, (B) aerobic growth with aromatic compounds, (C) anaerobic growth with aliphatic alcohols, ketones and carboxylic acids.

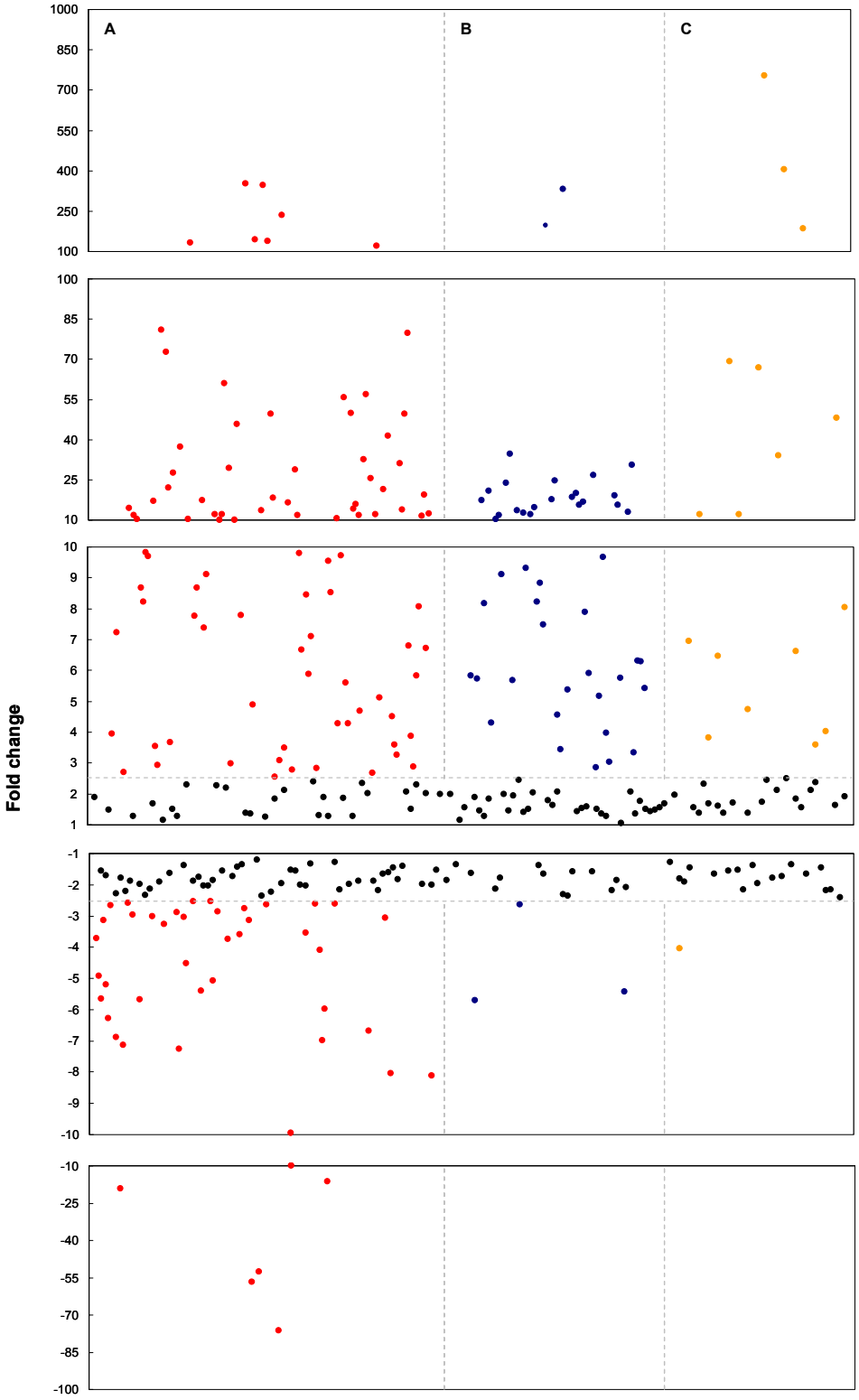


**Fig. 1.4.** Fold changes in protein abundance of all identified proteins. Proteins with no significant change in abundance are shown in black. Proteins specifically regulated during anaerobic growth with aromatic compounds are marked in red (column A). Blue dots represent proteins regulated during aerobic growth with aromatic compounds (column B) and proteins specifically regulated during anaerobic growth with aliphatic compounds are shown in orange (column C).

**Table 1.1.** Number of regulated as well as not regulated protein spots on the 2DE gels and their share of total protein.

| Substrates[a] | specific down-regulated (< -2.5)[b] | | | specific up-regulated (> 2.5)[b] | | | not regulated (> -2.5; < 2.5)[b] | | |
|---|---|---|---|---|---|---|---|---|---|
| | No of spots | share (%) | share of total protein (%)[c] | No of spots | share (%) | share of total protein (%)[c] | No of spots | share (%) | share of total protein (%)[c] |
| Pal -O | 69 | 5.3 | 5.3 | 64 | 4.9 | 16.2 | 1171 | 89.8 | 77.8 |
| Pac -O | 26 | 1.7 | 2.4 | 22 | 1.4 | 2.9 | 1490 | 96.9 | 94.4 |
| BzOH -O | 29 | 2.1 | 3.3 | 74 | 5.4 | 22.4 | 1269 | 92.5 | 74.3 |
| Bzal -O | 18 | 1.4 | 1.1 | 62 | 4.7 | 10.6 | 1250 | 94.0 | 88.3 |
| pCr -O | 45 | 3.5 | 4.2 | 110 | 8.6 | 26.9 | 1120 | 87.8 | 68.9 |
| Pol -O | 98 | 7.1 | 6.9 | 120 | 8.7 | 24.0 | 1157 | 84.1 | 69.1 |
| pHB -O | 44 | 3.4 | 4.8 | 51 | 3.9 | 7.1 | 1203 | 92.7 | 88.1 |
| mHB -O | 21 | 1.6 | 2.4 | 58 | 4.5 | 17.6 | 1210 | 93.9 | 80.0 |
| oAB -O | 47 | 3.5 | 3.5 | 71 | 5.3 | 22.1 | 1211 | 91.1 | 74.4 |
| *average* | *44* | *3.3* | *3.8* | *70* | *5.3* | *16.6* | *1345* | *91.4* | *79.5* |
| Bz +O | 20 | 1.4 | 1.2 | 57 | 4.0 | 24.7 | 1362 | 94.6 | 74.0 |
| Gen +O | 10 | 0.7 | 1.3 | 54 | 3.7 | 12.7 | 1408 | 95.7 | 86.0 |
| Pal +O | 8 | 0.5 | 0.5 | 42 | 2.4 | 9.1 | 1726 | 97.2 | 89.6 |
| Pac +O | 5 | 0.3 | 0.7 | 53 | 3.4 | 19.9 | 1488 | 96.2 | 79.4 |
| mHB +O | 17 | 1.1 | 1.5 | 98 | 6.5 | 39.0 | 1395 | 92.4 | 59.5 |
| *average* | *12* | *0.8* | *1.1* | *61* | *4.0* | *21.1* | *1548* | *91.4* | *77.7* |
| PrOH -O | 10 | 1.0 | 0.5 | 51 | 5.1 | 44.6 | 931 | 93.9 | 54.9 |
| Act -O | 6 | 0.5 | 0.4 | 52 | 4.0 | 32.2 | 1230 | 95.5 | 66.6 |
| BuOH -O | 6 | 0.6 | 0.9 | 64 | 6.6 | 46.9 | 899 | 92.8 | 52.2 |
| Bun -O | 9 | 0.9 | 1.1 | 59 | 5.8 | 39.2 | 953 | 93.3 | 59.8 |
| Prp -O | 14 | 1.5 | 2.4 | 19 | 2.0 | 3.7 | 932 | 96.6 | 93.9 |
| *average* | *9* | *0.9* | *1.0* | *49* | *4.7* | *33.3* | *1047* | *94.4* | *65.5* |

[a] Substrate abbreviations are as described in Fig. 3. -O indicates anaerobic, +O aerobic growth conditions.
[b] Average ratio as determined by DeCyder-anaylsis
[c] The volume of each spot on the 2DE gel was determined and its share of total spot volumes calculated. Values are summed up according to the respective category. Values with no corresponding average ratio are unaccounted for.

**Table 1.2.** Mean average ratio of not regulated protein spots of the three sub-experiments.

| | Mean average ratio[a] | Standard deviation | No of proteins included |
|---|---|---|---|
| Aromatics anaerobic | 1.34 | ± 0.31 | 146 |
| Aromatics aerobic | 1.30 | ± 0.29 | 43 |
| Aliphatics anaerobic | 1.33 | ± 0.30 | 24 |

[a] For each not significantly regulated identified protein, the mean of its average ratios of all test states was determined. Subsequently, these mean values were used to calculate the average value for all proteins.

**Table 1.3.** Mean of average ratios[a] of not regulated proteins, identified in all three experimental subgroups.

| Protein[b] | Aromatic anaerobic | Aromatics aerobic | Aliphatics anaerobic |
|---|---|---|---|
| AhpC | 1.25 ± 0.23 | 1.52 ± 0.35 | 1.20 ± 0.17. |
| AtpD | 1.46 ± 0.28 | 1.29 ± 0.20 | 1.43 ± 0.07 |
| EtfA | 1.28 ± 0.32 | 1.29 ± 0.19 | 1.59 ± 0.30 |
| GroeL | 1.16 ± 0.07 | 1.08 ± 0.06 | 1.07 ± 0.07 |
| GroeS | 1.35 ± 0.36 | 1.22 ± 0.16 | 1.06 ± 0.03 |
| HptG | 1.43 ± 0.21 | 1.16 ± 0.16 | 1.13 ± 0.37 |
| TyrB | 1.34 ± 0.27 | 1.13 ± 0.08 | 1.07 ± 0.03 |

[a] For each protein, the mean of its average ratio of all test-states was determined and is provided with standard deviation.
[b] protein abbreviations are as described in Rabus et al. 2005. All proteins were independently identified in at least one test state of the respective subgroup

.

**Table 1.4:** Proteins identified in this study (in order of Orf-No.). Orf-No., gene names and functions are as described by Rabus et al. 2005. Sequence coverage (Seq. Coverage), Meta-Score, Mascot-Score and Profound-Score are provided with standard deviation (SD).

| ORF No. | Gene | Function | No. of identifi-cations | Seq. Coverage | SD | Meta-Score | SD | Mascot-Score | SD | Profound-Score | SD |
|---|---|---|---|---|---|---|---|---|---|---|---|
| ebA118 | *folD* | bifunctional protein | 8 | 45,7 | 12,4 | 98,5 | 0,4 | 142,2 | 50,6 | 2,4 | 0,0 |
| ebA122 | *iorA* | indolepyruvate ferredoxin oxidoreductase, alpha SU | 4 | 30,7 | 11,7 | 98,4 | 1,4 | 228,3 | 55,9 | 2,4 | 0,0 |
| ebA135 | *aceF* | pyruvate dehydrogenase multienzyme complex, dihydrolipoamide acyltransferase component | 2 | 23,2 | 4,3 | 98,1 | 0,4 | 140,5 | 26,2 | 2,0 | 0,5 |
| ebA136 | *lpd* | pyruvate dehydrogenase multienzyme complex, dihydrolipoamide dehydrogenase component | 1 | 21,0 | | 98,1 | | 114,0 | | 2,2 | |
| ebA172 | *ascA* | acetyl-CoA synthetase | 14 | 33,3 | 8,9 | 98,8 | 0,4 | 178,7 | 56,8 | 2,4 | 0,1 |
| ebA173 | *fumA* | fumarate hydratase | 4 | 45,1 | 10,0 | 99,1 | 0,4 | 225,8 | 57,0 | 2,4 | 0,1 |
| ebA300 | *pchF* | probable *p*-cresol methylhydroxylase SU | 2 | 47,5 | 8,6 | 99,4 | 0,7 | 266,5 | 105,4 | 2,4 | 0,0 |
| ebA306 | *tioL* | predicted thiolase | 2 | 49,9 | 28,9 | 99,0 | 1,1 | 208,7 | 157,4 | 2,4 | 0,0 |
| ebA307 | *chnA* | cyclohexanol dehydrogenase | 2 | 74,8 | 31,7 | 99,4 | 0,6 | 271,0 | 90,5 | 2,4 | 0,0 |
| ebA332 | | conserved hypothetical protein | 3 | 49,6 | 21,5 | 99,2 | 0,9 | 237,0 | 127,5 | 2,3 | 0,1 |
| ebA310 | | FAD linked oxidase | 2 | 64,1 | 21,8 | 100,0 | 1,1 | 359,0 | 171,1 | 2,4 | 0,0 |
| ebA314 | *xccA* | putative carboxylase, SU of acetyl-CoA carboxylase-like enzyme | 3 | 53,4 | 13,5 | 99,5 | 0,7 | 292,3 | 94,1 | 2,4 | 0,0 |
| ebA318 | | conserved hypothetical protein | 2 | 64,5 | 34,6 | 99,4 | 1,0 | 268,5 | 145,0 | 2,4 | 0,0 |
| ebA570 | | hypothetical protein | 6 | 30,7 | 13,5 | 97,8 | 1,5 | 131,8 | 27,6 | 2,4 | 0,0 |
| ebA720 | | enoyl-CoA hydratase | 7 | 55,3 | 21,0 | 97,9 | 3,2 | 231,3 | 34,7 | 2,4 | 0,1 |
| ebA722 | | enoyl-CoA hydratase involved in 3-hydroxybenzoate metabolism | 29 | 45,3 | 20,5 | 97,5 | 3,5 | 173,0 | 64,9 | 2,4 | 0,0 |
| ebA723 | | putative alcohol dehydrogenase | 13 | 69,6 | 20,0 | 98,8 | 1,4 | 234,0 | 98,0 | 2,4 | 0,1 |
| ebA727 | *hbcL* | 3-hydroxybenzoate CoA ligase | 36 | 38,9 | 11,6 | 98,9 | 0,8 | 219,1 | 82,9 | 2,4 | 0,1 |
| ebA729 | *dctP* | dicarboxylate transport protein | 2 | 36,4 | 14,4 | 98,4 | 0,3 | 134,5 | 64,4 | 2,2 | 0,2 |

**Tab 1.4:** continued

| ORF No. | Gene | Function | No. of identifi-cations | Seq. Coverage | SD | Meta-Score | SD | Mascot-Score | SD | Profound-Score | SD |
|---|---|---|---|---|---|---|---|---|---|---|---|
| ebA736 | | putative acyl-CoA dehydrogenase | 21 | 61,1 | 19,1 | 99,1 | 0,8 | 252,9 | 78,1 | 2,3 | 0,2 |
| ebA741 | | predicted acetyltransferase | 3 | 65,0 | 20,7 | 99,3 | 1,2 | 261,7 | 166,4 | 2,4 | 0,0 |
| ebA741 | | predicted acetyltransferase | 13 | 45,5 | 6,3 | 98,2 | 0,7 | 130,0 | 20,6 | 2,3 | 0,1 |
| ebA742 | *hbrA* | *m*-hydroxybenzoyl-CoA reductase, SU A | 42 | 62,7 | 15,5 | 98,9 | 0,5 | 197,1 | 63,4 | 2,4 | 0,1 |
| ebA746 | *hbrB* | *m*-hydroxybenzoyl-CoA reductase, SU B | 20 | 32,7 | 13,6 | 98,4 | 0,5 | 136,9 | 60,6 | 2,3 | 0,1 |
| ebA748 | *hbrC* | *m*-hydroxybenzoyl-CoA reductase, SU C | 30 | 64,7 | 6,5 | 99,5 | 0,4 | 291,9 | 53,5 | 2,4 | 0,0 |
| ebA774 | *dapA* | dihydrodipicolinate synthetase | 7 | 50,4 | 16,3 | 98,9 | 0,6 | 204,8 | 84,6 | 2,4 | 0,0 |
| ebA775 | | conserved hypothetical protein | 4 | 54,6 | 21,5 | 98,4 | 0,3 | 144,5 | 58,7 | 2,0 | 0,3 |
| ebA819 | *glcB* | malate synthase G | 15 | 36,3 | 12,0 | 99,0 | 0,5 | 215,5 | 69,4 | 2,4 | 0,1 |
| ebA825 | | translation elongation factor G | 2 | 24,1 | 6,5 | 98,6 | 0,4 | 164,0 | 58,0 | 2,4 | 0,1 |
| ebA829 | *icd* | isocitrate dehydrogenase | 14 | 49,9 | 17,5 | 98,9 | 0,8 | 230,6 | 102,0 | 2,1 | 0,3 |
| ebA867 | *pheT* | phenylalanyl-tRNA synthetase, beta chain | 2 | 39,9 | 4,6 | 100,0 | 0,3 | 360,0 | 43,8 | 2,4 | 0,0 |
| ebA868 | *pheS* | phenylalanyl-tRNA synthetase, alfa chain | 4 | 32,5 | 7,4 | 98,4 | 0,3 | 127,0 | 42,2 | 2,4 | 0,0 |
| ebA888 | *nirS* | cytochrome cd1 nitrite reductase precursor | 7 | 43,8 | 11,8 | 99,1 | 0,4 | 221,4 | 54,0 | 2,4 | 0,0 |
| ebA896 | *cysM* | cystein synthase B | 2 | 39,0 | 4,5 | 98,4 | 0,1 | 120,0 | 17,0 | 2,4 | 0,0 |
| ebA903 | *rpsA* | 30S ribosomal protein S1 | 14 | 42,9 | 10,3 | 98,7 | 0,4 | 185,2 | 58,9 | 2,2 | 0,2 |
| ebA907 | *serC* | phosphoserine aminotransferase | 6 | 38,5 | 10,1 | 98,5 | 0,2 | 137,0 | 30,2 | 2,4 | 0,0 |
| ebA931 | *tyrS* | tRNA Synthetase, class Ib | 13 | 42,1 | 10,6 | 98,5 | 0,4 | 150,2 | 55,9 | 2,3 | 0,2 |
| ebA950 | *proS* | prolyl-tRNA synthetase | 4 | 37,9 | 12,2 | 99,1 | 0,6 | 235,0 | 84,3 | 2,4 | 0,1 |
| ebA969 | *tldD* | Zn-dependent peptidase, potential modulator of DNA gyrase | 7 | 61,8 | 21,9 | 99,6 | 0,7 | 308,9 | 105,2 | 2,2 | 0,2 |
| ebA993 | *ilvE* | branched-chain amino acid aminotransferase | 4 | 44,7 | 2,4 | 98,6 | 0,2 | 153,0 | 39,2 | 2,4 | 0,0 |
| ebA1027 | *mog* | molybdopterin biosynthesis protein | 3 | 36,6 | 5,0 | 98,3 | 0,1 | 119,3 | 18,6 | 2,4 | 0,0 |

**Tab 1.4:** continued

| ORF No. | Gene | Function | No. of identifi-cations | Seq. Coverage | SD | Meta-Score | SD | Mascot-Score | SD | Profound-Score | SD |
|---|---|---|---|---|---|---|---|---|---|---|---|
| ebA1033 | | putative exported solute binding protein | 12 | 41,3 | 14,6 | 98,1 | 1,3 | 164,0 | 50,4 | 2,3 | 0,1 |
| ebA1050 | | carboxy-terminal processing protease | 7 | 48,9 | 18,1 | 99,0 | 0,6 | 225,0 | 89,0 | 2,3 | 0,1 |
| ebA1052 | *gpmA* | 2,3-bisphosphoglycerate-dependent phosphoglycerate mutase | 4 | 48,8 | 12,3 | 98,5 | 0,4 | 136,9 | 58,6 | 2,3 | 0,0 |
| ebA1056 | *secB* | protein-export protein | 2 | 63,9 | 4,0 | 98,5 | 0,4 | 139,6 | 57,1 | 2,4 | 0,0 |
| ebA1102 | *gapA* | glyceraldehyde-3-phosphate dehydrogenase | 3 | 41,7 | 8,5 | 98,4 | 0,5 | 143,0 | 45,1 | 2,2 | 0,3 |
| ebA1103 | *pgk* | phosphoglyerate kinase | 7 | 56,9 | 24,3 | 98,4 | 2,0 | 256,5 | 75,8 | 2,1 | 0,2 |
| ebA1107 | *fbaA* | fructose-bisphosphate aldolase protein | 8 | 44,8 | 16,0 | 99,0 | 0,6 | 214,9 | 88,3 | 2,4 | 0,0 |
| ebA1153 | *purH* | bifunctional purine biosynthesis protein | 4 | 46,1 | 12,5 | 99,0 | 0,7 | 236,8 | 74,3 | 2,2 | 0,2 |
| ebA1155 | *purD* | phosphoribosylamine-glycine ligase | 4 | 37,8 | 6,1 | 98,7 | 0,4 | 168,5 | 57,6 | 2,4 | 0,0 |
| ebA1162 | *nirE* | uroporphyrin-III C-methyltransferase | 2 | 61,3 | 25,4 | 99,1 | 0,5 | 222,0 | 67,9 | 2,4 | 0,0 |
| ebA1170 | *argH* | argininosuccinate lyase | 2 | 33,8 | 0,0 | 98,4 | 0,0 | 153,0 | 0,0 | 2,2 | 0,0 |
| ebA1185 | *groEL* | chaperonin 60kDa SU | 81 | 52,3 | 14,5 | 99,0 | 0,7 | 227,7 | 81,7 | 2,4 | 0,0 |
| ebA1191 | *fbp* | fructose-1,6-bisphosphatase | 4 | 37,7 | 13,8 | 98,4 | 0,4 | 143,8 | 40,0 | 2,2 | 0,3 |
| ebA1195 | *sspA* | stringent starvation protein a | 6 | 52,8 | 9,6 | 98,4 | 0,2 | 124,8 | 26,1 | 2,3 | 0,1 |
| ebA1198 | *petA* | iron-sulfur subunit of cytochrome bc1 | 8 | 71,6 | 19,0 | 98,5 | 0,5 | 162,0 | 59,8 | 2,2 | 0,3 |
| ebA1206 | *acsA* | putative acetyl-CoA synthetase | 12 | 55,1 | 7,7 | 99,9 | 0,5 | 344,0 | 72,1 | 2,4 | 0,0 |
| ebA1220 | | serine proteases, subtilase family | 3 | 35,4 | 17,6 | 98,5 | 0,2 | 145,3 | 48,1 | 2,3 | 0,1 |
| ebA1250 | *hisZ* | ATP phosphoribosyltransferase regulatory SU | 1 | 66,1 | | 99,0 | | 213,0 | | 2,4 | |
| ebA1271 | *sucD* | succinyl-CoA synthetase, alpha chain | 3 | 44,8 | 3,7 | 98,8 | 0,8 | 196,0 | 106,9 | 2,3 | 0,2 |
| ebA1291 | *hisF* | imidazoleglycerol phosphate synthase | 2 | 71,8 | 3,4 | 98,9 | 0,6 | 222,0 | 59,4 | 2,1 | 0,4 |
| ebA1293 | *hisA* | 1-(5-phosphoribosyl)-5-[(5-phosphoribosylamino)methylideneamino]imidazole-4-carboxyamide isomerase | 5 | 54,1 | 14,0 | 98,6 | 0,3 | 154,6 | 45,0 | 2,4 | 0,0 |

**Tab 1.4:** continued

| ORF No. | Gene | Function | No. of identifi-cations | Seq. Coverage | SD | Meta-Score | SD | Mascot-Score | SD | Profound-Score | SD |
|---|---|---|---|---|---|---|---|---|---|---|---|
| ebA1299 | *hisD* | histidinol dehydrogenase | 2 | 36,5 | 3,5 | 99,0 | 0,0 | 215,0 | 2,8 | 2,3 | 0,0 |
| ebA1321 | *ech* | putative enoyl-CoA hydratase protein | 11 | 43,8 | 16,7 | 99,0 | 0,4 | 206,0 | 58,3 | 2,4 | 0,0 |
| ebA1323 | | conserved hypothetical protein, predicted phasin family | 15 | 70,1 | 16,6 | 98,4 | 0,6 | 155,7 | 45,1 | 2,3 | 0,2 |
| ebA1337 | | PhoH-like protein | 3 | 41,1 | 21,0 | 94,5 | 7,5 | 193,5 | 14,8 | 2,4 | 0,1 |
| ebA1373 | *nagI* | gentisate 1,2-dioxygenase | 24 | 32,8 | 13,2 | 98,6 | 0,4 | 163,4 | 56,5 | 2,4 | 0,1 |
| ebA1377 | *nagK* | fumarylpyruvate hydrolase | 20 | 64,0 | 13,9 | 98,7 | 0,6 | 188,1 | 42,2 | 2,4 | 0,1 |
| ebA1378 | *hbh* | putative hydroxybenzoate hydroxylase | 10 | 52,4 | 13,4 | 99,7 | 0,7 | 328,1 | 85,8 | 2,3 | 0,2 |
| ebA1379 | *nagL* | maleylpyruvate isomerase | 5 | 71,5 | 14,6 | 99,3 | 0,5 | 266,0 | 52,6 | 2,3 | 0,2 |
| ebA1395 | | putative zinc protease | 4 | 41,1 | 16,7 | 98,8 | 0,7 | 180,4 | 97,3 | 2,4 | 0,0 |
| ebA1403 | | conserved hypothetical protein | 2 | 24,5 | 4,5 | 98,5 | 0,1 | 142,5 | 17,7 | 2,4 | 0,0 |
| ebA1406 | | phosphoribosyl transferase | 4 | 44,0 | 12,5 | 99,0 | 0,6 | 213,9 | 85,3 | 2,4 | 0,0 |
| ebA1409 | *rplY* | 50S ribosomal protein L25 | 8 | 50,8 | 14,7 | 97,7 | 1,3 | 144,8 | 45,7 | 2,3 | 0,2 |
| ebA1438 | *ftsZ* | cell division transmembrane protein | 3 | 58,5 | 9,0 | 99,1 | 0,4 | 222,0 | 61,3 | 2,4 | 0,0 |
| ebA1442 | *ddlB* | D-alanine - D-alanine ligase (D-alanylalanine synthethase) | 1 | 35,6 | | 98,8 | | 177,0 | | 2,4 | |
| ebA1474 | *accC* | putative biotin carboxylase protein | 2 | 37,1 | 1,1 | 98,5 | 0,2 | 167,0 | 14,1 | 2,1 | 0,1 |
| ebA1594 | | probable rotamase | 10 | 56,0 | 9,1 | 98,3 | 1,1 | 157,5 | 36,4 | 2,4 | 0,0 |
| ebA1645 | *pcm* | putative protein-L-isoaspartate o-methyltransferase | 7 | 44,4 | 10,3 | 98,3 | 0,3 | 115,3 | 31,9 | 2,4 | 0,0 |
| ebA1743 | *hemL* | glutamate-1-semialdehyde 2,1-aminomutase | 3 | 48,3 | 8,4 | 98,7 | 0,5 | 174,3 | 64,4 | 2,3 | 0,1 |
| ebA1766 | *proC* | delta 1-pyrroline--5-carboxylate reductase | 3 | 43,0 | 11,0 | 97,7 | 1,2 | 127,0 | 2,8 | 2,4 | 0,1 |
| ebA1861 | | similar to uncharacterized protein probably involved in high affinity $Fe^{2+}$ transport | 15 | 48,7 | 11,5 | 98,1 | 0,9 | 124,9 | 37,9 | 2,3 | 0,1 |
| ebA1874 | *ahcY* | adenosylhomocysteinase | 3 | 44,4 | 8,3 | 99,2 | 0,1 | 242,0 | 13,9 | 2,4 | 0,0 |

**Tab 1.4:** continued

| ORF No. | Gene | Function | No. of identifi-cations | Seq. Coverage | SD | Meta-Score | SD | Mascot-Score | SD | Profound-Score | SD |
|---|---|---|---|---|---|---|---|---|---|---|---|
| ebA1929 | | conserved hypothetical protein | 7 | 57,0 | 11,3 | 98,8 | 0,5 | 184,6 | 69,9 | 2,4 | 0,0 |
| ebA1932 | | conserved hypothetical protein | 10 | 49,7 | 14,6 | 99,0 | 0,6 | 223,6 | 75,7 | 2,3 | 0,2 |
| ebA1936 | | conserved hypothetical protein | 3 | 53,5 | 5,8 | 99,5 | 0,4 | 284,0 | 49,0 | 2,4 | 0,0 |
| ebA1978 | *dps* | DNA-binding ferretin-like protein (oxidative damage protectant) | 12 | 44,6 | 6,1 | 98,4 | 0,3 | 125,0 | 31,6 | 2,4 | 0,0 |
| ebA2050 | *fcs* | putative ADP-producing CoA ligase, similar to feruloyl-CoA synthetase | 4 | 71,4 | 10,8 | 99,4 | 0,5 | 293,5 | 52,4 | 2,3 | 0,2 |
| ebA2051 | *hyuA* | hydantoin utilization protein A | 3 | 55,6 | 12,6 | 100,1 | 1,2 | 365,7 | 169,3 | 2,4 | 0,0 |
| ebA2053 | *hyuB* | hydantoin utilization protein B | 3 | 38,8 | 9,0 | 99,2 | 0,3 | 237,3 | 46,6 | 2,4 | 0,0 |
| ebA2060 | *sbmA* | methylmalonyl-CoA mutase, alpha SU | 3 | 56,2 | 10,7 | 99,2 | 0,9 | 268,7 | 103,6 | 2,1 | 0,4 |
| ebA2062 | | medium FAD-binding subunit of molybdenum enzyme | 4 | 55,9 | 5,3 | 99,1 | 0,2 | 233,0 | 30,7 | 2,4 | 0,0 |
| ebA2097 | | hypothetical protein | 3 | 78,2 | 30,7 | 97,4 | 2,0 | 146,0 | 49,5 | 2,4 | 0,0 |
| ebA2102 | *katA* | catalase | 9 | 58,4 | 19,7 | 99,6 | 0,7 | 299,9 | 108,9 | 2,4 | 0,1 |
| ebA2117 | *hemR* | hemin receptor precursor, TonB-dependent outer membrane uptake protein | 1 | 39,4 | | 98,4 | | 178,0 | | 2,0 | |
| ebA2168 | | cation efflux system transmembrane protein | 16 | 47,9 | 15,2 | 99,5 | 0,9 | 284,0 | 134,6 | 2,4 | 0,0 |
| ebA2178 | | hypothetical protein | 4 | 33,2 | 6,5 | 97,2 | 2,0 | 109,8 | 34,4 | 2,4 | 0,0 |
| ebA2251 | *gltA* | glutamate synthase, small SU | 6 | 58,8 | 13,1 | 99,0 | 1,5 | 316,0 | 49,2 | 2,2 | 0,2 |
| ebA2266 | *pilM* | type IV fimbrial biogenesis protein | 2 | 31,0 | 10,6 | 98,5 | 0,4 | 138,0 | 55,2 | 2,4 | 0,0 |
| ebA2271 | *lysA* | diaminopimelate decarboxylase | 4 | 54,3 | 16,6 | 98,9 | 0,5 | 225,5 | 60,9 | 2,1 | 0,4 |
| ebA2313 | | putative enoyl-CoA hydratase II | 3 | 48,9 | 4,7 | 98,2 | 0,3 | 124,7 | 35,1 | 2,2 | 0,2 |
| ebA2528 | | probable dehydrogenase | 2 | 63,3 | 15,6 | 98,0 | 0,1 | 115,5 | 9,2 | 1,8 | 0,2 |
| ebA2547 | | putative glutamate-cysteine ligase | 2 | 46,7 | 8,6 | 98,8 | 0,2 | 185,0 | 19,8 | 2,3 | 0,1 |
| ebA2621 | | conserved hypothetical protein | 4 | 49,1 | 7,4 | 98,4 | 0,2 | 129,6 | 27,8 | 2,4 | 0,0 |

**Tab 1.4:** continued

| ORF No. | Gene | Function | No. of identifi-cations | Seq. Coverage | SD | Meta-Score | SD | Mascot-Score | SD | Profound-Score | SD |
|---|---|---|---|---|---|---|---|---|---|---|---|
| ebA2623 | *cysH* | APS-reductase | 3 | 55,7 | 16,3 | 99,0 | 0,6 | 203,0 | 77,1 | 2,4 | 0,0 |
| ebA2625 | *cysD* | ATP sulfurylase, small SU | 3 | 54,2 | 16,3 | 98,4 | 0,9 | 162,3 | 93,4 | 2,1 | 0,4 |
| ebA2628 | *cysN* | ATP sulfurylase, large SU | 6 | 47,4 | 9,8 | 99,2 | 0,6 | 236,3 | 80,9 | 2,4 | 0,0 |
| ebA2654 | | hypothetical protein | 5 | 55,8 | 8,7 | 98,1 | 0,4 | 130,9 | 31,8 | 2,0 | 0,3 |
| ebA2717 | | putative metallo-beta-lactamase family protein | 3 | 78,7 | 8,7 | 98,9 | 0,4 | 198,3 | 46,0 | 2,3 | 0,2 |
| ebA2730 | | heat shock protein, HSP 20 family | 3 | 91,4 | 1,2 | 99,1 | 0,3 | 238,3 | 35,9 | 2,4 | 0,0 |
| ebA2753 | | lactonase | 3 | 46,8 | 17,2 | 98,5 | 0,8 | 162,3 | 91,7 | 2,3 | 0,1 |
| ebA2755 | | ABC-transporter | 9 | 49,3 | 8,1 | 98,7 | 0,3 | 167,4 | 43,6 | 2,4 | 0,0 |
| ebA2759 | *boxZ* | adehyde dehydrogenase | 10 | 61,3 | 11,7 | 99,6 | 0,6 | 293,8 | 99,8 | 2,4 | 0,0 |
| ebA2763 | *boxC* | enoyl-CoA hydratase/isomerase involved in isomerisation and hydrolytic ring opening of 2,3-dihydro-2,3-diol intermediate of benzoyl-CoA | 24 | 53,4 | 17,6 | 99,4 | 1,6 | 310,7 | 119,6 | 2,4 | 0,0 |
| ebA2765 | *boxB* | benzoyl-CoA oxygenase compinent B | 26 | 51,5 | 15,2 | 99,5 | 0,7 | 289,2 | 95,4 | 2,4 | 0,1 |
| ebA2771 | *phbP* | related to granule-associated proteins (phasins) | 1 | 60,8 | | 98,4 | | 121,0 | | 2,4 | |
| ebA2800 | | conserved hypothetical protein | 4 | 58,9 | 24,1 | 98,5 | 0,3 | 140,0 | 50,4 | 2,4 | 0,0 |
| ebA2822 | *hemE* | uroporphyrinogen decarboxylase | 3 | 31,7 | 6,7 | 98,5 | 0,3 | 161,3 | 9,7 | 2,2 | 0,4 |
| ebA2847 | *dnaN* | DNA-polymerase III, beta chain | 11 | 48,5 | 13,6 | 98,6 | 0,3 | 172,0 | 56,7 | 2,3 | 0,2 |
| ebA2907 | *spoOJ* | ParB-like partition protein | 2 | 45,5 | 13,0 | 98,5 | 0,1 | 143,0 | 19,8 | 2,4 | 0,0 |
| ebA2918 | *tpx* | probable thiol peroxidase | 7 | 78,9 | 10,2 | 98,9 | 0,3 | 197,6 | 38,3 | 2,4 | 0,0 |
| ebA2969 | *mucD* | putative serine protease | 11 | 40,9 | 9,5 | 98,9 | 0,4 | 201,1 | 60,8 | 2,4 | 0,1 |
| ebA2973 | *efp* | translation elongation factor P | 8 | 53,6 | 4,9 | 98,2 | 0,2 | 99,7 | 15,5 | 2,3 | 0,1 |
| ebA2993 | *gcdH* | glutaryl-CoA dehydrogenase | 35 | 50,3 | 13,3 | 98,7 | 1,0 | 190,7 | 59,6 | 2,4 | 0,1 |
| ebA3004 | *atpA* | F1-ATP synthase, alpha SU | 16 | 40,8 | 13,0 | 99,0 | 0,5 | 219,5 | 79,3 | 2,4 | 0,0 |

**Tab 1.4:** continued

| ORF No. | Gene | Function | No. of identifi-cations | Seq. Coverage | SD | Meta-Score | SD | Mascot-Score | SD | Profound-Score | SD |
|---|---|---|---|---|---|---|---|---|---|---|---|
| ebA3007 | *atpD* | F1-ATP synthase, beta SU | 59 | 57,0 | 14,6 | 98,9 | 0,8 | 215,8 | 59,9 | 2,3 | 0,2 |
| ebA3029 | *gatB* | aspartyl/glutamyl-tRNA amidotransferase, SU B | 4 | 40,8 | 16,7 | 98,0 | 1,7 | 204,0 | 44,2 | 2,3 | 0,2 |
| ebA3030 | *gatA* | glutamyl-tRNA amidotransferase, SU A | 4 | 42,3 | 9,9 | 98,7 | 0,3 | 159,5 | 45,1 | 2,4 | 0,0 |
| ebA3033 | *mreB* | ROD shape-determining protein | 4 | 50,1 | 9,1 | 98,8 | 0,4 | 199,5 | 39,7 | 2,3 | 0,3 |
| ebA3069 | | conserved hypothetical protein, probable involved in cell wall turnover | 2 | 60,7 | 14,3 | 98,5 | 0,2 | 128,0 | 31,1 | 2,4 | 0,0 |
| ebA3088 | | hypothetical protein | 3 | 47,3 | 8,8 | 98,6 | 0,4 | 153,0 | 52,2 | 2,4 | 0,0 |
| ebA3118 | | probable zinc-containing alcohol dehydrogenase | 8 | 47,5 | 13,3 | 98,5 | 0,4 | 150,2 | 51,6 | 2,4 | 0,1 |
| ebA3138 | *ppcA* | phenylphosphate carboxylase, alpha SU | 3 | 59,5 | 16,2 | 100,1 | 0,8 | 368,7 | 118,4 | 2,4 | 0,0 |
| ebA3149 | *korA2* | 2-oxoglutarate ferredoxin oxidoreductase, allpha SU | 14 | 57,1 | 12,3 | 100,0 | 0,6 | 354,4 | 92,8 | 2,4 | 0,0 |
| ebA3161 | *pchA* | *p*-hydroxybenzaldehyde dehydrogenase | 2 | 34,3 | 3,2 | 98,4 | 0,1 | 125,0 | 25,5 | 2,4 | 0,0 |
| ebA3165 | *pchF* | probable *p*-cresol methylhydroxylase, SU | 11 | 41,7 | 17,1 | 99,1 | 0,6 | 224,8 | 92,1 | 2,4 | 0,0 |
| ebA3166 | *adh* | benzyl alcohol dehydrogenase | 6 | 47,5 | 14,2 | 98,3 | 1,1 | 175,6 | 59,3 | 2,4 | 0,0 |
| ebA3175 | | putative amino acid ABC transporter | 15 | 62,3 | 18,4 | 99,3 | 0,8 | 254,6 | 118,4 | 2,4 | 0,0 |
| ebA3296 | | Zn-dependent hydrolase | 3 | 53,1 | 6,3 | 98,9 | 0,2 | 211,0 | 18,5 | 2,3 | 0,2 |
| ebA3488 | | conserved hypothetical protein, predicted DSBA oxidoreductase family | 4 | 51,0 | 11,5 | 98,5 | 0,5 | 131,7 | 65,0 | 2,4 | 0,0 |
| ebA3532 | | conserved hypothetical protein | 6 | 42,2 | 6,7 | 93,7 | 8,5 | 90,3 | 13,4 | 2,3 | 0,0 |
| ebA3541 | *paaZ* | protein involved in aerobic phenylacetate metabolism | 7 | 46,0 | 15,9 | 99,3 | 0,7 | 261,1 | 98,8 | 2,4 | 0,1 |
| ebA3542 | *paaG* | putative enoyl-CoA hydratase | 5 | 58,8 | 20,0 | 98,8 | 0,7 | 200,2 | 96,4 | 2,2 | 0,3 |
| ebA3547 | *paaA* | putative ring-oxidation complex protein 1 | 5 | 62,9 | 6,6 | 98,7 | 0,3 | 214,8 | 34,2 | 2,0 | 0,3 |
| ebA3550 | *paaC* | putative ring-hydroxylation complex protein 2 | 7 | 46,8 | 14,1 | 98,6 | 0,7 | 157,0 | 54,8 | 2,2 | 0,4 |
| ebA3553 | *paaE* | putative ring-hydroxylation complex protein 4 | 1 | 78,6 | | 100,5 | | 438,0 | | 2,4 | |

**Tab 1.4:** continued

| ORF No. | Gene | Function | No. of identifi-cations | Seq. Coverage | SD | Meta-Score | SD | Mascot-Score | SD | Profound-Score | SD |
|---|---|---|---|---|---|---|---|---|---|---|---|
| ebA3556 | | putative amino-acid-binding periplasmatic (PBP) ABC transporter protein | 11 | 38,5 | 13,3 | 97,8 | 1,2 | 124,6 | 39,5 | 2,3 | 0,1 |
| ebA3561 | *nemA* | flavoprotein NADH-dependent oxidoreductase | 12 | 61,0 | 22,3 | 99,1 | 0,9 | 239,3 | 125,3 | 2,3 | 0,2 |
| ebA3567 | *ribAB* | riboflavin biosynthesis bifunctional protein: GTP cyclohydrolase II, 3,4-dihydroxy-2-butanone-4-phosphate synthase | 8 | 60,3 | 11,3 | 99,1 | 0,3 | 217,9 | 49,2 | 2,4 | 0,1 |
| ebA3569 | *ribE* | riboflavin synthase, alpha chain | 12 | 59,2 | 23,2 | 98,6 | 0,4 | 147,8 | 57,6 | 2,4 | 0,0 |
| ebA3597 | *modB1* | molybdate or tungstate transport | 16 | 62,6 | 16,9 | 99,4 | 0,8 | 286,1 | 103,7 | 2,3 | 0,2 |
| ebA3628 | *phbC* | putative poly-beta-hydroxybutyrate synthase | 1 | 31,6 | | 99,0 | | 207,0 | | 2,4 | |
| ebA3640 | | putative acyl-CoA dehydrogenase oxidoreductase protein | 6 | 62,1 | 20,8 | 99,7 | 0,9 | 312,0 | 132,0 | 2,4 | 0,0 |
| ebA3642 | | putative enoyl-CoA hydratase protein | 1 | 37,3 | | 98,5 | | 146,0 | | 2,4 | |
| ebA3743 | *pccA* | propionyl-CoA carboxylase, alpha SU | 2 | 44,7 | 0,0 | 99,7 | 0,0 | 307,0 | 0,0 | 2,4 | 0,0 |
| ebA3811 | *nusG* | transcription antitermination protein | 10 | 50,9 | 16,6 | 97,8 | 1,9 | 166,6 | 57,4 | 2,3 | 0,1 |
| ebA3824 | *fusA* | elongation factor G1 (EF-G 1) | 4 | 40,1 | 8,0 | 98,8 | 0,3 | 187,0 | 42,7 | 2,4 | 0,0 |
| ebA3826 | *tufB* | elongation factor Tu | 43 | 56,6 | 16,8 | 98,8 | 1,2 | 229,5 | 83,5 | 2,3 | 0,2 |
| ebA3853 | *rpoA* | DNA-directed RNA polymerase alpha SU | 19 | 59,9 | 14,7 | 99,1 | 0,4 | 240,2 | 69,7 | 2,3 | 0,2 |
| ebA3861 | | Zn-dependent hydrolase | 1 | 47,2 | | 99,2 | | 241,0 | | 2,4 | |
| ebA3879 | *acpD* | acyl-carrier protein phosphodiesterase | 10 | 45,0 | 12,3 | 98,3 | 1,2 | 168,6 | 70,3 | 2,4 | 0,1 |
| ebA3937 | | TonB-dependent receptor | 14 | 46,9 | 16,7 | 99,0 | 1,1 | 269,6 | 93,5 | 2,2 | 0,2 |
| ebA3939 | | siderophor receptor, TonB-dependent | 8 | 55,2 | 10,0 | 100,0 | 0,8 | 366,8 | 107,9 | 2,4 | 0,2 |
| ebA3942 | *metK* | S-adenosylmethionine synthase; methionine adenosyltransferase | 3 | 42,6 | 21,1 | 99,0 | 0,7 | 211,7 | 97,1 | 2,3 | 0,1 |
| ebA3950 | *dapF* | diaminopimelate epimerase | 4 | 54,9 | 7,3 | 99,0 | 0,3 | 209,5 | 45,6 | 2,4 | 0,0 |

**Tab 1.4:** continued

| ORF No. | Gene | Function | No. of identifi-cations | Seq. Coverage | SD | Meta-Score | SD | Mascot-Score | SD | Profound-Score | SD |
|---|---|---|---|---|---|---|---|---|---|---|---|
| ebA3951 | | conserved hypothetical protein | 6 | 54,0 | 11,6 | 98,7 | 0,3 | 169,7 | 44,8 | 2,4 | 0,0 |
| ebA3964 | *cafA* | ribonuclease G (RNase G) | 1 | 23,1 | | 98,5 | | 135,0 | | 2,4 | |
| ebA3999 | *wcaG* | ADP-l-glycero-D-manno-heptose-6-epimerase | 5 | 55,1 | 26,6 | 99,2 | 0,7 | 235,2 | 109,8 | 2,4 | 0,0 |
| ebA4040 | *ppcK* | phosphoenoylpyruvate carboxykinase | 12 | 34,1 | 14,8 | 97,6 | 4,4 | 193,7 | 102,5 | 2,4 | 0,1 |
| ebA4065 | *glnS* | glutaminyl-tRNA synthethase | 1 | 18,5 | | 98,4 | | 118,0 | | 2,4 | |
| ebA4078 | *rplI* | 50S ribosomal protein L9 | 11 | 74,4 | 19,9 | 98,6 | 0,4 | 160,4 | 34,5 | 2,3 | 0,3 |
| ebA4105 | *coaE* | predicted dephospho-CoA kinase | 3 | 66,2 | 18,2 | 98,9 | 0,5 | 198,7 | 69,9 | 2,4 | 0,0 |
| ebA4113 | *birA* | probable biotin--acetyl-CoA-carboxylase ligase | 1 | 31,2 | | 98,5 | | 146,0 | | 2,4 | |
| ebA4139 | | predicted GTPase, probably involved in regulation of ribosome function | 6 | 61,8 | 5,6 | 99,0 | 0,3 | 211,5 | 26,4 | 2,3 | 0,2 |
| ebA4173 | *rpe* | ribulose-phosphate 3-epimerase | 3 | 39,3 | 2,7 | 98,4 | 0,0 | 129,7 | 1,2 | 2,4 | 0,1 |
| ebA4177 | *trpE* | anthranilate synthase, component I | 2 | 39,3 | 12,4 | 98,7 | 0,4 | 164,0 | 63,6 | 2,4 | 0,0 |
| ebA4199 | *pabA* | anthranilate synthase, component III | 2 | 48,7 | 22,2 | 98,6 | 0,7 | 154,3 | 102,9 | 2,4 | 0,1 |
| ebA4201 | *trpC* | indole-3-glycerol phosphate synthase | 3 | 36,3 | 14,2 | 96,6 | 3,4 | 155,5 | 61,5 | 2,4 | 0,0 |
| ebA4217 | | conserved hypothetical protein | 2 | 46,2 | 0,0 | 98,4 | 0,0 | 120,0 | 0,0 | 2,4 | 0,0 |
| ebA4244 | *ompC* | outer membrane protein (porin) | 2 | 45,6 | 7,7 | 98,4 | 0,0 | 120,0 | 2,8 | 2,4 | 0,0 |
| ebA4330 | *argB* | acetylglutamate kinase | 6 | 39,7 | 12,7 | 98,5 | 0,6 | 153,4 | 70,0 | 2,2 | 0,3 |
| ebA4332 | | small heat shock protein | 18 | 61,4 | 14,2 | 98,3 | 0,3 | 127,3 | 30,2 | 2,3 | 0,2 |
| ebA4339 | *aspS* | aspartyl-tRNA synthetase | 6 | 44,8 | 8,5 | 99,1 | 0,4 | 249,0 | 66,4 | 2,3 | 0,2 |
| ebA4380 | *proA* | gamma-glutamyl phosphate reductase | 4 | 42,2 | 12,6 | 98,7 | 0,6 | 177,7 | 80,4 | 2,3 | 0,1 |
| ebA4392 | *maeB1* | NADP-dependent malic enzyme | 9 | 44,2 | 17,7 | 99,5 | 0,9 | 282,7 | 124,3 | 2,4 | 0,0 |
| ebA4399 | *ahpC* | predicted peroxiredoxin | 58 | 74,4 | 12,1 | 98,6 | 0,4 | 169,8 | 48,5 | 2,2 | 0,2 |
| ebA4409 | *mrp* | Mrp-ATPases involved in chromosome partitioning | 5 | 37,9 | 5,6 | 98,6 | 0,3 | 160,8 | 35,4 | 2,4 | 0,0 |

**Tab 1.4:** continued

| ORF No. | Gene | Function | No. of identifi-cations | Seq. Coverage | SD | Meta-Score | SD | Mascot-Score | SD | Profound-Score | SD |
|---|---|---|---|---|---|---|---|---|---|---|---|
| ebA4440 | *ispA* | polyprenyl synthethase | 5 | 46,5 | 11,1 | 98,7 | 0,3 | 177,4 | 48,2 | 2,4 | 0,0 |
| ebA4444 | *ispH* | 4-hydroxy-3-methylbut-2-enyl diphosphate reductase | 4 | 44,9 | 5,4 | 98,8 | 0,3 | 190,8 | 41,4 | 2,4 | 0,1 |
| ebA4473 | *aceA* | isocitrate lyase | 33 | 42,1 | 12,1 | 98,2 | 3,1 | 206,5 | 86,3 | 2,4 | 0,1 |
| ebA4476 | *menG* | demethylmenaquinone methyltransferase | 6 | 69,6 | 22,1 | 98,7 | 0,5 | 154,4 | 56,8 | 2,4 | 0,0 |
| ebA4497 | *pntAA* | pyridine nucleotide transhydrogenase alpha subunit | 8 | 61,1 | 18,5 | 99,0 | 0,6 | 219,3 | 86,3 | 2,3 | 0,2 |
| ebA4512 | *ispB* | polyprenyl synthethase | 4 | 51,0 | 4,8 | 98,8 | 0,5 | 185,5 | 60,3 | 2,4 | 0,1 |
| ebA4561 | *gltI* | putative ABC-transporter, glutamate receptor | 18 | 58,8 | 19,2 | 98,3 | 1,7 | 204,8 | 70,6 | 2,3 | 0,3 |
| ebA4588 | *korA* | 2-ketoglutarate:NADP oxidoreductase, alpha SU | 10 | 35,4 | 11,3 | 98,6 | 1,3 | 215,1 | 65,8 | 2,4 | 0,0 |
| ebA4623 | *adhB* | alcohol dehydrogenase II | 10 | 40,6 | 11,6 | 98,6 | 0,4 | 161,1 | 43,5 | 2,3 | 0,2 |
| ebA4678 | *cysK* | cystein synthase A | 8 | 63,9 | 8,7 | 99,3 | 0,5 | 264,9 | 69,6 | 2,4 | 0,1 |
| ebA4700 | *acxA* | acetone carboxylase, beta SU | 12 | 57,0 | 23,4 | 99,5 | 2,0 | 365,8 | 131,7 | 2,3 | 0,2 |
| ebA4701 | *acxB* | acetone carboxylase, alpha SU | 11 | 31,9 | 9,5 | 98,8 | 0,4 | 208,4 | 64,3 | 2,2 | 0,2 |
| ebA4702 | *acxC* | acetone carboxylase, gamma SU | 19 | 46,0 | 10,4 | 98,6 | 0,3 | 157,6 | 41,5 | 2,3 | 0,2 |
| ebA4705 | | hypothetical protein | 4 | 80,5 | 12,9 | 99,2 | 0,4 | 248,5 | 52,6 | 2,4 | 0,0 |
| ebA4712 | | probable regulatory protein LysR | 12 | 27,9 | 12,7 | 98,5 | 1,5 | 199,9 | 95,7 | 2,3 | 0,1 |
| ebA4715 | | hypothetical protein | 15 | 57,9 | 13,1 | 99,6 | 0,6 | 302,7 | 95,0 | 2,4 | 0,1 |
| ebA4718 | *kctA* | succinyl-CoA:3-ketoacid-CoA tranferase, SU A | 15 | 79,0 | 11,5 | 99,3 | 0,4 | 257,2 | 46,8 | 2,3 | 0,2 |
| ebA4719 | *kctB* | succinyl-CoA:3-ketoacid-CoA tranferase, SU B | 12 | 54,1 | 14,6 | 98,2 | 1,2 | 151,8 | 34,3 | 2,4 | 0,0 |
| ebA4732 | *phbR* | predicted polyhydroxyalkanoate synthase repressor | 2 | 35,7 | 0,0 | 98,2 | 0,0 | 96,3 | 8,1 | 2,3 | 0,0 |
| ebA4742 | *hbdA* | 3-hydroxybutyryl-CoA dehydrogenase | 6 | 48,4 | 12,9 | 98,0 | 0,6 | 103,5 | 17,0 | 2,3 | 0,1 |
| ebA4757 | *leuC* | 3-isopropylmalate dehydrogenase large subunit | 8 | 44,8 | 9,1 | 99,0 | 0,4 | 212,6 | 62,1 | 2,4 | 0,0 |
| ebA4758 | *leuD* | 3-isopropylmalate dehydrogenase small subunit | 5 | 67,3 | 23,4 | 98,8 | 0,5 | 185,4 | 70,1 | 2,4 | 0,0 |

**Tab 1.4:** continued

| ORF No. | Gene | Function | No. of identifi-cations | Seq. Coverage | SD | Meta-Score | SD | Mascot-Score | SD | Profound-Score | SD |
|---|---|---|---|---|---|---|---|---|---|---|---|
| ebA4760 | *leuB* | 3-isopropylmalate dehydrogenase | 5 | 29,3 | 7,0 | 98,3 | 0,7 | 146,6 | 41,8 | 2,4 | 0,0 |
| ebA4761 | *asd* | aspartate-semialdehyde dehydrogenase | 8 | 40,7 | 14,3 | 98,6 | 0,4 | 153,9 | 54,5 | 2,4 | 0,0 |
| ebA4785 | *metZ* | putative cys/met metabolismus pyridoxal-phosphate-dependent enzyme | 6 | 40,7 | 13,5 | 97,6 | 2,0 | 143,4 | 42,6 | 2,3 | 0,2 |
| ebA4788 | *ppiB* | peptidyl-prolyl cis-trans isomerase B | 9 | 81,0 | 15,3 | 98,5 | 0,2 | 149,1 | 28,3 | 2,4 | 0,1 |
| ebA4794 | *dnaK* | chaperone protein | 13 | 41,1 | 16,2 | 99,2 | 0,9 | 244,3 | 113,1 | 2,3 | 0,2 |
| ebA4812 | *dapB* | putative dihydrodipicolinate reductase | 5 | 49,9 | 8,8 | 98,5 | 0,2 | 142,2 | 38,1 | 2,4 | 0,0 |
| ebA4813 | *carA* | carbamoyl-phosphate synthase, small chain | 2 | 44,9 | 12,6 | 99,1 | 0,3 | 234,0 | 41,0 | 2,4 | 0,1 |
| ebA4816 | *greA* | transcription elongation factor | 1 | 39,7 | | 98,4 | | 125,0 | | 2,4 | |
| ebA4824 | *dhpS* | dihydropteroate synthase | 2 | 40,6 | 5,4 | 98,5 | 0,1 | 136,5 | 2,1 | 2,4 | 0,0 |
| ebA4825 | *MRSA* | phosphoglucomutase and phosphomannomutase family | 4 | 26,6 | 8,1 | 98,4 | 0,5 | 132,4 | 61,8 | 2,4 | 0,0 |
| ebA4831 | *tpiA* | triosephosphat isomerase | 3 | 52,4 | 8,1 | 98,3 | 0,1 | 137,3 | 6,7 | 2,3 | 0,1 |
| ebA4836 | *nuoC* | NADH dehydrogenase I, chain C | 4 | 55,7 | 15,3 | 98,6 | 0,4 | 157,5 | 55,1 | 2,4 | 0,0 |
| ebA4840 | *nuoF* | NADH dehydrogenase I, chain F | 4 | 37,6 | 1,5 | 98,8 | 0,1 | 179,5 | 18,6 | 2,4 | 0,0 |
| ebA4865 | *hptG* | chaperone protein (high temperature protein G) | 11 | 49,4 | 17,3 | 99,2 | 0,8 | 247,9 | 112,1 | 2,4 | 0,1 |
| ebA4871 | | predicted ATPases of the AAA family | 6 | 52,0 | 10,9 | 99,1 | 0,5 | 219,2 | 70,8 | 2,4 | 0,0 |
| ebA4918 | | putative iron binding protein component of ABC iron transporter | 25 | 56,1 | 14,6 | 98,8 | 0,9 | 206,9 | 87,2 | 2,4 | 0,1 |
| ebA4952 | *thrA* | homoserine dehydrogenase | 10 | 58,4 | 13,1 | 99,5 | 0,3 | 287,4 | 46,5 | 2,4 | 0,0 |
| ebA4966 | *prkA* | protein kinase | 5 | 38,1 | 14,0 | 98,7 | 0,5 | 200,3 | 83,6 | 2,1 | 0,2 |
| ebA4969 | *tig* | trigger factor (TF) | 15 | 39,2 | 13,8 | 98,5 | 0,4 | 149,7 | 46,1 | 2,4 | 0,0 |
| ebA4994 | *dctP* | dicarboxylate transport, gene DCTP OR PM1525 | 1 | 36,2 | | 98,3 | | 107,0 | | 2,4 | |

**Tab 1.4:** continued

| ORF No. | Gene | Function | No. of identifi-cations | Seq. Coverage | SD | Meta-Score | SD | Mascot-Score | SD | Profound-Score | SD |
|---|---|---|---|---|---|---|---|---|---|---|---|
| ebA5004 | | ron-sulfur cluster-binding protein; potential subunit of aldehyde oxidoreductase | 4 | 83,1 | 15,1 | 99,1 | 0,5 | 200,0 | 79,0 | 2,4 | 0,0 |
| ebA5005 | | aldehyde:ferredoxin oxidoreductase | 4 | 58,9 | 14,8 | 99,4 | 0,4 | 285,3 | 76,9 | 2,2 | 0,2 |
| ebA5007 | | similar to ferredoxin:NADH oxidoreductases or NADH oxidases, potential subunit of aldehyde oxidoreductase | 7 | 67,6 | 10,4 | 99,5 | 0,7 | 309,0 | 74,3 | 2,2 | 0,3 |
| ebA5022 | | similar to YceI, base induced periplasmic protein | 2 | 46,0 | 0,4 | 98,2 | 0,1 | 96,1 | 11,2 | 2,4 | 0,0 |
| ebA5028 | | conserved hypothetical protein | 4 | 50,8 | 9,5 | 98,5 | 0,2 | 143,8 | 25,3 | 2,4 | 0,0 |
| ebA5076 | *gst* | conserved hypothetical protein | 8 | 38,7 | 16,8 | 97,3 | 3,0 | 123,5 | 43,2 | 2,3 | 0,1 |
| ebA5077 | *sodB* | superoxide dismutase [Fe] | 47 | 45,9 | 8,7 | 97,7 | 2,0 | 121,0 | 27,7 | 2,4 | 0,1 |
| ebA5087 | *adk* | adenylate kinase (ATP-AMP transphosphorylase) | 10 | 72,6 | 8,9 | 98,8 | 0,5 | 202,7 | 59,1 | 2,3 | 0,3 |
| ebA5097 | *argG* | argininosuccinate synthase | 10 | 64,5 | 11,5 | 99,3 | 0,4 | 253,9 | 60,3 | 2,4 | 0,0 |
| ebA5166 | | conserved hypothetical protein | 3 | 54,5 | 17,7 | 99,6 | 0,6 | 279,3 | 110,2 | 2,4 | 0,0 |
| ebA5202 | | putative thiolase | 19 | 48,8 | 16,0 | 98,7 | 1,5 | 214,3 | 65,6 | 2,3 | 0,1 |
| ebA5208 | *pgi* | glucose-6-phosphate isomerase | 2 | 28,1 | 2,5 | 98,5 | 0,3 | 139,0 | 41,0 | 2,4 | 0,0 |
| ebA5265 | *acnB* | aconitase | 21 | 32,1 | 13,8 | 99,1 | 0,7 | 216,1 | 107,6 | 2,4 | 0,0 |
| ebA5268 | | conserved hypothetical protein | 3 | 68,1 | 0,0 | 98,3 | 0,1 | 114,6 | 18,5 | 2,4 | 0,0 |
| ebA5282 | *bcrC* | benzoyl-CoA reductase, SU C | 33 | 63,8 | 16,1 | 99,6 | 0,7 | 296,3 | 101,0 | 2,4 | 0,1 |
| ebA5284 | *bcrB* | benzoyl-CoA reductase, SU B | 27 | 44,9 | 15,8 | 98,9 | 0,6 | 201,7 | 79,6 | 2,4 | 0,2 |
| ebA5286 | *bcrD* | benzoyl-CoA reductase, SU D | 85 | 63,7 | 20,7 | 98,3 | 3,9 | 203,0 | 68,1 | 2,4 | 0,1 |
| ebA5287 | *bcrA* | benzoyl-CoA reductase, SU A | | | | | | | | | |
| ebA5292 | *ORF3* | putative regulatory protein, conserved in anaerobic benzoate degradation gene cluster | 22 | 69,0 | 16,1 | 98,6 | 0,3 | 143,5 | 34,0 | 2,4 | 0,1 |

**Tab 1.4:** continued

| ORF No. | Gene | Function | No. of identifi-cations | Seq. Coverage | SD | Meta-Score | SD | Mascot-Score | SD | Profound-Score | SD |
|---|---|---|---|---|---|---|---|---|---|---|---|
| ebA5294 | *bzdV* | SU of oxidoreductase of unknown function, conserved in Azoarcus-type benzoate degradation gene cluster | 11 | 45,8 | 8,6 | 99,8 | 0,5 | 324,1 | 77,6 | 2,4 | 0,0 |
| ebA5296 | *dch* | dienoyl-CoA hydratase | 22 | 43,5 | 11,6 | 97,7 | 2,1 | 144,8 | 38,9 | 2,4 | 0,0 |
| ebA5298 | *oah* | probable 6-oxo-cyclohex-1-ene-carbonyl-CoA hydrolase | 36 | 48,7 | 11,4 | 98,8 | 0,6 | 186,9 | 58,1 | 2,4 | 0,1 |
| ebA5300 | *bzdZ* | putatvie dehydrogenase | 10 | 38,7 | 6,8 | 98,1 | 0,5 | 108,4 | 15,3 | 2,4 | 0,1 |
| ebA5301 | *bclA* | benzoate-CoA ligase | 16 | 39,4 | 12,0 | 98,8 | 0,5 | 187,4 | 75,0 | 2,4 | 0,1 |
| ebA5303 | | putative ABC-transporter, SU | 16 | 37,2 | 10,5 | 98,4 | 0,4 | 142,1 | 43,8 | 2,2 | 0,3 |
| ebA5307 | | putative ABC-transporter | 5 | 37,4 | 5,0 | 98,4 | 0,2 | 124,6 | 30,3 | 2,4 | 0,0 |
| ebA5317 | | long-chain-fatty-acid-CoA ligase | 3 | 58,6 | 8,6 | 100,1 | 0,4 | 375,0 | 50,7 | 2,4 | 0,0 |
| ebA5319 | | Putative beta-ketothiolase | 4 | 64,0 | 14,1 | 98,8 | 0,4 | 212,5 | 83,3 | 2,2 | 0,4 |
| ebA5320 | | putative 3-hydroxyacyl-CoA dehydrogenase precursor | 12 | 78,7 | 20,6 | 99,3 | 0,6 | 265,0 | 86,4 | 2,4 | 0,2 |
| ebA5333 | | putative TonB-dependent receptor | 14 | 54,3 | 17,2 | 99,9 | 1,1 | 348,8 | 152,3 | 2,4 | 0,1 |
| ebA5380 | | FAD dependent oxidase | 4 | 80,0 | 2,3 | 100,3 | 0,3 | 402,8 | 49,4 | 2,4 | 0,0 |
| ebA5381 | *phd* | probable phenylacetaldehyde dehydrogenase | 3 | 68,1 | 28,0 | 100,2 | 1,2 | 394,0 | 167,1 | 2,4 | 0,0 |
| ebA5395 | *padC* | phenylacetyl-CoA:acceptor oxidoreductase | 6 | 49,8 | 15,3 | 98,8 | 0,4 | 171,5 | 57,4 | 2,4 | 0,0 |
| ebA5399 | *padG* | phenylglyoxylate:acceptor oxidoreductase | 4 | 53,8 | 23,8 | 98,7 | 0,6 | 187,8 | 84,6 | 2,2 | 0,4 |
| ebA5400 | *padH* | phenylglyoxylate:acceptor oxidoreductase | 9 | 62,6 | 17,6 | 99,2 | 0,6 | 248,1 | 80,7 | 2,4 | 0,0 |
| ebA5402 | *padJ* | anaerobic phenylacetate CoA ligase | 15 | 50,1 | 15,0 | 98,8 | 0,8 | 212,3 | 67,5 | 2,3 | 0,2 |
| ebA5412 | | putative glycine clevage T-protein (aminomethyl transferase) | 9 | 54,4 | 18,1 | 98,8 | 0,5 | 181,4 | 68,2 | 2,4 | 0,0 |
| ebA5425 | *gdhA* | glutamate/leucine/phenylalanine/valine dehydrogenase | 3 | 35,5 | 10,5 | 98,6 | 0,2 | 173,0 | 36,0 | 2,3 | 0,0 |
| ebA5437 | *tyrB* | aromatic-amino-acid transaminase | 16 | 54,0 | 20,9 | 98,6 | 1,1 | 208,1 | 85,1 | 2,3 | 0,2 |

**Tab 1.4:** continued

| ORF No. | Gene | Function | No. of identifi-cations | Seq. Coverage | SD | Meta-Score | SD | Mascot-Score | SD | Profound-Score | SD |
|---|---|---|---|---|---|---|---|---|---|---|---|
| ebA5455 | *fabH* | 3-oxoacyl-(acyl-carrier-protein) synthase III | 6 | 38,1 | 16,3 | 97,0 | 3,1 | 134,3 | 44,4 | 2,4 | 0,0 |
| ebA5456 | *fabD* | probable malonyl-CoA (acyl-carrier-protein) transferase | 9 | 41,3 | 10,2 | 98,4 | 0,2 | 137,4 | 33,0 | 2,4 | 0,0 |
| ebA5459 | *fabF* | beta-ketoacyl-(acyl-carrier-protein) synthase | 6 | 50,5 | 15,5 | 98,6 | 0,4 | 174,5 | 60,1 | 2,1 | 0,3 |
| ebA5465 | *rseB* | putative sigma factor regulatory protein | 2 | 44,2 | 1,5 | 98,7 | 0,1 | 165,5 | 6,4 | 2,4 | 0,0 |
| ebA5637 | | mandelate racemase/muconate lactonizing enzyme familiy | 14 | 54,6 | 14,1 | 99,1 | 0,5 | 228,1 | 73,3 | 2,4 | 0,1 |
| ebA5640 | | acyl-CoA transferase, family III | 14 | 60,2 | 18,1 | 99,5 | 0,8 | 294,9 | 111,9 | 2,3 | 0,1 |
| ebA5641 | | acyl-CoA dehydrogenase | 15 | 72,4 | 19,0 | 99,7 | 1,1 | 326,5 | 154,9 | 2,3 | 0,2 |
| ebA5642 | *ald* | putative benzaldehyde dehydrogenase | 11 | 61,1 | 5,3 | 99,9 | 0,5 | 344,7 | 66,8 | 2,4 | 0,0 |
| ebA5643 | | acyl-CoA transferase, family III | 7 | 53,8 | 15,1 | 98,8 | 0,4 | 188,7 | 67,6 | 2,4 | 0,0 |
| ebA5660 | | probable ABC-transporter substrate binding protein | 9 | 64,0 | 10,6 | 99,7 | 0,6 | 316,0 | 96,7 | 2,4 | 0,1 |
| ebA5669 | *pimD* | putative pimeloyl-CoA dehydrogenase | 7 | 69,0 | 19,0 | 99,6 | 0,8 | 311,4 | 109,6 | 2,3 | 0,2 |
| ebA5671 | | predicted MaoC-like (R)-specific enoyl-CoA hydratase | 8 | 79,2 | 4,6 | 99,1 | 0,4 | 235,9 | 38,4 | 2,3 | 0,2 |
| ebA5722 | *paaC2* | similar to aerobic phenylacetate degradation protein | 6 | 51,9 | 9,8 | 98,7 | 0,3 | 163,4 | 43,4 | 2,4 | 0,0 |
| ebA5729 | *paaJ* | putative 3-ketoadipyl-CoA thiolase | 6 | 71,6 | 16,1 | 99,4 | 0,8 | 273,5 | 119,0 | 2,4 | 0,0 |
| ebA5761 | | putative oxidoreductase, zinc-containing alcohol dehydrogenase | 4 | 59,3 | 10,6 | 99,0 | 0,3 | 217,0 | 51,6 | 2,4 | 0,0 |
| ebA5764 | | conserved hypothetical protein, BNR domain protein | 3 | 64,9 | 6,4 | 99,2 | 0,1 | 243,0 | 8,5 | 2,4 | 0,0 |
| ebA5768 | | conserved hypothetical protein | 6 | 55,0 | 18,4 | 96,9 | 6,7 | 297,2 | 62,0 | 2,4 | 0,1 |
| ebA5783 | *ppsB* | hypothecial protein | 3 | 82,9 | 7,0 | 100,0 | 0,6 | 349,3 | 86,7 | 2,4 | 0,0 |
| ebA5789 | *ped2* | (S)-1-phenylethanol dehydrogenase | 6 | 49,8 | 11,2 | 98,4 | 0,3 | 135,5 | 45,0 | 2,4 | 0,1 |
| ebA5797 | | thiolase | 7 | 70,7 | 7,2 | 99,4 | 0,3 | 268,1 | 38,4 | 2,4 | 0,0 |

**Tab 1.4:** continued

| ORF No. | Gene | Function | No. of identifi-cations | Seq. Coverage | SD | Meta-Score | SD | Mascot-Score | SD | Profound-Score | SD |
|---|---|---|---|---|---|---|---|---|---|---|---|
| ebA5809 | *prfB* | peptide chain release factor 2 (RF-2), gene containing programmed frameshift site | 3 | 35,1 | 4,2 | 98,8 | 0,2 | 180,7 | 16,9 | 2,4 | 0,0 |
| ebA5846 | *pnp* | polyribonucleotide nucleotidtransferase protein | 9 | 37,5 | 12,2 | 99,0 | 0,7 | 222,0 | 108,8 | 2,4 | 0,1 |
| ebA5873 | *wbpP* | epimerase | 4 | 63,9 | 16,0 | 99,2 | 0,7 | 232,8 | 97,9 | 2,4 | 0,0 |
| ebA5895 | | hypothetical ATP-binding protein | 1 | 27,1 | | 98,4 | | 122,0 | | 2,4 | |
| ebA596 | *pat* | aromatic-amino-acid aminotransferase | 11 | 53,2 | 17,7 | 98,8 | 1,0 | 220,4 | 78,2 | 2,4 | 0,0 |
| ebA5987 | *tsf* | elongation factor Ts (EF-Ts) | 13 | 58,0 | 15,3 | 98,8 | 0,7 | 196,0 | 77,0 | 2,3 | 0,2 |
| ebA5996 | | probable outer membrane protein/surface antigen | 9 | 48,3 | 16,5 | 98,8 | 3,3 | 364,3 | 87,8 | 2,3 | 0,2 |
| ebA6038 | *rbr* | rubrerythrin/nigerythrin-like protein | 13 | 52,6 | 12,3 | 98,5 | 0,3 | 148,2 | 35,6 | 2,4 | 0,0 |
| ebA605 | *tnaA* | tyrosine phenol-lyase | 2 | 35,7 | 6,2 | 99,0 | 0,4 | 218,5 | 61,5 | 2,4 | 0,0 |
| ebA6073 | | conserved hypothetical protein | 5 | 68,5 | 16,5 | 98,7 | 0,6 | 179,8 | 76,6 | 2,4 | 0,0 |
| ebA6101 | | conserved hypothetical protein | 11 | 43,1 | 11,6 | 98,0 | 1,1 | 121,5 | 23,2 | 2,4 | 0,0 |
| ebA6107 | *gcvR* | glycine cleavage system regulatory protein | 3 | 63,1 | 5,0 | 98,9 | 0,1 | 162,0 | 30,5 | 2,4 | 0,0 |
| ebA6110 | *fpr* | ferredoxin-NADP reductase | 2 | 55,7 | 1,3 | 98,6 | 0,1 | 144,0 | 4,2 | 2,4 | 0,0 |
| ebA6149 | | putative TonB-dependent receptor | 4 | 55,3 | 9,0 | 99,7 | 0,6 | 316,0 | 88,7 | 2,4 | 0,0 |
| ebA6152 | | conserved hypothetical protein | 10 | 54,5 | 14,0 | 99,1 | 0,5 | 226,8 | 73,1 | 2,4 | 0,1 |
| ebA6162 | *eno* | enolase | 9 | 41,3 | 12,1 | 99,1 | 0,5 | 228,3 | 67,2 | 2,4 | 0,0 |
| ebA6204 | *cysP* | periplasmatic thiosulfate-binding protein | 11 | 54,2 | 10,3 | 99,2 | 0,4 | 239,9 | 62,1 | 2,4 | 0,0 |
| ebA6294 | | conserved hypothetical protein | 8 | 53,1 | 18,6 | 97,5 | 1,7 | 120,1 | 33,0 | 2,3 | 0,1 |
| ebA6332 | | hypothetical protein | 4 | 23,5 | 2,4 | 98,2 | 0,2 | 104,3 | 21,2 | 2,3 | 0,1 |
| ebA6376 | *typA* | GTP-binding protein with elongation factor-like domain | 3 | 23,6 | 3,3 | 98,3 | 0,4 | 121,8 | 46,1 | 2,4 | 0,1 |
| ebA6378 | *epsT* | UDP-glucose pyrophosphorylase | 5 | 29,1 | 9,9 | 95,1 | 4,3 | 142,4 | 68,4 | 2,3 | 0,1 |

**Tab 1.4:** continued

| ORF No. | Gene | Function | No. of identifi-cations | Seq. Coverage | SD | Meta-Score | SD | Mascot-Score | SD | Profound-Score | SD |
|---|---|---|---|---|---|---|---|---|---|---|---|
| ebA6386 | *dapD* | tetrahydrodipicolinate succinylase | 11 | 45,5 | 18,5 | 98,8 | 0,8 | 193,1 | 102,8 | 2,4 | 0,0 |
| ebA6393 | *btuE* | putative glutathion peroxidase protein | 4 | 65,3 | 25,1 | 98,6 | 0,5 | 174,3 | 47,5 | 2,2 | 0,3 |
| ebA6396 | *hscA* | chaperone protein, involved in Fe-S cluster synthesis (DnaK paralog) | 6 | 42,3 | 18,7 | 99,4 | 1,4 | 279,1 | 188,4 | 2,3 | 0,2 |
| ebA6410 | *suhB* | inositol monophosphatase | 1 | 48,5 | | 98,5 | | 149,0 | | 2,4 | |
| ebA6506 | | acyl-CoA dehydrogenase | 10 | 47,3 | 23,2 | 99,5 | 1,0 | 288,1 | 139,8 | 2,3 | 0,2 |
| ebA6510 | *etfA* | electron transfer flavoprotein, alpha SU | 48 | 50,2 | 9,6 | 98,5 | 0,3 | 142,8 | 30,7 | 2,4 | 0,1 |
| ebA6516 | | enoyl CoA hydratase | 1 | 34,2 | | 98,5 | | 143,0 | | 2,4 | |
| ebA6545 | *pdc* | probable phenylpyruvate decarboxylase | 6 | 45,2 | 18,0 | 99,0 | 0,9 | 223,7 | 108,8 | 2,3 | 0,3 |
| ebA6645 | *guaA* | GMP synthase | 5 | 34,9 | 13,2 | 98,8 | 0,6 | 183,3 | 88,1 | 2,4 | 0,0 |
| ebA6664 | *fabI* | enoyl-[acyl-carrier-protein] reductase | 9 | 36,4 | 10,4 | 98,3 | 1,4 | 179,8 | 90,0 | 2,4 | 0,1 |
| ebA6665 | *ppiD* | PpiC-type peptidyl-prolyl cis-trans isomerase | 3 | 50,4 | 7,5 | 100,0 | 0,1 | 353,3 | 17,9 | 2,4 | 0,0 |
| ebA6667 | *clpB* | ClpB protein | 4 | 24,5 | 16,4 | 98,3 | 1,3 | 202,3 | 104,5 | 2,4 | 0,1 |
| ebA6684 | *sucB* | 2-oxoglutarate dehydrogenase complex, dihydrolipoamide succinyltransferase | 4 | 45,0 | 11,6 | 98,5 | 0,5 | 147,8 | 73,8 | 2,3 | 0,1 |
| ebA6687 | *gltA* | citrate synthase | 22 | 55,8 | 9,7 | 99,4 | 0,5 | 276,3 | 72,0 | 2,4 | 0,1 |
| ebA6689 | *sdhB* | succinate dehydrogenase, iron-sulfur protein | 7 | 55,6 | 9,9 | 98,6 | 0,8 | 197,7 | 33,6 | 2,4 | 0,0 |
| ebA6690 | *sdhA* | succinate dehydrogenase, flavoprotein SU | 14 | 44,5 | 11,7 | 98,8 | 0,6 | 192,4 | 78,2 | 2,3 | 0,3 |
| ebA6736 | | probable FAD/FNM-containing oxidoreductase | 2 | 52,3 | 25,7 | 99,1 | 0,9 | 225,5 | 139,3 | 2,4 | 0,1 |
| ebA6773 | *acnA2* | aconitase | 1 | 26,7 | | 99,3 | | 259,0 | | 2,4 | |
| ebA6817 | *selD* | selenide, water dikinase (selenophosphate synthethase) | 3 | 48,8 | 17,7 | 97,3 | 2,6 | 206,0 | 116,0 | 2,2 | 0,2 |
| ebA6822 | | conserved hypothetical protein | 2 | 59,8 | 13,2 | 98,5 | 0,5 | 137,4 | 68,7 | 2,3 | 0,1 |

**Tab 1.4:** continued

| ORF No. | Gene | Function | No. of identifi-cations | Seq. Coverage | SD | Meta-Score | SD | Mascot-Score | SD | Profound-Score | SD |
|---|---|---|---|---|---|---|---|---|---|---|---|
| ebA6832 | | predicted aldolase 1-epimerase | 4 | 47,3 | 18,1 | 98,3 | 1,0 | 181,3 | 71,2 | 2,4 | 0,0 |
| ebA6837 | *minC* | septum site-determining protein | 5 | 49,0 | 15,5 | 98,7 | 0,4 | 168,0 | 56,9 | 2,4 | 0,0 |
| ebA6838 | *minD* | septum site-determining protein | 6 | 69,4 | 16,9 | 99,3 | 0,6 | 247,7 | 79,7 | 2,4 | 0,1 |
| ebA6852 | | probable phasin | 7 | 71,5 | 26,8 | 98,2 | 1,0 | 163,6 | 68,4 | 2,2 | 0,3 |
| ebA7042 | *trxB* | FAD-dependent pyridine nucleotide-disulfide oxidoreductase | 7 | 41,2 | 9,2 | 98,6 | 0,4 | 164,1 | 60,0 | 2,4 | 0,1 |
| ebA7053 | *ppa* | inorganic diphosphatase | 8 | 78,7 | 18,0 | 98,4 | 1,6 | 197,4 | 56,8 | 2,3 | 0,1 |
| ebA7104 | *purM* | phosphoribosylformylglycinamidine cyclo-ligase | 6 | 44,8 | 3,2 | 98,8 | 0,2 | 181,5 | 28,1 | 2,4 | 0,0 |
| ebA7120 | *panC* | pantoate-beta-alanine ligase | 2 | 57,1 | 1,8 | 98,8 | 0,0 | 185,5 | 2,1 | 2,4 | 0,0 |
| ebA7121 | | conserved hypothetical protein | 2 | 56,8 | 8,6 | 98,3 | 0,3 | 112,6 | 35,9 | 2,4 | 0,0 |
| ebA7134 | *ilvC* | ketol-acid reductoisomerase | 12 | 40,1 | 15,4 | 98,7 | 0,6 | 178,9 | 78,8 | 2,4 | 0,1 |
| ebA7154 | *leuA* | 2-isopropylmalate synthase | 7 | 49,8 | 17,0 | 98,8 | 0,9 | 212,2 | 107,6 | 2,2 | 0,3 |
| ebA7220 | *prpE* | propionate-CoA ligase | 1 | 46,5 | | 99,4 | | 269,0 | | 2,4 | |
| ebB167 | *fur* | ferric uptake regulation protein | 1 | 37,4 | | 98,2 | | 99,7 | | 2,4 | |
| ebB35 | *groES* | chaperonin cpn10 | 9 | 88,3 | 10,7 | 98,5 | 0,3 | 149,5 | 37,0 | 2,3 | 0,1 |
| ebB88 | | putative heat shock protein | 5 | 53,8 | 17,7 | 98,3 | 0,6 | 127,2 | 63,6 | 2,4 | 0,1 |
| ebB9 | *xccB* | biotin carboxyl carrier protein of inknown carboxylase | 3 | 43,4 | 2,6 | 98,3 | 0,3 | 113,0 | 41,6 | 2,4 | 0,0 |
| ebD6 | *ppcC* | phenylphosphate carboxylase, gamma SU | 3 | 56,2 | 0,0 | 98,7 | 0,2 | 175,7 | 27,0 | 2,3 | 0,1 |
| c1A46 | *thiG* | thiamine biosynthesis protein, gene: THIG | 3 | 43,9 | 15,4 | 97,0 | 3,0 | 181,0 | 29,7 | 2,3 | 0,1 |
| c2A172 | | beta-Ketoadipyl CoA thiolase | 13 | 74,1 | 13,4 | 99,6 | 0,6 | 296,9 | 93,7 | 2,4 | 0,1 |
| c2A306 | *bssE* | chaperone | 4 | 94,0 | 2,8 | 100,2 | 0,3 | 381,0 | 53,0 | 2,4 | 0,0 |
| c2A309 | *bssH* | putative E-phenylitaconyl-CoA hydratase | 8 | 66,8 | 8,5 | 99,2 | 0,4 | 240,1 | 56,7 | 2,4 | 0,0 |

**Tab 1.4:** continued

| ORF No. | Gene | Function | No. of identifi-cations | Seq. Coverage | SD | Meta-Score | SD | Mascot-Score | SD | Profound-Score | SD |
|---|---|---|---|---|---|---|---|---|---|---|---|
| c2A316 | *bbsA* | subunit of benzoylsuccinyl-CoA thiolase | 8 | 82,4 | 8,6 | 98,7 | 0,4 | 171,5 | 57,9 | 2,4 | 0,0 |
| p1B315 | *terD* | protein involved in tellurid resistance | 11 | 74,8 | 10,7 | 98,6 | 0,2 | 162,1 | 23,0 | 2,4 | 0,1 |
| p1B317 | *terE* | protein involved in tellurid resistance | 8 | 71,0 | 16,1 | 98,7 | 0,3 | 172,3 | 42,2 | 2,4 | 0,1 |

# 2. Cellular functions

## 2.1. DNA replication, recombination and repair

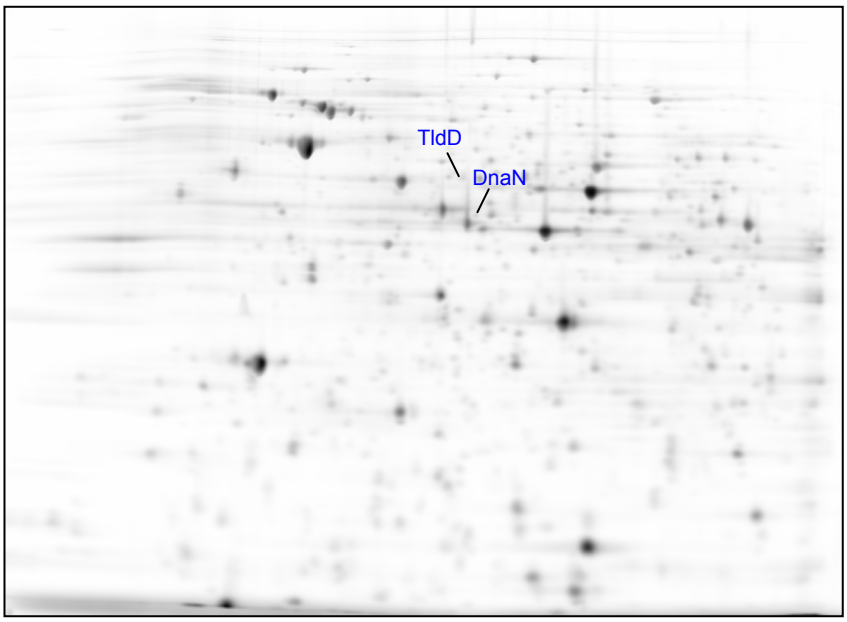


**Fig. 2.1.** 2DE gel (pH 4-7) of cells grown anaerobically with benzoate. Identified proteins related to DNA replication, recombination and repair are annotated.

**Table 2.1.** Identified protein related to DNA-replication, recombination and repair.

| Orf-No. | Gene | Functional description |
|---|---|---|
| ebA969 | *tldD* | Zn-dependent peptidase, potential modulator of DNA gyrase |
| ebA2847 | *dnaN* | DNA-polymerase III, beta chain |

### 2.1.1. DNA replication

The DNA polymerase III holoenzyme of *E. coli* is composed of 10 subunits. This proteincomplex, in cooperation with other replication proteins, carries out the duplication of the entire chromosome. The enzyme contains four distinct functional components. (1) The core polymerase, composed of α, ε and θ, contains both DNA polymerase (α) and proofreading exonuclease (ε) activities. (2) The sliding clamp, a β-dimer (**DnaN**), provides processivity by tethering the holoenzyme to the template DNA. (3) The clamp loader or γ-

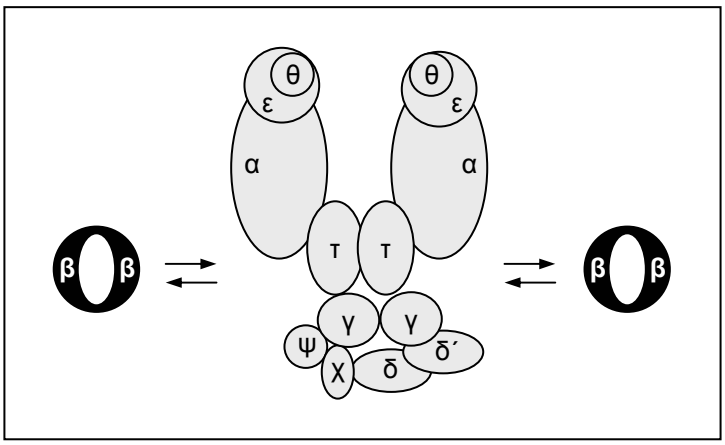


**Fig 2.1.1.**: Schematic illustration of DNA polymerase III holoenzyme composition. The identified β-subunit (**DnaN**) is marked in black.

complex (γ2δ1δ´1χ1ψ1), assembles β-clamps onto the DNA in an ATP-dependent reaction. (4) The linker protein (τ2) is associated with two core polymerase molecules and one γ-complex, forming the holoenzyme (Herendeen and Kelly 1996).

The identified β-subunit (**DnaN**) forms ring shaped dimers (sliding clamp) which encircle the DNA. Thereby the binding of DNA polymerase III to DNA strands is stabilized, enabling processive replication over length of several kilobases. In the absence of DNA, the core polymerase appears to have a relatively low affinity for β-dimers (Kawakami et al. 2001).

**TldD** was found to suppress mutations in *letD* an inhibitor of DNA gyrase. Therefore it has been hypothesised that the TldD protein modulate the activity of DNA gyrase (Murayama et al. 1996).

## 2.2. Transcription

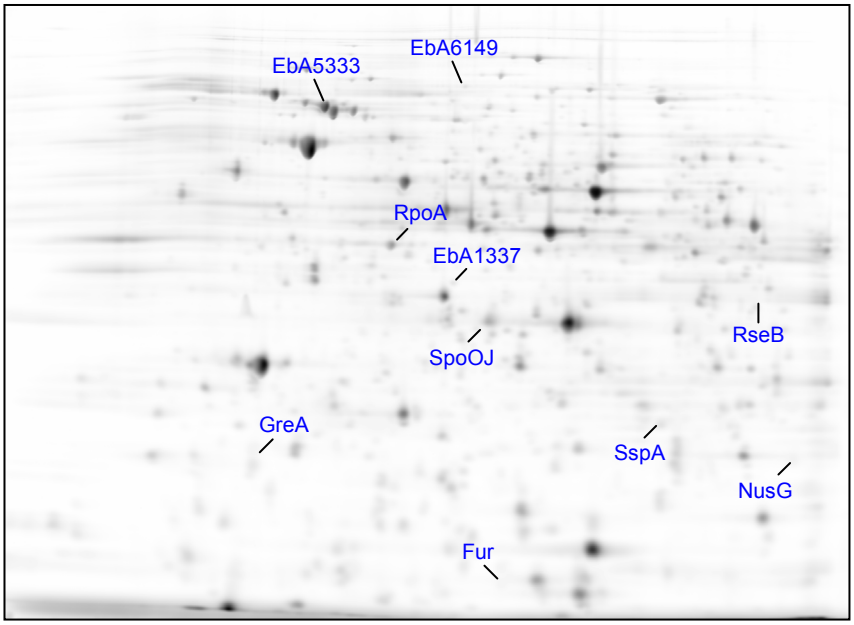


**Fig. 2.2.** 2DE gel (pH 4-7) of cells grown anaerobically with benzoate. Identified proteins related to transcription are annotated.

**Table 2.2.** Identified proteins related to transcription.

| Orf-No. | Gene | Functional description |
|---|---|---|
| ebA1195 | *sspA* | Stringent starvation protein A |
| ebA1337 | | PhoH-like protein |
| ebA2907 | *spoOJ* | ParB-like partition protein |
| ebA3853 | *rpoA* | DNA-directed RNA polymerase, α-subunit |
| ebA3811 | *nusG* | Transcription anti-termination protein |
| ebA4816 | *greA* | Transcription elongation factor |
| ebA5333 | | Putative TonB-dependent receptor |
| ebA5465 | *rseB* | Putative sigma factor regulatory protein |
| ebA6149 | | Putative TonB-dependent receptor |
| ebB167 | *fur* | Transcriptional regulator |

## 2.2.1. DNA-dependent RNA polymerase and sigma factors

The RNA polymerase holoenzyme is composed of the core enzyme and one of multiple σ-subunits, which provide promotor recognition activity. The core enzyme is made up of two large subunits (β and β´) and two smaller α-subunits. The core $\alpha_2\beta\beta'$ RNA polymerase forms the catalytic unit for RNA polymerisation but is incapable of accurate initiation. The proteomically identified α-subunit (**RpoA**) possesses two functional domains, mediating the assembly of the $\alpha_2\beta\beta'$ core enzyme by the pathway $2\alpha \rightarrow \alpha_2 \rightarrow \alpha_2\beta \rightarrow \alpha_2\beta\beta'$. The N-terminal domains (αNTD) contact the other subunits, while the C-terminal domains (αCTD) are in contact with the AT-rich sequence element near base -43. The identified **RseB**, together with RseAC, is involved in regulation of the activity of the sigma factor $\sigma^E$ (Coulombe and Burton 1999).

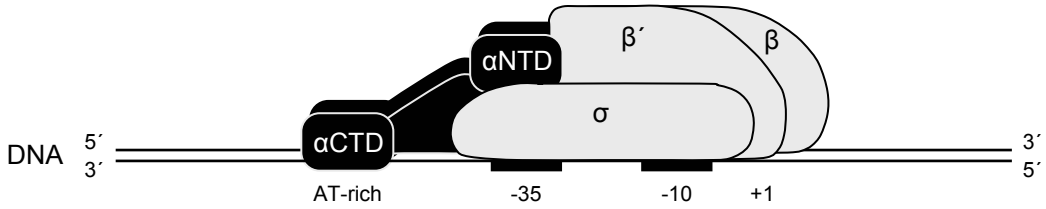


**Fig 2.2.1.** Schematic depiction of RNA polymerase interacting with the promotor.

## 2.2.2. Factors affecting RNA polymerase

Like transcription initiation, the elongation and termination of transcription serve as important targets for regulatory factors in procaryotes. Such factors affect RNA polymerase processivity by modulating transcription pausing, termination or anti-termination.

The transcription factor **GreA** supresses RNA polymerase pausing and arrest by stimulating its intrinsic nucleolytic activity. When RNA polymerase encounters a block, Gre-induced cleavage of the 3´-end enables the polymerase to transcribe over the block and resume elongation. In contrast to GreB, GreA is only able to prevent transcription arrest (Borukhov et al. 2005).

The transcription factor **NusG**, in a complex with the essential multifunctional factor NusA (as well as NusB and NusE), stimulates anti-termination at both ρ-dependent and ρ-independent terminators. Depending on the RNA/DNA sequence context, and the presence or absence of auxiliary factors, NusA may have opposite effects on transcription (Borukhov et al. 2005).

**SspA** is a transcription activator associated with the RNA-polymerase. In *E. coli*, its expression is induced during stationary phase growth and upon starvation for carbon, amino acids, nitrogen and phosphate as well as upon phage λ infection (Hansen et al. 2003).

The ATP-binding protein PhoH (**EbA1337**) belongs to the phosphate regulon of *E. coli*. Interestingly it is homologous to the N-terminal part of superfamily I helicases, comprising conserved amino acid residues corresponding to motives I-V of superfamily I helicases. Its distinct function is not known up to now (Koonin and Rudd 1996).

## 2.2.3. Classes of transcriptional regulators

An efficient response to changing environmental conditions is essential for all cells. Therefore effective repression or activation of gene transcription is a central mechanism, achieved via diverse transcriptional regulators. **Fur**-like regulators act as classical repressors, blocking transcription in the presence of their corresponding effector molecule (Coy and Neilands 1991).

## 2.3 Translation

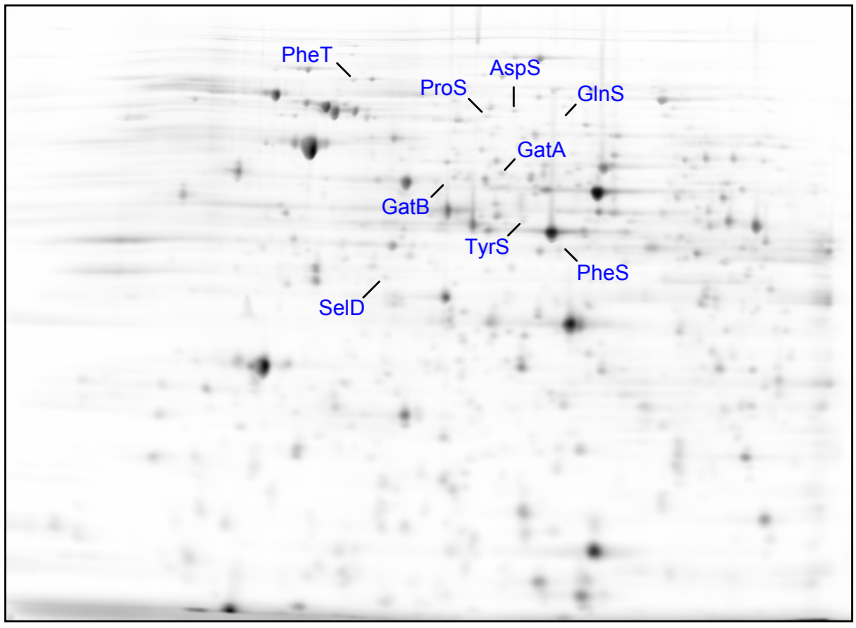


**Fig. 2.3.** 2DE gel (pH 4-7) of cells grown anaerobically with benzoate. Identified proteins related to translation are annotated (excluding translation factors; see Fig. 2.3.3.).

**Table 2.3.** Identified proteins related to translation.

| Orf-No. | Gene | Functional description |
|---|---|---|
| ebA3030 | *gatA* | Glutamyl-tRNA synthetase, α-subunit |
| ebA3029 | *gatB* | Glutamyl-tRNA synthetase, β-subunit |
| ebA4065 | *glnS* | Glutaminyl-tRNA synthetase |
| ebA4339 | *asp* | Aspartyl-tRNA synthetase |
| ebA868 | *pheS* | Phenylalanyl-tRNA synthetase, α-subunit |
| ebA867 | *pheT* | Phenylalanyl-tRNA synthetase, β-subunit |
| ebA931 | *tyrS* | Tyrosyl-tRNA synthetase |
| ebA950 | *proS* | Prolyl-tRNA synthetase |
| ebA6817 | *selD* | Selenophosphate synthetase |

### 2.3.1. tRNA synthetases

The aminoacyl-tRNA synthetases covalently link an amino acid to a nucleic acid adaptor molecule (tRNA), that contains the triplet anticodon for that amino acid. This is a crucial step in protein synthesis, since synthetase and its associated amino acid and tRNA have to form a correctly aminoacetylated tRNA (Cusack 1997).

Despite their conserved mechanisms of catalysis, the aminoacyl-tRNA synthetases are devided into two classes (I and II). In class I synthetases the active site contains a Rossmann dinucleotide-binding domain, whereas this fold is absent in class II, which instead contain a novel antiparallel β-fold (Ibba and Söll 2000).

Out of the 21 amino acids, eight proteins belonging to six aminoacyl-tRNA synthetases of both classes have been identified (Fig. 2.3.1.).

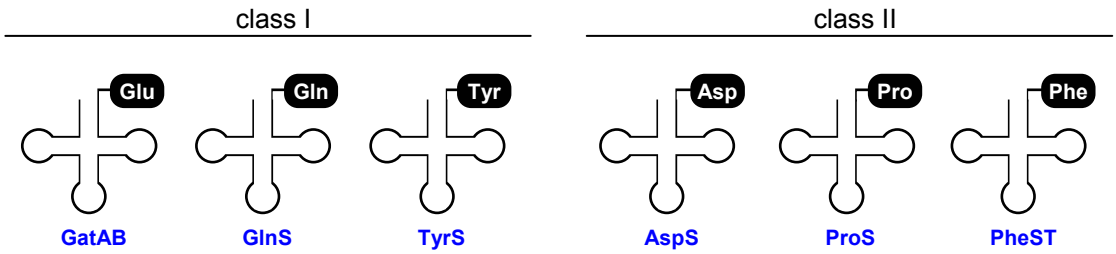


**Fig. 2.3.1.** Illustration of tRNAs synthesized by identified tRNA-synthethases (indicated below; enzyme abbreviations are as indicated in Tab. 2.3.)

## 2.3.2. tRNA/rRNA modification

The identified **SelD** protein is involved in selenium metabolism. In *E. coli* it could be shown, that SelD is required for the incorporation of selenium into the modified nucleoside 5-methylaminomethyl-2-selenouridine of tRNA. Furthermore, it is involved in the biosynthesis of selenocystein from an L-serine residue esterbonded to $tRNA^{Ser}$, functioning as a donor for reduced selenium (Leinfelder et al. 1990).

## 2.3.3. Translation factors

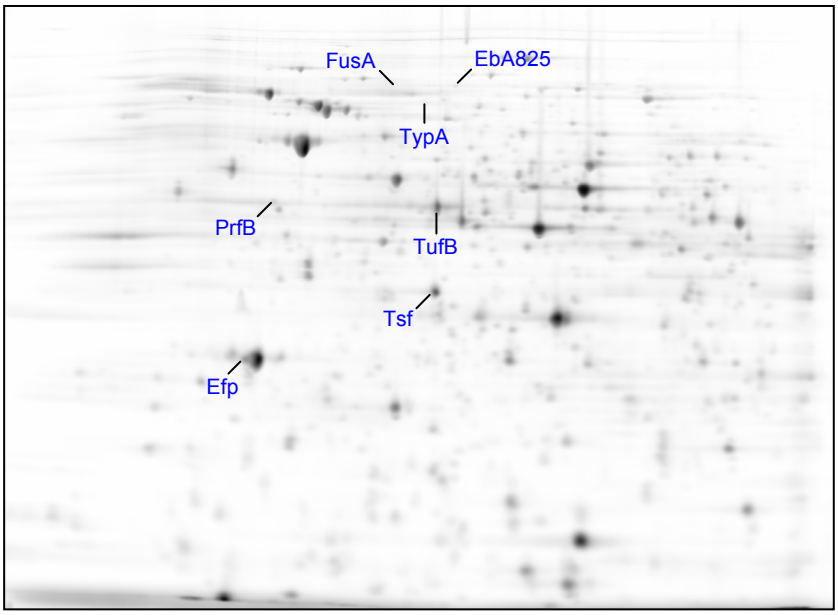


**Fig. 2.3.3.** 2DE gel (pH 4-7) of cells grown anaerobically with benzoate. Identified translation factors are annotated.

**Table 2.3.3.** Identified translation factors.

| Orf-No. | Gene | Functional description |
|---|---|---|
| ebA825 | | Elongation factor G |
| ebA2973 | *efp* | Elongation factor P |
| ebA3824 | *fusA* | Elongation factor G1 |
| ebA3826 | *tufB* | Elongation factor Tu |
| ebA5809 | *prfB* | Peptide chain release factor 2 (RF-2) |
| ebA5987 | *tsf* | Elongation factor Ts |
| ebA6376 | *typA* | GTP-binding protein with elongation factor-like domain |

During initiation of translation, the functional 70S ribosome, composed of 30S and 50S ribosomal subunit, mRNA and the initiating fMet-tRNA$^{fMet}$, is formed, supported by the initiation factors IF-1, IF-2 and IF-3.

In the first step of elongation, the appropriate incoming aminoacyl-tRNA is bound to a complex of GTP-bound EF-Tu (**TufB**). This complex binds to the A site of the 70S ribosome, GTP is hydrolyzed and the resulting EF-Tu·GDP complex is released. The EF-Tu·GTP complex is regenerated in a process involving EF-Ts (**Tsf**) and GTP (Nelson and Cox 2000).

Following formation of the peptide bond, promoted by EF-P (**Efp**), translocation takes place. This movement, supported by EF-G (**EbA826** and **FusA**) and GTP hydrolysis, shifts the anticodon of the dipeptidyl-tRNA from the A site to the P site, also shifting the deacetylated tRNA from the P to the E site. The structure of EF-G mimics the structure of the EF-Tu/tRNA complex, suggesting that EF-G may bind at the A site and displace the peptidyl-tRNA (Aoki et al. 1991, Nelson and Cox 2000). The role of **TypA**-like proteins is not clearly solved. It is suggested, that it increases the translation efficiency of some mRNA-species and therefore might have a regulatory function (Owens et al. 2004).

Elongation continues until the ribosome reaches the last aminoacid encoded by the mRNA. Immediately following the final coded amino acid, one of three termination codons (UAA, UAG, UGA) signal the termination of translation. Three release factors are involved in this process. RF-1 recognized the termination codons UAG and UAA, RF-2 (**PrfB**) recognizes UGA and UAA. Depending on the present codon, RF-1 or RF-2 bind at a termination codon and induce the peptidyl transferase to transfer the polypeptide to a water molecule. The release factor RF-3 stimulates, in the presence of RF-1 or RF-2, the dissociation of the ribosome, supported by the ribosome recycling factor and hydrolysis of GTP. (Nelson and Cox 2000, Grentmann et al. 1998)

## 2.3.4. Ribosomal proteins and modifying factors

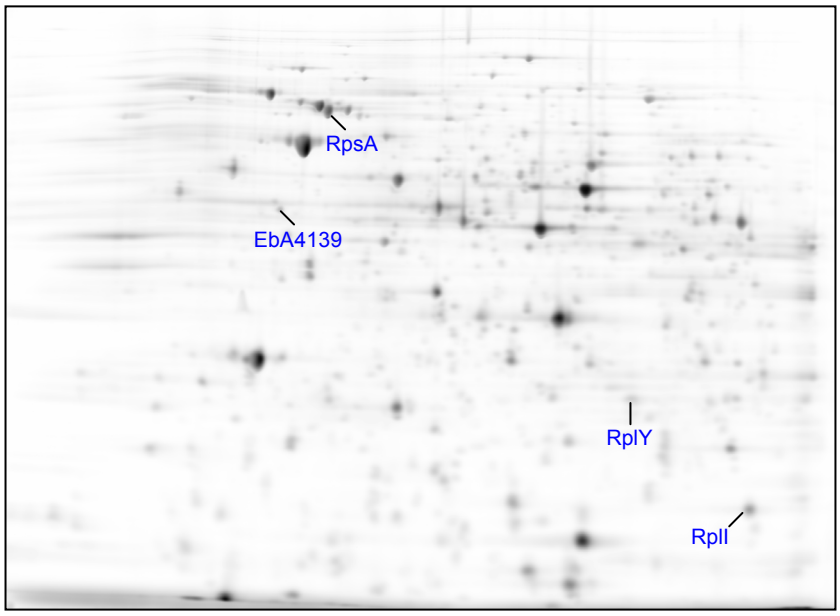


**Fig. 2.3.4.** 2DE gel (pH 4-7) of cells grown anaerobically with benzoate. Identified ribosomal proteins and modifying factors are annotated.

**Table 2.3.4.** Identified ribosomal proteins and modifying factors.

| Orf-No. | Gene | Functional description |
|---|---|---|
| ebA903 | *rpsA* | 30S ribosomal protein S1 |
| ebA1409 | *rplY* | 50S ribosomal protein L25 |
| ebA4078 | *rplI* | 50S ribosomal protein L9 |
| ebA4139 | | Predicted GTPase, probably involved in regulation of ribosome function |

Bacterial ribosomes are composed of two subunits, the large 50S and the small 30S subunit. Approximately one third of the total mass of the ribosome (~2.5 MDa) is constituted by proteins. With some possible variations, the small subunit consists of 21 ribosomal proteins (S1-21), while the large subunit contains 36 (L1-36; Al-Karadaghi et al. 2000).

In Gram-negative bacteria, the S1 protein (**RpsA**) plays an essential role in facilitating the initiation of translation by interacting with both the ribosome and with sequences in the mRNA upstream from the ribosome binding site. A sequence motive of about 70 amino acids, first identified in the S1-protein, is also found in a number of other proteins (e.g. translation initiation factor 1; Bycroft et al. 1997).

In the ribosome, the protein L9 (**RplI**) is located close to the components of the peptidyltransferase activity, but is not part of it. Besides L1, L9 is the only protein that interacts with the 3´-end of the 23S rRNA without cooperating with other L-proteins. It is suggested, that it is an essential scaffold molecule that maintains the correct folding of this region of the 23S rRNA (Hoffman et al. 1994).

The ribosomal protein L25 (**RplY**) is bound to the 5S rRNA in the ribosome. It consists a six stranded β-barrel structure, containing four parallel strands and two short α-helices, representing an uncommon fold for ribosomal proteins (Stoldt et. al, 1998).

## 2.3.5. Heat shock proteins and chaperons

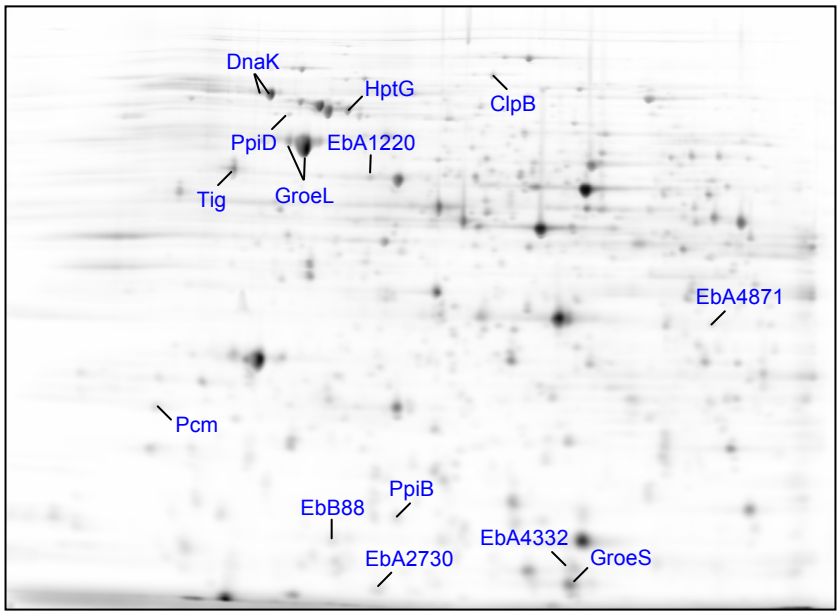


**Fig. 2.3.5.** 2DE gel (pH 4-7) of cells grown anaerobically with benzoate. Identified heat shock proteins and chaperons are annotated.

**Table 2.3.5.** Identified heat shock proteins and chaperons.

| Orf-No. | Gene | Functional description |
|---|---|---|
| ebA1185 | *groEL* | Chaperonin, 60 kDa subunit |
| ebB35 | *groES* | Chaperonin, cpn10 |
| ebA1220 | | Serine proteases, subtilase family |
| ebA1645 | *pcm* | Putative protein-L-isoaspartate *o*-methyltransferase |
| ebA2730 | | Heat shock protein, Hsp20 family |
| ebB88 | | Putative heat shock protein |
| ebA4332 | | Small heat shock protein |
| ebA4788 | *ppiB* | Peptidyl-prolyl isomerase B |
| ebA4794 | *dnaK* | Chaperonine protein |
| ebA4865 | *hptG* | Chaperonine protein (high temperature protein G) |
| ebA4871 | | Predicted ATPase of the AAA+ superfamily |
| ebA4966 | *tig* | Trigger factor |
| ebA6665 | *ppiD* | PpiC-type peptidyl-prolyl *cis-trans* isomerase |
| ebA6667 | *clpB* | Heat shock protein |

In general, chaperons represent a functionally related set of proteins. According to their molecular weight, molecular chaperons are devided into several classes or families. This complicated and sophisticated machinery of proteins assists in protein folding and allows the functional state of proteins to be maintained under conditions in which they would normally unfold and aggregate (Walter and Buchner 2002).

The most extensively studied molecular chaperones are the GroE proteins (**GroEL** and **GroES**). The quartery structure of GroEL resembles a barrel open at both ends, formed by fourteen subunits which are assembled in two seven-membered rings. The co-chaperone GroES is a dome-shaped ring structure, also formed by seven subunits. Initially in the functional cycle a polypeptide substrate binds to one GroEL ring. Binding of Mg/ATP and GroES to the same ring creates a folding-active *cis* complex inducing major conformational changes in the GroEL tetradecamer. The polypeptide is discharged into the protected environment of the *cis* cavity and starts to fold. The bound ATP is hydrolyzed and a second conformational change primes GroEL for the release of GroES by binding ATP to the *trans* ring. Finally the polypeptide is released from the cavity, irrespective of its folding state (Walter and Buchner 2002).

On the 2DE gel of strain EbN1, **GroEL** is one of the most abundant spots under all condtions. Its share of the total protein ranges from 5 to 7.5 %, depending on the growth condition. Also **GroES** is highly abundant representing approximately 3 % of the total protein. Both, GroEL and GroES, show no significant changes in abundance thoughout all examined 20 conditions. This underlines the importance of this chaperonin in general cellular metabolism.

The Hsp90 chaperone system (including **HptG**) is more complex than Groe. It includes the Hsp70 system and comprises a large number of cofactors. At present it seems that under physiological conditions Hsp90 does not play a major general role in the *de novo* folding of proteins. However, it is of critical importance for the folding of a number of proteins involved in regulatory processes. As principle of action is suggested a passing of the polypeptide through several Hsp90 complexes that differ in the composition of partner proteins. Thereby, the functional conformation of the target protein is promoted through the interactions with the different Hsp90 complexes (Walter and Buchner 2002).

**DnaK**, like other Hsp70 proteins, constitutes a central part of an ubiquitous chaperone system, present in most compartments of eucaryotic cells, in eubacteria and many archaea. It is involved in a wide range of cellular processes, including protein folding and degradation of instable proteins. Binding of short hydrophobic segments of partially folded polypeptides, thereby preventing aggregation and arresting of the folding process, seems to be the common function of Hsp70 proteins (Hartl 1996).

In *E. coli* the trigger tactor (**Tig**) is one of three major chaperones (along with DnaK and GroEL) which cooperate in the folding of newly synthesized cytoplasmic proteins. The majority of nascent polypeptides interact first with Tig at the ribosome, which binds at the ribosomal proteins L23 and L29 at the polypeptide exit site. Tig is thought to interact primarily with short nascent chains and its function overlaps with that of DnaK, which interacts with longer nascent chains downstream of Tig. Although deletion mutants of either *tig* or *dnaK* are viable, their combined deletion is lethal at temperatures above 30 degrees (Deuerling et al. 1999; Kramer et al. 2002).

In bacteria, representatives of the AAA+ superfamily (**EbA4871**, **ClpB)** are involved in functions as diverse as transcription and protein degradation and play an important tole in the protein quality control network. Often they employ a common mechanism to mediate an ATP-dependent unfolding/disassambly of protein-protein or DNA-protein complexes. Many bacterial chaperons of the AAA+ superfamily participate in proteolysis, although they do not contain a peptidase module (i.e. ClpA, ClpC and ClpX). These proteins regulate protein degradation by association with a ring-shaped peptidase. In contrast, **ClpB** is not involved in proteolysis but rather acts in collaboration with the DnaK-system to disassemble and refold large protein aggregates. The refolding of aggregated proteins by this bichaperone machinery could be separated into two phases. Resolubilisation of aggregated proteins is achieved by both ClpB and DnaK, while the subsequent refolding of the substrate requires only DnaK. The precise mechanism of DnaK/ClpB cooperation is still unknown (Dougan et al. 2002).

In contrast to the other classes of chaperones, small heat shock proteins (sHsps), like **EbA4332**, show a characteristic heterogenety in sequence and size. All known sHsps form

oligomeric complexes, mainly of 12 to 42 subunits, forming a hollow spherical structure. They exhibit a remarkable binding capacity, preventing aggregation of the bound proteins. Possibly, up to one target protein per subunit can be bound, regardless of the size of the protein. Subsequent refolding of the bound proteins might be achieved by Hsp70 or other potential ATP-dependent chaperone systems, allowing binding and folding to be seperated in space and time (Walter and Buchner 2002).

**EbA1594**, **PpiB** and **PpiD** are peptidyl-prolyl *cis-trans*-isomerase (rotamase) catalyzing the conformational isomerization of prolyl residues in peptides. *Cis-trans* isomerization of prolyl peptide bonds is a slow step in protein folding, and thus peptidyl-prolyl *cis-trans* isomerase is thought to facilitate proper protein folding (Compton et al. 1992).

Three classes of protein carboxyl methyltransferases have been distinguished according to their methyl-acceptor substrate specificity. **Pcm** belongs to the type II methyltransferases, which are found in a variety of cell types and methylates proteins and peptides containing D-aspartyl and L-isoaspartyl residues. This enzyme is postulated to participate in the metabolism of aged and damaged proteins (Fu et al. 1991).

## 2.3.6. Other translational functions

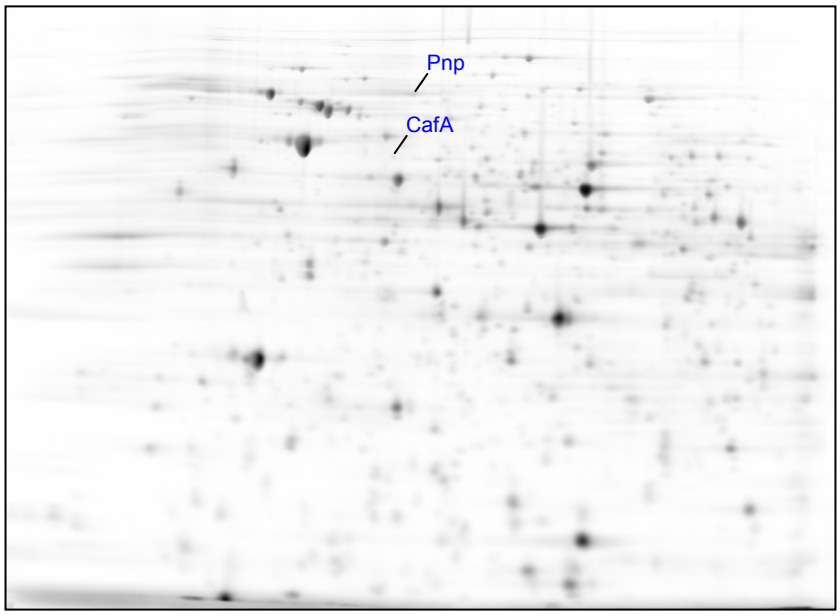


**Fig. 2.3.6.** 2DE gel (pH 4-7) of cells grown anaerobically with benzoate. Identified proteins related to translational factors are annotated.

**Table 2.3.6.** Identified proteins related to translational factors.

| Orf-No. | Gene | Functional description |
|---|---|---|
| ebA3964 | *cafA* | Ribonuclease G (RNase G) |
| ebA5846 | *pnp* | Polyribonuleotide nucleotidyltransferase protein |

The RNase G (**CafA**) is an endonuclease responsible for 5′-end processing of 16S rRNA. It shows high sequence similarity with the N-terminal half of RNase E which is involved in rRNA processing as well as in mRNA stability. RNase G is dependent on the nature of the 5′-end of the substrate. It cleaves 5′-monophosphorylated substrates efficiently but does not cleave the 5′-hydroxylated ones. Results from mutagenesis experiments indicate, that RNase G is not only involved in rRNA processing, but also, at least in part, responsible for *in vivo* mRNA degradation (Umitsuki et al. 2001).

In *E. coli*, the degradation of mRNA is mediated by the combined action of endo- and exonucleases. Two enzymes, RNase II and polynucleotide phosphorylase (PNPase; **Pnp**), degrade RNA in a 3′→ 5′ pathway. Thereby, PNPase uses inorganic phosphate yielding nucleotide diphosphates (ADP, CDP, UDP and GDP). Together with the DEAD-box RNA helicase B, RNase E and PNPase are the major components of the RNA degradasome. The association of RNase E and PNPase in a complex provides a direct physical link for their cooperation in the degradation of mRNA (Carpousis 2002).

## 2.3.7. Proteases

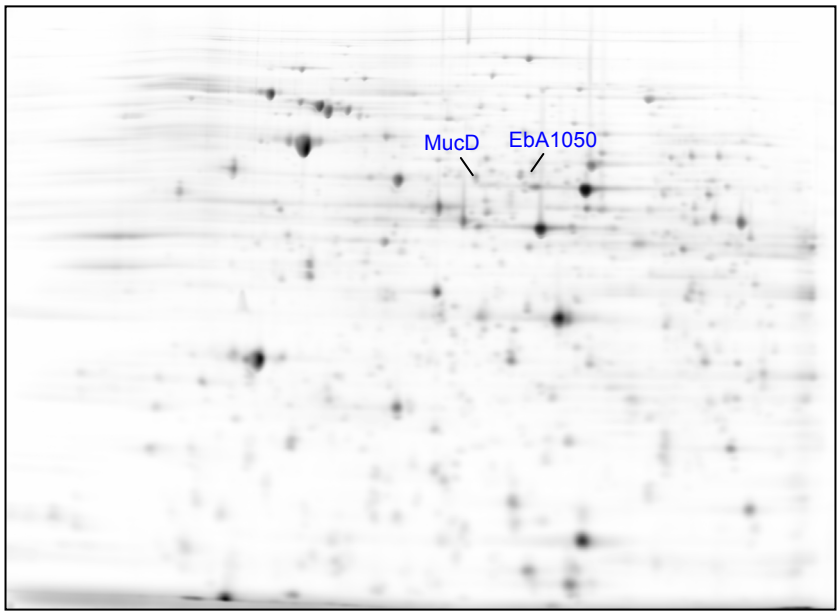


**Fig. 2.3.7.** 2DE gel (pH 4-7) of cells grown anaerobically with benzoate. Identified proteins related to proteases are annotated.

**Table 2.3.7.** Identified proteins related to proteases.

| Orf-No. | Gene | Functional description |
|---|---|---|
| ebA1050 | | Carboxy-terminal processing protease |
| ebA2969 | *mucD* | Putative serine protease |

## 2.4. Cell envelope biosynthesis

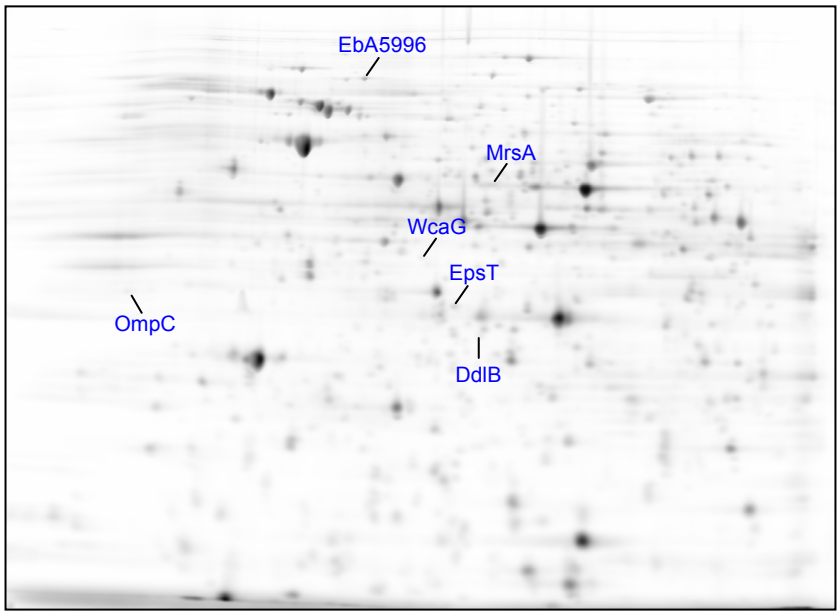


**Fig. 2.4.** 2DE gel (pH 4-7) of cells grown anaerobically with benzoate. Identified proteins related to cell envelope biosynthesis are annotated.

**Table 2.4.** Identified proteins related to cell envelope biosynthesis.

| Orf-No. | Gene | Functional description |
|---|---|---|
| ebA1442 | *ddlB* | D-alanine – D-alanine ligase (D-alanylalanine-synthetase) |
| ebA3999 | *wcaG* | ADP-I-glycero-D-manno-heptose-6-isomerase |
| ebA4244 | *ompC* | Outer membrane protein (porin) |
| ebA4825 | *mrsA* | Phosphoglucomutase and phosphomannomutase family |
| ebA5996 | | Probable outer membrane protein/surface antigen |
| ebA6378 | *epsT* | UTP:α-D-glucose-1-phosphate uridylyltransferase |

### 2.4.1. N-acetylglucosamine and murein synthesis and turnover

The peptidoglycan layer is the main component that enables bacteria to be resistant to osmotic pressure. In the crosslinking reaction of the peptidoglycan precursors, D-alanine plays an important role as bridge molecule. D-alanine, generated by alanine racemase, is a substrate for the D-alanine-D-alanine ligase (**DdlB**). The catalyzed ATP-dependent reaction leads to the dipeptide D-alanine-D-alanine, which is incorporated into the peptidoglycan precursor (Noda et al. 2004).

Phosphoglucomutase (**MrsA**) catalyzes the interconversion of D-glucose 1-phosphate and D-glucose 6-phosphate. This is a central reaction of energy metabolism in all cells and is essential to the synthesis of cell wall polysaccharides in bacterial cells (Lahiri et al. 2002).

UDP-glucose is of central importance in the synthesis of the components of the cell envelope of *E. coli* and in both galactose and trehalose metabolism. The biosynthesis of lipopolysaccharide, capsular polysaccharide and membrane-derived oligosaccharids all require UDP-glucose as a glucosyl donor. The UTP:α-D-glucose-1-phosphate uridylyltransferase (**EpsT**) is predicted to catalyse a reversible reaction converting UTP and glucose-1-phosphate into UDP-glucose and PPi, probably involving the galF gene product (Weissborn et al. 1994; Marolda and Valvano 1996).

### 2.4.2. Lipopolysaccharide synthesis

ADP-L-*glycero*-D-*manno*-heptose 6-epimerase (**WcaG**) is a bacterial enzyme that interconverts the unusual seven-carbon β-linked sugar nucleotides ADP-*β*-L-*glycero*-D-*manno*-heptose and ADP-*β*-D-*glycero*-D-*manno*-heptose. In Gram-negative bacteria this enzyme plays a key role in the biosynthesis of cell surface lipopolysaccharide as it provides the ADP-*β*-L-*glycero*-D-*manno*-heptose that is a component of the inner core tetrasaccharide (Read et al. 2004).

### 2.4.3. Porins and outer membrane proteins

The outer membrane porin **OmpC** is a member of the GMP family. It forms a trimeric porin allowing ions and other hydrophilic solutes to cross the outer membrane (Neidhardt et al. 1996). OmpC is tightly but noncovalently associated with the peptidoglycan layer and the solutes tend to be less than 500 Daltons (Lambert 1988).

## 2.5. Cell division

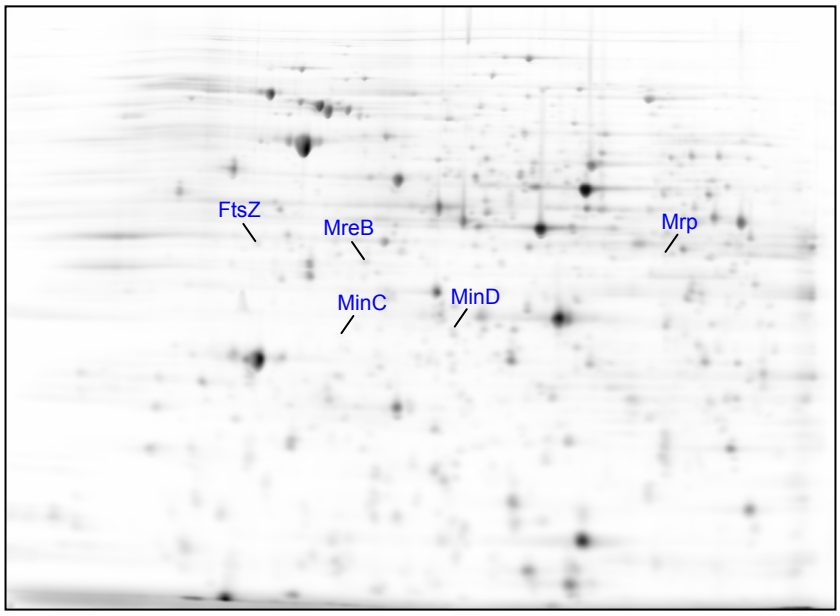


**Fig. 2.5.** 2DE gel (pH 4-7) of cells grown anaerobically with benzoate. Identified proteins related to cell division are annotated.

**Table 2.5.** Identified proteins related to cell division.

| Orf-No. | Gene | Functional description |
|---|---|---|
| ebA1438 | *ftsZ* | Cell division transmembrane protein |
| ebA3033 | *mreB* | Rod shape-determining protein |
| ebA4409 | *mrp* | MRP-ATPases involved in chromosome partitioning |
| ebA6837 | *minC* | Septum site-determining protein |
| ebA6838 | *minD* | Septum site-determining protein |

### 2.5.1. Chromosome partitioning

Plasmids encode partitioning genes (*par*) that are required for accurate plasmid segregation at cell division. These *par*-loci were also identified on bacterial chromosomes. Components encoded by the *par* genes in conjunction with host-encoded factors support directional movement and positioning of newly replicated plasmids and chromosomes (Gerdes et al. 2000).

Two of these genes encode *trans*-acting proteins that form a nucleoprotein complex at the centromere. In all cases one protein is an ATPase which is essential for partitioning. Two types of partitioning ATPases are known, one that contains the Walker-type ATPase motif and one that belongs to the actin/hsp70 superfamily of ATPases. The identified **Mrp** protein comprises a deviant Walker-type ATPase motif; the function is unknown (Gerdes et al. 2000).

### 2.5.2. Cell division

Cell division proceeds via the coordinated growth of all three layers of the cells envelope (cytoplasmatic membrane, peptidoglycan wall and outer membrane). It is mediated by a collection of proteins that localize to the division site, where they appear to assemble into a multiprotein complex – the septal ring (Z ring). The process starts with the polymerisation of the tubuline-like protein **FtsZ** which is highly conserved in almost all bacteria and many archaea. Like tulin, purified FtsZ exhibits GTPase activity and undergoes reversible, GTP-dependent, polymerisation into filaments (Weiss 2004).

Regulation of cell division is accomplished primarily at the level of Z ring assembly. The **MinC** and **MinD** proteins form a complex (MinCD) which binds to FtsZ and prevents Z ring formation (Weiss 2004). At the cell poles, a high concentration of MinCD is maintained and a low concentration at midcell. This leaves the midcell site as the only available location for formation of the division septum (Rothfield et al. 2005).

Bacterial cells possess several different actin-like proteins. The actin ortholog **MreB** has a dual functuion, it is vital for the formation of proper rod shape of the cells, and for regular chromosome segregation. MreB filaments do not form a closed cytoskeleton like structure, but different forms of filaments within a single cell. These filaments can strech along a half turn up to a full turn underneath the membrane, but are not clearly connected with each other. The membrane bound MreC and MreD proteins are required for the formation of proper helical MreB filaments, establishing a link between MreB and the membrane (Defeu Soufo et al. 2005).

An important function of MreB in *Bacillus subtilis* is the positioning of the replication machinery. After depletion of MreB, the replisome loses its central position in the cell, before a change in cell shape is apparent. Therefore it is speculated, that MreB also has a function in DNA movement to the cell poles (Defeu Soufo et al. 2005).

## 2.6. Chemotaxis, motility and secretion

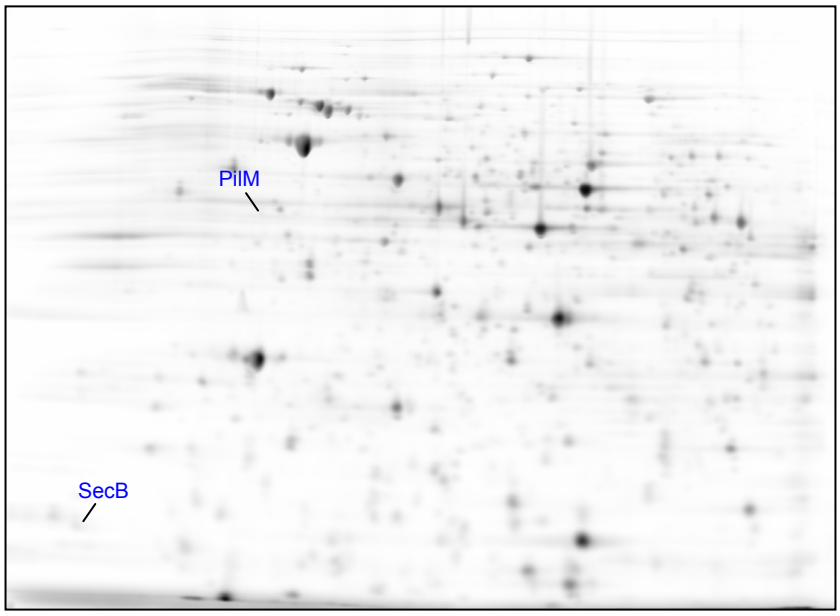


**Fig. 2.6.** 2DE gel (pH 4-7) of cells grown anaerobically with benzoate. Identified proteins related to chemotaxis, motility or secretion are annotated.

**Table 2.6.** Identified proteins related to chemotaxis, motility and secretion.

| Orf-No. | Gene | Functional description |
|---|---|---|
| ebA1056 | *secB* | Protein-export protein |
| ebA2266 | *pilM* | Type IV fimbrial biogenesis protein |

### 2.6.2. Twitching motility

Twitching motility is mediated by type IV pili located at one or both poles of the cell. Type IV pili are typically 5-7 nm in diameter and can extend to several µm in length. Apart from cell movement, functional type IV pili are also required for a wide variety of other processes including transformation, conjugation and bacteriophage infection (Mattick 2002).

Type IV pili are primarily composed of one small protein (PilA or pilin), which is arranged in helical conformation. In *P. aeruginosa* 40 genes have been identified whose products are required for twitching motility. The identified **PilM** contains motifs conserved in the ATP-binding domain of actin and shows homology with the rod-shape determining protein MreB from *E. coli*. This suggests, that the assembly of type IV pili may be linked to cell shape and is possibly directed through PilM to the cell pole (Mattick 2002).

### 2.6.2.3. sec-dependent pathway

**SecB** is a molecular chaperone specialized in the post-translational protein translocation pathway of some Proteobacteria. It binds to newly synthesized precursor polypeptides and stabilizes them in an unfolded and non-aggregated state after they exit from the ribosome translation tunnel. It also delivers these precursors to the membrane-embedded translocon via its specific interaction with SecA, an ATPase, that provides part of the actual energy for translocation (Zhou and Xu 2005).

## 2.7. Transport

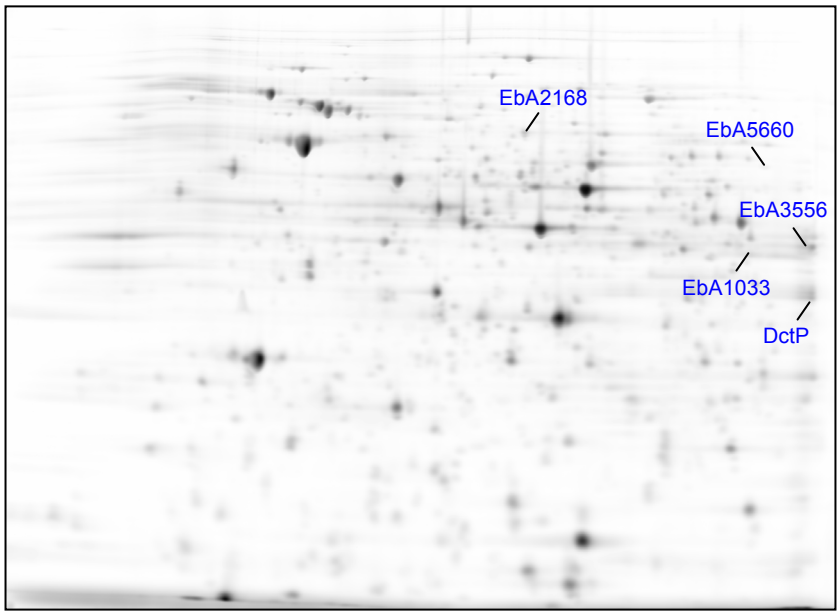


**Fig. 2.7.** 2DE gel (pH 4-7) of cells grown anaerobically with benzoate. Identified proteins related to transport are annotated.

**Table 2.7.** Identified proteins related to transport.

| Orf-No. | Gene | Functional description |
|---|---|---|
| ebA1033 | | Putative exported solute binding portein |
| ebA2168 | | Cation efflux system transmembrane protein |
| ebA3556 | | Putative amino-acid-binding periplasmatic (PBP) ABC transporter protein |
| ebA4994 | *dctP* | Dicarboxylate transport protein |
| ebA5660 | | Probabale ABC-transporter substrate binding protein |

## 2.9. Coenzymes and vitamins

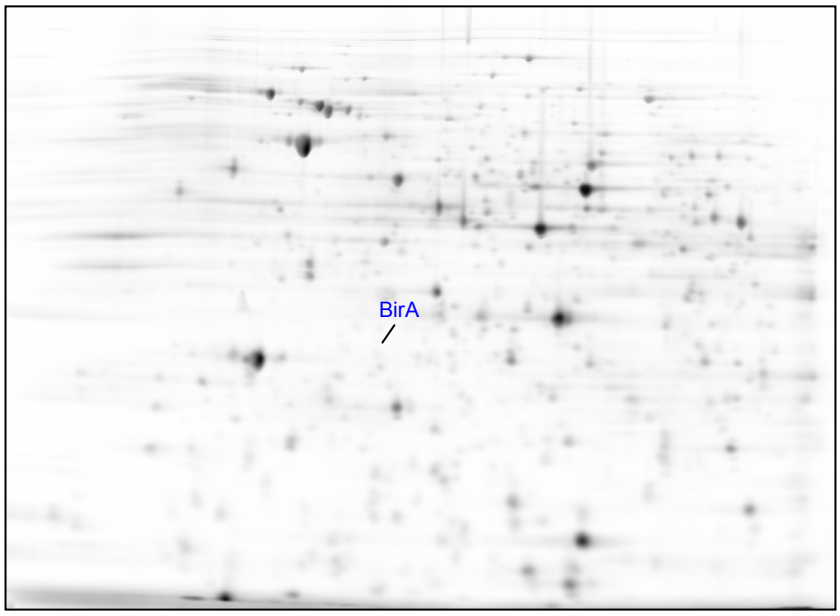


**Fig. 2.9.** 2DE gel (pH 4-7) of cells grown anaerobically with benzoate. Identified proteins related to coenzymes and vitamins are annotated.

**Table 2.9.** Identified proteins related to coenzymes and vitamins.

| Orf-No. | Gene | Functional description |
|---|---|---|
| ebA4113 | *birA* | Probable biotin-acetyl-CoA-carboxylase ligase |

### 2.9.1. Biotin

Biotin is a coenzyme essential to all life forms. It is synthesized by most bacteria and plays vital metabolic roles. But only when covalently bound to a protein. Biotin is covalently attached at the active site of certain enzymes that transfer carbon dioxide from bicarbonate to organic acids to form cellular metabolites. These biotin dependent enzymes have key roles in gluconeogenesis, lipogenesis, amino acid metabolism and energy transduction (Chapman-Smith and Cronan 1999).

**BirA** is a bifunctional protein that exhibits biotin ligase activity and also acts as the DNA binding transcriptional repressor of the biotin operon. The effector of BirA transcriptional repression activity, biotinyl-5'-adenylate, is also a substrate in the BirA-mediated biotinylation of the biotin carboxyl carrier protein monomer (apoBCCP), and this relationship results in repression of the biotin operon when the abundance of apoBCCP (and therefore the cellular demand for biotin) is reduced (Chapman-Smith and Cronan 1999).

# 3. Special degradation pathways

# 3.1. Anaerobic aromatic compound degradation

## 3.1.1. Phenylalanine

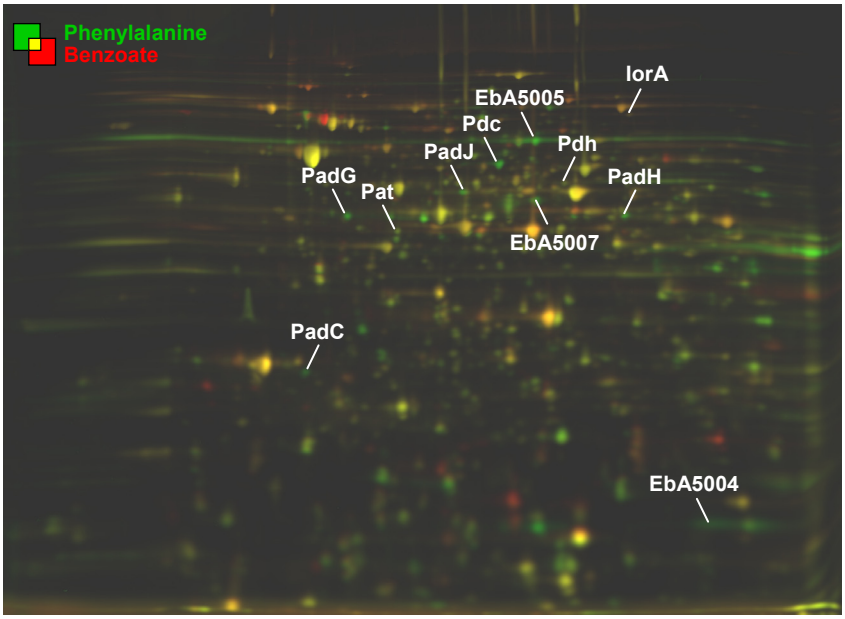


**Fig 3.1.1.1.** Overlay image of 2D DIGE gels (pH 4-7). Protein spots appearing in green are up-regulated when cells were anaerobically grown with phenylalanine. Whereas spots appearing in red are more abundant when cells were anaerobically grown with the reference substrate benzoate. Spots related to anaerobic phenylalanine degradation are annotated.

**Table 3.1.1.** Identified proteins related to anaerobic phenylalanine degradation.

| Orf-No.[a] | Gene[a] | Functional description | Fold change[b] | Share of total protein[b] |
|---|---|---|---|---|
| **Phenylalanine pathway**[c] | | | | |
| ebA122 | *iorA* | Indolepyruvate ferredoxin oxidoreductase, α-subunit | -2.0 | 0.013 |
| ebA596 | *pat* | Aromatic-amino-acid aminotransferase | 1.4 | 0.073 |
| ebA6545 | *pdc* | Probable phenylpyruvate decarboxylase | 27.5 | 0.399 |
| ebA5381 | *pdh* | Probable phenylacetaldehyde dehhydrogenase | -1.4 | 0.015 |
| **Phenylacetate pathway**[c] | | | | |
| ebA5402 | *padJ* | Anaerobic phenylacetate CoA ligase | 9.1 | 0.224 |
| ebA5395 | *padC* | Phenylacetyl-CoA:acceptor oxidoreductase | 14.1 | 0.072 |
| ebA5399 | *padG* | Phenylacetyl-CoA:acceptor oxidoreductase | 16.1 | 0.209 |
| ebA5400 | *padH* | Phenylacetyl-CoA:acceptor oxidoreductase | 6.5 | 0.226 |
| **Proteome prediction** | | | | |
| ebA5004 | | Predicted 4Fe-4S ferredoxin | 49.7 | 0.237 |
| ebA5005 | | Aldehyde:ferredoxin oxidoreductase | 9.7 | 0.370 |
| ebA5007 | *TM0359* | Ferredoxin:NADH oxidoreductase | 6.0 | 0.278 |

[a] listed in order of catalytic activity in the pathway
[b] average ratio and share of total protein (%) are indicated for cells grown anaerobically with phenylalanine
[c] as predicted by genome analysis (Rabus et al. 2005)

## Biochemical background

The degradation of phenylalanine was previously suggested to proceed in analogy to the Ehrlich pathway via transamination and decarboxylation to phenylacetaldehyde and then via dehydrogenation to phenylacetate (Fig. 3.1.1.2.; Schneider et al. 1997, Rabus et al. 2005). The proposed genes *pat* (phenylalanine aminotransferase), *pdc* (phenylpyruvate decarboxylase) and *pdh* (phenylacetaldehyde dehydrogenase) are not organized in an operon-like structure, but rather widely distributed across the chromosome of strain EbN1 (Fig. 3.1.1.2.). The proteomic analysis suggested involvement of EbA5005, most probably supported by EbA5004 and EbA5007, instead of Pdh in the pathway.

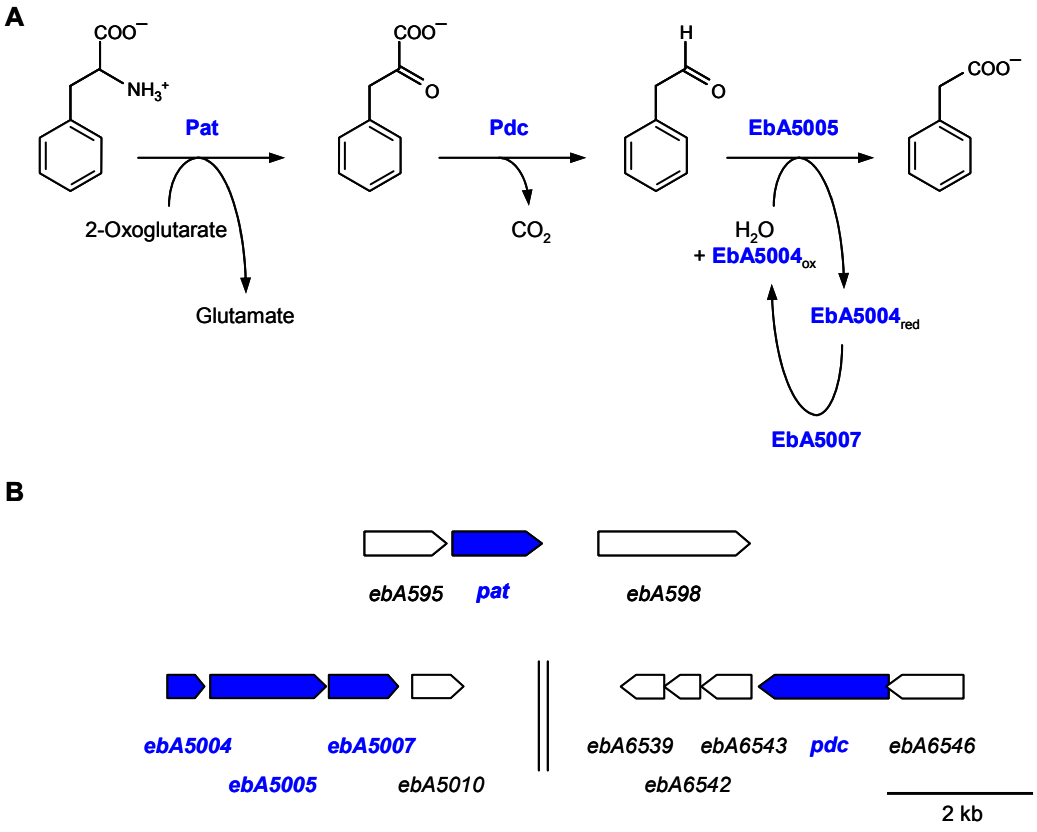


**Fig 3.1.1.2** (**A**) Pathway of anaerobic phenylalanine degradation. Enzyme names of indicated gene products are as described in Rabus et al. 2005. (**B**) Scale model for the organisation of the involved genes. Identified proteins and genes are highlighted in blue (modified from Rabus et al. 2005).

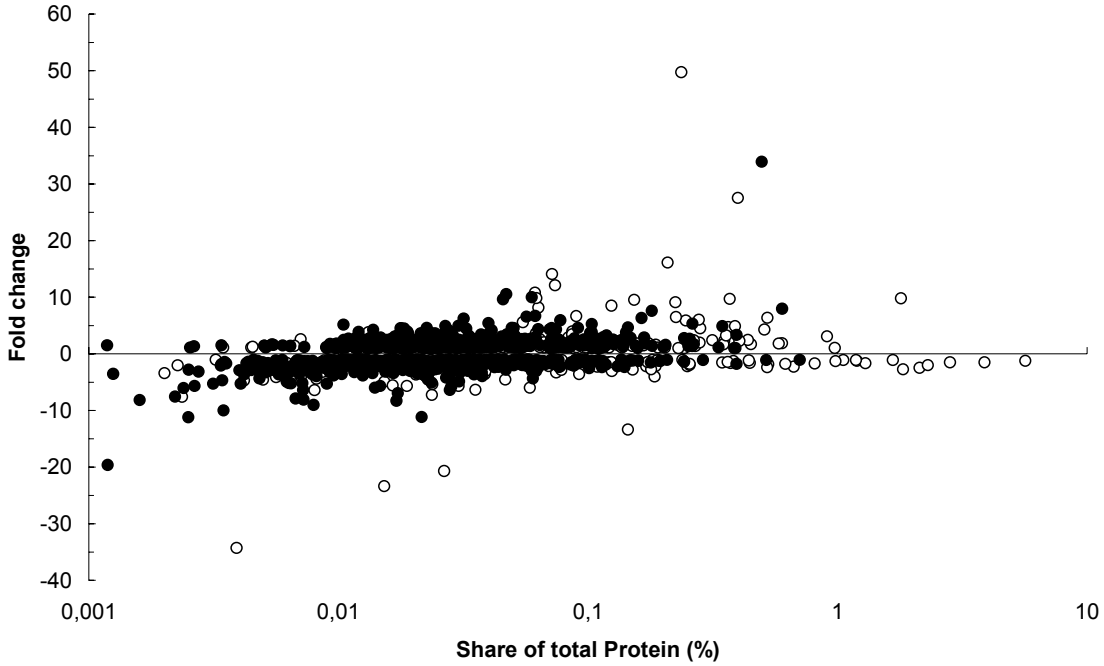


**Fig 3.1.1.3.** Fold changes in protein abundance and their relative share of total protein in cells anaerobically grown with phenylalanine. Each dot represents a spot on the 2D-gel, except for repeatedly identified proteins (fold changes averaged and spot volumes summed up) (○) identified (●) not identified.

## 3.1.2. Phenylacetate

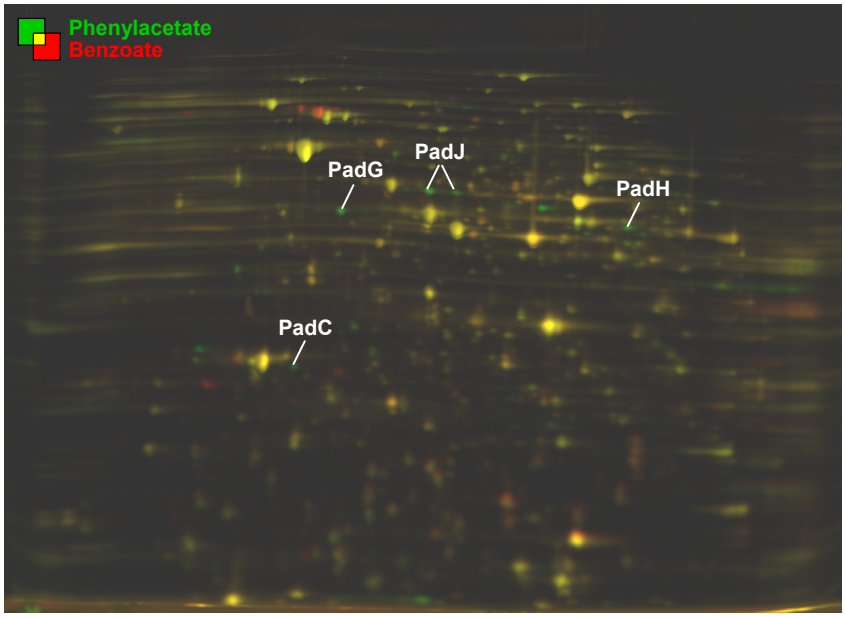


**Fig 3.1.2.1.** Overlay image of 2D DIGE gels (pH 4-7). Protein spots appearing in green are up-regulated when cells were anaerobically grown with phenylacetate. Whereas spots appearing in red are more abundant when cells were anaerobically grown with the reference substrate benzoate. Spots related to anaerobic phenylacetate degradation are annotated.

**Table 3.1.2.** Identified proteins related to anaerobic phenylacetate degradation.

| Orf-No.[a] | Gene [a] | Functional description | Fold change[b] | Share of total protein[b] |
|---|---|---|---|---|
| **Phenylalanine pathway**[c] | | | | |
| ebA122 | *iorA* | Indolepyruvate ferredoxin oxidoreductase, α-subunit | -1.0 | 0.018 |
| ebA596 | *pat* | Aromatic-amino-acid aminotransferase | -1.2 | 0.036 |
| ebA6545 | *pdc* | Probable phenylpyruvate decarboxylase | 2.2 | 0.023 |
| ebA5381 | *pdh* | Probable phenylacetaldehyde dehhydrogenase | -1.9 | 0.009 |
| **Phenylacetate pathway**[c] | | | | |
| ebA5402 | *padJ* | Anaerobic phenylacetate CoA ligase | 5.5 | 0.131 |
| ebA5395 | *padC* | Phenylacetyl-CoA:acceptor oxidoreductase | 15.8 | 0.080 |
| ebA5399 | *padG* | Phenylacetyl-CoA:acceptor oxidoreductase | 29.5 | 0.297 |
| ebA5400 | *padH* | Phenylacetyl-CoA:acceptor oxidoreductase | 10.1 | 0.266 |
| **Proteome prediction** | | | | |
| ebA5004 | | Predicted 4Fe-4S ferredoxin | 1.5 | 0.006 |
| ebA5005 | | Aldehyde:ferredoxin oxidoreductase | 1.0 | 0.018 |
| ebA5007 | *TM0359* | Ferredoxin:NADH oxidoreductase | 10.1 | 0.281 |

[a] listed in order of catalytic activity in the pathway
[b] average ratio and share of total protein (%) are indicated for cells grown anaerobically with phenylacetate
[c] as predicted by genome analysis (Rabus et al. 2005)

## Biochemical background

The phenylacetate degradation pathway was suggested to proceed via activation to phenylacetyl-CoA and subsequent α-oxidation and decarboxylation yielding the central intermediate benzoyl-CoA (Mohammed and Fuchs 1993, Rhee and Fuchs 1999). Genes encoding the involved enzymes *padJ* (phenylacetate-CoA ligase), *padBCD* (phenylacetyl-CoA:acceptor oxidoreductase) and *padEFGHI* (phenylglyoxylate:acceptor oxidoreductase) form an operon on the chromosome of strain EbN1 (Fig. 3.1.2.2.). Four protein subunits (PadJ, PadC, PadG and PadH) were identified and specifically increased in abundance during anaerobic growth with phenylacetate and phenylalanine.

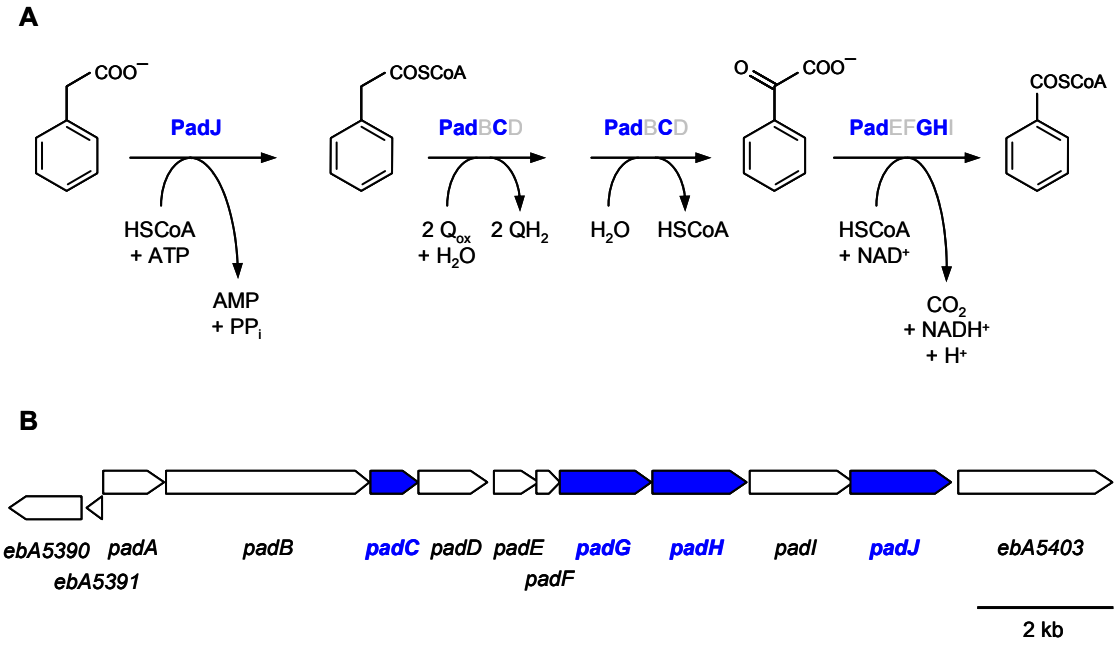


**Fig 3.1.2.2** (**A**) Pathway of anaerobic phenylacetate degradation. Enzyme names of indicated gene products are as described in Rabus et al. 2005. (**B**) Scale model for the organisation of the involved genes. Identified proteins and genes are highlighted in blue (modified from Rabus et al. 2005).

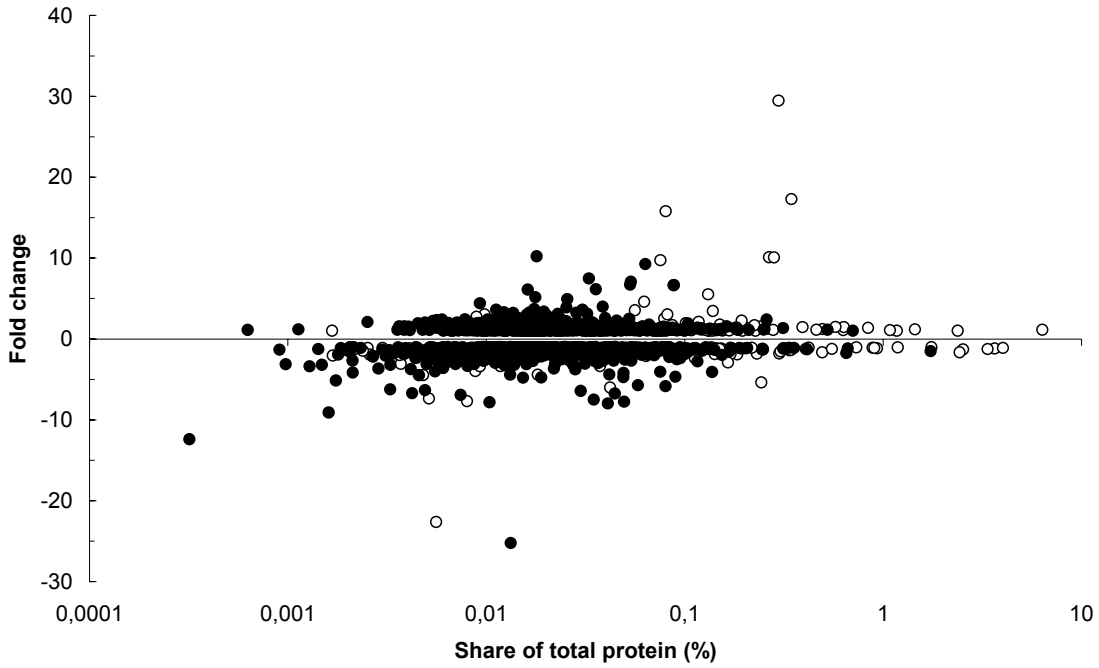


**Fig 3.1.2.3.** Fold changes in protein abundance and their relative share of total protein in cells anaerobically grown with phenylacetate. Each dot represents a spot on the 2D-gel, except for repeatedly identified proteins (fold changes averaged and spot volumes summed up) (○) identified (●) not identified.

## 3.1.3.1. Benzyl alcohol

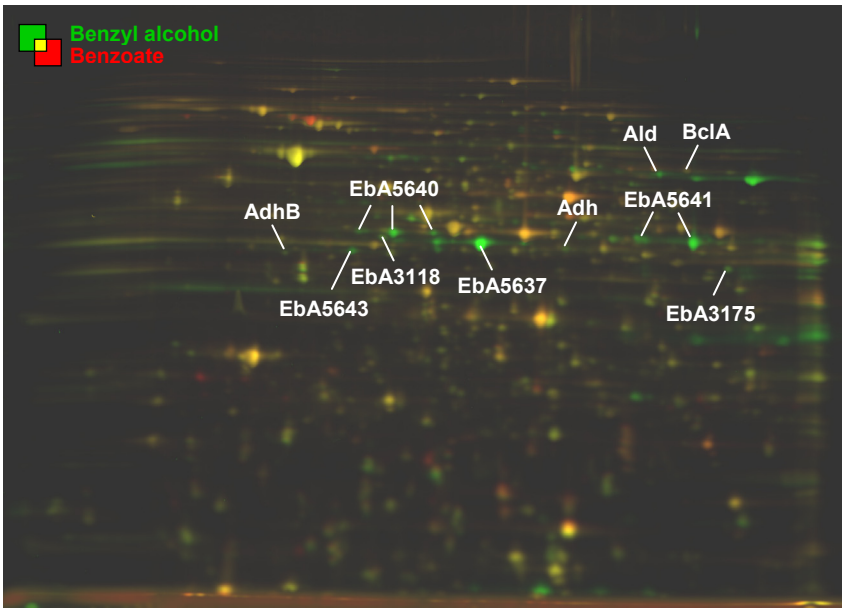


**Fig 3.1.3.1.** Overlay image of 2D DIGE gels (pH 4-7). Protein spots appearing in green are up-regulated when cells were anaerobically grown with benzyl alcohol. Whereas spots appearing in red are more abundant when cells were anaerobically grown with the reference substrate benzoate. Spots related to anaerobic benzyl alcohol degradation are annotated.

**Table 3.1.3.1.** Identified proteins related to anaerobic benzyl alcohol degradation

| Orf-No.[a] | Gene [a] | Functional description | Fold change[b] | Share of total protein[b] |
|---|---|---|---|---|
| **Benzyl alcohol pathway**[c] | | | | |
| ebA3166 | *adh* | Benzyl alcohol dehydrogenase | 1.5 | 0.059 |
| ebA4623 | *adhB* | Alcohol dehydrogenase II | 3.0 | 0.032 |
| **Benzaldehyde pathway**[c] | | | | |
| ebA5642 | *ald* | Putative benzaldehyde dehydrogease | 37.3 | 0.305 |
| ebA5301 | *bclA* | Benzoate CoA-ligase | -1.7 | 0.062 |
| **Proteome prediction** | | | | |
| ebA3118 | | Alcohol dehydrogenase (Zn-containing) | 5.5 | 0.129 |
| ebA3175 | | Putative amino acid ABC transporter | 5.7 | 0.084 |
| ebA5637 | | Mandelate racemase/muconate lactonizing enzyme family | 144.5 | 0.398 |
| ebA5640 | | Acyl-CoA transferase, family III | 45.7 | 0.050 |
| ebA5641 | | Acyl-CoA dehydrogenase | 22.4 | 0.303 |
| ebA5643 | | Acyl-CoA transferase, family III | 49.6 | 0.205 |

[a] listed in order of catalytic activity in the pathway
[b] average ratio and share of total protein (%) are indicated for cells grown anaerobically with benzyl alcohol
[c] as predicted by genome analysis (Rabus et al. 2005)

## Biochemical background

Anaerobic degradation of benzyl alcohol is predicted to proceed via benzaldehyde to benzoate, catalyzed by the respective dehydrogenases as known from other bacteria (MacKintosh and Fewson 1988; Chalmers et al. 1991). Analysis of the strain EbN1 genome suggested the presence of various dehydrogenases for aromatic alcohols and aldehydes (rabus et al. 2005).

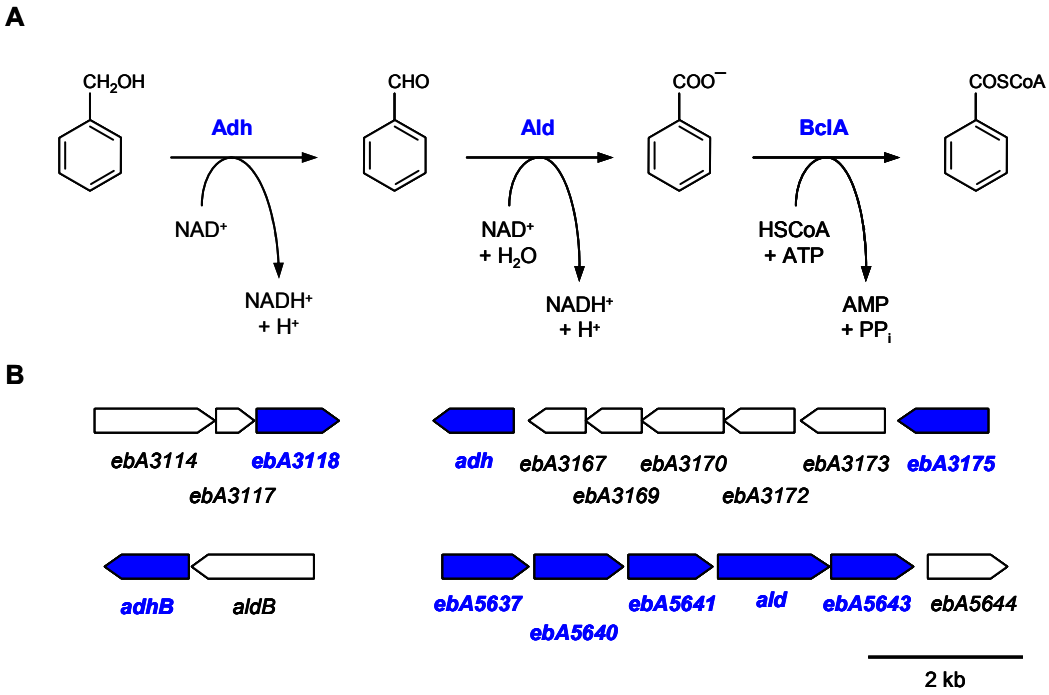


**Fig 3.1.3.2** (**A**) Pathway of anaerobic benzyl alcohol and benzaldehyde degradation. Enzyme names of indicated gene products are as described in Rabus et al. 2005. (**B**) Scale model for the organisation of the involved genes. Identified proteins and genes are highlighted in blue (modified from Rabus et al. 2005).

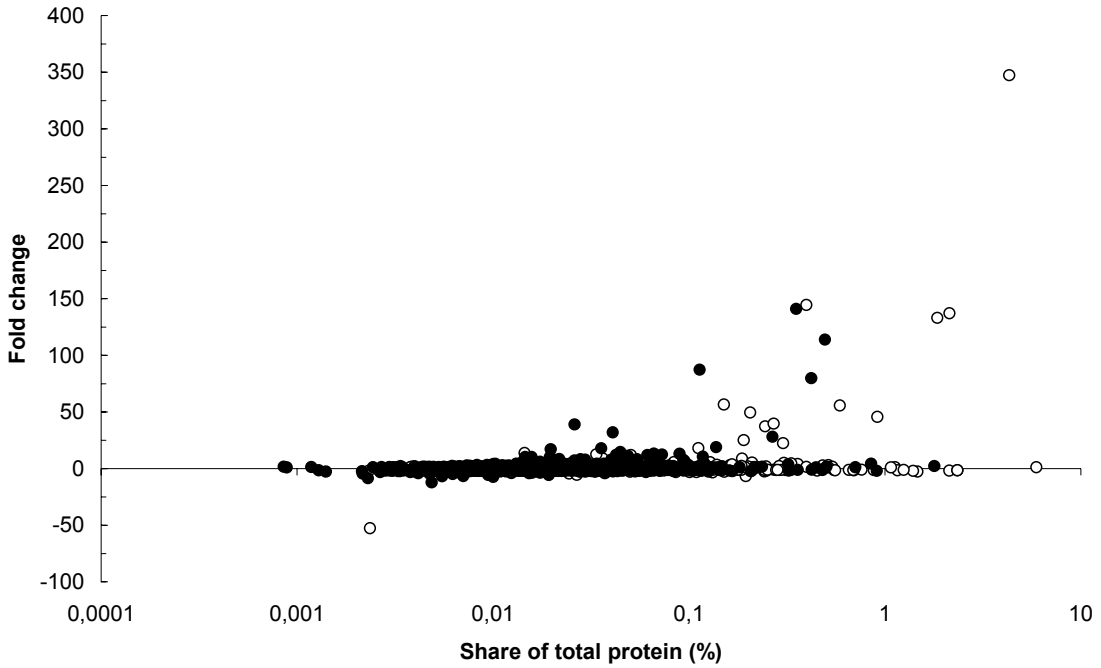


**Fig 3.1.3.3.** Fold changes in protein abundance and their relative share of total protein in cells anaerobically grown with benzyl alcohol. Each dot represents a spot on the 2D-gel, except for repeatedly identified proteins (fold changes averaged and spot volumes summed up) (○) identified (●) not identified.

## 3.1.3.2. Benzaldehyde

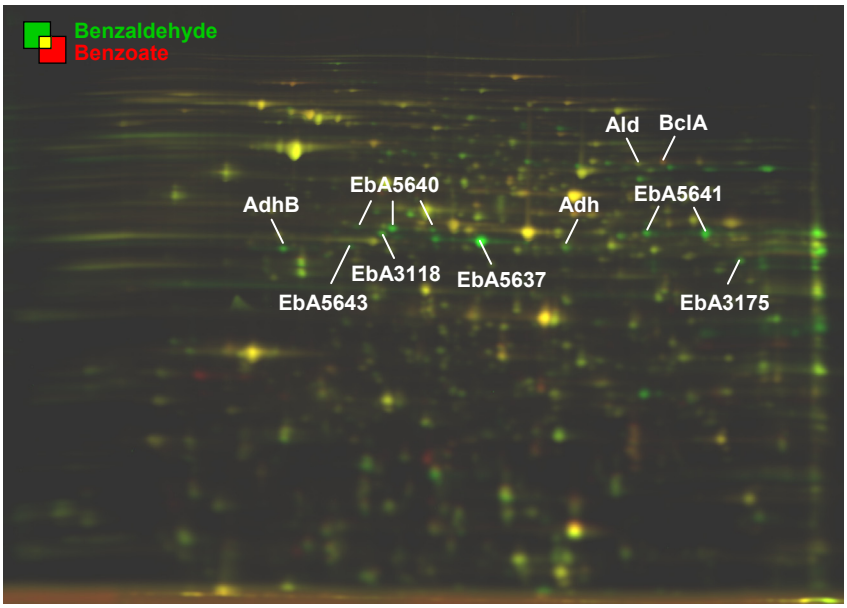


**Fig 3.1.3.4.** Overlay image of 2D DIGE gels (pH 4-7). Protein spots appearing in green are up-regulated when cells were anaerobically grown with benzaldehyde. Whereas spots appearing in red are more abundant when cells were anaerobically grown with the reference substrate benzoate. Spots related to anaerobic benzaldehyde degradation are annotated.

**Table 3.1.3.2.** Identified proteins related to anaerobic benzaldehyde degradation

| Orf-No.[a] | Gene [a] | Functional description | Fold change[b] | Share of total protein[b] |
|---|---|---|---|---|
| **Benzyl alcohol pathway**[c] | | | | |
| ebA3166 | *adh* | Benzyl alcohol dehydrogenase | 2.3 | 0.193 |
| ebA4623 | *adhB* | Alcohol dehydrogenase II | 16.4 | 0.230 |
| **Benzaldehyde pathway**[c] | | | | |
| ebA5642 | *ald* | Putative benzaldehyde dehydrogease | 10.8 | 0.156 |
| ebA5301 | *bclA* | Benzoate CoA-ligase | -2.6 | 0.050 |
| **Proteome prediction** | | | | |
| ebA3118 | | Alcohol dehydrogenase (Zn-containing) | 7.8 | 0.220 |
| ebA3175 | | Putative amino acid ABC transporter | 7.3 | 0.161 |
| ebA5637 | | Mandelate racemase/muconate lactonizing enzyme family | 66.2 | 0.238 |
| ebA5640 | | Acyl-CoA transferase, family III | 16.3 | 0.015 |
| ebA5641 | | Acyl-CoA dehydrogenase | 16.6 | 0.226 |
| ebA5643 | | Acyl-CoA transferase, family III | 15.6 | 0.065 |

[a] listed in order of catalytic activity in the pathway
[b] average ratio and share of total protein (%) are indicated for cells grown anaerobically with benzaldehyde
[c] as predicted by genome analysis (Rabus et al. 2005)

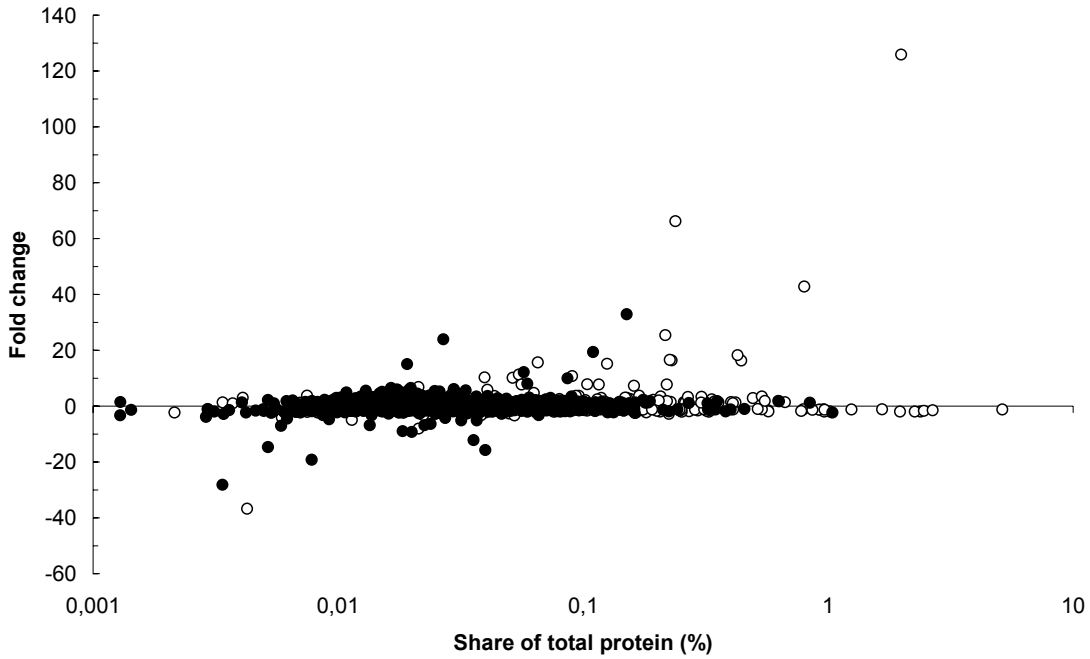


**Fig 3.1.3.5.** Fold changes in protein abundance and their relative share of total protein in cells anaerobically grown with benzaldehyde. Each dot represents a spot on the 2D-gel, except for repeatedly identified proteins (fold changes averaged and spot volumes summed up) (○) identified (●) not identified.

## 3.1.3.3. Regulation of the benzyl alcohol and benzaldehyde pathway

In the genome sequence of strain EbN1, two benzyl alcohol dehydrogenases (*adh* and *adhB*) and two benzaldehyde dehydrogenases (*ald* and *aldB*) were identified and *adh* and *ald* predicted to be involved in the pathway (Rabus et al. 2005). However, Adh did not display a significant increase in abundance at all, suggesting no function in the benzyl alcohol pathway. In contrast, the iron containing AdhB revealed an increased abundance in benzyl alcohol and benzaldehyde grown cells (3.0-fold and 16.4-fold respectively), but also in cells grown with *p*-cresol, phenol, *p*-hydroxybenzoate and *o*-aminobenzoate (3.0- to 7.8-fold) which might indicate a more general function. Interestingly, another predicted Zn-containing alcohol dehydrogenase (EbA3118) was specifically increased in abundance with benzyl alcohol and benzaldehyde (5.5- and 7.8-fold, respectively) and only slightly with phenylalanine (2.9-fold). In *Acinetobacter calcoaceticus* and *Pseudomonas putida* the dehydrogenation of benzyl alcohol is catalyzed by Zn-containing dehydrogenases which are induced by both benzyl alcohol and benzaldehyde (Chalmers et al. 1991; Gillooly et al. 1998). Furthermore, sequence similarity of EbA3118 with the known benzyl alcohol dehydrogenases from *A. calcoaceticus* and *P. putida* (see Tab. 3.1.3.3.) suggests an involvement of EbA3118 rather than AdhB in the pathway.

The *ald* gene product was increased in abundance in both benzyl alcohol and benzaldehyde grown cells (37.3-fold and 10.8-fold, respectively) and also in *p*-cresol and phenol grown cells (20.9- and 8.5-fold) providing no clear evidence for its involvement in benzaldehyde oxidation. In contrast to *adh* and *ald*, which are located at different sites of

the chromosome, *adhB* and *aldB* form an operon-like structure analogous to genes encoding benzyl alcohol dehydrogenase and benzaldehyde dehydrogenase in *A. calcoaceticus* (Fig 3.1.3.6.; Gillooly et al. 1998). The unidentified AldB possesses a theoretical isoelectric point of 6.4 and a molecular weight of 55 kDa, being in the analyzed pI- and mass range. Concerning benzyl alcohol as well as benzaldehyde grown cells, none of the significantly increased, unidentified protein spots possesses these attributes, presuming no increased abundance of AldB and therefore most likely no involvement in the benzyl alcohol pathway of strain EbN1.

**Table 3.1.3.3.** Sequence similarities (%) of predicted benzyl alcohol dehydrogenases from strain EbN1 with benzyl alcohol dehydrogenases from *Acinetobacter calcoaceticus* (XylB[a]) and *Pseudomonas putida* (XylB[b]).

| Strain EbN1 | *A. calcoaceticus* | | *P. putida* | |
|---|---|---|---|---|
| | identity | positives | identity | positives |
| EbA3118 | 26 | 40 | 26 | 40 |
| Adh (EbA3166) | 51 | 68 | 49 | 68 |
| AdhB (EbA4623) | n.s.[c] | n.s.[c] | n.s.[c] | n.s.[c] |

[a] gi1408294
[b] gi18077189
[c] no significant similarities

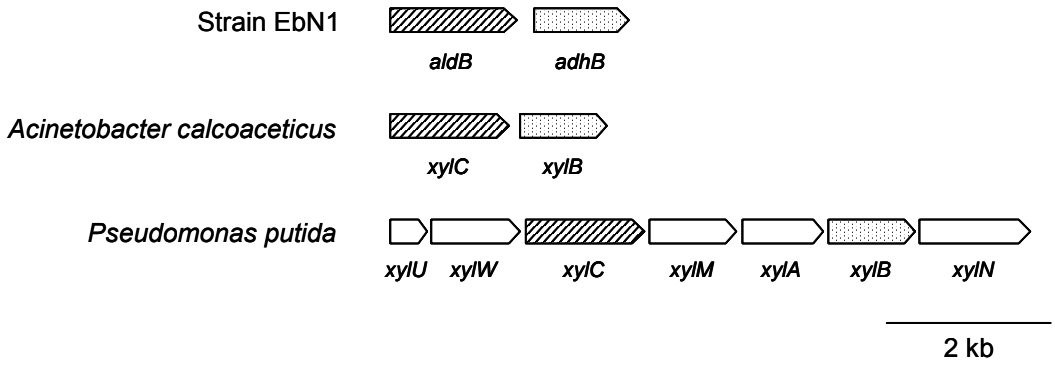


**Fig. 3.1.3.6.** Comparison of the genetic organisation of benzyl alcohol dehydrogenases (dottet) and benzaldehyde dehydrogenases (hatched) encoding genes of strain EbN1, *Acinetobacter calcoaceticus* and *Pseudomonas putisa*. (Gillooly et al. 1998; Greated et al. 2002; Rabus et al. 2005).

### 3.1.3.4. Induction of mandelate-racemase during growth with benzyl alcohol and benzaldehyde

Mandelic acid is an aromatic $\alpha$-hydroxy acid of plant origin, whose D-(-)- and L-(+)-isomers occur naturally (Carles and Bourget 1957). The degradative pathway, proceeding via L-(+)-mandelate, benzylformate, benzaldehyde, benzoate and catechol, is well studied in *P. putida* and *A. calcoaceticus* and also known for other genera (Fig. 3.1.3.7.; Cook et al. 1975; Hegemann 1966). In *P. putida* the genes for mandelate degradation are organized in an operon, except for the benzaldehyde dehydrogenase I, being in close proximity, but transcribed in opposite direction (Fig 3.1.3.7.; McLeish et al. 2003; Tsou et al. 1990). However, all five enzymes of the pathway are coordinately regulated and are induced by D-(-)-mandelate, L-(+)-mandelate or benzylformate (Hegemann 1966; Rosenberg 1971). In *A. calcoaceticus* the pathway-genes are only induced by L-(+)-mandelate and benzylformate, since the bacteria do not possess a mandelate racemase (Kennedy and Fewson 1968). Benzaldehyde does not induce the mandelate pathway in neither of the two organisms, other benzaldehyde dehydrogenases as well as benzyl alcohol dehydrogenases being induced utilizing benzaldehyde (Livingstone and Fewson 1971; Rosenberg 1971).

Strain EbN1 is not able to use either of the mandelate isomers as sole source of carbon and energy with or without oxygen (data not shown). This inability is supported by the lack of genes for mandelate dehydrogenase and benzylformate dehydrogenase in the genome sequence (Rabus et al. 2005). In addition, the genetic neighborhood, including acyl-CoA transferases and dehydrogenases, is quite different to *P. putida* (Fig. 3.1.3.7.). Therefore, the induction of the mandelate racemase and its complete operon appears to be non specific. This might also be true concerning induction by *p*-cresol, since the enzymes of the mandelate pathway also oxidize *p*-hydroxymandelate yielding *p*-hydroxybenzoate (Kennedy and Fewson 1968).

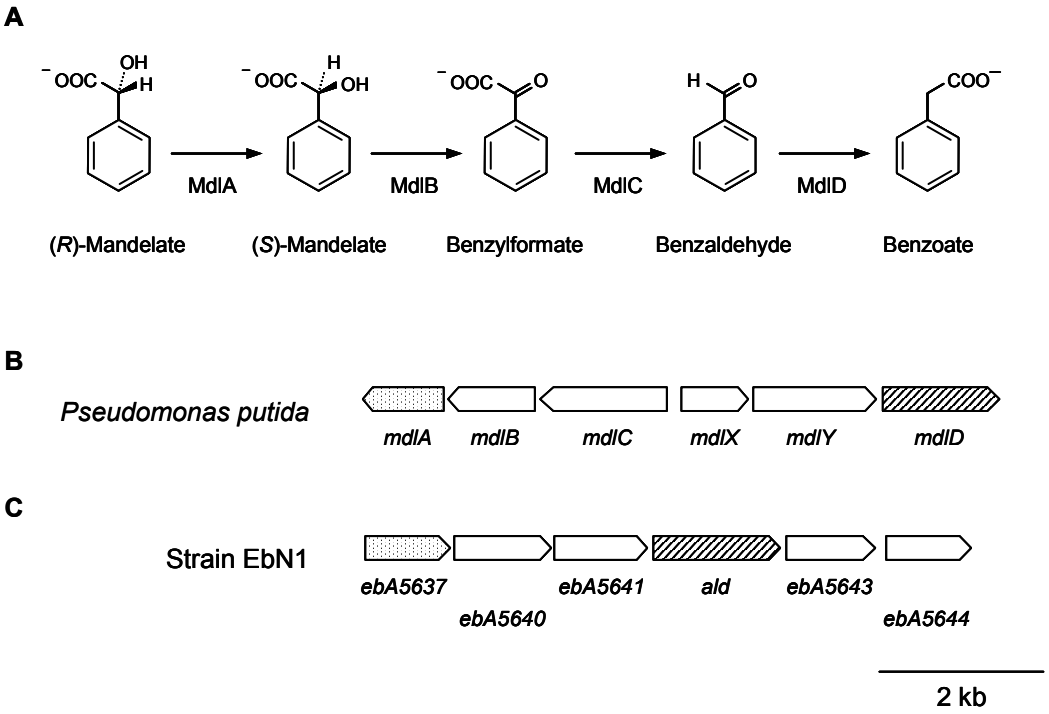


**Fig. 3.1.3.7.** (A) Mandelate degradation pathway of *Pseudomonas putida* and (B) scale model of the involved genes. Enzyme names of indicated gene products are as follows: MdlA, mandelate racemase; MdlB, (*S*)-mandelate dehydrogenase; MdlC, benzoylformate decarboxylase; MdlD, benzaldehyde dehydrogenase (adapted from Tsou et al. 1990). (C) Genetic neighborhood of the mandelate racemase encoding gene of strain EbN1. Gene names and Orf numbers are as described (Rabus et al. 2005). Mandelate racemase is indicated by dots, benzaldehyde dehydrogenase genes are hatched.

## 3.1.4. *p*-Cresol

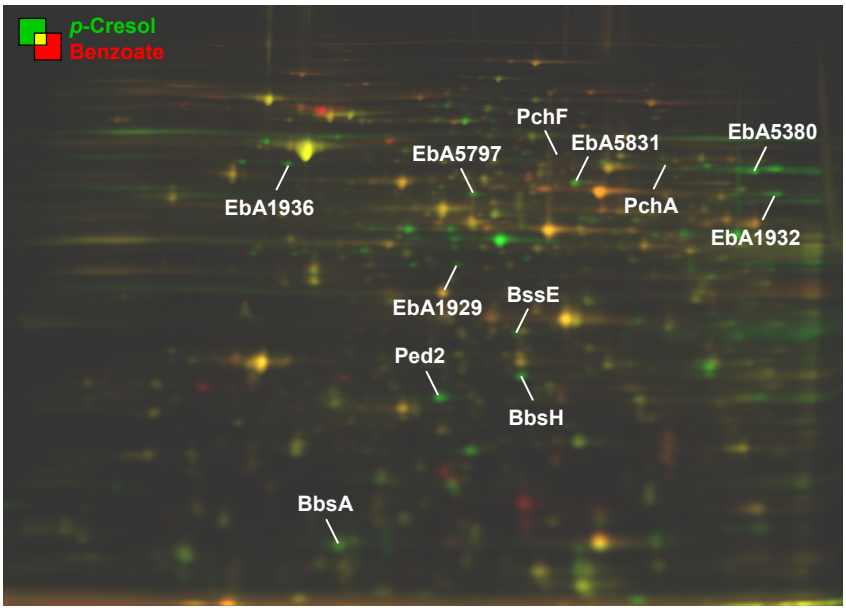


**Fig 3.1.4.1.** Overlay image of 2D DIGE gels (pH 4-7). Protein spots appearing in green are up-regulated when cells were anaerobically grown with *p*-cresol. Whereas spots appearing in red are more abundant when cells were anaerobically grown with the reference substrate benzoate. Spots related to anaerobic *p*-cresol degradation are annotated.

**Table 3.1.4.** Identified proteins related to anaerobic *p*-cresol degradation.

| Orf-No.[a] | Gene [a] | Functional description | Fold change[b] | Share of total protein[b] |
|---|---|---|---|---|
| ***p*-Cresol pathway**[c] | | | | |
| ebA3165 | *pchF* | Benzyl alcohol dehydrogenase | 1.1 | 0.008 |
| ebA3161 | *pchA* | Alcohol dehydrogenase II | 1.2 | 0.014 |
| **Toluene pathway and related genes**[c] | | | | |
| c2A306 | *bssE* | Chaperone | 10.6 | 0.094 |
| c2A316 | *bbsA* | Subunit of benzoylsuccinyl-CoA thiolase | 6.8 | 0.473 |
| c2A309 | *bbsH* | Putative E-phenylitaconyl-CoA hydratase | 57.0 | 0.396 |
| ebA1929 | | Conserved hypothetical protein | 11.9 | 0.053 |
| ebA1932 | | Conserved hypothetical protein | 60.9 | 0.543 |
| ebA1936 | | Conserved hypothetical protein | 72.7 | 0.138 |
| **Paralogous ethylbenzene pathway**[c] | | | | |
| ebA5789 | *ped2* | Predicted (*S*)-1-phenylethanol dehydrogenase | 235.4 | 0.626 |
| ebA5797 | | Predicted thiolase | 12.1 | 0.216 |
| **Proteome prediction** | | | | |
| ebA5380 | | Predicted *p*-cresol methylhydroxylase | 352.2 | 0.732 |
| ebA5381 | *pdh* | Putative p-hydroxybenzaldehyde dehydrogenase | 7.4 | 0.431 |

[a] listed in order of catalytic activity in the pathway
[b] average ratio and share of total protein (%) are indicated for cells grown anaerobically with *p*-cresol
[c] as predicted by genome analysis (Rabus et al. 2005)

## Biochemical background

Anaerobic oxidation of *p*-cresol via *p*-hydroxybenzaldehyde to *p*-hydroxybenzoate has been intensively studied in *Pseudomonas putida* as well as in several *Thauera* and *Azoarcus* strains (Hopper and Taylor 1977; Rudolphi et al. 1991). Corresponding genes for *p*-cresol methylhydroxylase (*pchCF*) and *p*-hydroxybenzaldehyde dehydrogenase (*pchA*), were also predicted for strain EbN1 (Rabus et al. 2005). PchA and PchF could be identified in the present proteomic study. However, they did not display significant increases in abundance during anaerobic growth with *p*-cresol. The proteomic analysis indicated involvement of EbA5380 and EbA5381 instead of PchCF and PchF.

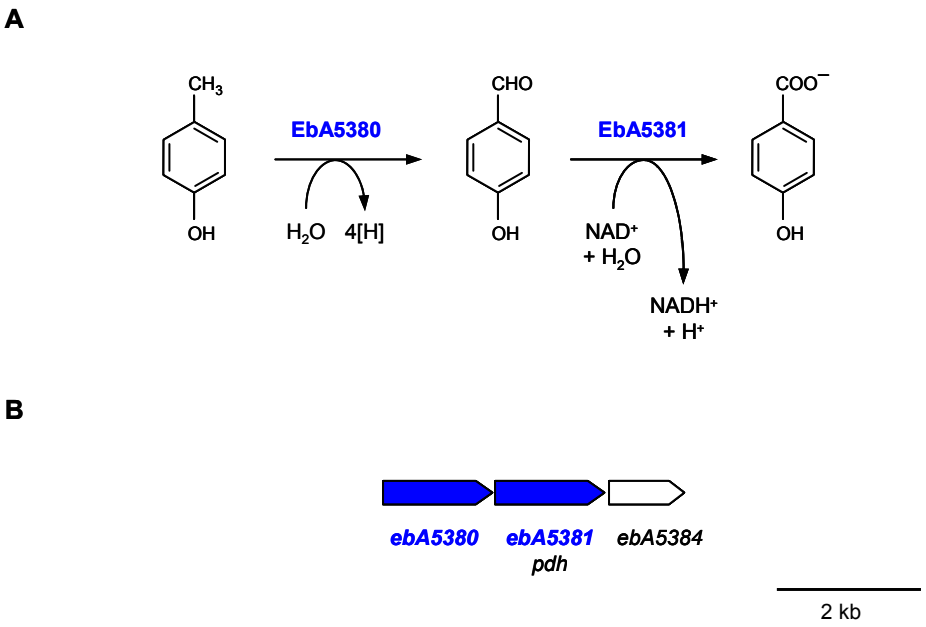


**Fig 3.1.4.2** (**A**) Pathway of anaerobic *p*-cresol degradation. Enzyme names of indicated gene products are as described in Rabus et al. 2005. (**B**) Scale model for the organisation of the involved genes. Identified proteins and genes are highlighted in blue (modified from Rabus et al. 2005).

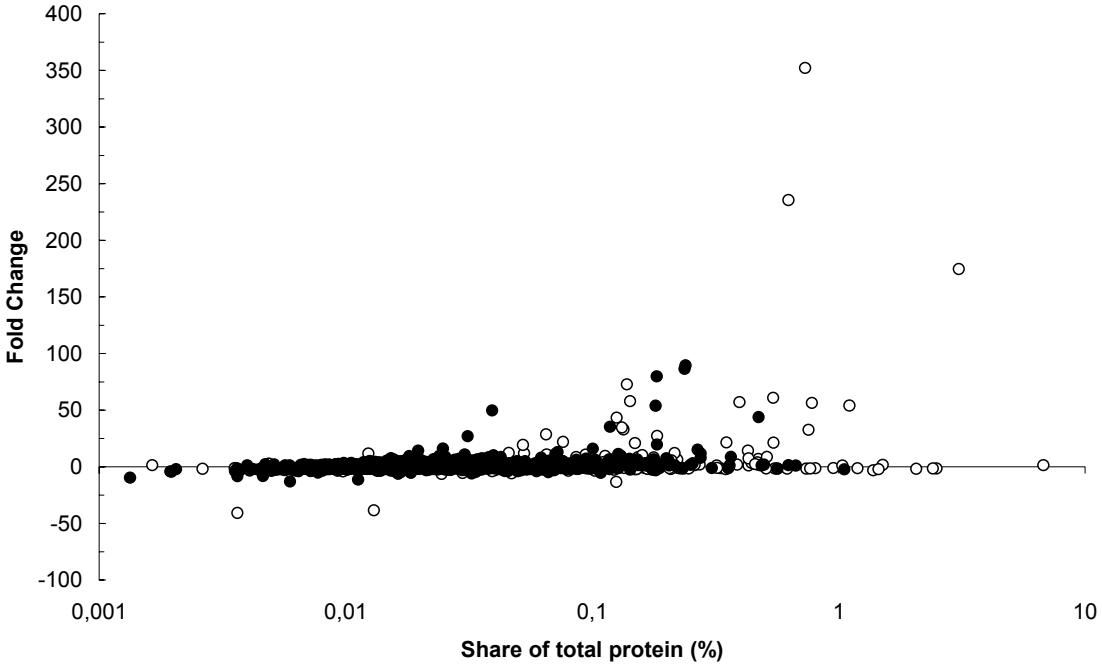


**Fig 3.1.4.3.** Fold changes in protein abundance and their relative share of total protein in cells anaerobically grown with *p*-cresol. Each dot represents a spot on the 2D-gel, except for repeatedly identified proteins (fold changes averaged and spot volumes summed up) (○) identified (●) not identified.

## 3.1.5. Phenol

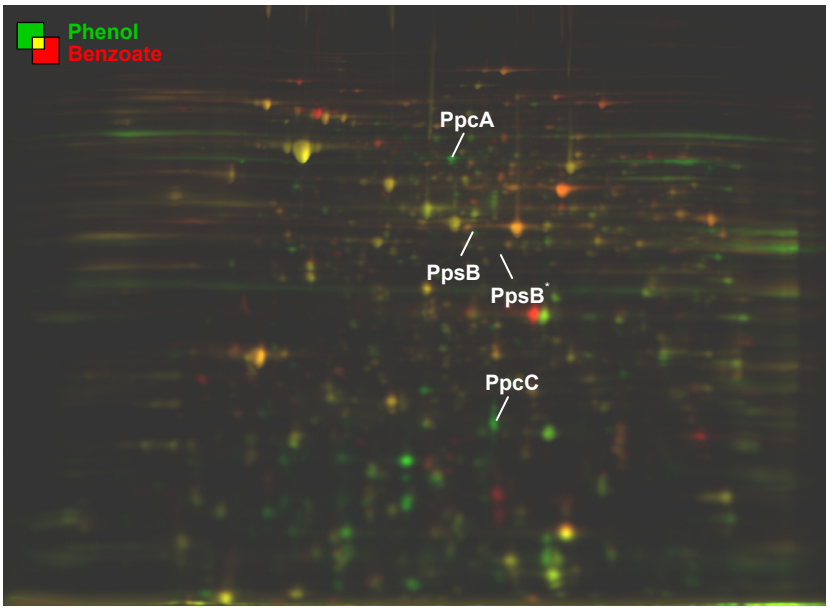


**Fig 3.1.5.** Overlay image of 2D DIGE gels (pH 4-7). Protein spots appearing in green are up-regulated when cells were anaerobically grown with phenol. Whereas spots appearing in red are more abundant when cells were anaerobically grown with the reference substrate benzoate. Spots related to anaerobic phenol degradation are annotated (PpsB* represents EbA5783).

**Table 3.1.5.** Identified proteins related to anaerobic phenol degradation.

| Orf-No.[a] | Gene [a] | Functional description | Fold change[b] | Share of total protein[b] |
|---|---|---|---|---|
| **Phenol pathway**[c] | | | | |
| ebA3143 | *ppsB* | Phenylphosphate synthase β-subunit | 3.6 | 0.068 |
| ebA5783 | *ppsB* | Similar to subunit B of phenylphosphate synthetase or Phenoylpyruvate synthase | 1.9 | 0.006 |
| ebA3138 | *ppcA* | Phenylphosphate carboxylase, α-subunit | 81.0 | 0.355 |
| ebD6 | *ppcC* | Phenylphosphate carboxylase, γ-subunit | 120.3 | 0.663 |

[a] listed in order of catalytic activity in the pathway
[b] average ratio and share of total protein (%) are indicated for cells grown anaerobically with phenol
[c] as predicted by genome analysis (Rabus et al. 2005)

## Biochemical background

In *Thauera aromatica*, the initial reactions of anaerobic phenol degradation involve activation to phenylphosphate followed by a carboxylation to *p*-hydroxybenzoate (Schmeling et al. 2004; Schühle and Fuchs 2004). Genes encoding these enzymes, phenylphosphate synthase (*ppsABC*) and phenylphosphate carboxylase (*ppcABCD*), are clustered with other genes of unknown function (Breinig et al. 2000). An orthologous and similarly organized ″phenol″ gene cluster was also identified in the genome of strain EbN1. At a different chromosomal position, strain EbN1 also possesses *ppsAB* paralogs (*ebA5781* and *ebA5783*) co-localized with carboxylase encoding genes in an operon-like structure (Rabus et al. 2005).

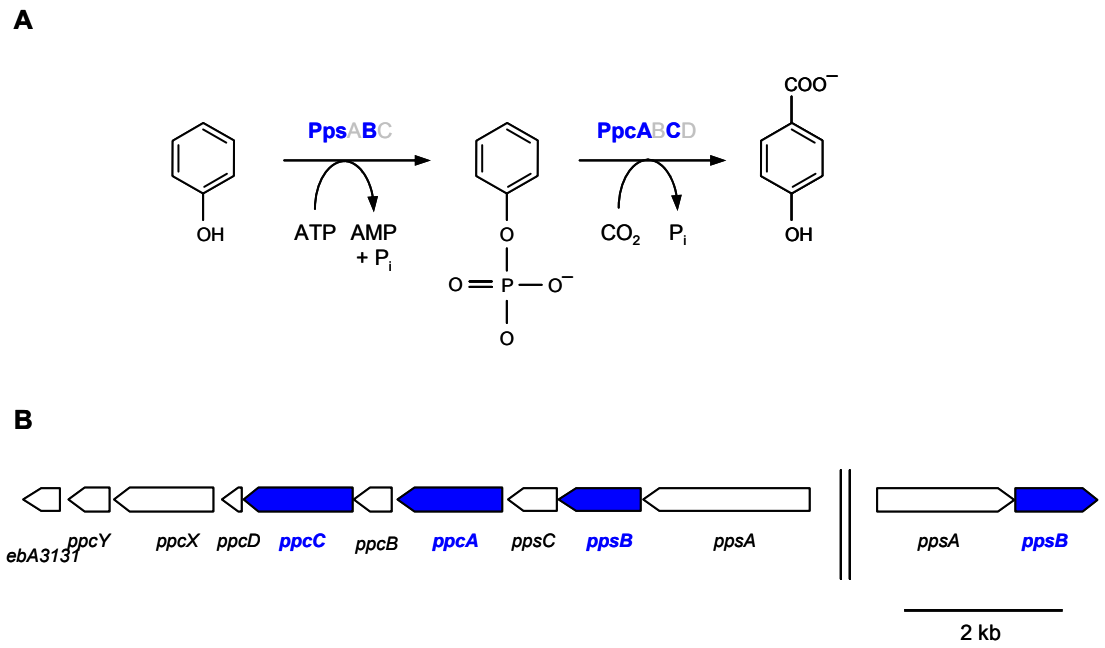


**Fig 3.1.5.2** (**A**) Pathway of anaerobic phenol degradation. Enzyme names of indicated gene products are as described in Rabus et al. 2005. (**B**) Scale model for the organisation of the involved genes. Identified proteins and genes are highlighted in blue (modified from Rabus et al. 2005).

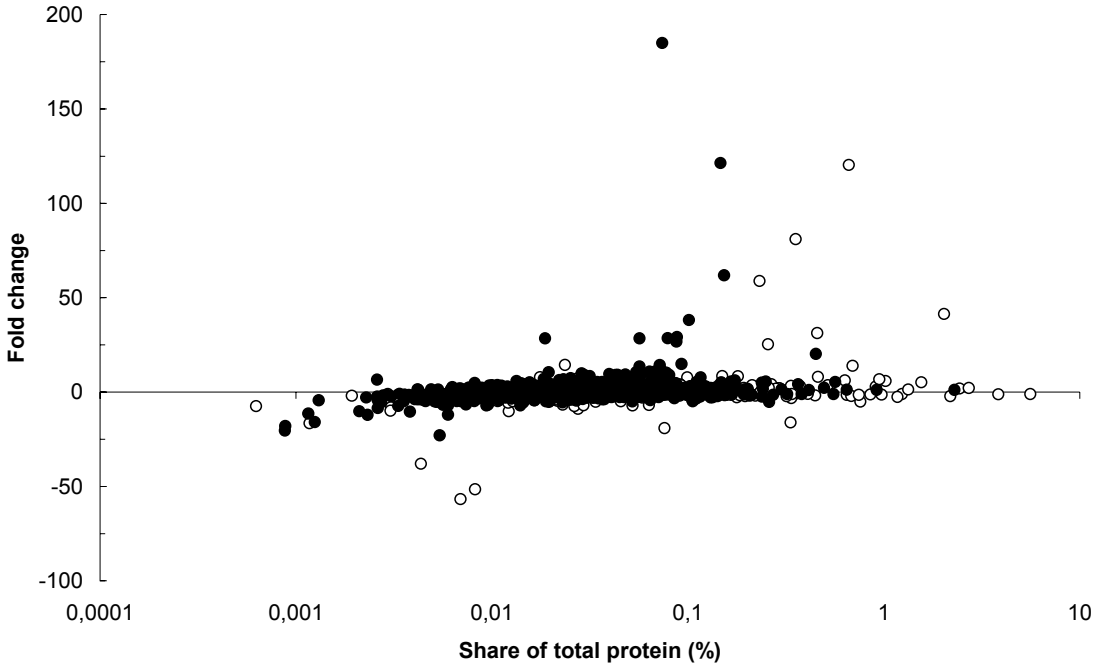


**Fig 3.1.5.3.** Fold changes in protein abundance and their relative share of total protein in cells anaerobically grown with phenol. Each dot represents a spot on the 2D-gel, except for repeatedly identified proteins (fold changes averaged and spot volumes summed up) (○) identified (●) not identified.

## 3.1.6. *p*-Hydroxybenzoate

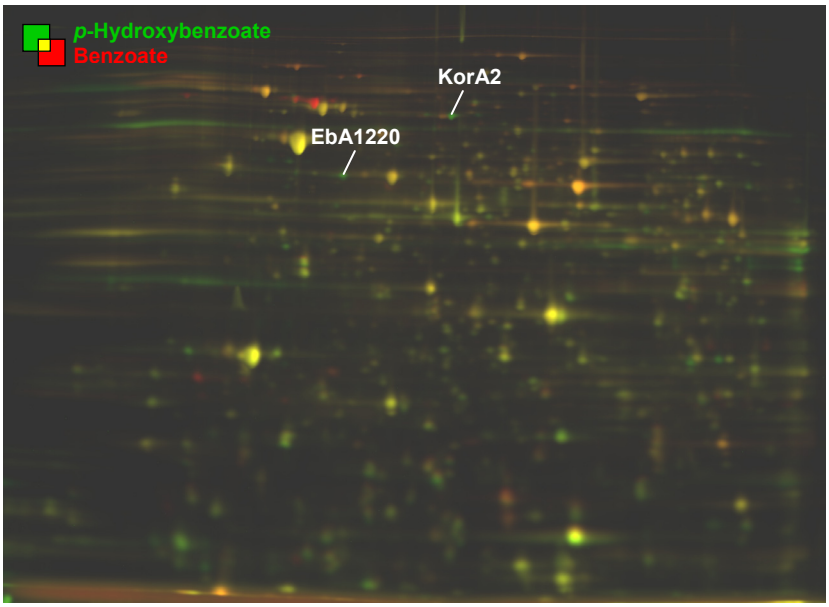


**Fig 3.1.6.1.** Overlay image of 2D DIGE gels (pH 4-7). Protein spots appearing in green are up-regulated when cells were anaerobically grown with *p*-hydroxybenzoate. Whereas spots appearing in red are more abundant when cells were anaerobically grown with the reference substrate benzoate. Spots related to anaerobic *p*-hydroxybenzoate degradation are annotated.

**Table 3.1.6.** Identified proteins related to anaerobic *p*-hydroxybenzoate degradation.

| Orf-No. | Gene | Functional description | Fold change[a] | Share of total protein[a] |
|---|---|---|---|---|
| **Unrelated, up-regulated proteins** | | | | |
| ebA1220 | | Serine proteases, subtilase family | 10.2 | 0.174 |
| ebA3149 | *korA2* | 2-oxoglutarate ferredoxin oxidoreductase α-subunit | 7.4 | 0.244 |

[a] average ratio and share of total protein (%) are indicated for cells grown anaerobically with *p*-hydroxybenzoate
[b] as predicted by genome analysis (Rabus et al. 2005)

### Biochemical background

The degradation pathway of *p*-hydroxybenzoate was mainly elucidated with *Thauera aromatica* and *Rhodopseudomonas palustris*. Initial activation to the CoA-ester is performed by a specific *p*-hydroxybenzoate CoA-ligase (HbcL-1). Subsequently, *p*-hydroxybenzoyl-CoA reductase (HcrCAB) catalyzes the reductive dehydroxylation to benzoyl-CoA (Gibson et al. 1994; Gibson et al. 1997, Brackmann and Fuchs 1993; Breese and Fuchs 1998). While the orthologous genes are present on the chromosome of strain EbN1 (Rabus et al. 2003), none of their products could be identified in the present study

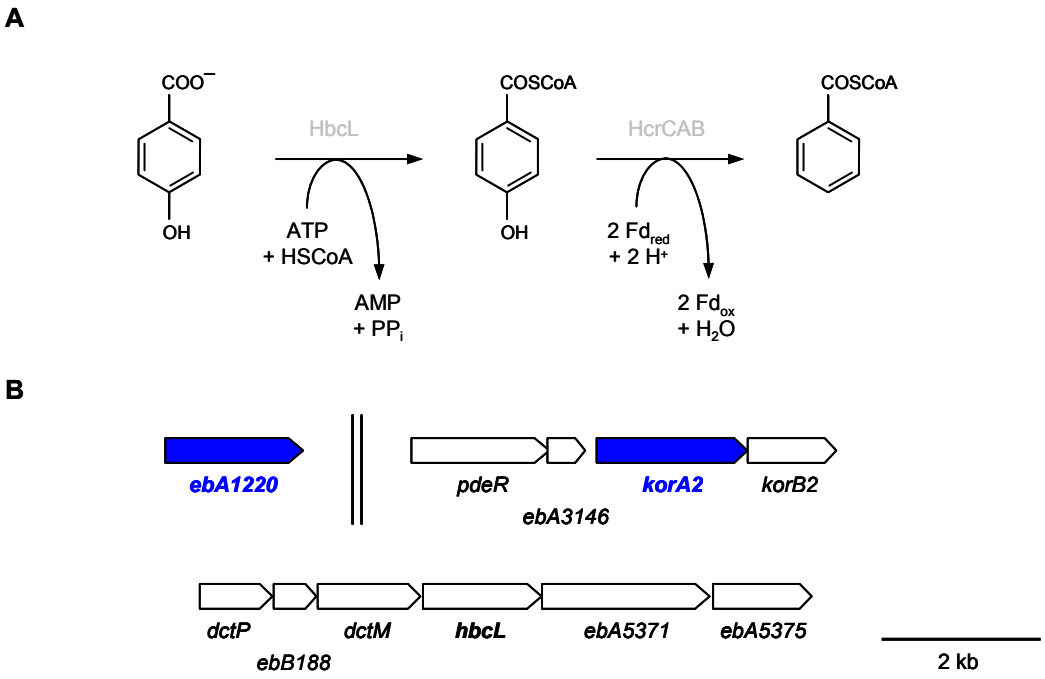


**Fig 3.1.6.2** (**A**) Pathway of anaerobic *p*-hydroxybenzoate degradation. Enzyme names of indicated gene products are as described in Rabus et al. 2005. (**B**) Scale model for the organisation of the involved genes. Identified proteins and genes are highlighted in blue (modified from Rabus et al. 2005).

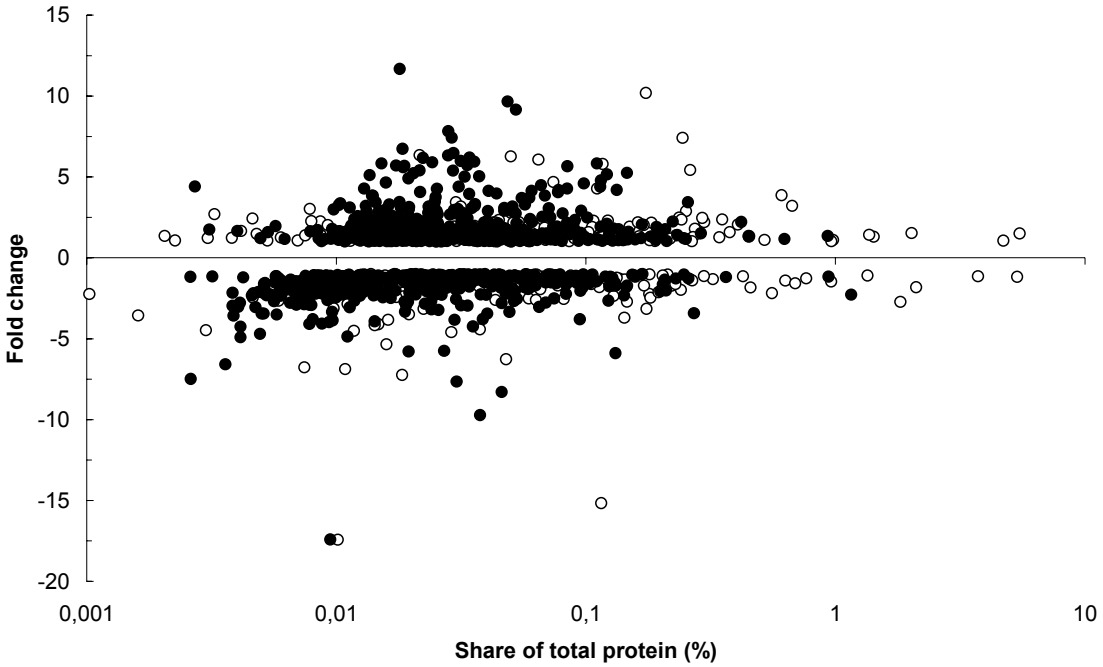


**Fig 3.1.6.3.** Fold changes in protein abundance and their relative share of total protein in cells anaerobically grown with *p*-hydroxybenzoate. Each dot represents a spot on the 2D-gel, except for repeatedly identified proteins (fold changes averaged and spot volumes summed up) (○) identified (●) not identified.

### 3.1.6.1. Up-regualation of proteins not related to the pathway

The spot revealing the largest increase in abundance in cells anaerobically grown with *p*-hydroxybenzoate is EbA1220 (10.2-fold), a protein of the serine protease family, which is also significantly up-regulated during growth with *m*-hydroxybenzoate. The function of this extra cellular protease is unclear.

A strong induction (7.4-fold) was observed for KorA2, the α-subunit of 2-oxoglutarate:ferredoxin oxidoreductase (KGOR). In *T. aromatica* reduced ferredoxin serves as electron donor for the reductive dearomatisation of benzoyl-CoA by benzoyl-CoA reductase, the ferredoxin being regenerated by KGOR (Dörner and Boll 2002). The protein is also increased in abundance during growth with *p*-cresol, the reason is unknown.

## 3.1.9. Benzoate

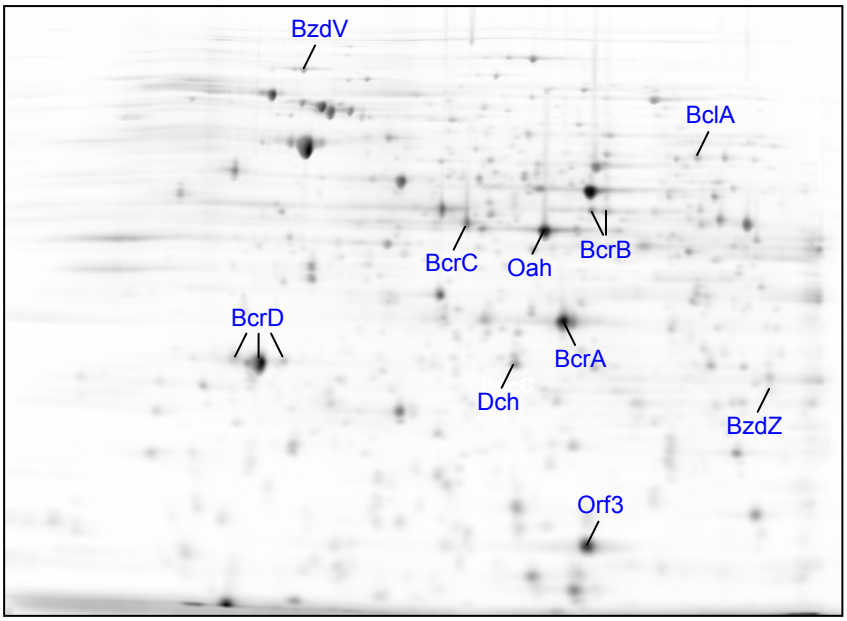


**Fig. 3.1.9.** 2DE gel (pH 4-7) of cells grown anaerobically with benzoate. Identified proteins related to anaerobic benzoate degradation are annotated.

**Table 3.1.9.** Identified proteins related to anaerobic benzoate degradation.

| Orf-No.[a] | Gene [a] | Functional description |
|---|---|---|
| **Benzoate pathway**[b] | | |
| ebA5301 | *bclA* | Benzoate-CoA ligase |
| ebA5282 | *bcrC* | Benzoyl-CoA reductase, subunit C |
| ebA5284 | *bcrB* | Benzoyl-CoA reductase, subunit B |
| ebA5286 | *bcrD* | Benzoyl-CoA reductase, subunit D |
| ebA5287 | *bcrA* | Benzoyl-CoA reductase, subunit A |
| ebA5296 | *dch* | Dienyl-CoA hydratase |
| ebA5298 | *oah* | Probable 6-oxo-cyclohex-1-ene-carbonyl-CoA hydrolase |
| **Genetically related proteins**[b] | | |
| ebA5292 | *orf3* | Putative regulatory protein |
| ebA5294 | *bzdV* | Oxidoreductase of unknown function, subunit |
| ebA5300 | *bzdZ* | Putative dehydrogenase |

[a] listed in order of catalytic activity in the pathway
[b] as predicted by genome analysis (Rabus et al. 2005)

## Biochemical background

Benzoate degradation is initiated by activation to benzoyl-CoA, the central intermediate of anaerobic aromatic compound degradation, catalyzed by benzoate-coenzyme A ligase (BclA) as described for different organisms, e.g. *T. aromatica, A. evansii* and *R. palustris* (Harwood et al. 1998; Heider and Fuchs 1997). Subsequent reductive dearomatisation is catalyzed by the ATP-dependent benzoyl-CoA reductase (BcrCABD; Boll et al. 2002). In *T. aromatica* following reactions of hydratases and dehydrogenases involve cyclohexa-1,5-diene-1-carboxyl-CoA hydratase (Dch), 6-hydroxycyclohex-1-ene-1-carbonyl-CoA dehydrogenase (Had) and 6-oxocyclohex-1-ene-1cabonyl-CoA hydrolase (Oah) yieldng 3-hydroxypimelyl-CoA (Laempe et al. 1998, 1999).

The genome of strain EbN1 contains a large gene cluster baering all genes of anaerobic benzoate degradation. Except Had, all gene products of the anaerobic benzoate pathway were identified.

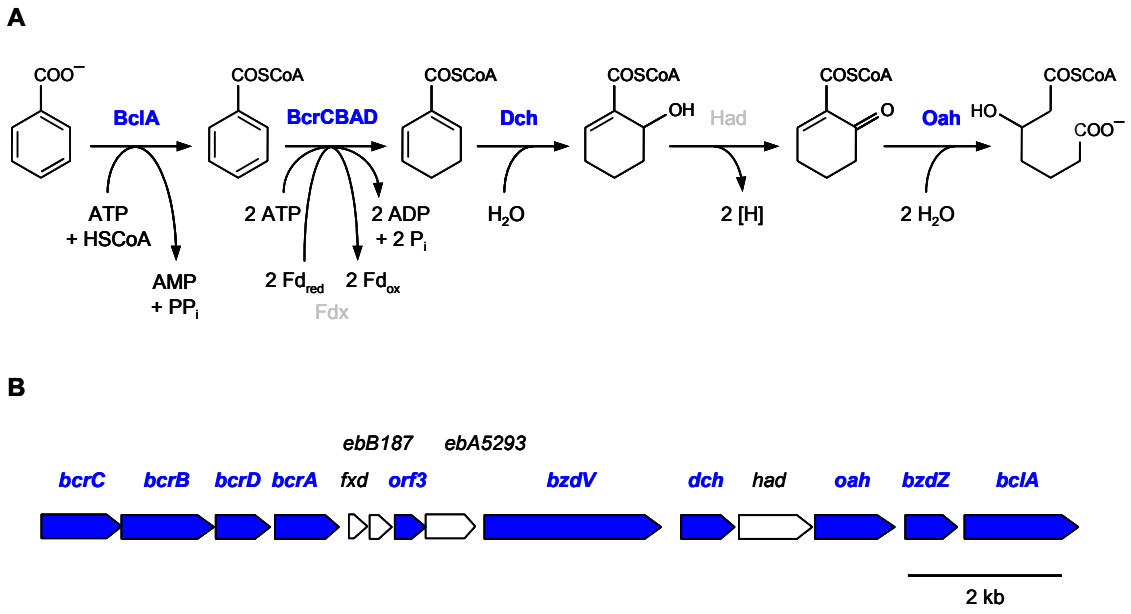


**Fig 3.1.9.2** (**A**) Pathway of anaerobic benzoate degradation. Enzyme names of indicated gene products are as described in Rabus et al. 2005. (**B**) Scale model for the organisation of the involved genes. Identified proteins and genes are highlighted in blue (modified from Rabus et al. 2005).

## 3.1.10. *m*-Hydroxybenzoate

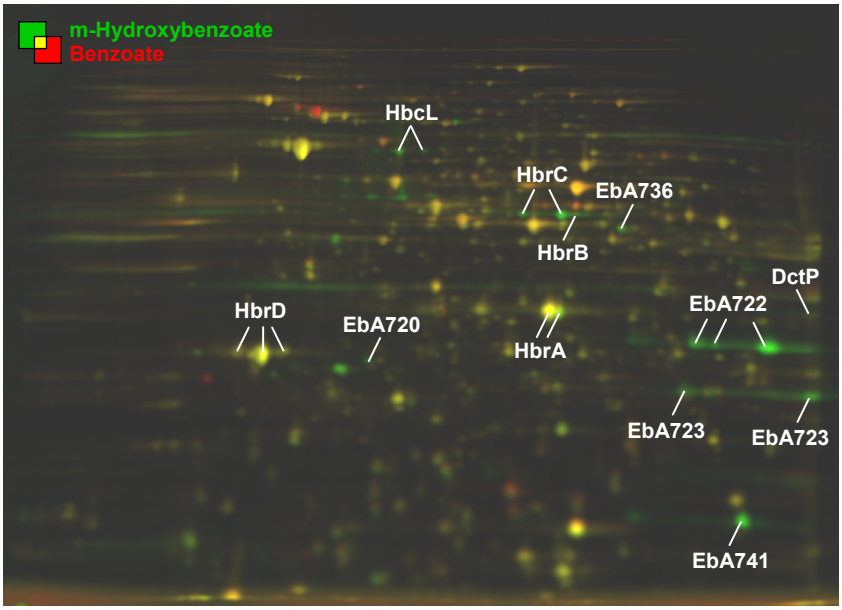


**Fig 3.1.10.1.** Overlay image of 2D DIGE gels (pH 4-7). Protein spots appearing in green are up-regulated when cells were anaerobically grown with *m*-hydroxybenzoate. Whereas spots appearing in red are more abundant when cells were anaerobically grown with the reference substrate benzoate. Spots related to anaerobic *m*-hydroxybenzoate degradation are annotated.

**Table 3.1.10.** Identified proteins related to anaerobic *m*-hydroxybenzoate degradation.

| Orf-No.[a] | Gene [a] | Functional description | Fold change[b] | Share of total protein[b] |
|---|---|---|---|---|
| ***m*-Hydroxybenzoate pathway**[c] | | | | |
| ebA727 | *hbcL* | *m*-Hydroxybenzoate CoAligase | 17.2 | 0.493 |
| ebA748 | *hbrC* | Hydroxybenzoyl-CoA reductase, subunit C | 82.1 | 2.648 |
| ebA746 | *hbrB* | Hydroxybenzoyl-CoA reductase, subunit B | 23.4 | 1.044 |
| ebA744 | *hbrD*[d] | Hydroxybenzoyl-CoA reductase, subunit D | 1.2 | 4.620 |
| ebA742 | *hbrA*[d] | Hydroxybenzoyl-CoA reductase, subunit A | 1.2 | 4.982 |
| ebA720 | | Enoyl-CoA hydratase | -1.5 | 0.003 |
| ebA722 | | Enoyl-CoA hydratase | -6.4 | 0.027 |
| ebA723 | | Putative alcohol dehydrogenase | 1.5 | 0.159 |
| ebA736 | | Putative acyl-CoA dehydrogenase | 13.5 | 0.562 |
| **Genetically related proteins**[c] | | | | |
| ebA729 | *dctP* | Dicarboxylate transport protein | 4.4 | 0.218 |
| ebA741 | | Predicted acetyltransferase | 79.7 | 3.780 |

[a] listed in order of catalytic activity in the pathway
[b] average ratio and share of total protein (%) are indicated for cells grown anaerobically with *m*-hydroxybenzoate
[c] as predicted by genome analysis (Rabus et al. 2005)
[c] HbrA and HbrD exhibit 100 % sequence identity to BcrA and BcrD, respectively, and are therefore not distrainable by MS

## Biochemical background

The pathway of anaerobic *m*-hydroxybenzoate degradation is initiated by a specific CoA-ligase (HbcL) followed by reductive dearomatization performed by a paralogue of benzoyl-CoA reductase, the *m*-hydroxybenzoyl-CoA reductase (HbrCABD; Laempe et al. 2001). The further metabolism of the alicyclic dienoyl-CoA product involves hydrolases and dehydrogenases (EbA720, EbA722, EbA723, EbA736 and EbA738). All postulated gene products (encoded in two adjacent gene clusters) were identified.

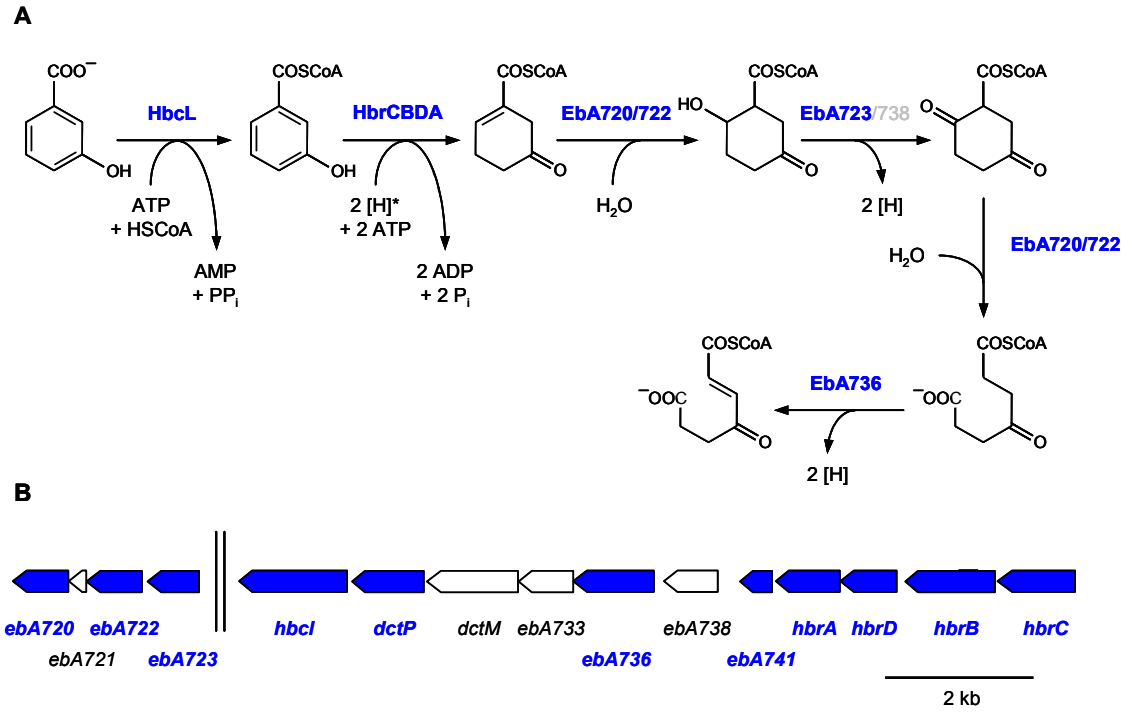


**Fig 3.1.10.2** (**A**) Pathway of anaerobic *m*-hydroxybenzoate degradation. Enzyme names of indicated gene products are as described in Rabus et al. 2005. (**B**) Scale model for the organisation of the involved genes. Identified proteins and genes are highlighted in blue. *one may speculate that ferredoxin also serves as electron donor for *m*-hydroxybenzoyl-CoA reductase (see Fig 3.9.1.2. A; modified from Rabus et al. 2005).

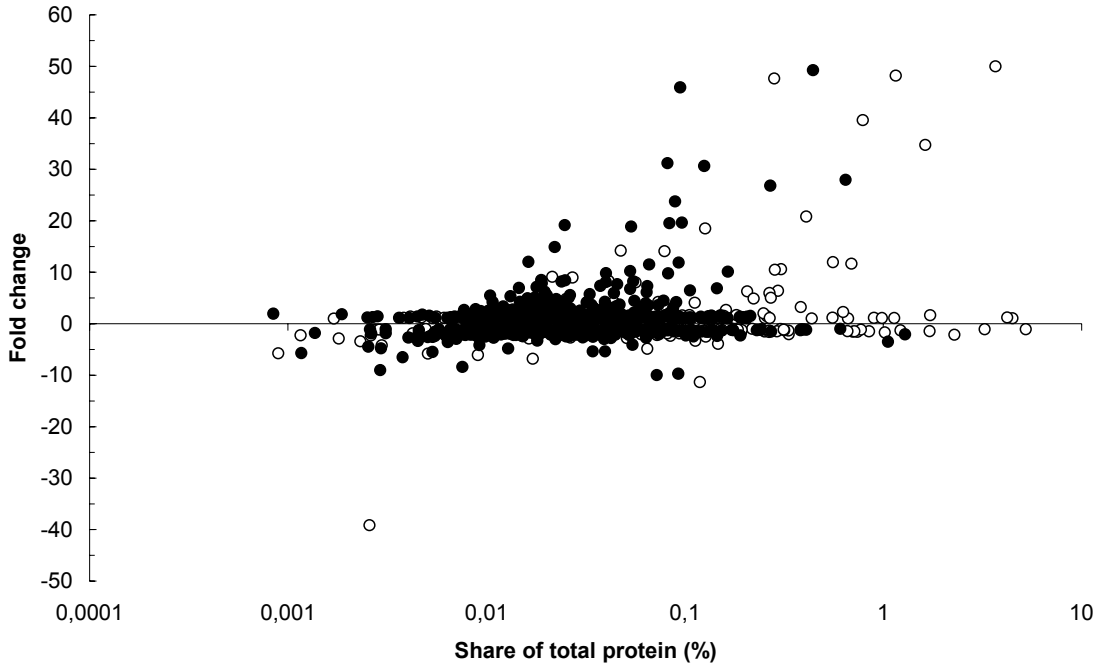


**Fig 3.1.10.3.** Fold changes in protein abundance and their relative share of total protein in cells anaerobically grown with *m*-hydroxybenzoate. Each dot represents a spot on the 2D-gel, except for repeatedly identified proteins (fold changes averaged and spot volumes summed up) (○) identified (●) not identified.

## 3.1.11. *o*-Aminobenzoate

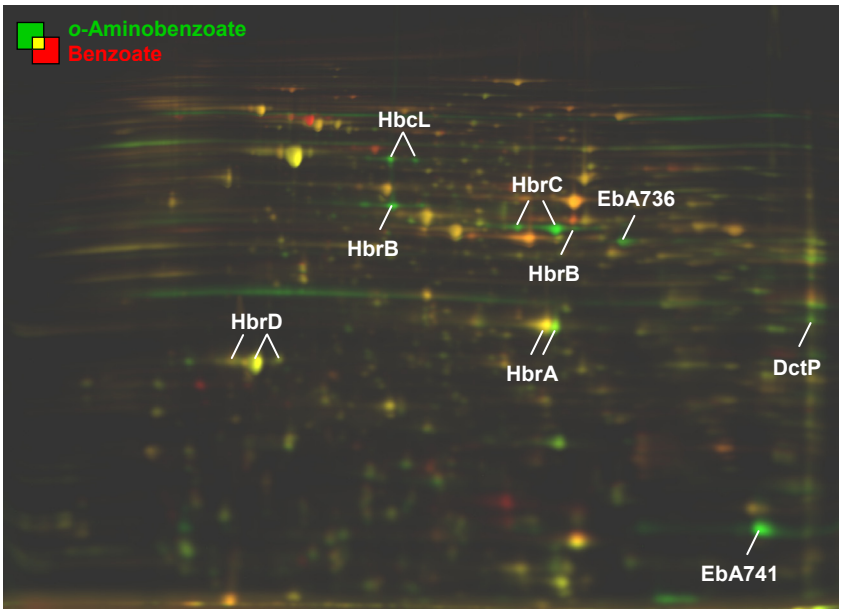


**Fig 3.1.11.1.** Overlay image of 2D DIGE gels (pH 4-7). Protein spots appearing in green are up-regulated when cells were anaerobically grown with *o*-amino-benzoate. Whereas spots appearing in red are more abundant when cells were anaerobically grown with the reference substrate benzoate. Spots related to anaerobic *o*-aminobenzoate degradation are annotated.

**Table 3.1.11.** Identified proteins related to anaerobic *o*-aminobenzoate degradation.

| Orf-No.[a] | Gene [a] | Functional description | Fold change[b] | Share of total protein[b] |
|---|---|---|---|---|
| ***m*-Hydroxybenzoate pathway**[c] | | | | |
| ebA727 | *hbcL* | *m*-Hydroxybenzoate CoAligase | 17.2 | 0.493 |
| ebA748 | *hbrC* | Hydroxybenzoyl-CoA reductase, subunit C | 82.1 | 2.648 |
| ebA746 | *hbcB* | Hydroxybenzoyl-CoA reductase, subunit B | 23.4 | 1.044 |
| ebA744 | *hbrD* | Hydroxybenzoyl-CoA reductase, subunit D | 1.4 | 4.753 |
| ebA742 | *hbrA* | Hydroxybenzoyl-CoA reductase, subunit A | 1.1 | 5.683 |
| ebA720 | | Enoyl-CoA hydratase | -1.5 | 0.003 |
| ebA722 | | Enoyl-CoA hydratase | -6.4 | 0.027 |
| ebA723 | | Putative alcohol dehydrogenase | 1.5 | 0.158 |
| ebA736 | | Putative acyl-CoA dehydrogenase | 13.5 | 0.562 |
| **Genetically related proteins**[c] | | | | |
| ebA729 | *dctP* | Dicarboxylate transport protein | 4.4 | 0.218 |
| ebA741 | | Predicted acetyltransferase | 79.7 | 3.781 |

[a] listed in order of catalytic activity in the pathway
[b] average ratio and share of total protein (%) are indicated for cells grown anaerobically with *o*-aminobenzoate
[c] as predicted by genome analysis (Rabus et al. 2005)
[c] HbrA and HbrD exhibit 100 % sequence identity to BcrA and BcrD, respectively, and are therefore not distrainable by MS

## Biochemical background

Anthranilic acid (*o*-aminobenzoate) is an intermediate of tryptophan synthesis as well as degradation. In *Thauera aromatica* anaerobic degradation of *o*-aminobenzoate proceeds via activation to *o*-aminobenzoyl-CoA, reductive deamination to benzoyl-CoA and subsequent ring reduction to yield alicyclic acyl-CoA compounds (Lochmeyer et al. 1992).

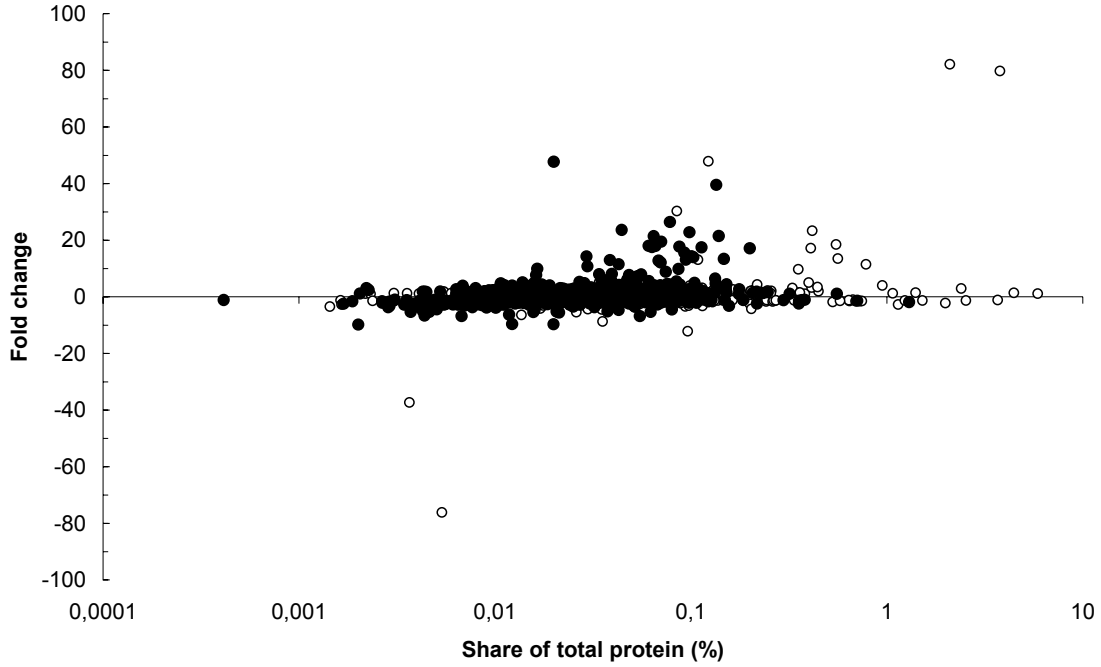


**Fig 3.1.11.2.** Fold changes in protein abundance and their relative share of total protein in cells anaerobically grown with *o*-aminobenzoate. Each dot represents a spot on the 2D-gel, except for repeatedly identified proteins (fold changes averaged and spot volumes summed up) (○) identified (●) not identified.

# 3.2. Aerobic aromatic compound degradation

## 3.2.1. Benzoate

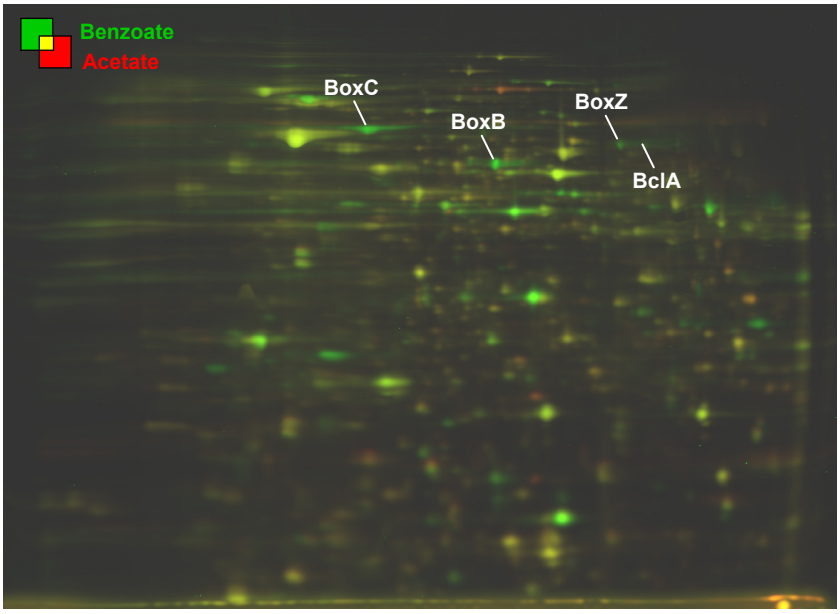


**Fig 3.2.1.1.** Overlay image of 2D DIGE gels (pH 4-7). Protein spots appearing in green are up-regulated when cells were aerobically grown with benzoate. Whereas spots appearing in red are more abundant when cells were aerobically grown with the reference substrate acetate. Spots related to aerobic benzoate degradation are annotated.

**Table 3.2.1.** Identified proteins related to aerobic benzoate degradation.

| Orf-No.[a] | Gene [a] | Functional description | Fold change[b] | Share of total protein[b] |
|---|---|---|---|---|
| **Benzoate pathway**[c] | | | | |
| ebA2753 | *bclA* | Benzoate-CoA ligase | 4.4 | 0.095 |
| ebA2765 | *boxB* | Benzoyl-CoA oxygenase, component B | 34.8 | 0.845 |
| ebA2763 | *boxC* | Enoyl-CoA hydratase/isomerase involved in isomerisation and hydrolytic ring opening of 2,3-dihydro-2,3-diol intermediate of benzoyl-CoA | 5.7 | 1.417 |
| ebA2759 | *boxZ* | Aldehyde dehydrogenase | 10.3 | 0.139 |

[a] listed in order of catalytic activity in the pathway
[b] average ratio and share of total protein (%) are indicated for cells grown aerobically with benzoate
[c] as predicted by genome analysis (Rabus et al. 2005)

## Biochemical background

A new pathway for aerobic benzoate catabolism was previously described for *Azoarcus evansii*. It involved initial activation of benzoate to the respective CoA-thioester followed by a 2,3-dioxygenation. Subsequent isomerization and dehydrogenation yield β-ketoadipyl-CoA (Gescher et al. 2002, Gescher et al. 2006). All predicted genes are present in the genome of strain EbN1 (Rabus et al. 2005). Four of these five predicted gene products, namely benzoate-CoA ligase (BclA-1), one subunit of benzoyl-CoA oxygenase (BoxB), enoyl-CoA-hydratase/isomerase (BoxC), and the aldehyde dehydrogenase involved in ring opening (BoxZ), could be identified in the present proteomic study.

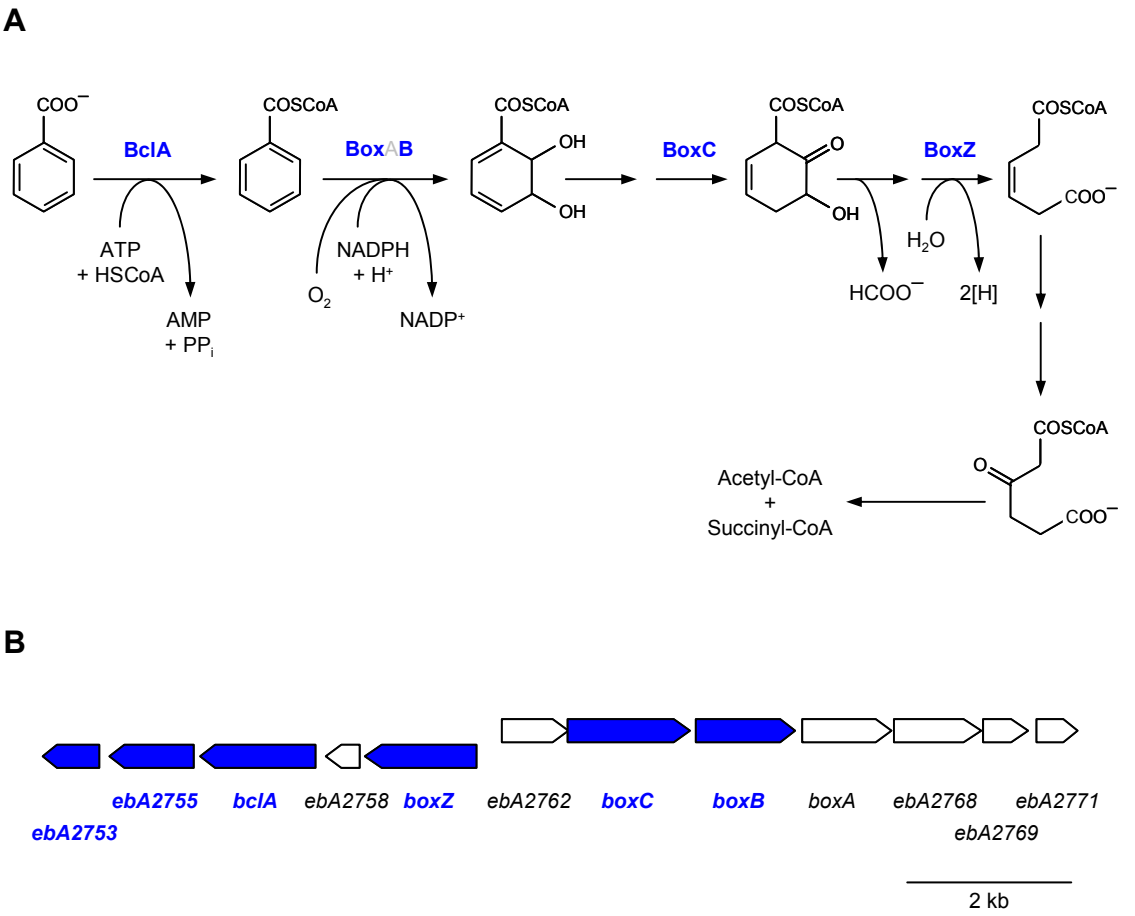


**Fig 3.2.1.2** (**A**) Pathway of aerobic benzoate degradation. Enzyme names of indicated gene products are as described in Rabus et al. 2005. (**B**) Scale model for the organisation of the involved genes. Identified proteins and genes are highlighted in blue. (modified from Rabus et al. 2005).

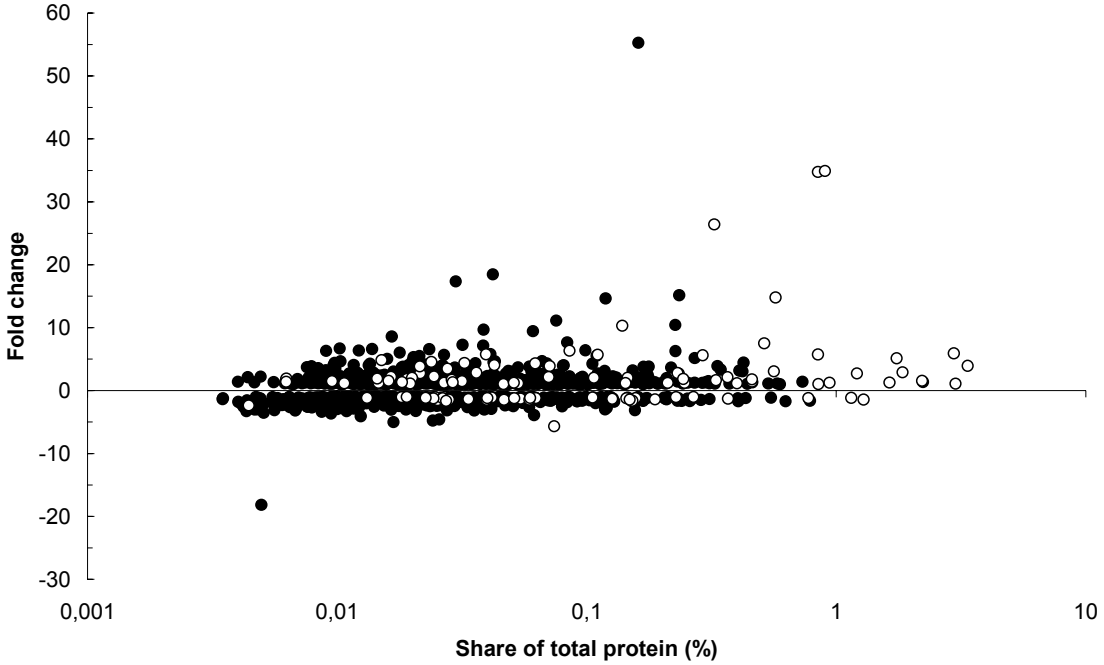


**Fig 3.2.1.3.** Fold changes in protein abundance and their relative share of total protein in cells aerobically grown with benzoate. Each dot represents a spot on the 2D-gel, except for repeatedly identified proteins (fold changes averaged and spot volumes summed up) (○) identified (●) not identified.

## 3.2.2. Gentisate (2,5-Dihydroxybenzoate)

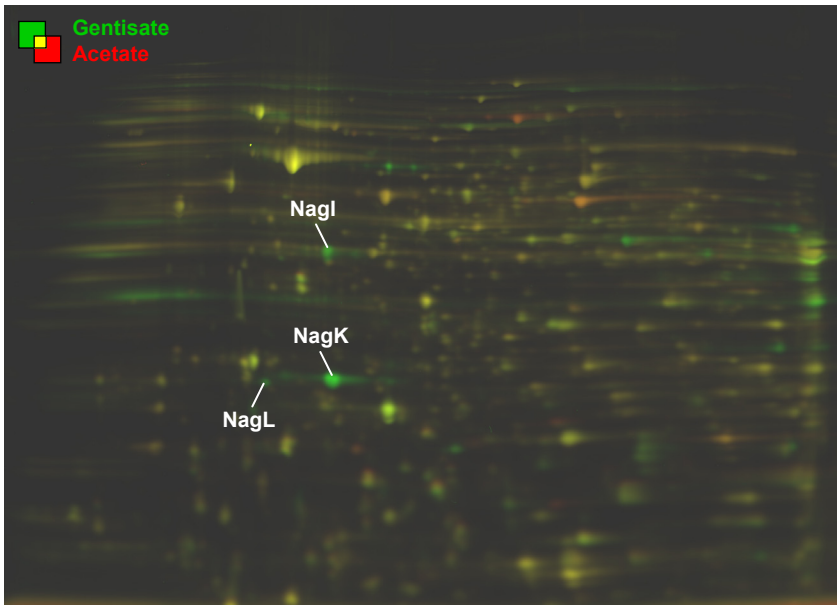


**Fig 3.2.2.1.** Overlay image of 2D DIGE gels (pH 4-7). Protein spots appearing in green are up-regulated when cells were aerobically grown with gentisate. Whereas spots appearing in red are more abundant when cells were aerobically grown with the reference substrate acetate. Spots related to aerobic gentisate degradation are annotated.

**Table 3.2.2.** Identified proteins related to aerobic gentisate degradation.

| Orf-No.[a] | Gene [a] | Functional description | Fold change[b] | Share of total protein[b] |
|---|---|---|---|---|
| **Gentisate pathway**[c] | | | | |
| ebA1373 | *nagI* | Gentisate 1,2-dioxygenase | 16.7 | 0.927 |
| ebA1379 | *nagL* | Maleylpyruvate isomerase | 17.5 | 0.179 |
| ebA1377 | *nagK* | Fumarylpyruvate hydrolase | 120.3 | 3.003 |
| **Genetically related proteins**[c] | | | | |
| ebA1378 | *hbh* | Hydroxybenzoate hydroxylase | 10.7 | 0.255 |

[a] listed in order of catalytic activity in the pathway
[b] average ratio and share of total protein (%) are indicated for cells grown aerobically with gentisate
[c] as predicted by genome analysis (Rabus et al. 2005)

## Biochemical background

The aerobic gentisate pathway was originally described in *Pseudomonas* spp. (Wheelis et al. 1967). Initially, a gentisate 1,2-dioxygenase (NagI) forms maleylpyruvate, which is subsequently isomerized to fumarylpyruvate (maleylpyruvate isomerase, NagL) and hydrolytically cleaved (fumarylpyruvate hydroxylase, NagK) to fumarate and pyruvate. Orthologous genes (*nagIKL*) are organized together with the *s5h* gene in an operon-like structure on the chromosome of strain EbN1 (Rabus et al. 2005). All four proteins encoded in this operon were identified.

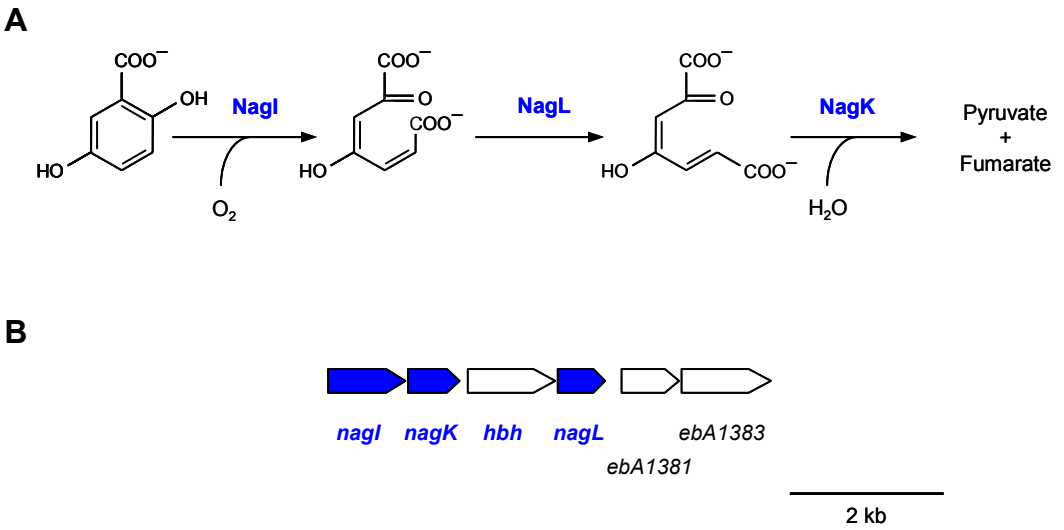


**Fig 3.2.2.2** (**A**) Pathway of aerobic gentisate degradation. Enzyme names of indicated gene products are as described in Rabus et al. 2005. (**B**) Scale model for the organisation of the involved genes. Identified proteins and genes are highlighted in blue. (modified from Rabus et al. 2005).

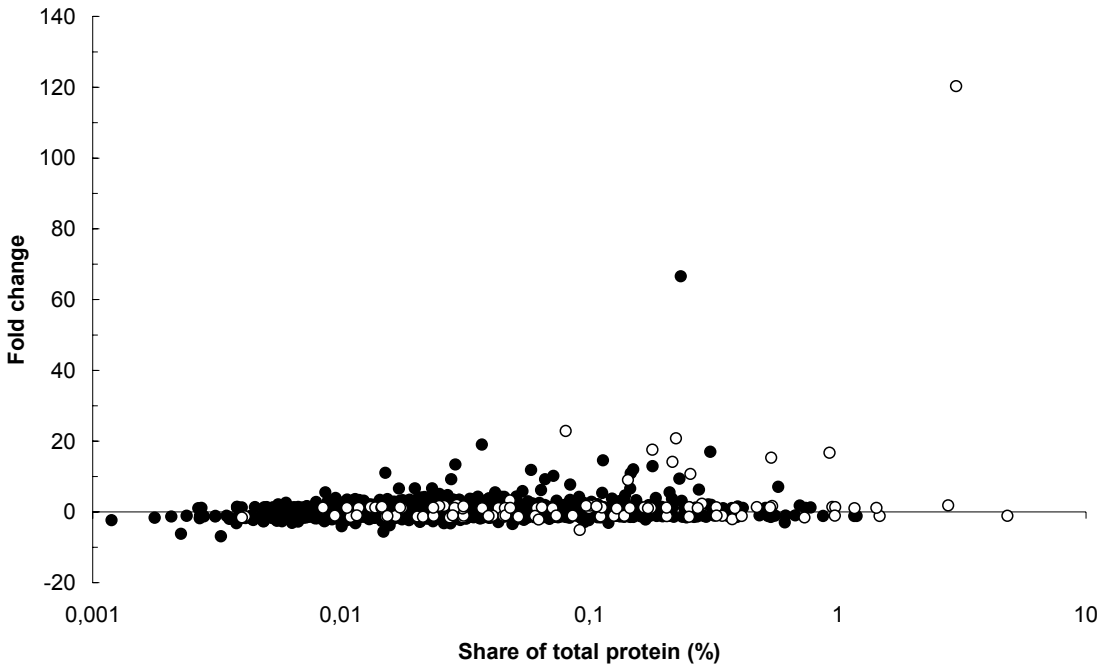


**Fig 3.2.2.3.** Fold changes in protein abundance and their relative share of total protein in cells aerobically grown with gentisate. Each dot represents a spot on the 2D-gel, except for repeatedly identified proteins (fold changes averaged and spot volumes summed up) (○) identified (●) not identified.

## 3.2.3. Phenylacetate

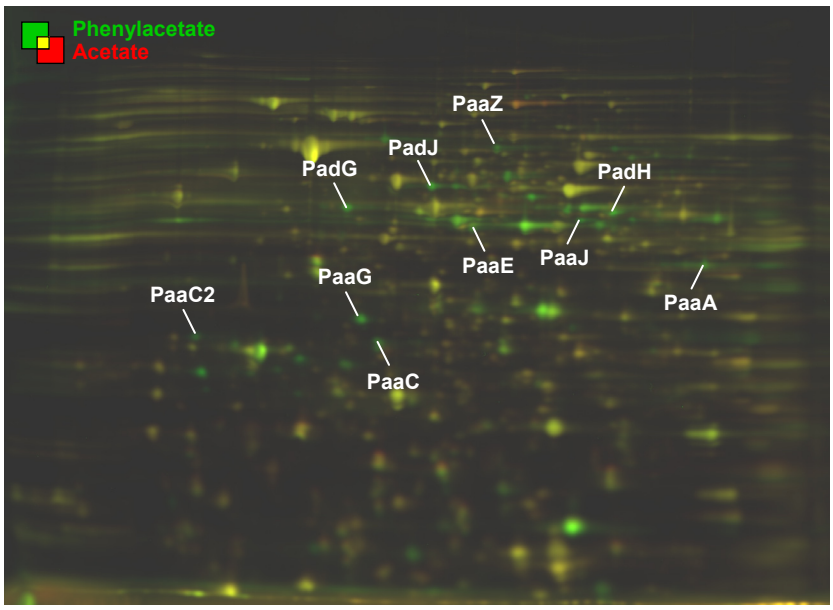


**Fig 3.2.3.1.** Overlay image of 2D DIGE gels (pH 4-7). Protein spots appearing in green are up-regulated when cells were aerobically grown with phenylacetate. Whereas spots appearing in red are more abundant when cells were aerobically grown with the reference substrate acetate. Spots related to aerobic phenylacetate degradation are annotated.

**Table 3.2.3.** Identified proteins related to aerobic phenylacetate degradation.

| Orf-No.[a] | Gene[a] | Functional description | Fold change[b] | Share of total protein[b] |
|---|---|---|---|---|
| **Phenylacetate pathway**[c] | | | | |
| ebA3547 | *paaA* | Putative ring-oxidation complex protein 1 | 6.0 | 0.280 |
| ebA3550 | *paaC* | Putative ring-hydroxylation complex protein 2 | 6.9 | 0.19. |
| ebA5722 | *paaC2* | Similar to aerobic phenylacetate degradation protein | 5.2 | 0.050 |
| ebA3553 | *paaE* | Putative ring-hydroxylation complex protein 4 | 3.5 | 0.236 |
| ebA3542 | *paaG* | Putative enoyl-CoA hydratase | 21.6 | 0.275 |
| ebA3541 | *paaZ* | Protein involved in aerobic phenylacetate metabolism | 8.2 | 0.125 |
| ebA5729 | *paaJ* | Putative 3-ketoadipyl-CoA thiolase | 24.8 | 0.113 |
| **Anaerobic Phenylacetate pathway** | | | | |
| ebA5402 | *padJ* | Anaerobic phenylacetate CoA ligase | 13.4 | 0.429 |
| ebA5399 | *padG* | Phenylacetyl-CoA:acceptor oxidoreductase | 14.8 | 0.265 |
| ebA5400 | *padH* | Phenylacetyl-CoA:acceptor oxidoreductase | 8.8 | 0.359 |

[a] listed in order of catalytic activity in the pathway
[b] average ratio and share of total protein (%) are indicated for cells grown aerobically with phenylacetate
[c] as predicted by genome analysis (Rabus et al. 2005)

## Biochemical background

The aerobic pathway of phenylacetate degradation is initiated by activation to phenylacetyl-CoA by a specific ligase (PaaK) in *E. coli* K12, *P. putida* and *A. evansii* (Mohamed et al. 2002, Diaz et al. 2001, Olivera et al. 1998). Dihydrodiol formation is then supposed to be catalyzed by a specific phenylacetyl-CoA dioxygenase (PaaABCDE). Subsequent isomerisation and hydrolytic ring opening are presumed to be achieved by an enoyl-CoA hydratase/isomerase (PaaG) and an aldehyde dehydrogenase (PaaZ). Finally, β-oxidation steps lead to succinyl-CoA and acetyl-CoA, catalyzed by PaaFH and PaaJ.

In strain EbN1 two large gene clusters were detected, bearing in each case most of the genes of the aerobic phenylacetate pathway (Rabus et al. 2005). The first cluster (at approx. 2.1 Mb) encodes all proteins involved in the predicted pathway, except for enoyl-CoA hydratase (PaaF*)* and 3-ketoadipyl-CoA thiolase (PaaJ). Although the second cluster (at approx. 3.4 Mb) contains the *paaF* and *paaJ* genes, here genes for the ring opening enzymes (*paaGZ*), the regulator (*paaR*) and two proteins of unknown function (*paaI* and *paaX*) are missing.

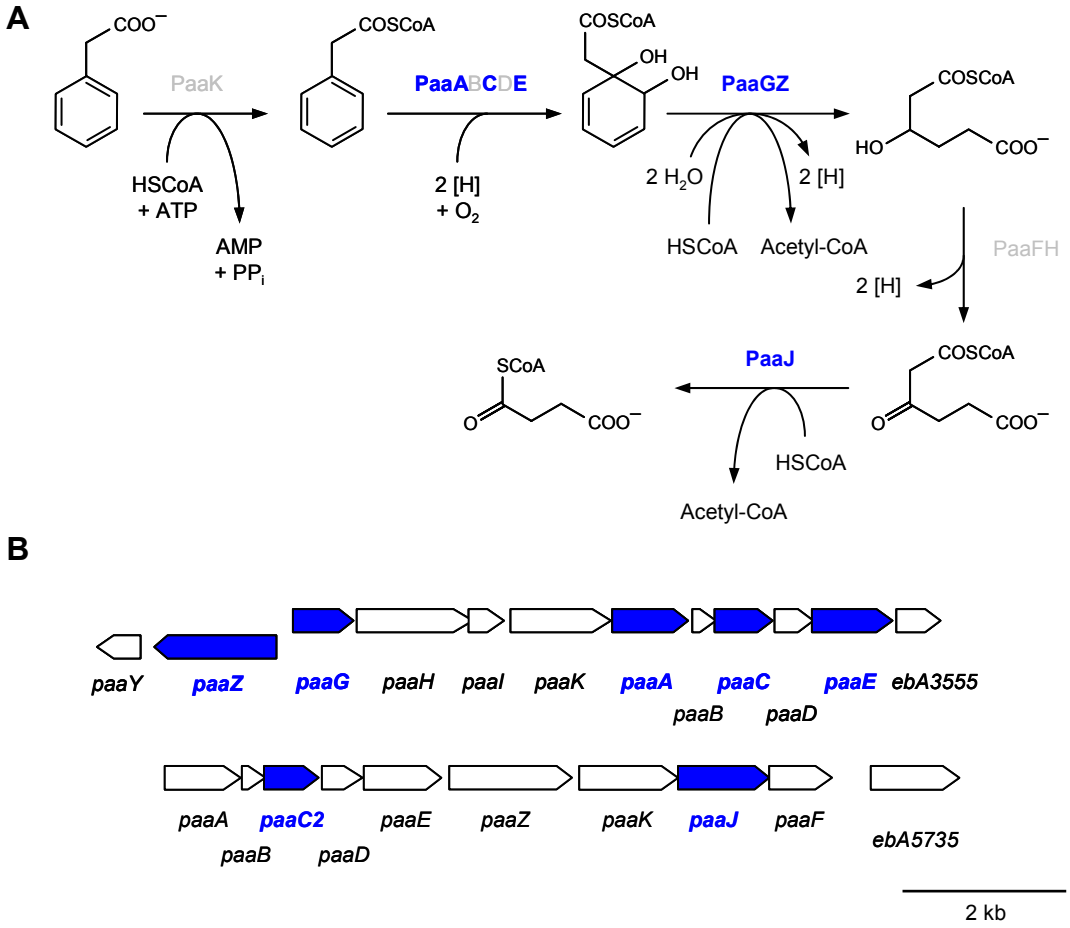


**Fig 3.2.3.2** (**A**) Pathway of aerobic phenylacetate degradation. Enzyme names of indicated gene products are as described in Rabus et al. 2005. (**B**) Scale model for the organisation of the involved genes. Identified proteins and genes are highlighted in blue. (modified from Rabus et al. 2005).

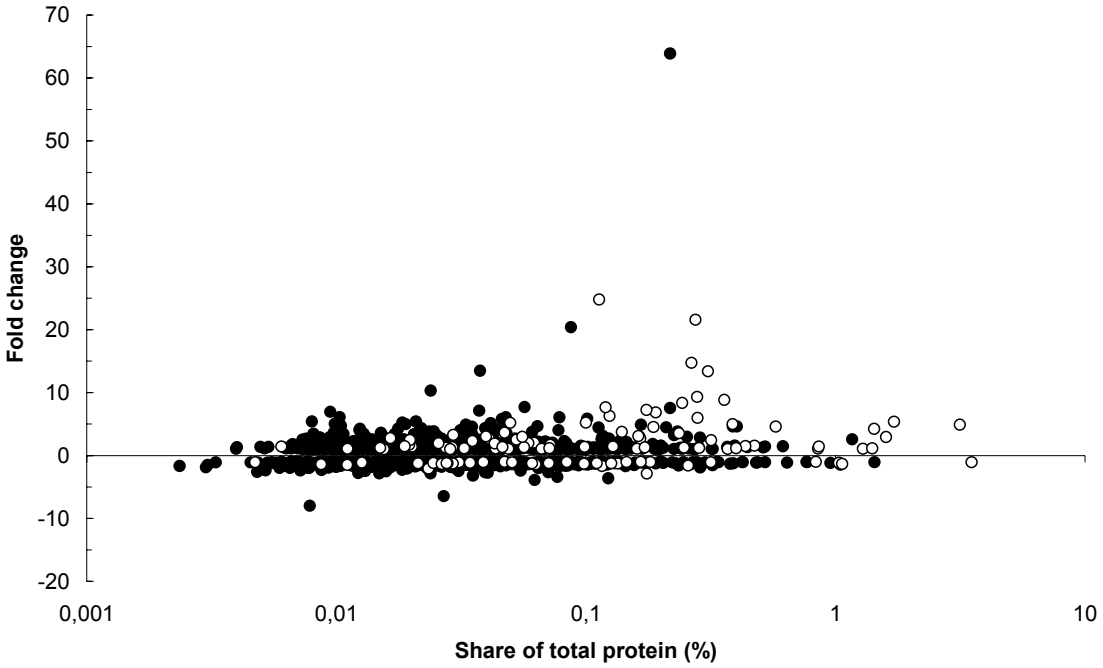


**Fig 3.2.3.3.** Fold changes in protein abundance and their relative share of total protein in cells aerobically grown with phenylacetate. Each dot represents a spot on the 2D-gel, except for repeatedly identified proteins (fold changes averaged and spot volumes summed up) (○) identified (●) not identified.

## 3.2.4. Phenylalanine

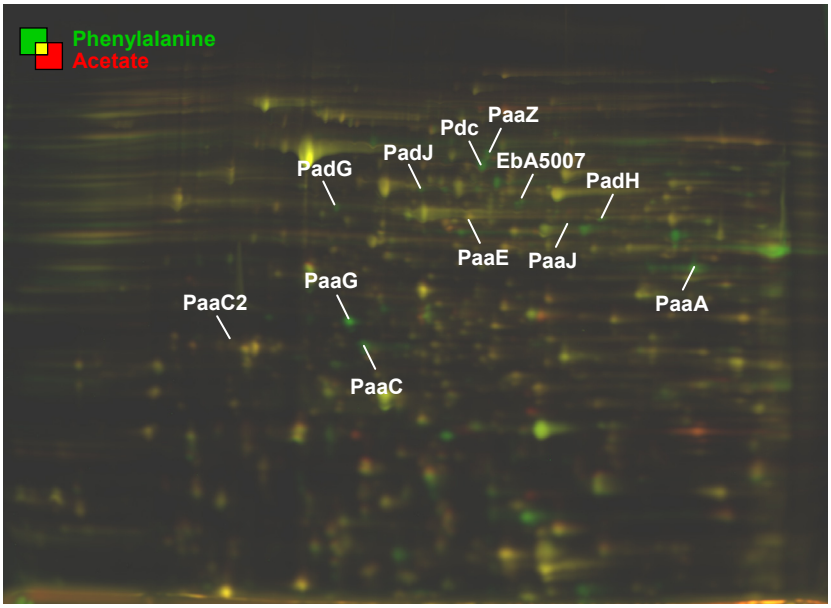


**Fig 3.2.4.1.** Overlay image of 2D DIGE gels (pH 4-7). Protein spots appearing in green are up-regulated when cells were aerobically grown with phenylalanine. Whereas spots appearing in red are more abundant when cells were aerobically grown with the reference substrate acetate. Spots related to aerobic phenylalanine degradation are annotated.

**Table 3.2.4.** Identified proteins related to aerobic phenylalanine degradation.

| Orf-No.[a] | Gene [a] | Functional description | Fold change[b] | Share of total protein[b] |
|---|---|---|---|---|
| **Phenylacetate pathway**[c] | | | | |
| ebA3547 | *paaA* | Putative ring-oxidation complex protein 1 | 7.9 | 0.328 |
| ebA3550 | *paaC* | Putative ring-hydroxylation complex protein 2 | 9.7 | 0.293 |
| ebA5722 | *paaC2* | Similar to aerobic phenylacetate degradation protein | 1.0 | 0.010 |
| ebA3553 | *paaE* | Putative ring-hydroxylation complex protein 4 | 1.8 | 0.097 |
| ebA3542 | *paaG* | Putative enoyl-CoA hydratase | 26.6 | 0.597 |
| ebA3541 | *paaZ* | Protein involved in aerobic phenylacetate metabolism | 6.3 | 0.120 |
| ebA5729 | *paaJ* | Putative 3-ketoadipyl-CoA thiolase | 4.7 | 0.024 |
| **Anaerobic Phenylalanine pathway**[d] | | | | |
| ebA5007 | | Ferredoxin:NADH oxidoreductase | 2.8 | 0.059 |
| **Anaerobic Phenylacetate pathway**[c] | | | | |
| ebA5402 | *padJ* | Anaerobic phenylacetate CoA ligase | 3.2 | 0.124 |
| ebA5399 | *padG* | Phenylacetyl-CoA:acceptor oxidoreductase | 3.2 | 0.056 |
| ebA5400 | *padH* | Phenylacetyl-CoA:acceptor oxidoreductase | 2.6 | 0.126 |

[a] listed in order of catalytic activity in the pathway
[b] average ratio and share of total protein (%) are indicated for cells grown aerobically with phenylalanine
[c] as predicted by genome analysis (Rabus et al. 2005)
[d] as predicted by this proteomic study

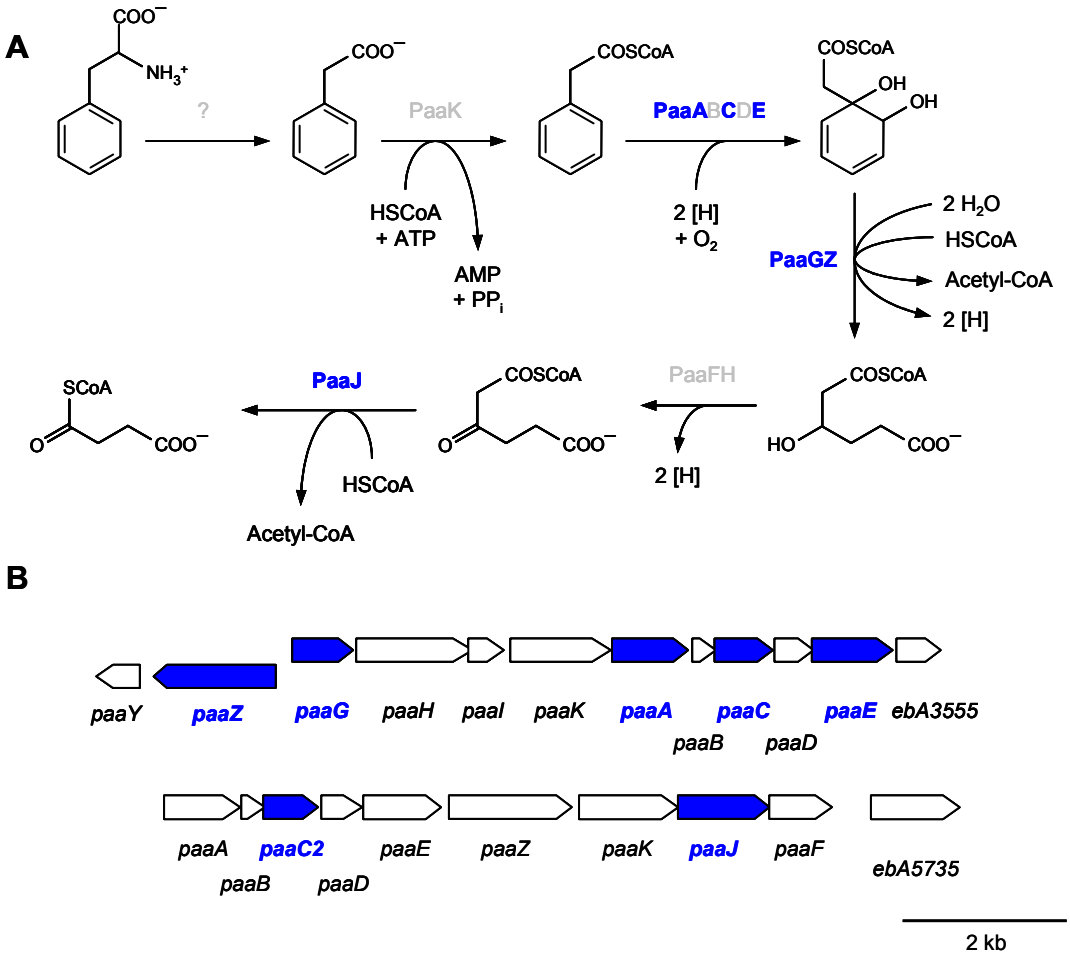


**Fig 3.2.3.2** (**A**) Proposed pathway of aerobic phenylalanine degradation. Enzyme names of indicated gene products are as described in Rabus et al. 2005. (**B**) Scale model for the organisation of the involved genes. Identified proteins and genes are highlighted in blue. (modified from Rabus et al. 2005).

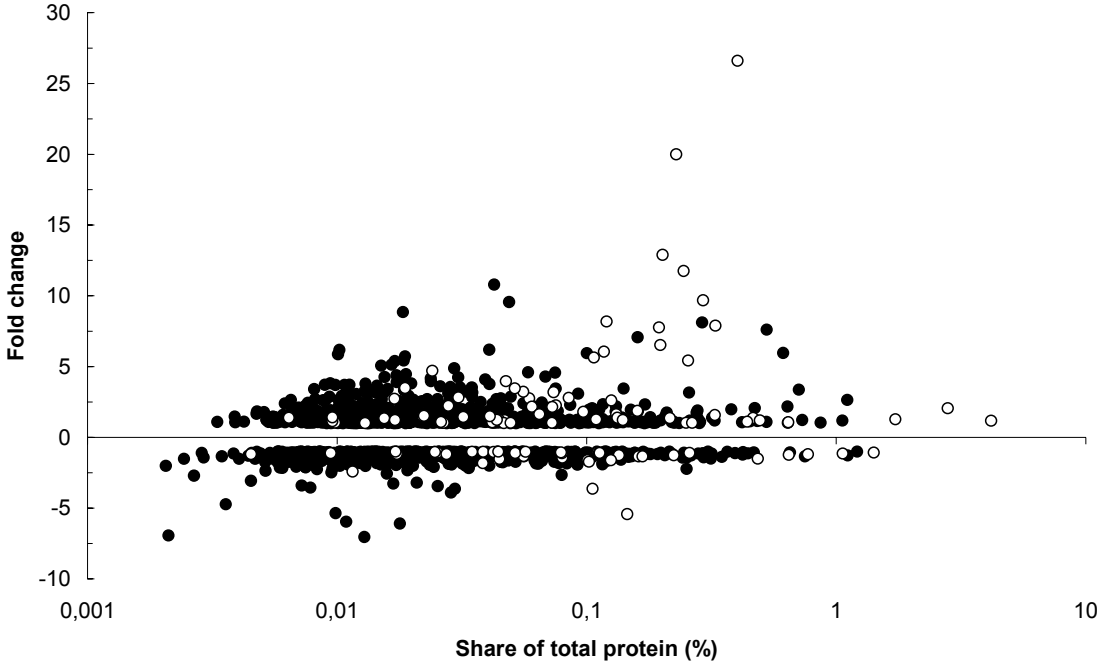


**Fig 3.2.4.3.** Fold changes in protein abundance and their relative share of total protein in cells aerobically grown with phenylalanine. Each dot represents a spot on the 2D-gel, except for repeatedly identified proteins (fold changes averaged and spot volumes summed up) (○) identified (●) not identified.

## 3.2.5. *m*-Hydroxybenzoate

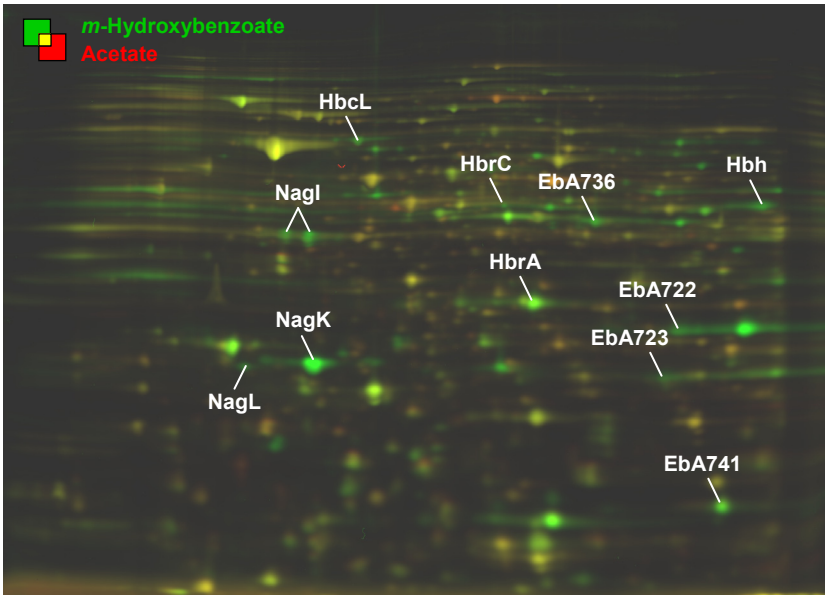


**Fig 3.2.5.1.** Overlay image of 2D DIGE gels (pH 4-7). Protein spots appearing in green are up-regulated when cells were aerobically grown with *m*-hydroxybenzoate. Whereas spots appearing in red are more abundant when cells were aerobically grown with the reference substrate acetate. Spots related to aerobic *m*-hydroxybenzoate degradation are annotated.

**Table 3.2.5.** Identified proteins related to aerobic *m*-hydroxybenzoate degradation.

| Orf-No.[a] | Gene [a] | Functional description | Fold change[b] | Share of total protein[b] |
|---|---|---|---|---|
| ***m*-hydroxybenzaote pathway**[c] | | | | |
| ebA1378 | *hbh* | Hydroxybenzoate hydroxylase | 17.6 | 0.345 |
| **Gentisate pathway**[d] | | | | |
| ebA1373 | *nagI* | Gentisate 1,2-dioxygenase | 16.5 | 0.826 |
| ebA1379 | *nagL* | Maleylpyruvate isomerase | 19.0 | 0.144 |
| ebA1377 | *nagK* | Fumarylpyruvate hydrolase | 197.0 | 3.373 |
| **Anaerobic *m*-hydroxybenzoate pathway**[c] | | | | |
| ebA727 | *hbcL* | *m*-Hydroxybenzoate CoAligase | 9.5 | 0.129 |
| ebA748 | *hbrC* | Hydroxybenzoyl-CoA reductase, subunit C | 8.2 | 0.641 |
| ebA742 | *hbrA* | Hydroxybenzoyl-CoA reductase, subunit A | 2.5 | 0.784 |
| ebA722 | | Enoyl-CoA hydratase | 25.8 | 3.210 |
| ebA723 | | Putative alcohol dehydrogenase | 5.8 | 0.270 |
| ebA736 | | Putative acyl-CoA dehydrogenase | 18.6 | 0.476 |
| ebA741 | | Predicted acetyltransferase | 6.3 | 1.218 |

[a] listed in order of catalytic activity in the pathway
[b] average ratio and share of total protein (%) are indicated for cells grown aerobically with *m*-hydroxybenzoate
[c] as predicted by this proteomic study
[d] as predicted by genome analysis (Rabus et al. 2005)

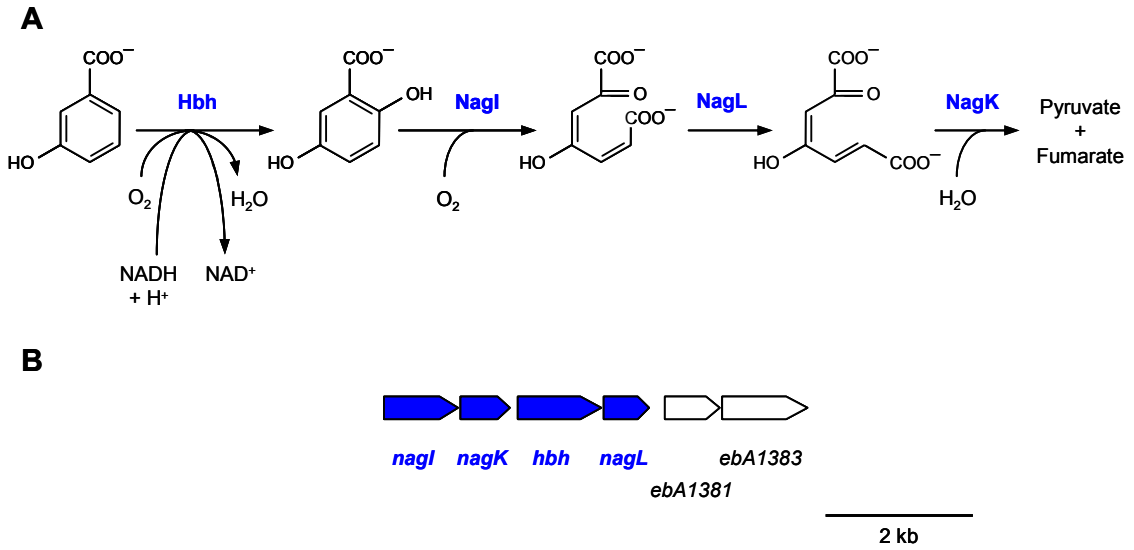


**Fig 3.2.5.2** (**A**) Predicted pathway of aerobic *m*-hydroxybenzoate degradation. Enzyme names of indicated gene products are as described in Rabus et al. 2005. (**B**) Scale model for the organisation of the involved genes. Identified proteins and genes are highlighted in blue. (modified from Rabus et al. 2005).

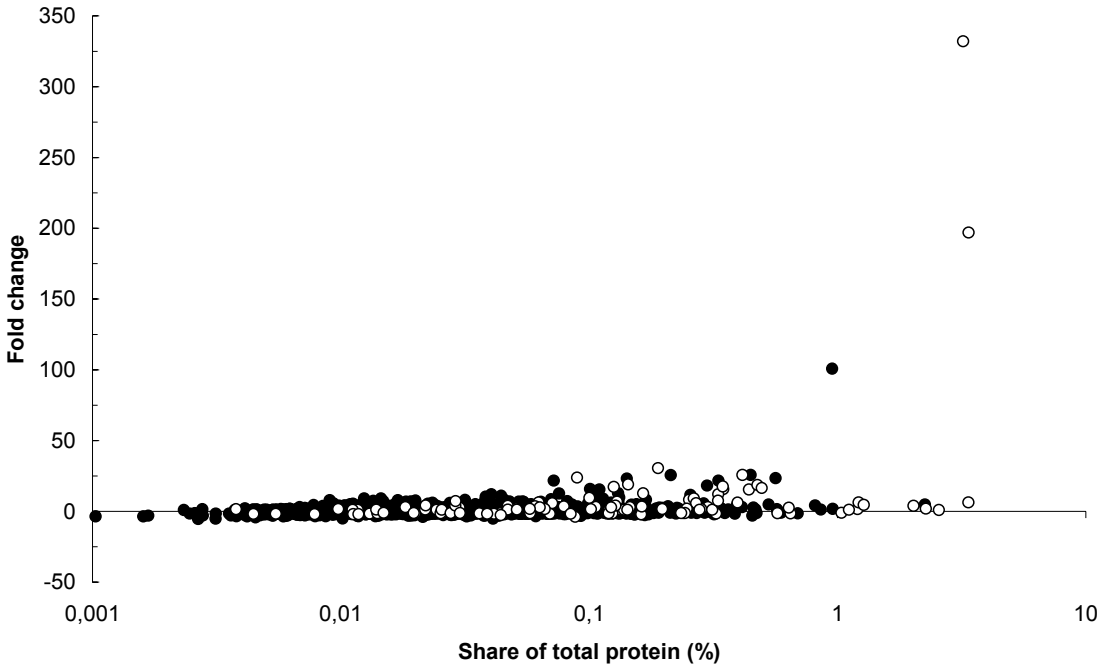


**Fig 3.2.5.3.** Fold changes in protein abundance and their relative share of total protein in cells aerobically grown with *m*-hydroxybenzoate. Each dot represents a spot on the 2D-gel, except for repeatedly identified proteins (fold changes averaged and spot volumes summed up) (○) identified (●) not identified.

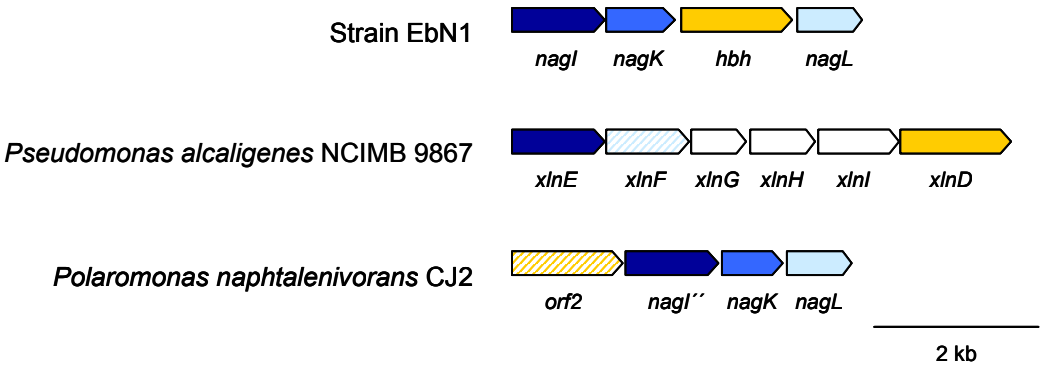


**Fig. 3.2.5.4.** Comparison of gene clusters containing genes of the gentisate/*m*-hydroxybenzoate pathway of strain EbN1, *Pseudomonas alcaligenes* NCIMB 9867 and *Polaromonas naphtalenivorans* CJ2. Colors indicate same function. Hatching indicates high sequence similarities to respective genes of strain EbN1 (adapted from Jeon et al. 2006, Rabus et al. 2005, Yeo et al. 2003).

# 3.3. Anaerobic degradation of aliphatic alcohols, ketones and organic acids

## 3.3.1. Alcohols and ketones

### 3.3.1.1. 2-Propanol

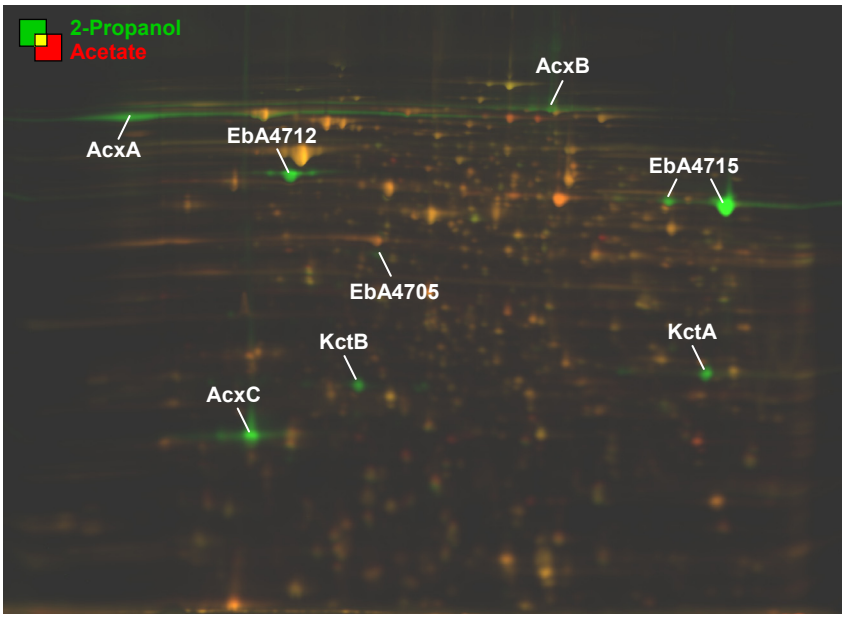


**Fig 3.3.1.1.** Overlay image of 2D DIGE gels (pH 4-7). Protein spots appearing in green are up-regulated when cells were anaerobically grown with 2propanol. Whereas spots appearing in red are more abundant when cells were anaerobically grown with the reference substrate acetate. Spots related to anaerobic 2-propanol degradation are annotated.

**Table 3.3.1.1.** Identified proteins related to anaerobic 2-propanol degradation.

| Orf-No.[a] | Gene [a] | Functional description | Fold change[b] | Share of total protein[b] |
|---|---|---|---|---|
| **2-Propanol degradation**[c] | | | | |
| ebA4700 | *acxA* | Acetone carboxylase, β-subunit | 68.1 | 0.593 |
| ebA4701 | *acxB* | Acetone carboxylase, β-subunit | 11.8 | 0.760 |
| ebA4702 | *acxC* | Acetone carboxylase, γ-subunit | 175.4 | 3.888 |
| ebA4718 | *kctA* | Succinyl-CoA:3ketoacid-CoA transferase, subunit A | 48.0 | 1.716 |
| ebA4719 | *kctB* | Succinyl-CoA:3ketoacid-CoA transferase, subunit B | 66.9 | 0.860 |
| **Genetically related proteins**[c] | | | | |
| ebA4705 | | Hypothetical protein | 6.4 | 0.079 |
| ebA4712 | | Probable regulatory protein LysR | 754.7 | 3.846 |
| ebA4715 | | Hypothetical protein | 406.3 | 11.287 |

[a] listed in order of catalytic activity in the pathway
[b] average ratio and share of total protein (%) are indicated for cells grown anaerobically with 2-propanol
[c] as predicted by genome analysis (Rabus et al. 2005)

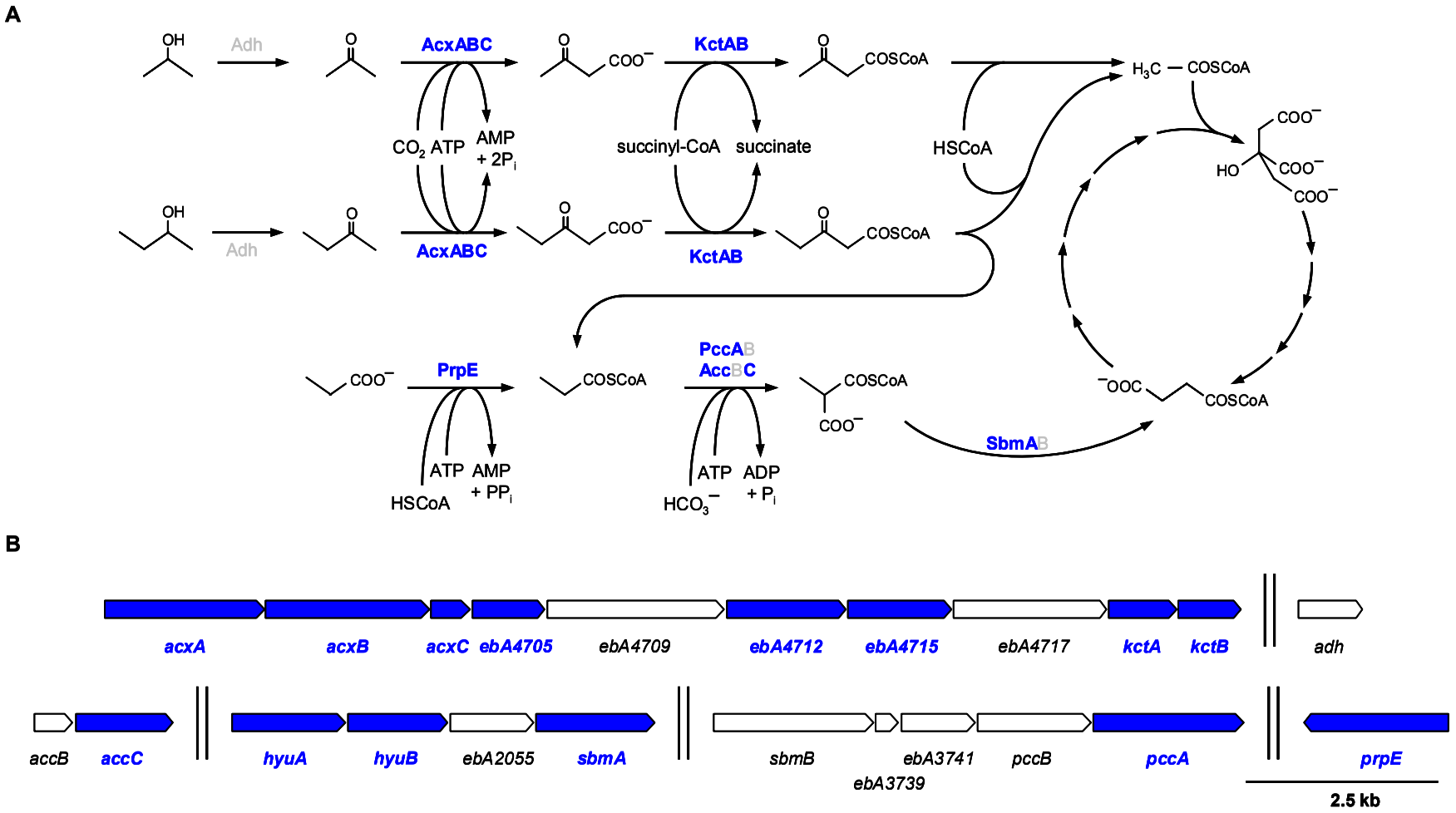


**Fig 3.3.1.** (**A**) Pathway of aerobic 2-propanol, acetone, 2-butanol, 2-butanone and propionate degradation. Enzyme names of indicated gene products are as described in Rabus et al. 2005. (**B**) Scale model for the organisation of the involved genes. Identified proteins and genes are highlighted in blue. (modified after Rabus et al. 2005).

## Biochemical baclground

Anaerobic degradation of acetone is initiated by carboxylation to acetoacetate (Sluis et al. 2002). Following activation to acetoacetyl-CoA, thiolytic cleavage yields two acetyl-CoA. Corresponding alcohols (e.g. 2-propanol) are channeled into this pathway via short-chain alcohol dehydrogenases.

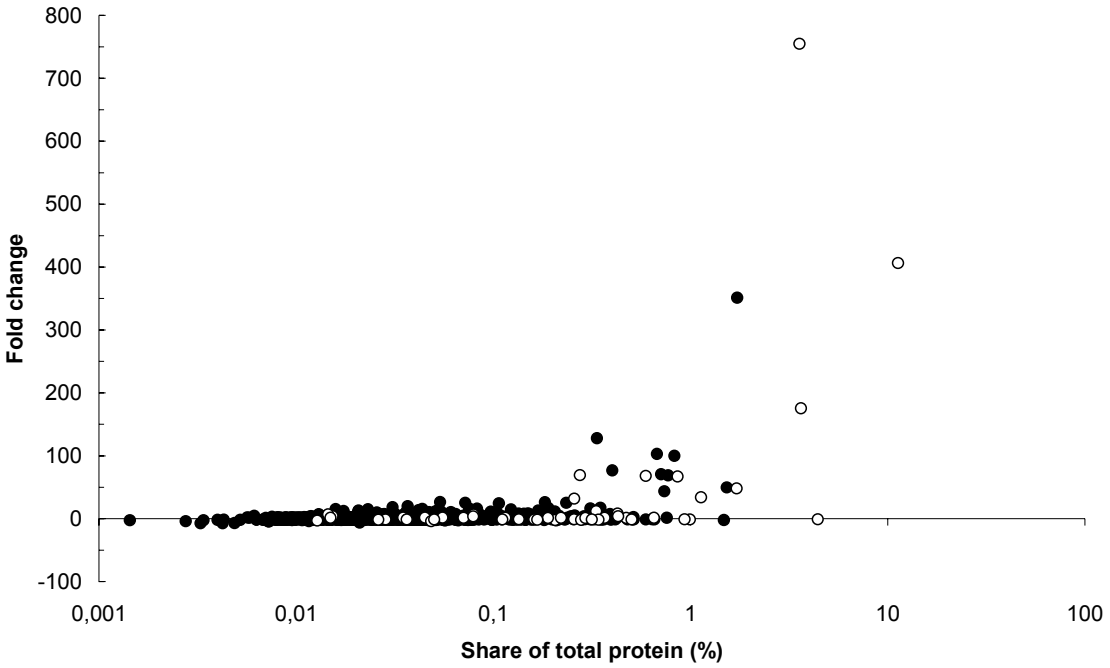


**Fig 3.3.1.1.2.** Fold changes in protein abundance and their relative share of total protein in cells aerobically grown with 2-propanol. Each dot represents a spot on the 2D-gel, except for repeatedly identified proteins (fold changes averaged and spot volumes summed up) (○) identified (●) not identified.

## 3.3.1.2. Acetone

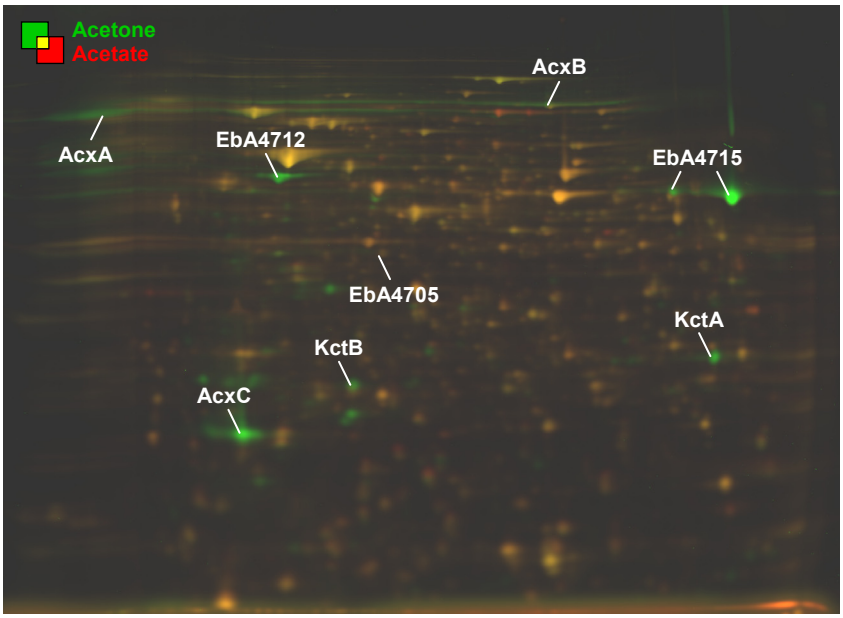


**Fig 3.3.1.2** Overlay image of 2D DIGE gels (pH 4-7). Protein spots appearing in green are up-regulated when cells were anaerobically grown with acetone. Whereas spots appearing in red are more abundant when cells were anaerobically grown with the reference substrate acetate. Spots related to anaerobic acetone degradation are annotated.

**Table 3.3.1.2.** Identified proteins related to anaerobic acetone degradation.

| Orf-No.[a] | Gene [a] | Functional description | Fold change[b] | Share of total proteinb[a] |
|---|---|---|---|---|
| **acetone degradation**[c] | | | | |
| ebA4700 | *acxA* | Acetone carboxylase, β-subunit | 45.7 | 0.319 |
| ebA4701 | *acxB* | Acetone carboxylase, β-subunit | 8.6 | 0.435 |
| ebA4702 | *acxC* | Acetone carboxylase, γ-subunit | 124.9 | 4.528 |
| ebA4718 | *kctA* | Succinyl-CoA:3ketoacid-CoA transferase, subunit A | 30.6 | 1.030 |
| ebA4719 | *kctB* | Succinyl-CoA:3ketoacid-CoA transferase, subunit B | 44.8 | 0.717 |
| **Genetically related proteins**[c] | | | | |
| ebA4705 | | Hypothetical protein | 3.8 | 0.026 |
| ebA4712 | | Probable regulatory protein LysR | 409.3 | 1.770 |
| ebA4715 | | Hypothetical protein | 219.0 | 3.905 |

[a] listed in order of catalytic activity in the pathway
[b] average ratio and share of total protein (%) are indicated for cells grown anaerobically with acetone
[c] as predicted by genome analysis (Rabus et al. 2005)

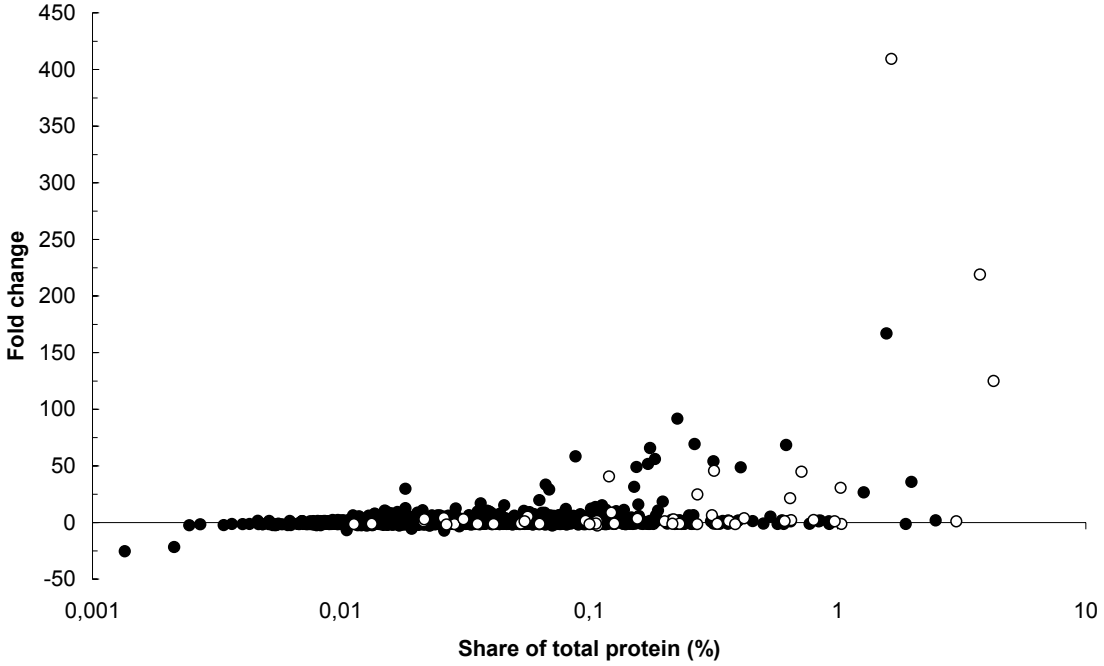


**Fig 3.3.1.2.1** Fold changes in protein abundance and their relative share of total protein in cells aerobically grown with acetone. Each dot represents a spot on the 2D-gel, except for repeatedly identified proteins (fold changes averaged and spot volumes summed up) (○) identified (●) not identified.

## 3.3.1.3. 2-Butanol

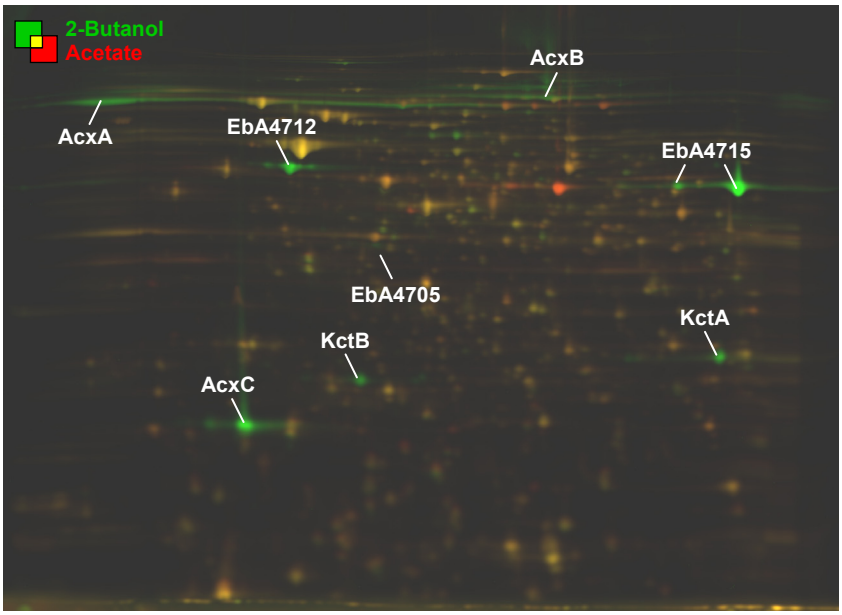


**Fig 3.3.1.3** Overlay image of 2D DIGE gels (pH 4-7). Protein spots appearing in green are up-regulated when cells were anaerobically grown with 2-butanol. Whereas spots appearing in red are more abundant when cells were anaerobically grown with the reference substrate acetate. Spots related to anaerobic 2-butanol degradation are annotated.

**Table 3.3.1.3.** Identified proteins related to anaerobic 2-butanol degradation.

| Orf-No.[a] | Gene [a] | Functional description | Fold change[b] | Share of total protein[b] |
|---|---|---|---|---|
| **acetone degradation**[c] | | | | |
| ebA4700 | *acxA* | Acetone carboxylase, β-subunit | 69.3 | 0.491 |
| ebA4701 | *acxB* | Acetone carboxylase, β-subunit | 12.0 | 0.875 |
| ebA4702 | *acxC* | Acetone carboxylase, γ-subunit | 185.6 | 4.879 |
| ebA4718 | *kctA* | Succinyl-CoA:3ketoacid-CoA transferase, subunit A | 46.9 | 1.436 |
| ebA4719 | *kctB* | Succinyl-CoA:3ketoacid-CoA transferase, subunit B | 64.3 | 0.785 |
| **Genetically related proteins**[c] | | | | |
| ebA4705 | | Hypothetical protein | 6.6 | 0.050 |
| ebA4712 | | Probable regulatory protein LysR | 689.0 | 3.048 |
| ebA4715 | | Hypothetical protein | 350.4 | 10.506 |

[a] listed in order of catalytic activity in the pathway
[b] average ratio and share of total protein (%) are indicated for cells grown anaerobically with 2-butanol
[c] as predicted by genome analysis (Rabus et al. 2005)

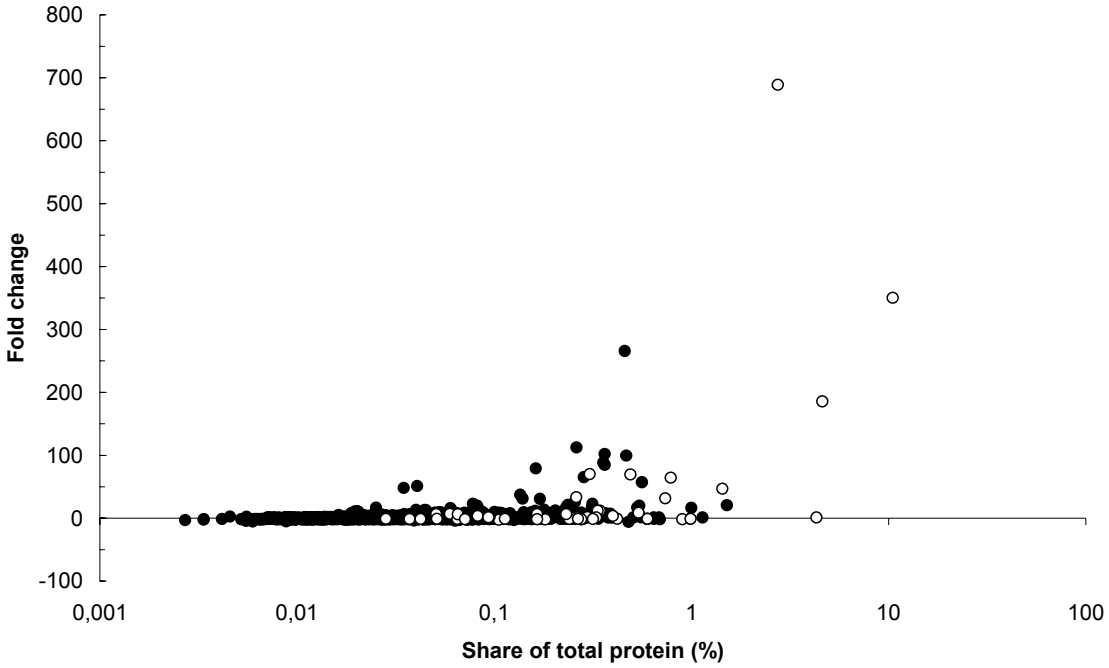


**Fig 3.3.1.3.1** Fold changes in protein abundance and their relative share of total protein in cells aerobically grown with 2-butanol. Each dot represents a spot on the 2D-gel, except for repeatedly identified proteins (fold changes averaged and spot volumes summed up) (○) identified (●) not identified.

## 3.3.1.4. 2-Butanone

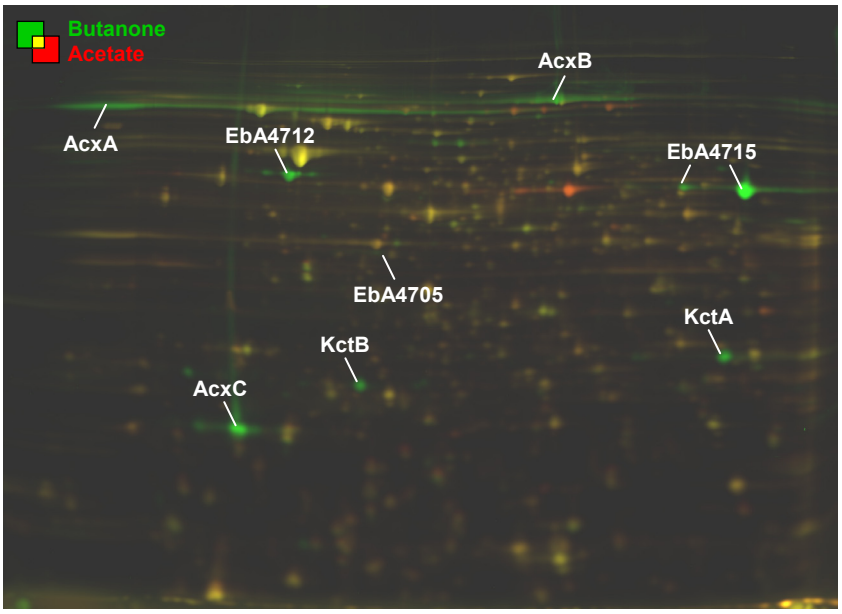


**Fig 3.3.1.4.** Overlay image of 2D DIGE gels (pH 4-7). Protein spots appearing in green are up-regulated when cells were anaerobically grown with 2-butanone. Whereas spots appearing in red are more abundant when cells were anaerobically grown with the reference substrate acetate. Spots related to anaerobic 2-butanone degradation are annotated.

**Table 3.3.1.4.** Identified proteins related to anaerobic 2-butanone degradation.

| Orf-No.[a] | Gene [a] | Functional description | Fold change[b] | Share of total protein[b] |
|---|---|---|---|---|
| **acetone degradation**[c] | | | | |
| ebA4700 | *acxA* | Acetone carboxylase, β-subunit | 56.9 | 0.440 |
| ebA4701 | *acxB* | Acetone carboxylase, β-subunit | 10.1 | 0.965 |
| ebA4702 | *acxC* | Acetone carboxylase, γ-subunit | 149.5 | 3.846 |
| ebA4718 | *kctA* | Succinyl-CoA:3ketoacid-CoA transferase, subunit A | 39.4 | 1.322 |
| ebA4719 | *kctB* | Succinyl-CoA:3ketoacid-CoA transferase, subunit B | 52.9 | 0.673 |
| **Genetically related proteins**[c] | | | | |
| ebA4705 | | Hypothetical protein | 4.6 | 0.047 |
| ebA4712 | | Probable regulatory protein LysR | 466.9 | 2.391 |
| ebA4715 | | Hypothetical protein | 242.2 | 7.666 |

[a] listed in order of catalytic activity in the pathway
[b] average ratio and share of total protein (%) are indicated for cells grown anaerobically with 2-butanone
[c] as predicted by genome analysis (Rabus et al. 2005)

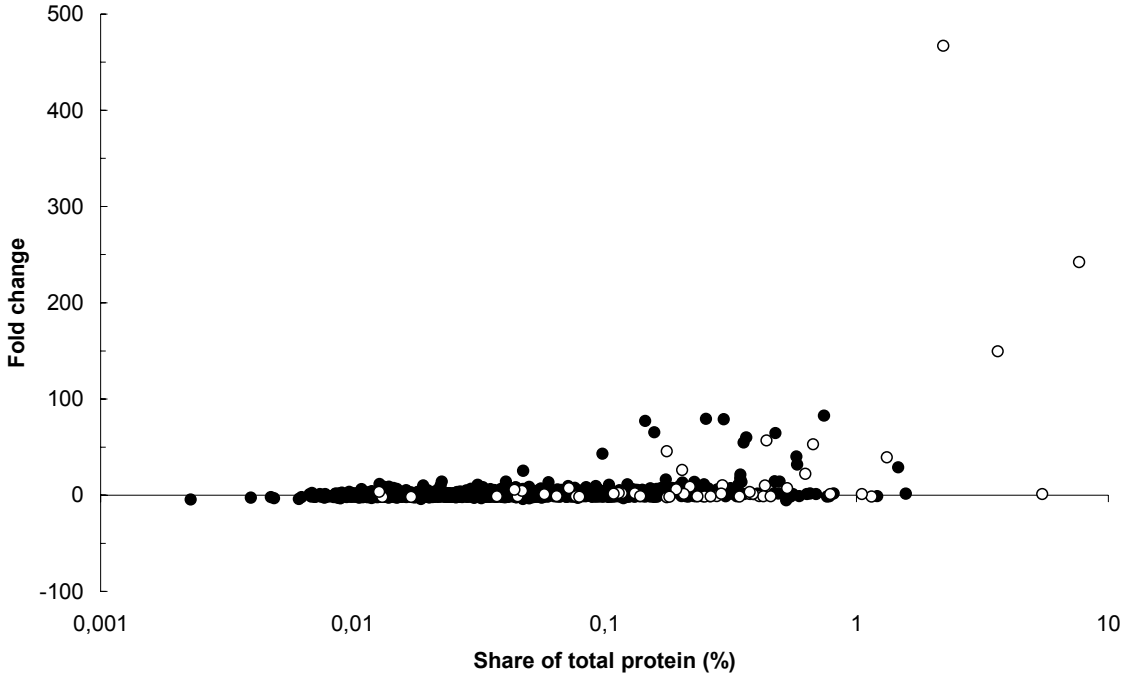


**Fig 3.3.1.4.1.** Fold changes in protein abundance and their relative share of total protein in cells aerobically grown with 2-butanone. Each dot represents a spot on the 2D-gel, except for repeatedly identified proteins (fold changes averaged and spot volumes summed up) (○) identified (●) not identified.

## 3.3.2. Propionate

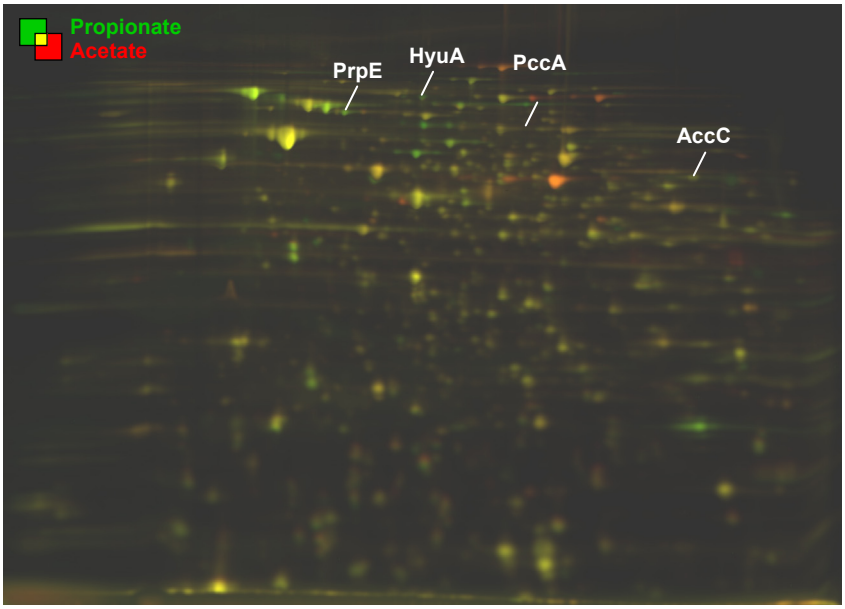


**Fig 3.3.2.1.** Overlay image of 2D DIGE gels (pH 4-7). Protein spots appearing in green are up-regulated when cells were anaerobically grown with propionate. Whereas spots appearing in red are more abundant when cells were anaerobically grown with the reference substrate acetate. Spots related to anaerobic propionate degradation are annotated.

**Table 3.3.2.** Identified proteins related to anaerobic propionate degradation.

| Orf-No.[a] | Gene [a] | Functional description | Fold change[b] | Share of total protein[b] |
|---|---|---|---|---|
| **acetone degradation**[c] | | | | |
| ebA7220 | *prpE* | Propionate-CoA ligase | -1.5 | 0.056 |
| ebA1474 | *pccA* | Propionyl-CoA carboxylase, α-subunit | 8.1 | 0.097 |
| ebA3743 | *accC* | Putative biotin carboxylase protein | 1.4 | 0.156 |
| **Genetically related proteins**[c] | | | | |
| ebA2051 | *hyuA* | Hydantoin utilization protein A | 2.1 | 0.089 |

[a] listed in order of catalytic activity in the pathway
[b] average ratio and share of total protein (%) are indicated for cells grown anaerobically with propionate
[c] as predicted by genome analysis (Rabus et al. 2005)

### Biochemical background

The pathway of propionate degradation was proposed to proceed via the methylmalonyl-CoA pathway (Rabus et al. 2005), involving propionyl-CoA ligase (PrpE), propionyl-CoA carboxylase (PccAB) and methylmalonyl-CoA mutase (SbmAB). In the present proteomic study, PrpE, PccA and the biotin carboxylase subunit (AccC), possibly delivering carboxylated biotin carrier protein, were identified

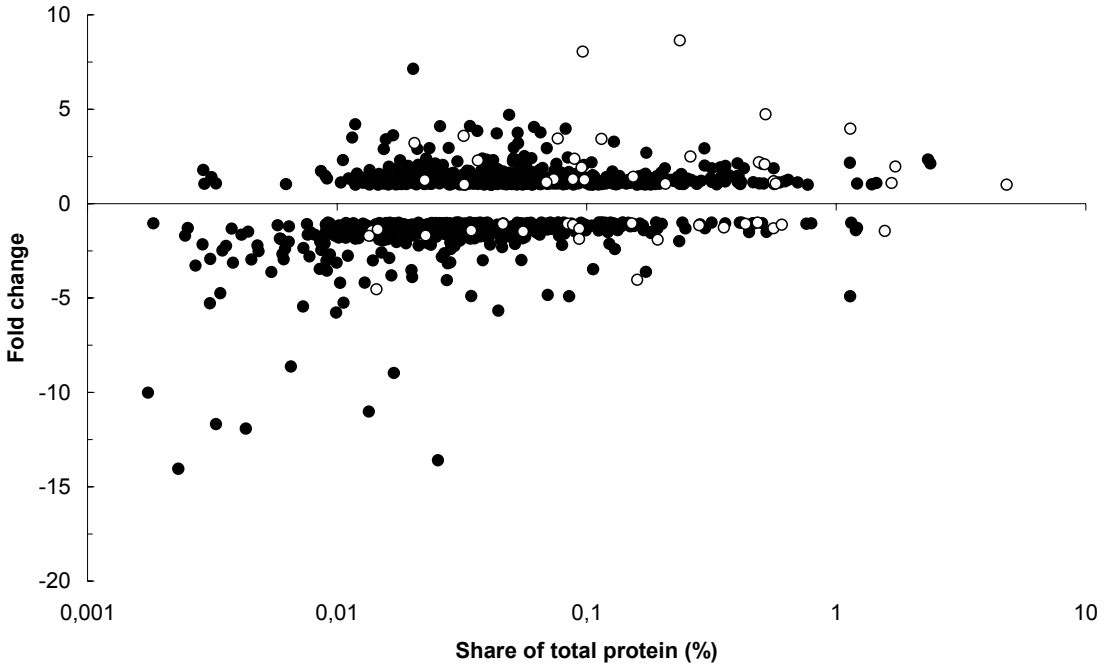


**Fig 3.3.2.2.** Fold changes in protein abundance and their relative share of total protein in cells aerobically grown with propionate. Each dot represents a spot on the 2D-gel, except for repeatedly identified proteins (fold changes averaged and spot volumes summed up) (○) identified (●) not identified.

# 4. Central and other metabolic features

# 4.4. Glycolysis and gluconeogenesis, glyoxylate shunt and TCA-cycle

## 4.4.1 Glycolysis and gluconeogenesis

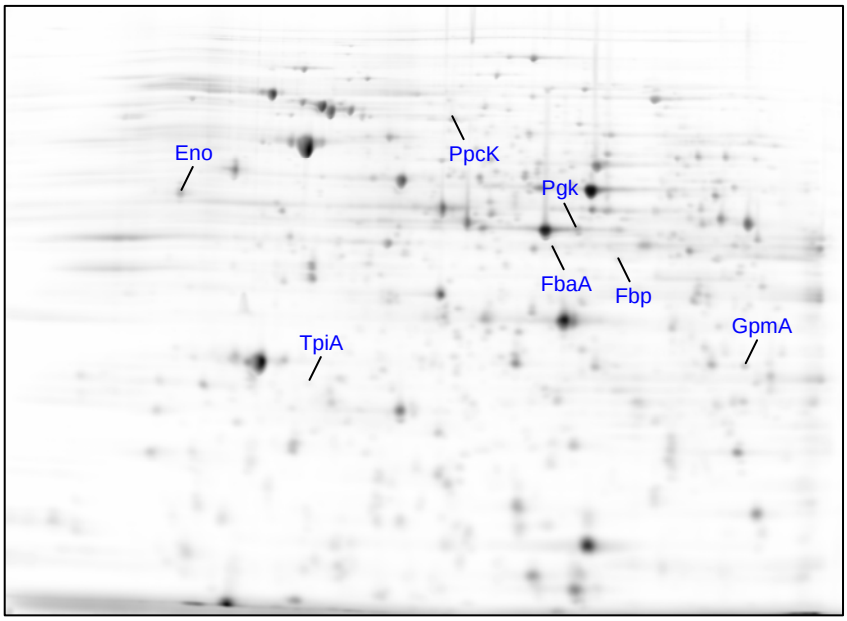


**Fig.4.4.1.** 2DE gel (pH 4-7) of cells grown anaerobically with benzoate. Identified proteins related to glycolysis and gluconeogenesis are annotated.

**Table 4.4.1.** Identified proteins related to glycolysis and gluconeogenesis.

| Orf-No. | Gene | Functional description |
|---|---|---|
| ebA1052 | *gpmA* | 2,3-bisphosphoglycerate-dependent phosphoglycerate mutase |
| ebA1102 | *gapA* | Glyceraldehyde-3-phosphate dehydrogenase |
| ebA1103 | *pgk* | Phosphoglycerate kinase |
| ebA1107 | *fbaA* | Fructose-1,6-bisphosphate aldolase |
| ebA1191 | *fbp* | Fructose-1,6-bisphosphatase |
| ebA4040 | *ppcK* | Phosphoenoylpyruvate carboxykinase |
| ebA4831 | *tpiA* | Triosephosphate isomerase |
| ebA5208 | *pgi* | Glucose-6-phosphate isomerase |
| ebA6162 | *eno* | Enolase |

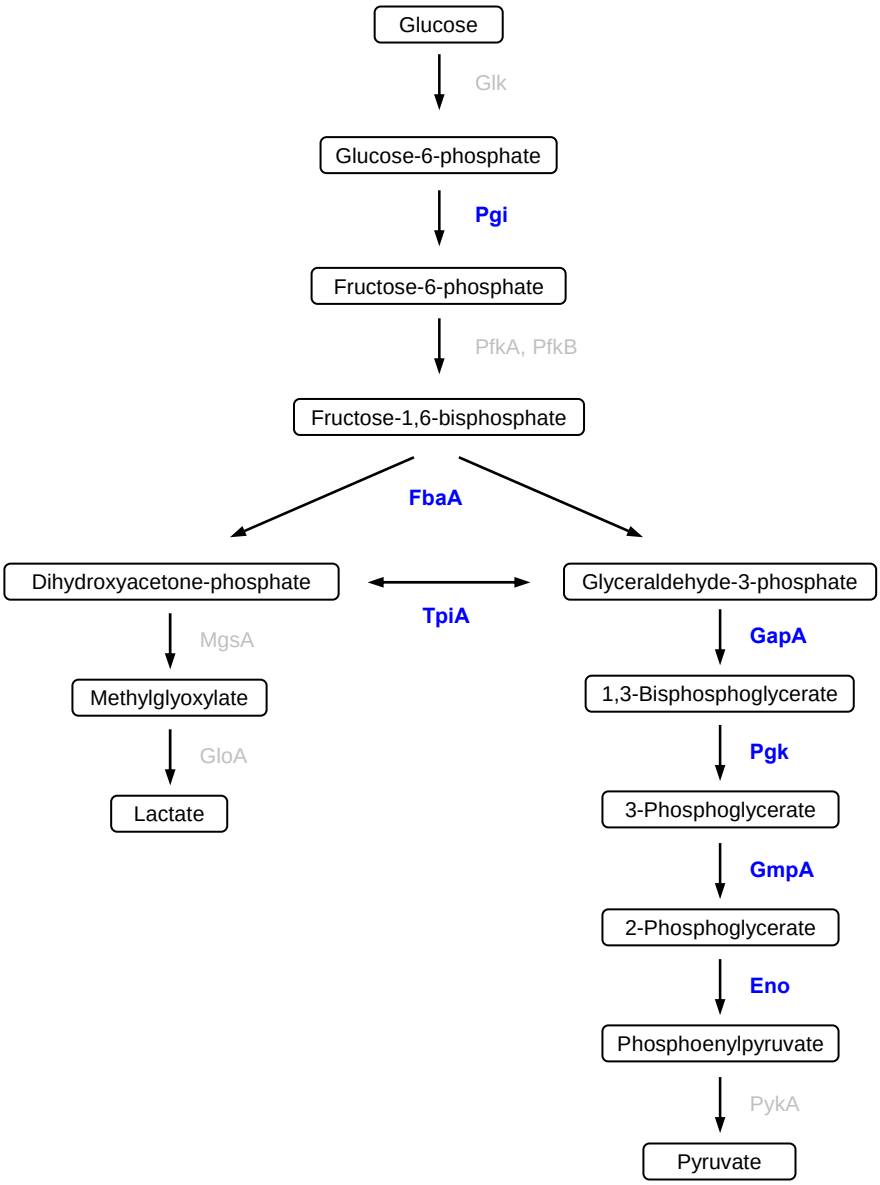


**Fig 4.4.1.1.** Schematic representation of glycolysis. Proteins involved in the different steps are indicated next to the arrows. Substrates and intermediates are framed. Identified proteins are highlighted in blue (modified from Rabus et al. 2005).

## 4.4.2 Glyoxylate shunt

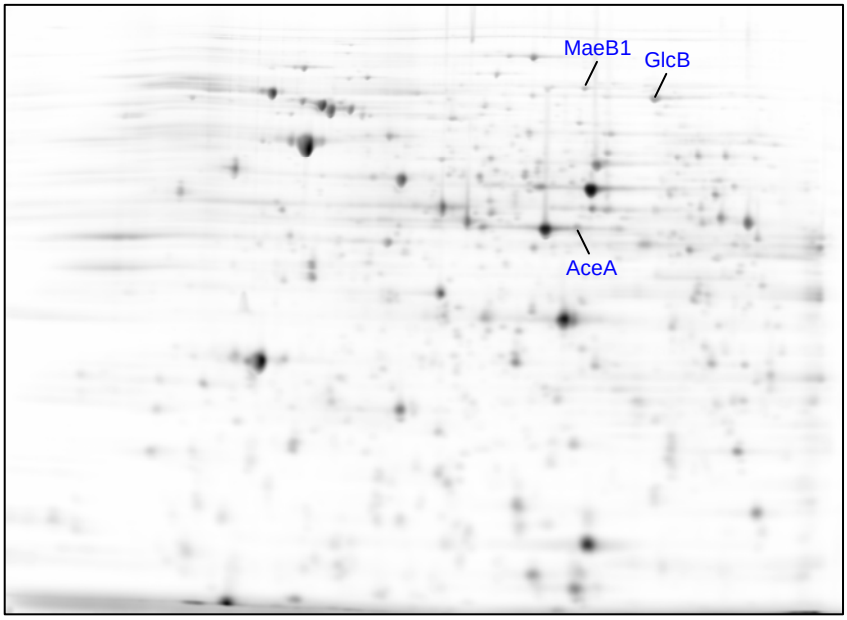


**Fig.4.4.2.** 2DE gel (pH 4-7) of cells grown anaerobically with benzoate. Identified proteins related to the glyoyxlate shunt are annotated.

**Table 4.4.2.** Identified proteins related to the glyoxylate shunt.

| Orf-No. | Gene | Functional description |
|---|---|---|
| ebA819 | *glcB* | Malate synthase G |
| ebA4382 | *maeB1* | NADP-dependent malic enzyme |
| ebA4473 | *aceA* | Isocitrate lyase |

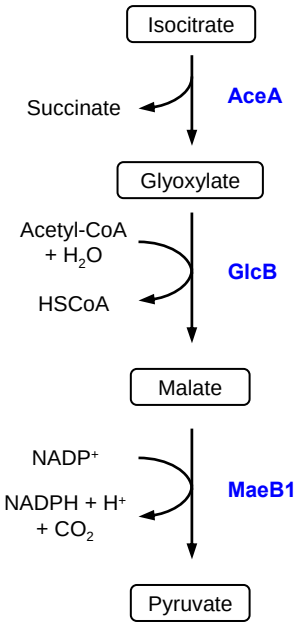


**Fig 4.4.2.1.** Schematic representation of the glyoxylate shunt. Proteins involved in the different steps are indicated next to the arrows. Substrates and intermediates are framed. Identified proteins are highlighted in blue (modified from Rabus et al. 2005).

## 4.4.3 TCA-cycle

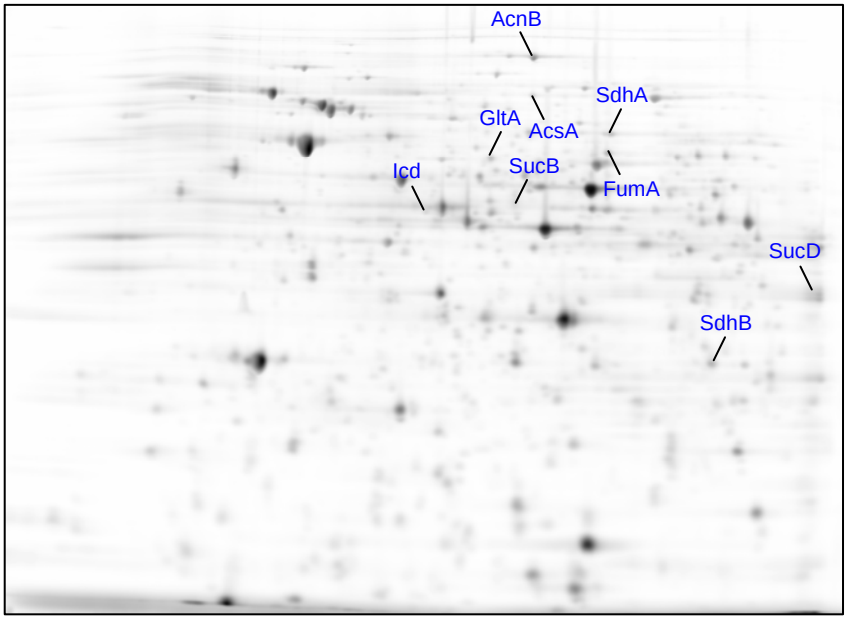


**Fig.4.4.3.** 2DE gel (pH 4-7) of cells grown anaerobically with benzoate. Identified proteins related to the TCA-cycle are annotated.

**Table 4.4.3.** Identified proteins related to the TCA-cycle.

| Orf-No. | Gene | Functional description |
|---|---|---|
| ebA172 | *acsA* | Acetyl-CoA synthetase |
| ebA173 | *fumA* | Fumarate hydratase |
| ebA829 | *icd* | Isocitrate dehydrogenase |
| ebA1271 | *sucD* | Succinyl-CoA synthetase, α-chain |
| ebA5265 | *acnB* | Aconitase |
| ebA6684 | *sucB* | 2-oxoglutarate dehydrogenase complex, dihydrolipoamide succinyltransferase |
| ebA6687 | *gltA* | Citrate synthase |
| ebA6689 | *sdhA* | Succinate dehydrogenase, iron-sulfur protein |
| ebA6690 | *sdhB* | Succinate dehydrogenase, flavoprotein subunit |

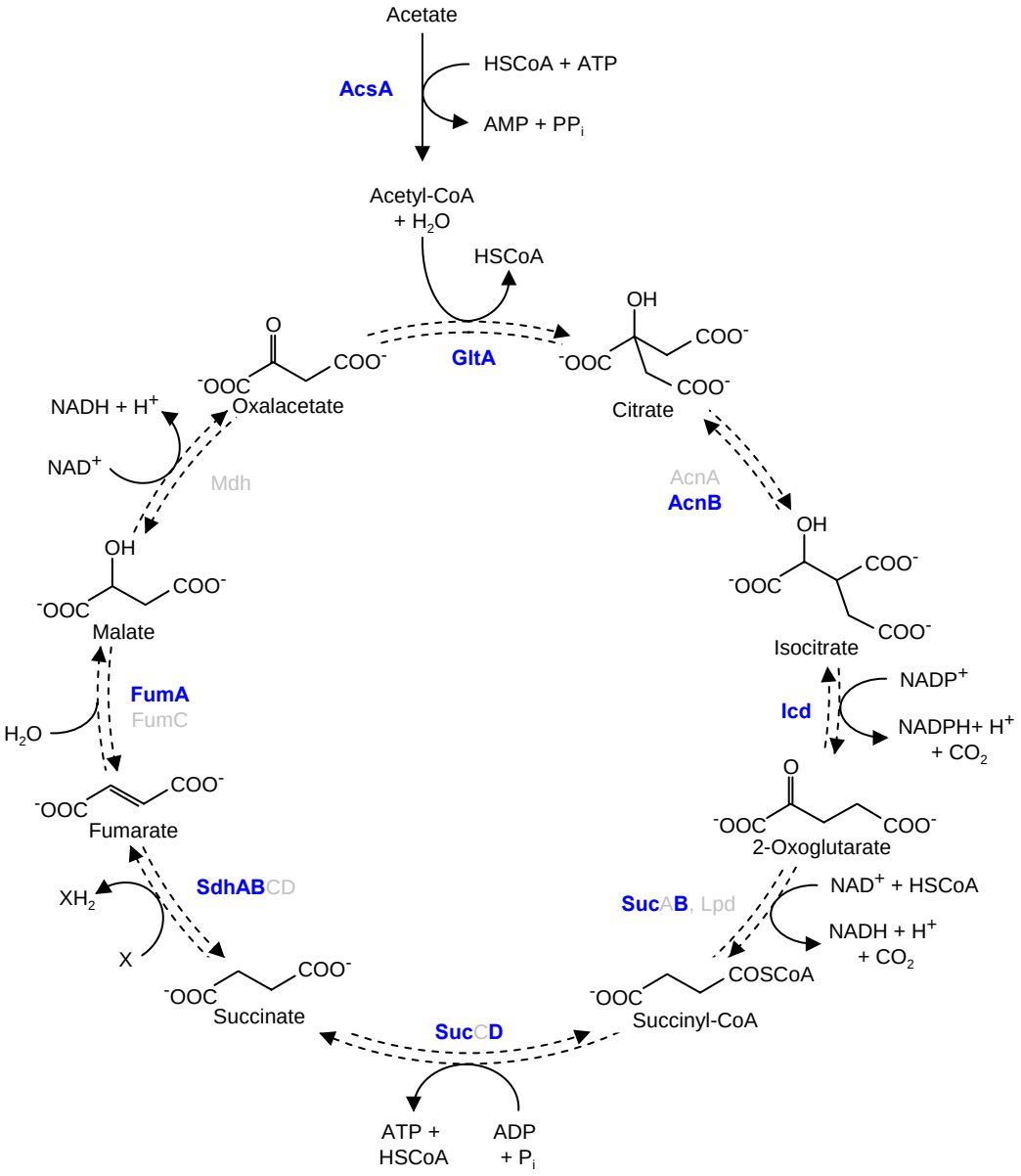


**Fig 4.4.3.1.** Schematic representation of the TCA-cycle. Proteins involved in the different steps are indicated next to the arrows. Substrates and intermediates are framed. Identified proteins are highlighted in blue (modified from Rabus et al. 2005).

## 4.5. Respiratory energy generation

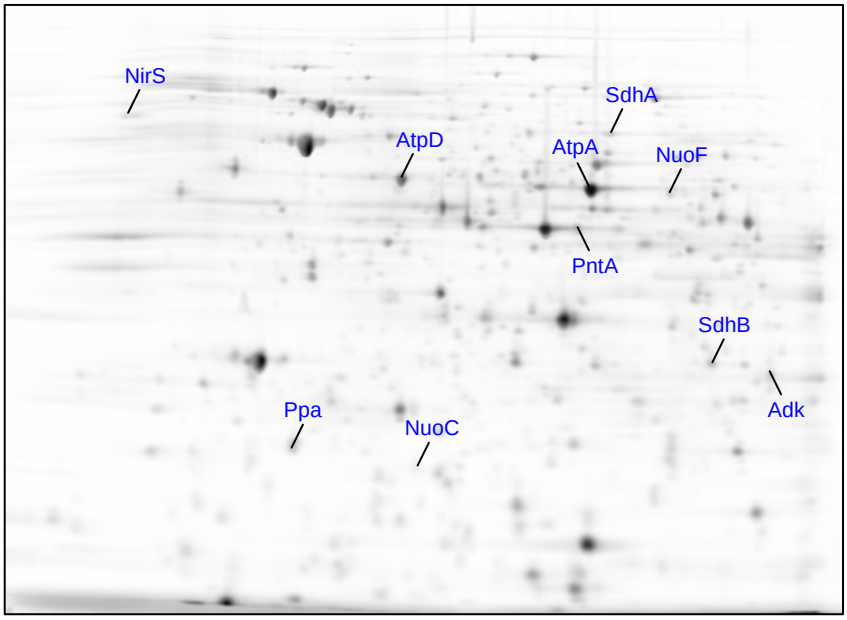


**Fig.4.5.** 2DE gel (pH 4-7) of cells grown anaerobically with benzoate. Identified proteins related to respiratory energy generation are annotated.

**Table 4.5.** Identified proteins related to respiratory energy generation

| Orf-No. | Gene | Functional description |
|---|---|---|
| ebA888 | *nirS* | Cytochrome cd1 nitrite reductase precursor |
| ebA3004 | *atpA* | F1-ATP synthase, α-subunit |
| ebA3007 | *atpD* | F1-ATP synthase, β-subunit |
| ebA4497 | *pntA* | Pyridine nucleotide transhydrogenase, α-subunit |
| ebA4836 | *nuoC* | NADH dehydrogenase I, chain C |
| ebA4840 | *nuoF* | NADH dehydrogenase I, chain F |
| ebA5087 | *adk* | Adenylate kinase |
| ebA6689 | *sdhB* | Succinate dehydrogenase, iron-sulfur protein |
| ebA6690 | *sdhA* | Succinate dehydrogenase, flavoprotein subunit |
| ebA7053 | *ppa* | Inorganic diphosphatase |

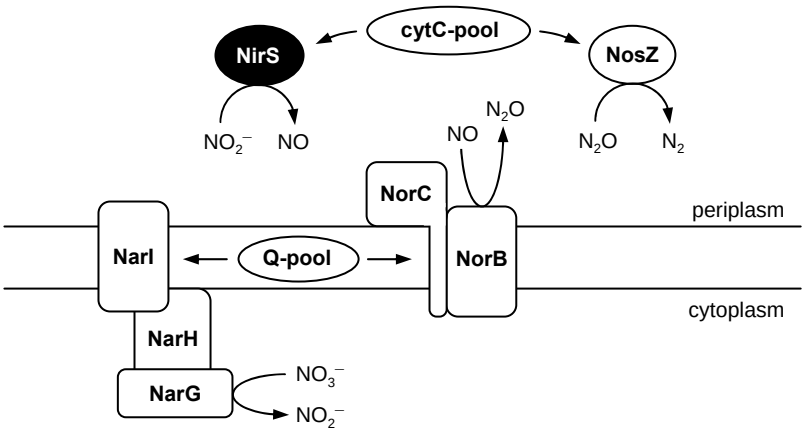


**Fig.4.5.1.** Schematic depiction of dissimilatory nitrate reduction to dinitrogen. The identified nitrate reductase (**NirS**) is indicated in black (modified from Shapleigh, 2006).

## 4.5.2. NADH:ubiquinol oxidoreductase

The $F_0F_1$ ATP synthase is a large multisubunit complex that couples translocation of protons down an electrochemical gradient to the synthesis of ATP. The $\alpha_3\beta_3$ hexamer (**AtpA** and **AtpD**) containing the catalytic sites in each of the β subunits surrounds the rotor shaft made up of the γ subunit coiled coil. The rest of the proposed rotor consists of the ε and c subunits. The stator $\alpha_3\beta_3$ and the a subunits are connected by the δ and two b subunits. The 10-12 c subunits are believed to be arranged in a ring, with subunit a on the side. Proton transport is mediated between the a and c subunits (Fig 4.5.2.; Nakamoto et al. 1999).

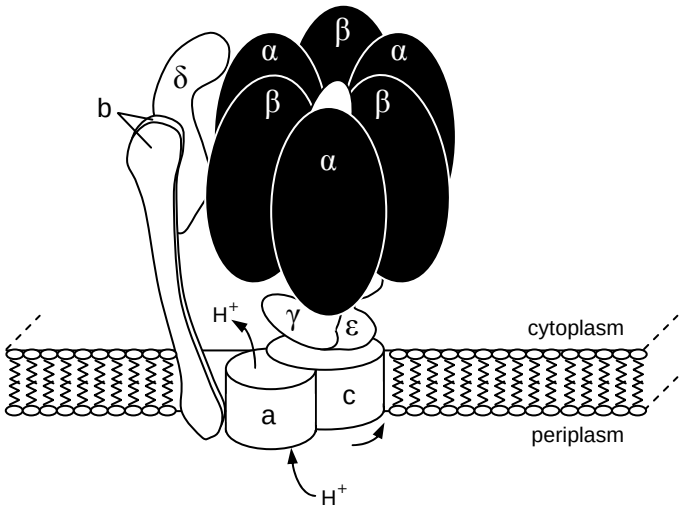


**Fig 4.5.2.** Schematic subunit arrangement of the $F_0F_1$ ATP synthase and the proposed proton pathway in $F_0$. The identified α (**AtpA**) and β subunit (**AtpD**) are indicated in black (modified from Nakamoto et al. 1999).

## 4.5.3. Oxygen respiration

The succinate dehydrogenase is a tetrameric protein of the TCA-cycle as well as of the respiratory chain. It is a membrane bound flavoprotein with remarkably similar physical and catalytic properties compared to fumarate reductase. The enzyme catalyzes the oxidation of succinate to fumarate as one step of the TCA cycle and transfers the electrons directly to the ubiquinone pool (Ackrell 2000).

The complex can be resolved in two parts. (I) the hydrophilic domain, containing a flavoprotein subunit (**SdhA**), in which the covalent FAD co-factor of the enzyme is part of the catalytic site, and an iron sulfur subunit (**SdhB**), containing three different clusters $[2Fe\text{-}S]^{2+,\,1+}$, $[4Fe\text{-}4S]^{2+,\,1+}$, and $[3Fe\text{-}4S]^{1+,\,0}$ for electron transfer between FAD and membrane quinone (Ackrell 2000). (II) the hydrophobic domain, containing two membrane embedded polypeptides (SdhC and SdhD) that interact with ubiquinone and anchor the catalytic domain at the membrane surface (Cecchini et al. 2002).

The NADH dehydrogenase I is a multisubunit complex, catalyzing the electron transfer from NADH to quinone coupled with the translocation of four protons across the membrane, contributing to the proton motive force. In general, the bacterial complex consists of 14 different subunits. Homologues of these are part of complex I in all species known so far. The 14 different subunits can be classified in two groups: (I) seven subunits (**Nuo**B**C**DE**F**GI) are peripheral proteins including the subunits that bear all known redox groups of complex I. In addition, NuoF contains the NADH binding site and NuoB and D are probably involved in quinone binding. (II) The remaining seven subunits (NuoAHJKLMN) are mostly hydrophobic proteins predicted of folding inti 54 α-helices across the membrane. These subunits do not contain typical cofactor-binding motives, but are most likely involved in proton translocation (Friedrich and Böttcher 2004).

### 4.5.5. Other related proteins

Pyridine nucleotide transhydrogenase (**PntA**B) catalyzes the reversible transfer of a hydride ion equivalent between NAD and NADP and is a major source of NADPH in *E. coli*. In the course of the reaction one H atom is transferred from inside the cell to the outside (Fig. 4.5.5.). This reaction is an important redox exchange reaction, functioning as a proton pump across the inner membrane. In *E. coli* the functional enzyme assembles as a tetramer composed of two alpha and two beta subunits. PntAB is a major source of NADPH in the cell (Sauer et al. 2004).

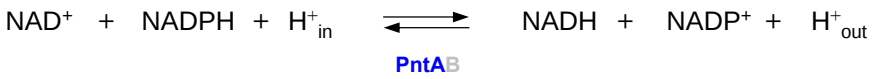


**Fig 4.5.5.** Reaction catalyzed by the pyridine nucleotide transhydrogenase (PtnAB) in *E. coli* (modified from Sauer et al. 2004).

Adenylate kinase (**Adk**) is an essential enzyme, responsible for recycling AMP in energetically active cells. The enzyme can utilize both ribo- and desoxyribonucleotides as substrates. Although highly specific for AMP and dAMP, detectable activity is observed when ATP or dATP is replaced by a variety of ribonucleoside triphosphates. Adenylate kinase also has nucleoside diphosphate kinase activity. Using ATP as the phosphate donor it can convert ribonucleoside diphosphates and desoxyribonucleoside triphosphates to the respective nucleoside triphosphate (Ishige and Noguchi 2000).

# 4.6. β-oxidation

## 4.6.1 CoA-ligases

## 4.6.4 Acyl-CoA dehydrogenases

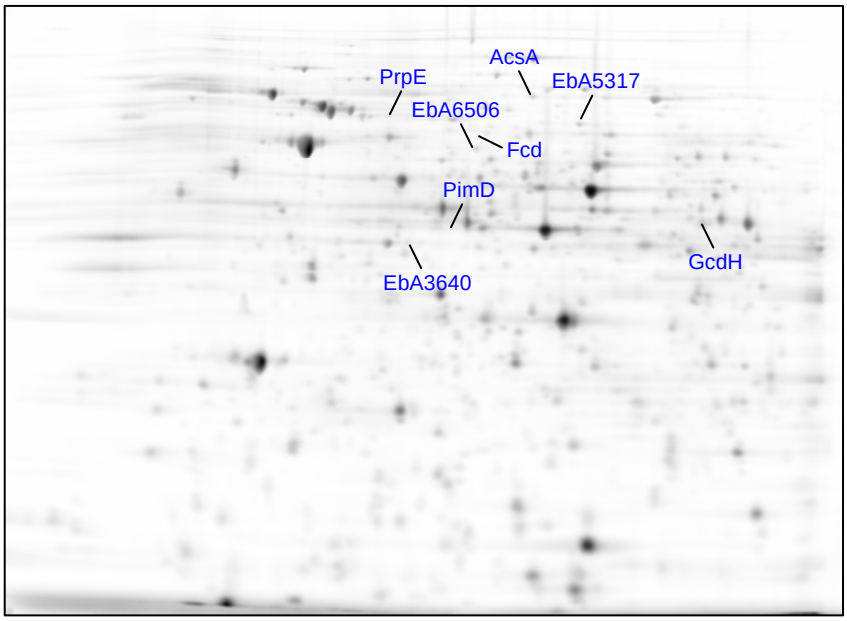


**Fig.4.6.1.** 2DE gel (pH 4-7) of cells grown anaerobically with benzoate. Identified proteins related to β-oxidation (CoA-ligases and acyl-CoA dehydrogenases) are annotated.

**Table 4.6.1.** Identified proteins related to CoA-ligases

| Orf-No. | Gene | Functional description |
|---|---|---|
| ebA1206 | *acsA* | Putative acetyl-CoA synthetase |
| ebA2050 | *fcd* | Putative ADP-producing CoA ligase, similar to feruloly-CoA synthetase |
| ebA5317 | | Long-chain-fatty-acid-CoA ligase |
| ebA7220 | *prpE* | Propionate-CoA ligase |

**Table 4.6.2.** Identified proteins related to acyl-CoA dehydrogenases

| Orf-No. | Gene | Functional description |
|---|---|---|
| ebA5669 | *pimD* | Putative pimeloyl-CoA dehydrogenase |
| ebA3640 | | Putative acyl-CoA dehydrogenase oxidoreductase protein |
| ebA6506 | | Acyl-CoA dehydrogenase |
| ebA2993 | *gcdH* | Glutaryl-CoA dehydrogenase |

## 4.6.5 Electron transfer flavoproteins

## 4.6.6 Enoyl-CoA hydratases / isomerases

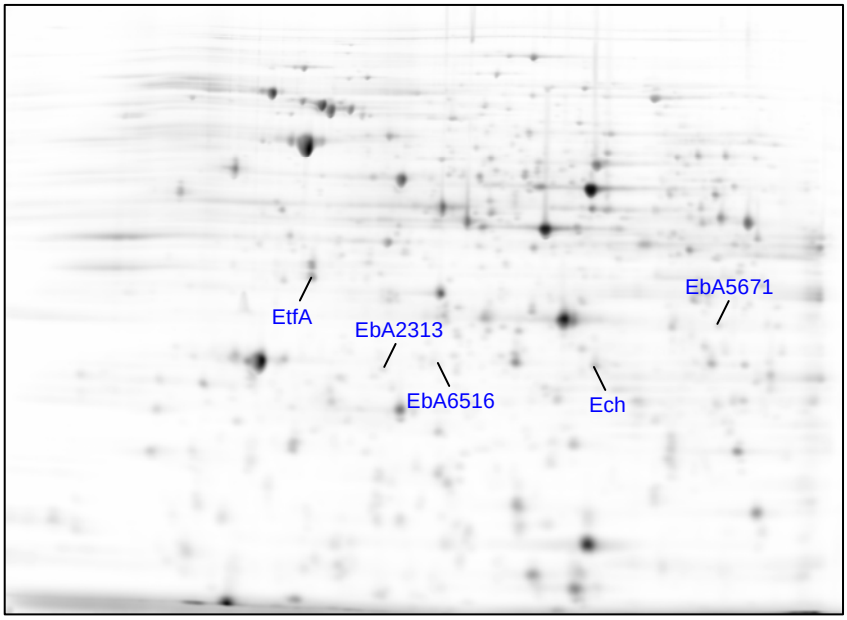


**Fig.4.6.1.** 2DE gel (pH 4-7) of cells grown anaerobically with benzoate. Identified proteins related to β-oxidation (electron transfer flavoproteins and enoyl-CoA hydratases / isomerases) are annotated.

**Table 4.6.5.** Identified protein related to electron transfer flavoproteins

| Orf-No. | Gene | Functional description |
|---|---|---|
| ebA6510 | *etfA* | Electron transfer flavoprotein, α-subunit |

**Table 4.6.6.** Identified proteins related to enoyl-CoA hydratases / isomerases

| Orf-No. | Gene | Functional description |
|---|---|---|
| ebA1321 | *ech* | Putative enoyl-CoA hydratase protein |
| ebA2313 | | Putative enoyl-CoA hydratase II |
| ebA5671 | | Predicted MaoC-like (R)-specific enoyl-CoA hydratase |
| ebA6516 | | Enoyl-CoA hydratase |

## 4.6.7 Short chain alcohol dehydrogenases

## 4.6.8 Thiolases

## 4.6.9 Other alcohol and aldehyde dehydrogenases

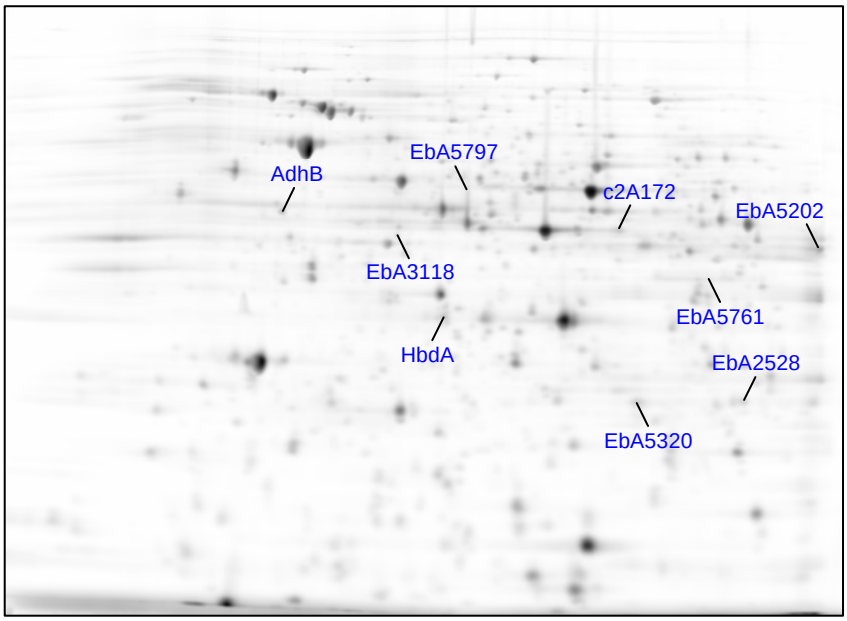


**Fig.4.6.2.** 2DE gel (pH 4-7) of cells grown anaerobically with benzoate. Identified proteins related to β-oxidation (short chain alcohol dehydrogenases, thiolases and other alcohol and aldehyde dehydrogenases) are annotated.

**Table 4.6.7.** Identified proteins related to short chain alcohol dehydrogenases

| Orf-No. | Gene | Functional description |
|---|---|---|
| ebA2528 | | Probable dehydrogenase |
| ebA4742 | *hbdA* | 3-hydroxybutyryl-CoA dehydrogenase |
| ebA5320 | | Putative 3-hydroxyacyl-CoA dehydrogenase precursor |

**Table 4.6.8.** Identified proteins related to thiolases

| Orf-No. | Gene | Functional description |
|---|---|---|
| ebA5202 | | Putative thiolase |
| ebA5797 | | Thiolase |
| c2A172 | | β-ketoadipyl-CoA thiolase |

**Table 4.6.9.** Identified protein related to other alcohol and aldehyde dehydrogenases

| Orf-No. | Gene | Functional description |
|---|---|---|
| ebA3118 | | Probable zinc-containing alcohol dehydrogenase |
| ebA4623 | *adhB* | Alcohol dehydrogenase II |
| ebA5761 | | Putative oxidoreductase, zinc-containing alcohol dehydrohgenase |

## β-oxidation in general

The initial step of β-oxidation is the conversion of free fatty acids into metabolically active conenzyme A thioesters. This reaction is catalyzed by either AMP- or ADP-forming acyl-CoA synthetases (or ligases respectively; **AcsA**, **EbA5317**, **PrpE**; Kunau et al. 1995).

The first step in the degradation of the activated fatty acids is performed by acyl-CoA dehydrogenases (e.g. **PimD**, **EbA6506**). These enzymes catalyze the desaturation at positions α,β (α,β-dehydrogenation) of various CoA-conjugated fatty acids that stem from either the β-oxidation cycle or amino acid metabolism. In this process, two reducing equivalents are generated that are transferred to an electron transferring flavoprotein (ETF; **EtfA**) and from this to the respiratory chain via ETF dehydrogenase (Ghisla and Thorpe 2004).

The addition of water, catalyzed by a enoyl-CoA hydratase (e.g. **Ech**, **EbA2313**), is followed by a $NAD^+$-specific β-hydroxyacyl-CoA dehydrogenase (e.g. **HbdA**, **EbA2528**) reaction. Finally, cleavage of the β-oxoacyl-CoA with CoA proceeds under catalysis of β-ketothiolases (e.g. **EbA5202**, **EbA5797**).

Even-numbered fatty acids yield only acetyl-CoA. With odd-numbered fatty acids, the final β-oxidation cycle yields acetyl-CoA and propionyl-CoA, which can be further metabolized via the methylmalonyl-pathway (for details see 3.3.3.) yielding succinyl-CoA.

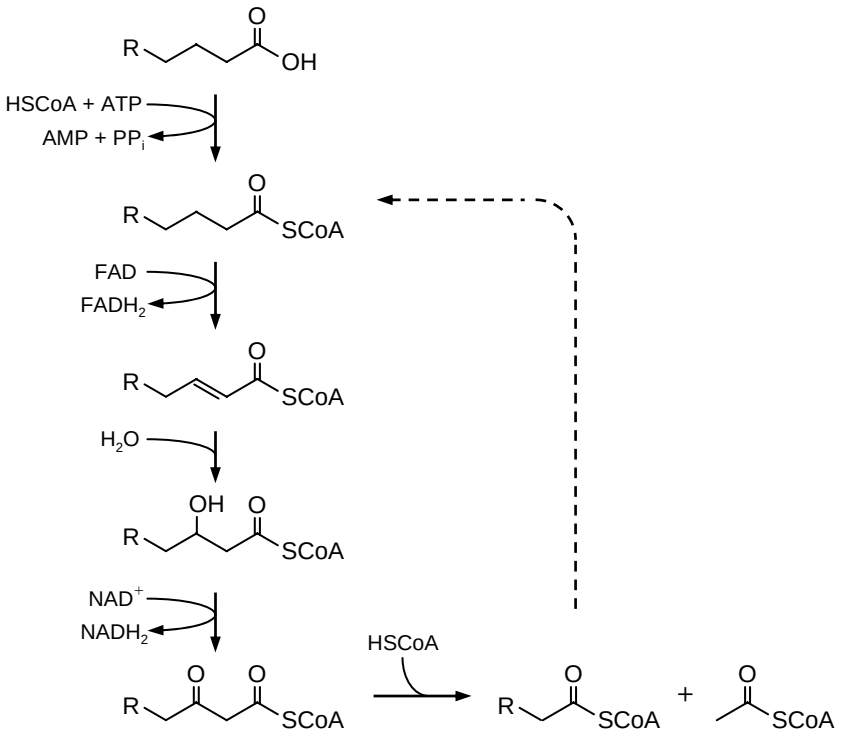


**Fig.4.6.3.** β-oxidation of fatty acids.

# 4.7. Metalloenzymes and related proteins

## 4.7.7. Aconitase and endonuclease III

## 4.7.8. Ferredoxins

## 4.7.10. Fe-S cluster biosynthesis

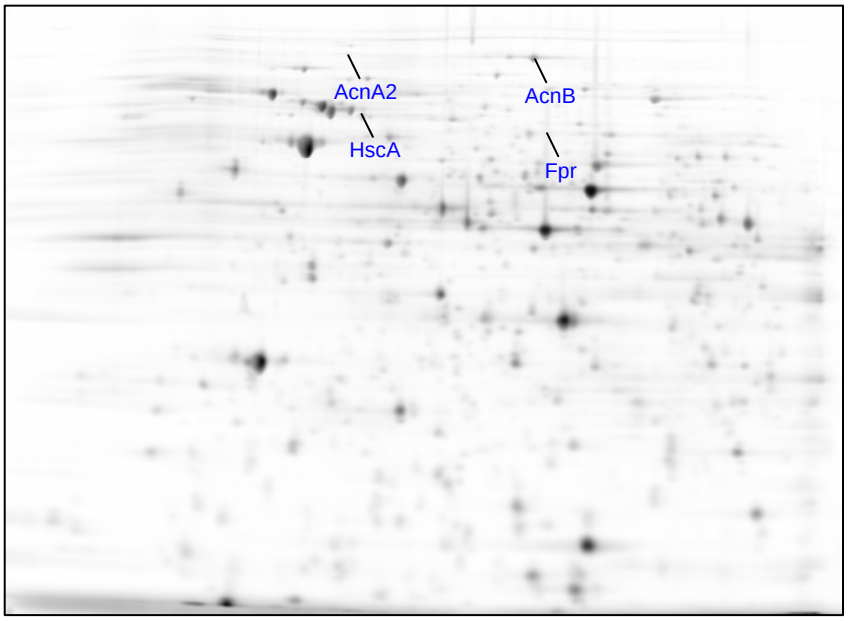


**Fig.4.7.1.** 2DE gel (pH 4-7) of cells grown anaerobically with benzoate. Identified proteins related to aconitase and endonuclease III and Fe-S cluster biosynthesis are annotated.

**Table 4.7.7.** Identified proteins related to aconitase and Fe-S cluster biosynthesis.

| Orf-No. | Gene | Functional description |
|---|---|---|
| ebA5265 | *acnB* | Aconitase |
| ebA6110 | *fpr* | Ferredoxin-NADP reductase |
| ebA6396 | *hscA* | Chaperone protein involved in Fe-S cluster synthesis (DnaK paralog) |
| ebA6773 | *acnA2* | Aconitase |

### 4.7.7. Aconitase

Aconitases catalyze the interconversion of citrate and isocitrate via *cis*-aconitate in the TCA and glyoxylate cycles. They are monomeric enzymes that contain one [4Fe-4S] cluster that is essential for catalytic activity. *E. coli* contains two genetically and biochemically distinct aconitases (AcnA and AcnB). Physiological and enzymological studies have shown that **AcnB** is the major TCA cycle enzyme synthesized during exponential phase, whereas AcnA (**AcnA2**) is a more stable stationary-phase enzyme, which is also specifically induced by iron and oxidative stress (Tang et al. 2002).

### 4.7.8. Ferredoxins

Ferredoxin-NADP(H) reductases (FNRs; **Fpr**) are ubiquitous, monomeric enzymes harbouring one molecule of noncovalently bound FAD as prosthetic group. They catalyze the reversible electron transfer between NADP(H) and the iron-sulfur protein ferredoxin or FMN-containing flavodoxin. Flavoproteins with FNR activity have beeen found in plastids, phototrophic and heterotrophic bacteria, mitochondria and apicoplasts of obligate intracellular parasites. FNR operates as a general electronic switch at the bifurcation steps of many different electron transfer pathways. The ability of these flavoenzymes to split electrons between obligatory one- and two-electron carriers is most relevant to FNR function in vivo (Ceccarelli et al. 2004).

### 4.7.10. Fe-S cluster biosynthesis

Iron-sulfur cluster proteins are widely distributed in nature and can be found in anaerobic, aerobic and photosynthetic bacteria as well as in eukaryotes. They serve a variety of biological roles, including electron transport, catalytic, structural and sensory roles. The fact, that the cluster can be reconstituted in the absence of protein mediators provides an important indicator of the intracellular roles for many proteins of the Fe-S cluster assembly pathway. Such proteins are more correctly viewed as carrier proteins, rather than as catalysts for the reaction, that circumvent the toxicity of free iron and sulfide and allow delivery at lower intracellular concentrations of this species (Mansy and Cowan 2004).

## 4.7.12. Cytochrome c biosynthesis

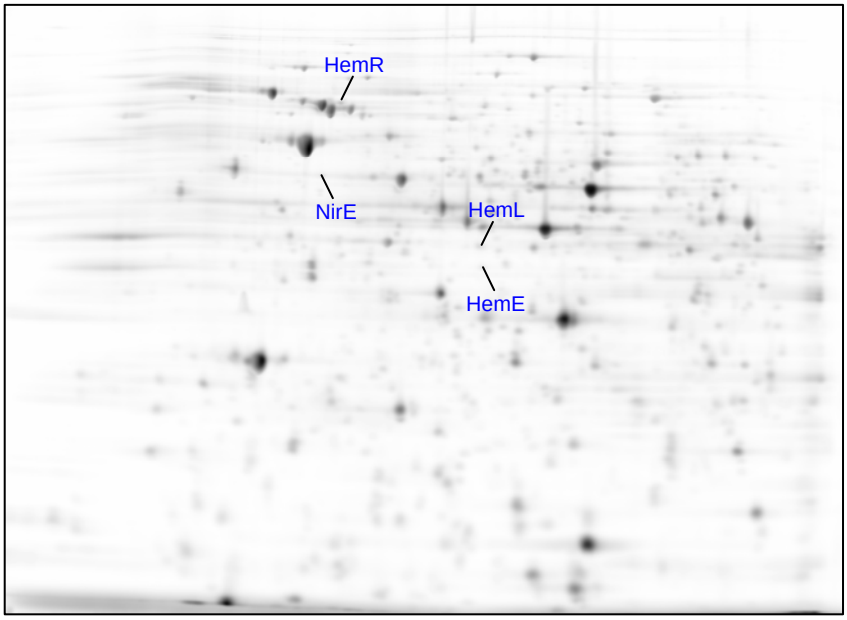


**Fig.4.7.12.** 2DE gel (pH 4-7) of cells grown anaerobically with benzoate. Identified proteins related to cytochrome c biosynthesis are annotated.

**Table 4.7.12.** Identified proteins related to cytochrome c biosynthesis.

| Orf-No. | Gene | Functional description |
|---|---|---|
| ebA1162 | *nirE* | Uroporphyrin III C-methyltransferase |
| ebA1743 | *hemL* | Glutamate-1-semialdehyde 2,1-aminomutase |
| ebA2117 | *hemR* | Hemin receptor precursor, TonB-dependent outer membrane uptake protein |
| ebA2822 | *hemE* | Uroporphyrinogen decarboxylase |

One of the major protein classes characterized by covalent cofactor attachment are the c-type cytochromes. The characteristic heme-binding mode of c-type cytochromes requires the formation of two covalent bonds between two cysteine residues in the protein and two vinyl groups of heme. Heme attachment is a complex post-translational process that occurs in the periplasmasic space and involves the participation of many proteins (Stevens et al. 2005).

In the biosynthesis of the heme cofactor, the first heme precursor for tetrapyrrole synthesis is δ-aminolevulinate (ALA). Most bacteria use the $C_5$-pathway, by which glutamate serves as a precursor and is converted to ALA in a three-step reaction involving glutamyl-tRNA. The last reaction of this sequence is catalyzed by the glutamate-1-semialdehyde 2,1-aminotransferase (**HemL**) forming ALA out of glutamate semidaldehyde (Thöny-Meyer 1997).

At the stage of uroporphyrinogen III in heme biosynthesis, a side pathway for the synthesis of heme $D_1$ branches of. The **Nir**CD**E**F proteins appear to play a role in heme $D_1$ formation, their precise role remaining unclear until now. Uroporphyrinogen III is decarboxylated by the uroporphyrinogen III decarboxylase (**HemE**) and further reactions lead to heme B, as a precursor of heme A, C, D and O (Thöny-Meyer 1997).

The ability to use hemin as an iron source is widespread among Gram-negative bacteria. In order to utilize micromolar quantities of free hemin many bacteria possess highly efficient hemin uptake systems. Thereby, hemin is transported through the otherwise impermeable outer membrane via the TonB-dependent outer membrane receptor **HemR**. In Gram-negative bacteria, such systems can also be involved in the uptake of iron-siderophore complexes, colicins and vitamin B12 (Stojiljkovic and Hantke 1994).

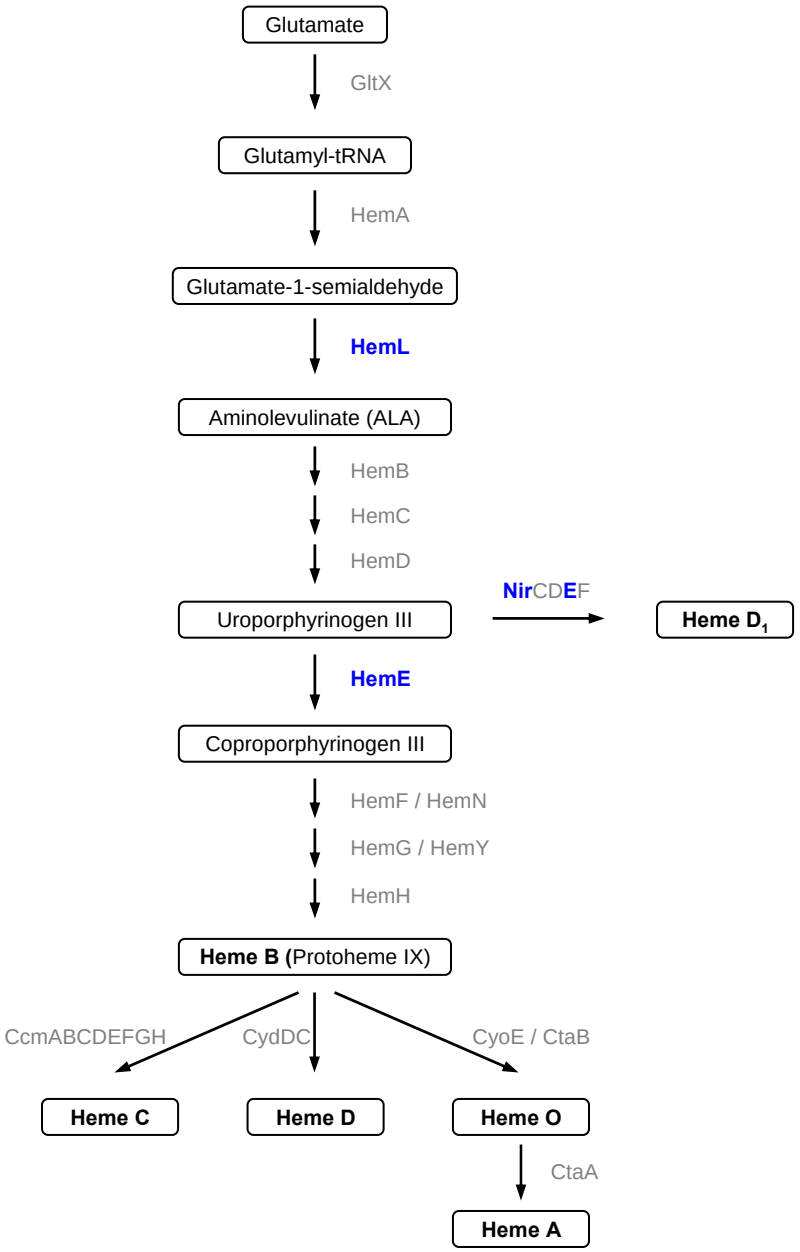


**Fig 4.7.12.1.** Schematic representaion of heme biosynthetic pathway in Gram-negative bacteria. Proteins involved in the different biosynthesis steps are indicated next to the arrows. Substrates and intermediates are framed; heme products are shown in bold type; identified Proteins are highlighted in blue (modified from Thömy-Meyer 1997).

## 4.7.15. Oxygen and NO detoxification

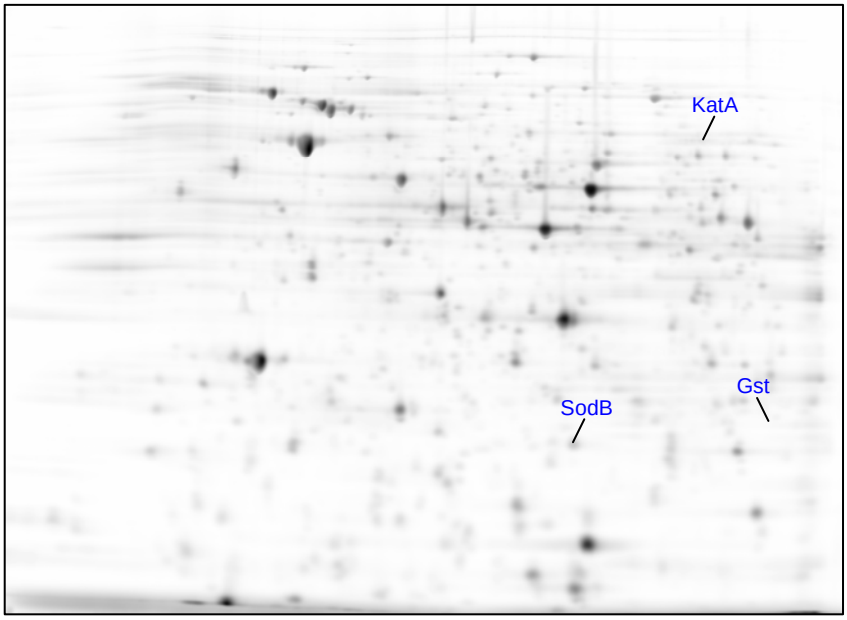


**Fig.4.7.12.** 2DE gel (pH 4-7) of cells grown anaerobically with benzoate. Identified proteins related to oxygen and NO detoxification are annotated.

**Table 4.7.15.** Identified proteins related to oxygen and NO detoxification.

| Orf-No. | Gene | Functional description |
|---|---|---|
| ebA2102 | *katA* | Catalase |
| ebA5076 | *gst* | Putative glutathione S-transferase |
| ebA5077 | *sodB* | Superoxide dismutase [Fe] |

Reactive by-products of oxygen, such as superoxide anion radicals ($O_2^-$), hydrogen peroxides ($H_2O_2$) and the highly reactive hydroxyl radicals ($^{\cdot}OH$) are generated continuously in cells grown aerobically. The biological targets of these highly reactive oxygen species are DNA, RNA, proteins and lipids. Much of the damage is caused by hydroxyl radicals generated from $H_2O_2$ via the Fenton reaction (Cabiscol et al. 2000).

Some molecules are constitutively present and help to maintain an intracellular reducing environment or to scavenge chemically reactive oxygen. Among these molecules are nonenzymatic antioxidants such as NADPH and NADH pools, β-carotene, ascorbic acid and glutathione. In addition, specific enzymes decrease the steady-state levels of reactive oxygen. The superoxide dismutase (**SodB**), an iron containing enzyme, converts $O_2^-$ to $H_2O_2$ and $O_2$, whose expression is modulated by intracellular iron concentration in *E. coli*. The $H_2O_2$ is removed by catalase (**KatA**) yielding $H_2O$ and $O_2$ (Cabiscol et al. 2000).

Glutathione S-transferase (**Gst**) is predicted to act as a detoxifying enzyme. It is thought to protect the cell from foreign compounds via binding of glutathione. It was demonstrated, that fosfomycin resistant *E. coli* exert the antibiotic conjugated to with a molecule of glutathione, resulting in opening of the epoxide group essential for antimicrobial activity (Arca et al. 1990).

## 4.7.16. Peroxidases

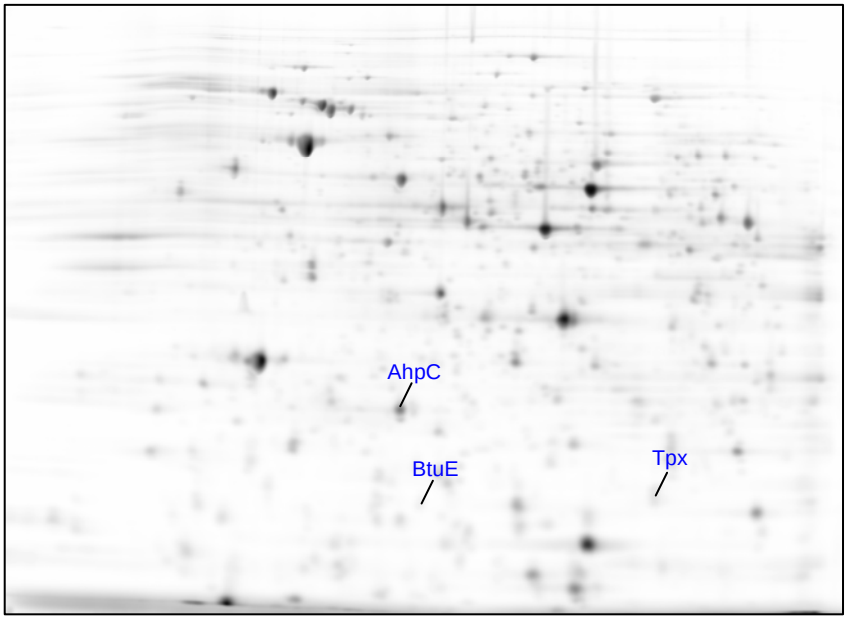


**Fig.4.7.16.** 2DE gel (pH 4-7) of cells grown anaerobically with benzoate. Identified proteins related to peroxidases are annotated.

**Table 4.7.16.** Identified proteins related to peroxidases.

| Orf-No. | Gene | Functional description |
|---|---|---|
| ebA2918 | *tpx* | Probable thiol peroxidase |
| ebA4399 | *ahpC* | Predicted peroxiredoxin |
| ebA6393 | *btuE* | Putative glutathion peroxidase protein |

Bacterial defenses against peroxide-mediated oxidative damage include a family of non-heme, non-selenium proteins, distinct from catalases and glutathione peroxidases, which catalyze the reduction, and resulting detoxification, of organic hyperoxides, hydrogen peroxide and peroxynitrite. Mechanistic studies have clarified the role of reactive cysteinyl residues in the peroxidatic process and have highlighted the cascade of dithiol-disulfide interchange reactions that take place in support of this process (Poole 2005).

As a representative of a very large and ubiquitous family of cystein-based peroxidases, now designated as peroxiredoxins, **AhpC** is a peroxide reducing protein. In many eubacteria recycling of AhpC is achieved by a flavoprotein (AhpF) acting as a „AhpC reductase“. This NAD(P)H-dependent reaction can also be mediated by the thioredoxin reductase or thioredoxin system or other organism specific reductase systems (Poole 2005).

The thiol peroxidase (**Tpx**) has been characterized as a periplasmatic protein despite the lack of a signal sequence for periplasmatic transport. It is capable of reducing $H_2O_2$ and alkyl hydroperoxide and protecting against glutamine synthetase inactivation by a metal-catalyzed oxidation system (Cha et al. 2004).

Gluthatione peroxidase (**BtuE**) is a selenoprotein oxoreductase that plays important roles in the protection of cells against oxidation of DNA and maintenance of cellular redox balance (Brenot et al. 2004).

## 4.7.18. Gene clusters related to iron transport

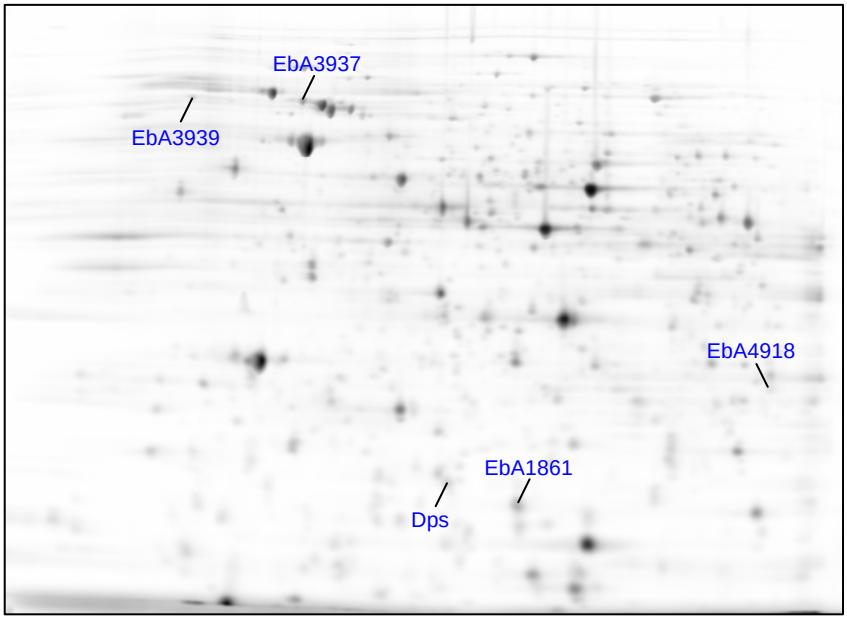


**Fig.4.7.18.** 2DE gel (pH 4-7) of cells grown anaerobically with benzoate. Identified proteins related to gene cluster related to iron transport are annotated.

**Table 4.7.18.** Identified proteins related to gene clusters related to iron transport.

| Orf-No. | Gene | Functional description |
|---|---|---|
| ebA1861 | | Similar to uncharacterized protein probably involved in high affinity $Fe^{2+}$ transport |
| ebA1978 | *dps* | DNA-binding ferritin-like protein (oxidative damage protectant) |
| ebA3937 | | TonB-dependent receptor |
| ebA3939 | | TonB-dependent siderophor receptor |
| ebA4918 | | Putative iron binding protein component of ABC iron transporter |

Iron is essential to virtually all organisms, but poses problems of toxicity and poor solubility. Highly efficient iron acquisition systems are used to scavenge iron from the environment under iron-restricted conditions. In many cases, this involves the secretion and internalization of extracellular ferric chelators called siderophors, to solubilize iron prior to transport (Andrews et al. 2003).

Gram-negative bacteria take up ferri-siderophore complexes via specific outer membrane (OM) receptors (**EbA3937** and **EbA3939**) in a process that is driven by the cytoplasmic membrane (CM) potential and mediated by the energy-transducing TonB-ExbB-ExbD system. Periplasmic binding proteins (**EbA4918**) shuttle ferri-siderophores from the OM receptors to CM ATP-binding cassette (ABC) transporters that, in turn, deliver the ferri-siderophores to the cytosol (Andrews et al. 2003).

Extracellular iron is not the only source of iron available to bacteria. Many bacteria deposit intracellular reserves of iron within iron storage proteins. One type of iron storage proteins is **Dps**. It is composed of 12 identical subunits that assemble to form an approximately spherical protein shell surrounding a central cavity that acts as an iron storage reservoir. Indeed, the primary role of Dps in *E. coli* is in protecting DNA against the combined action of ferrous iron and $H_2O_2$ in the production of the hydroxy free radical (Andrews et al. 2003).

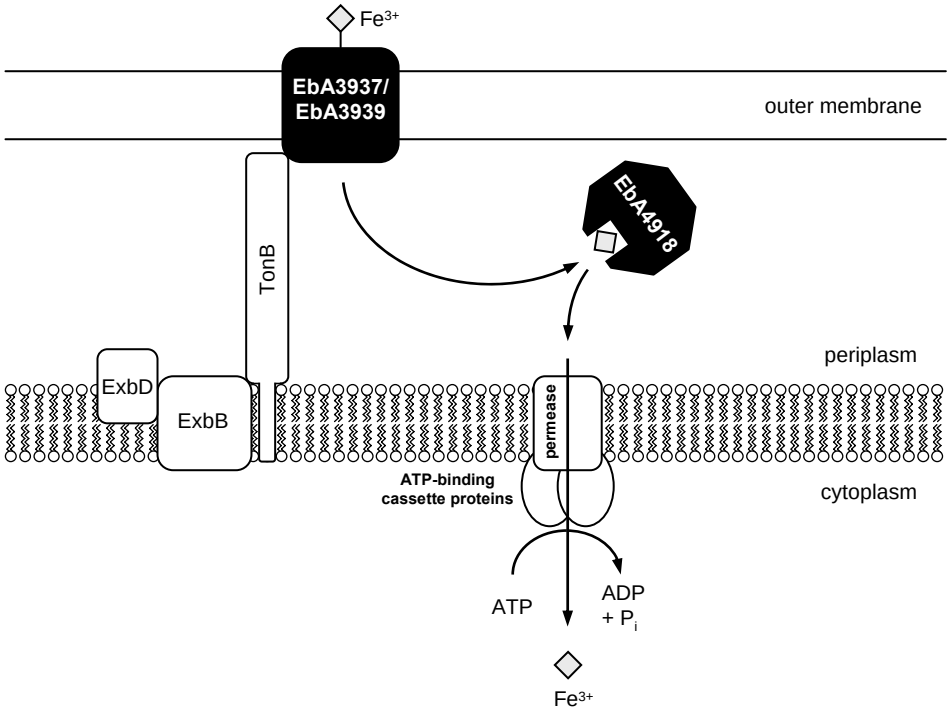


**Fig 4.7.18.1.** Schematic representation of siderphore-mediated iron uptake in Gram-negative bacteria. Identified proteins involved in this process (**EbA3937**, **EbA3939** and **EbA4918**) are marked in black. Genes encoding the energy-transducing TonB-ExbB-ExbD system have been identified in the genome as well as several genes encoding ABC-transporters (Rabus et al. 2005; modified from Andrews et al. 2003).

## 4.7.19. Transport of other metals

## 4.7.20. Zinc containing proteins

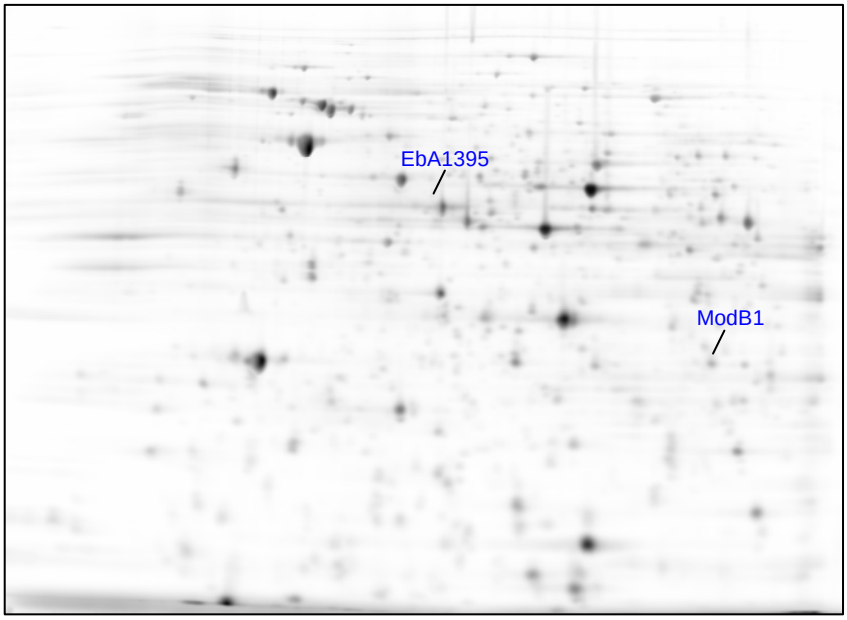


**Fig.4.7.19.** 2DE gel (pH 4-7) of cells grown anaerobically with benzoate. Identified proteins related to transport of other metals and zinc containing proteins are annotated.

**Table 4.7.19.** Identified protein related to transport of other metals.

| Orf-No. | Gene | Functional description |
|---|---|---|
| ebA3597 | *modB1* | Molybdate or tungstate transport |

**Table 4.7.20.** Identified protein related to zinc containing proteins.

| Orf-No. | Gene | Functional description |
|---|---|---|
| ebA1395 | | Putative zinc protease |

### 4.7.19. Transport of other metals

Although required only in trace amounts, molybdenum plays a critical role in several metabolic pathways in all organisms. These pathways contribute to energy production, e.g. denitrification. The largest of the three subunits of nitrate reductase (NarG) contains molybdenum. In bacteria molybdenum is transported by a high-affinity transport system composed of a periplasmic binding protein (ModA), an integral membrane protein (**ModB1**) and an energy-transducing protein (ModC). The membrane channel, through which molybdenum transverses across the membrane, is presumably composed of a ModB homopolymer (Grunden and Shanmugam 1997).

### 4.7.20. Zinc containing proteins

Microbial proteases, catalyzing the hydrolysis of peptide bonds in proteins or peptides, are predominantly extracellular and can be classified into four groups: (I) serine proteases, (II) cysteine proteases, (III) aspartate proteases and (IV) metalloproteases (**EbA1395**), mostly zinc-containing proteins. The ubiquity and conservation of extracellular zinc-containing metalloproteases in the microbial world suggest that they must provide survival advantages (Häse and Finkelstein 1993).

## 4.7.23. Flavin enzymes

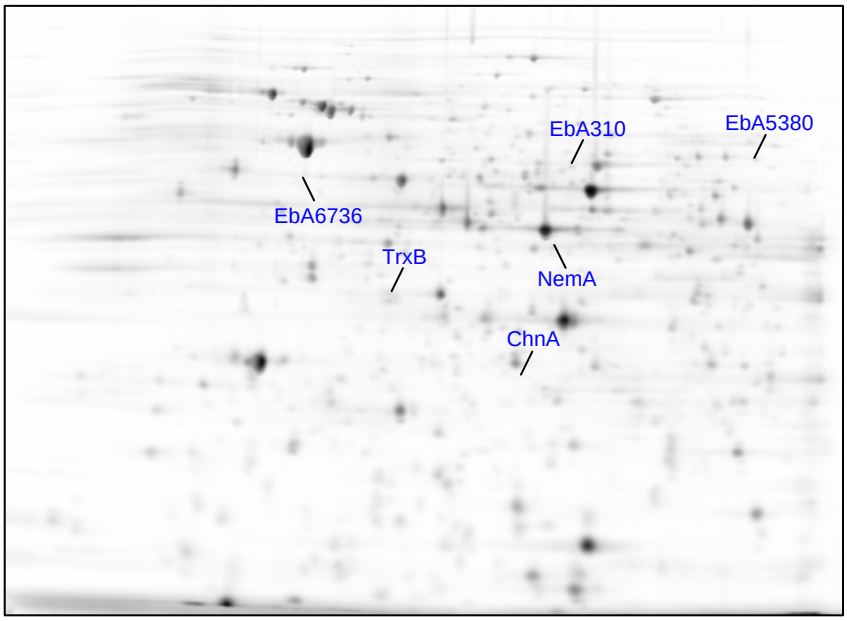


**Fig.4.7.23.** 2DE gel (pH 4-7) of cells grown anaerobically with benzoate. Identified proteins related to flavin enzymes are annotated.

**Table 4.7.23.** Identified proteins related to flavin enzymes.

| Orf-No. | Gene | Functional description |
|---|---|---|
| ebA307 | *chnA* | Cyclohexanol dehydrogenase |
| ebA310 | | FAD-linked oxidase |
| ebA3561 | *nemA* | Flavoprotein, NADH-dependent oxidoreductase |
| ebA5380 | | Probable *p*-cresol methylhydroxylase |
| ebA6736 | | Probable FAD/FMN-containing oxidoreductase |
| ebA7042 | *trxB* | FAD-dependent pyridine nucleotide-disulfide oxidoreductase |

Flavin enzymes are a group of about 70 oxidoreductases present in animals, plants and microorganisms containing mostly FAD, more seldom FMN. These coenzymes are reversibly reduced through hydrogen transfer, either from the substrate or from NAD(P)H.

In contrast to other enzyme classes (e.g. the haemoglobins), flavin enzymes do not share a basic structure. According to the main reactions catalyzed, flavin enzymes can be grouped: (I) oxidases, (II) reductases and (III) dehydrogenases. Furthermore, more complex flavin enzymes are known (e.g. formic acid dehydrogenase), which contain metals, sulfhydryl-disulfide-systems or haemin-groups in addition to the flavin component.

## 4.10. Hypothetical and conserved hypothetical proteins

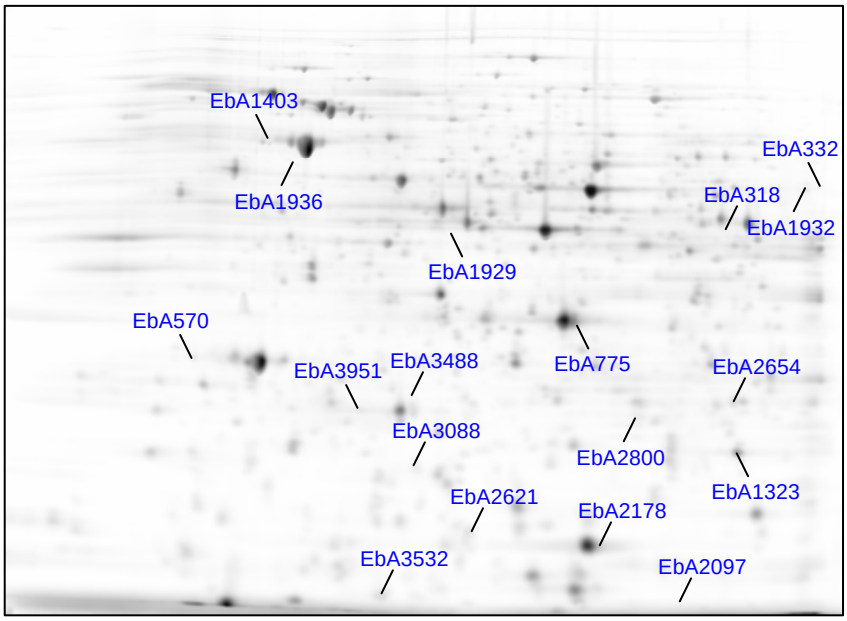


**Fig.4.10.1** 2DE gel (pH 4-7) of cells grown anaerobically with benzoate. Identified hypothetical and conserved hypothetical proteins are annotated.

**Table 4.10.** Identified proteins related to flavin enzymes.

| Orf-No. | Gene | Functional description |
|---|---|---|
| ebA318 | | Conserved hypothetical protein |
| ebA332 | | Conserved hypothetical protein |
| ebA570 | | Hypothetical protein |
| ebA775 | | Conserved hypothetical protein |
| ebA1323 | | Conserved hypothetical protein |
| ebA1403 | | Conserved hypothetical protein |
| ebA1929 | | Conserved hypothetical protein |
| ebA1932 | | Conserved hypothetical protein |
| ebA1936 | | Conserved hypothetical protein |
| ebA2097 | | Hypothetical protein |
| ebA2178 | | Hypothetical protein |
| ebA2621 | | Conserved hypothetical protein |
| ebA2654 | | Hypothetical protein |
| ebA2800 | | Conserved hypothetical protein |
| ebA3088 | | Hypothetical protein |
| ebA3488 | | Conserved hypothetical protein |
| ebA3532 | | Conserved hypothetical protein |
| ebA3951 | | Conserved hypothetical protein |

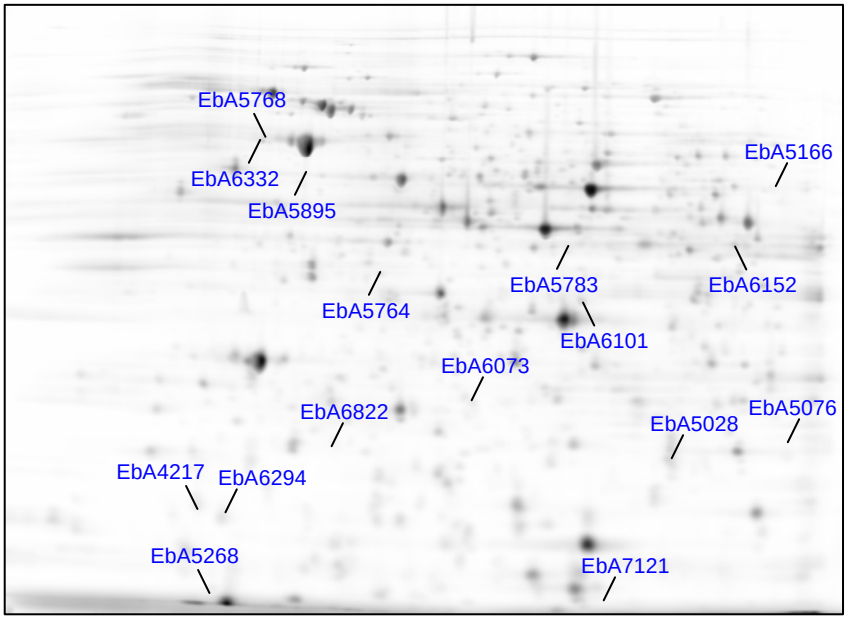


**Fig.4.10.2** 2DE gel (pH 4-7) of cells grown anaerobically with benzoate. Identified hypothetical and conserved hypothetical proteins are annotated.

**Table 4.10.** continued

| Orf-No. | Gene | Functional description |
|---|---|---|
| ebA4217 | | Conserved hypothetical protein |
| ebA4705 | | Hypothetical protein |
| ebA4715 | | Hypothetical protein |
| ebA5028 | | Conserved hypothetical protein |
| ebA5076 | | Conserved hypothetical protein |
| ebA5166 | | Conserved hypothetical protein |
| ebA5268 | | Conserved hypothetical protein |
| ebA5764 | | Conserved hypothetical protein |
| ebA5768 | | Conserved hypothetical protein |
| ebA5783 | | Hypothetical protein |
| ebA5895 | | Hypothetical protein |
| ebA6073 | | Conserved hypothetical protein |
| ebA6101 | | Conserved Hypothetical protein |
| ebA6152 | | Conserved hypothetical protein |
| ebA6294 | | Conserved Hypothetical protein |
| ebA6332 | | Hypothetical protein |
| ebA6822 | | Conserved hypothetical protein |
| ebA7121 | | Conserved hypothetical protein |

# 5. Biosynthesis

## 5.1. Amino acid synthesis

## 5.1.1. α-Ketoglutarate family

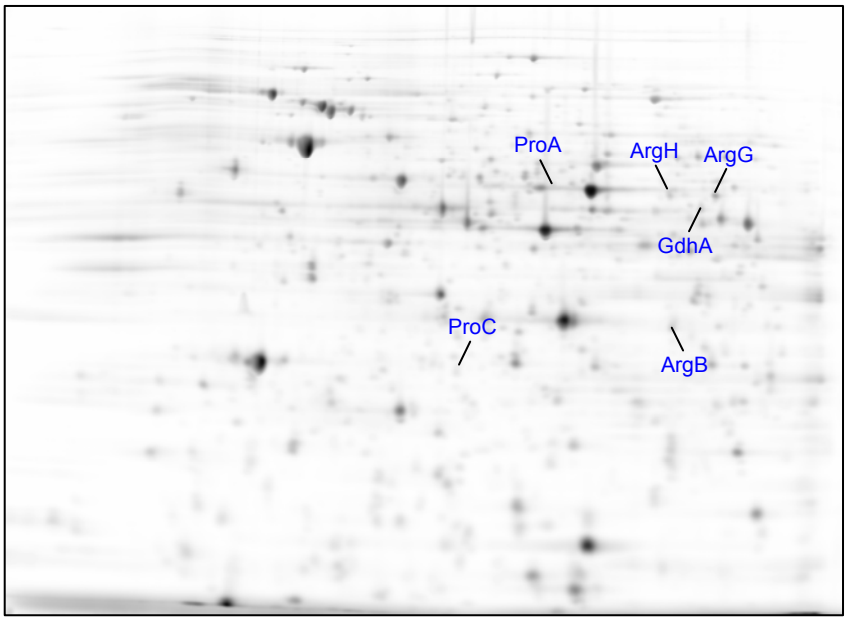


**Fig.5.1.1.** 2DE gel (pH 4-7) of cells grown anaerobically with benzoate. Identified proteins related to amino acid synthesis (α-ketoglutarate family) are annotated.

**Table 5.1.1.** Identified proteins related to amino acid synthesis (α-ketoglutarate family).

| Orf-No. | Gene | Functional description |
|---|---|---|
| ebA1170 | *argH* | Argininosuccinate lyase |
| ebA1766 | *proC* | 1-pyrroline-5-carboxylate reductase |
| ebA4330 | *argB* | Acetylglutamate kinase |
| ebA4380 | *proA* | γ-glutamyl phosphate reductase |
| ebA5097 | *argG* | Argininosuccinate synthase |
| ebA5425 | *gdhA* | Glutamate dehydrogenase |

### Glutamate and glutamine

Glutamate and glutamine play a central role in amino acid biosynthesis by the ready transfer of amino or amide groups, respectively, in the synthesis of other amino acids via transamination or transamidation reactions. Glutamate is synthesized via reductive transamination of the TCA intermediate α-ketoglutarate, catalyzed by the glutamate-synthase or glutamate dehydrogenase (**GdhA**). Glutamine is synthesized from glutamate with the participation of ammonia and ATP (Fig 5.1.1.1.; Moat and Foster 1995).

### Proline

The synthesis of proline involves the formation of γ-glutamylphosphate from L-glutamate and ATP by γ-glutamyl-kinase. In the presence of NADPH, γ-glytamylphosphate is reduced to glutamate γ-semialdehyde, catalyzed by γ-glutamyl phosphate reductase (**ProA**). Glutamate γ-semialdehyde can cyclize spontaneously to form 1-pyrroline-5-carboxylate, which is converted to proline by the 1-pyrroline-5-carboxylate reductase (**ProC**; Fig 5.1.1.1.; Moat and Foster 1995).

## Arginine

Bacteria synthesize ornithine via a series of N-acteyl derivates of glutamate. The function of the *N*-acetyl groups is to prevent the premature cyclisation of 1-pyrrole 5-carboxylate to proline as shown in Fig 5.1.1.1. (Moat and Foster 1995).
*N*-acetylglutamate (NAG) is synthesized by the NAG synthase and further activated to *N*-acetylglutamyl phosphate by the acetylglutamate kinase (**ArgB**). Subsequent reactions lead to citrulline, which is converted to arginino succinate by the argininosuccinate synthase (**ArgG**). Arginine is formed by the argininosuccinate lyase (**ArgH**), releasing fumarate (Fig 5.1.1.1.; Caldovic and Tuchman 2003)

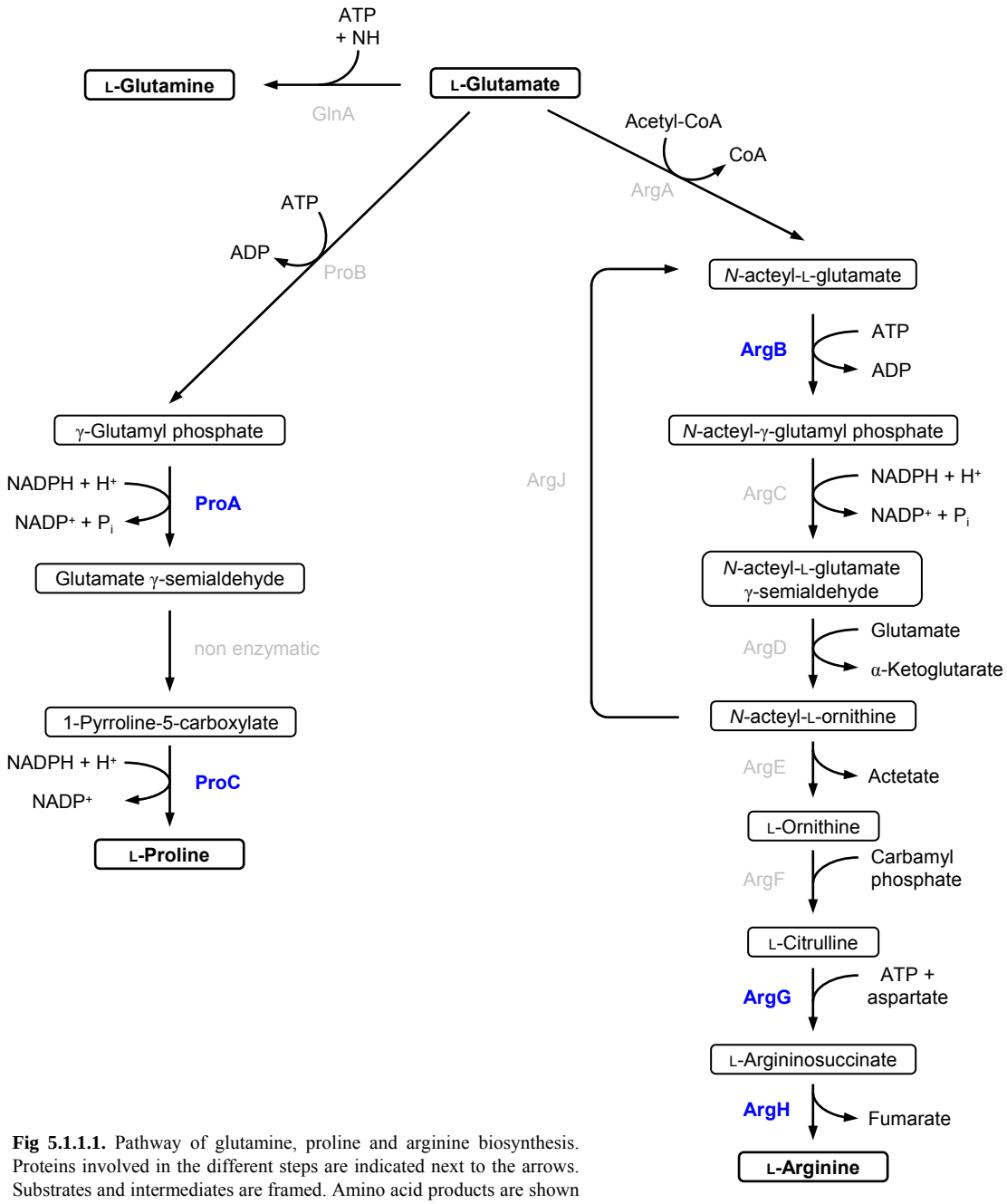


**Fig 5.1.1.1.** Pathway of glutamine, proline and arginine biosynthesis. Proteins involved in the different steps are indicated next to the arrows. Substrates and intermediates are framed. Amino acid products are shown in bold type. Identified proteins are highlighted in blue (modified from Moat and Foster 1995 and Caldovic and Tuchman 2003).

## 5.1.2. Aspartate family

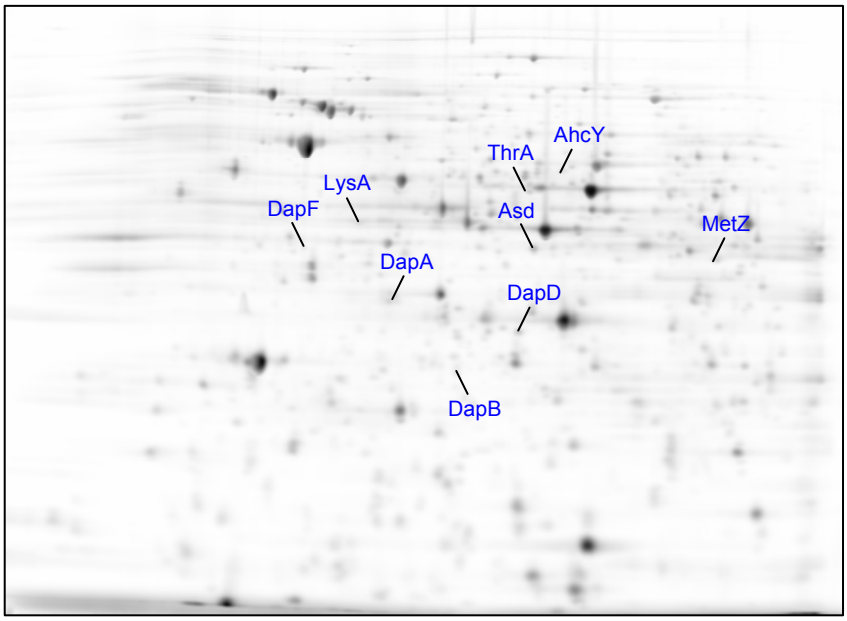


**Fig.5.1.2.** 2DE gel (pH 4-7) of cells grown anaerobically with benzoate. Identified proteins related to amino acid synthesis (aspartate family) are annotated.

**Table 5.1.2.** Identified proteins related to amino acid synthesis (aspartate family).

| Orf-No. | Gene | Functional description |
|---|---|---|
| ebA774 | *dapA* | Dihydrodipicolinate synthase |
| ebA1874 | *ahcY* | Adenosylhomocysteinase |
| ebA2271 | *lysA* | Diaminopimelate decarboxylase |
| ebA3950 | *dapF* | Diaminopimelate epimerase |
| ebA4761 | *asd* | Aspartate-semialdehyde dehydrogenase |
| ebA4785 | *metZ* | *O*-Succinylhomoserine sulfhydrylase |
| ebA4812 | *dapB* | Putative dihydrodipicolinate reductase |
| ebA4952 | *thrA* | Homoserine dehydrogenase |
| ebA6386 | *dapD* | Tetrahydrodipicolinate succinylase |

### Aspartate and Asparagine

Aspartate is synthesized from the TCA intermediate oxalacetate via a transaminase reaction. Asparagine is synthesized from aspartate, ammonia (or glutamate) and ATP by the asparagine synthase (Fig 5.1.2.1.; Moat and Foster 1995).

### Methionine and Threonine

The enzymes aspartokinase and aspartate semialdehyde dehydrogenase initiate the aspartate pathway of amino acid biosynthesis. Apartokinase I (**ThrA**) is specific for the threonine pathway, apartokinase II (MetL) and III (LysC) are specific for the methionine and lysine branch, respectively. Asparatate semialdehyde dehydrogenase (**Asd**) forms aspartate β-semialdehyde by removal of phosphate from

aspartyl phosphate and reduction using NADPH. Reduction of aspartate β-semialdehyde to homoserine is catalyzed by homoserine dehydrogenase I (**ThrA**), which is specific for the threonine branch, or homoserine dehydrogenase II (MetL) specific for the methionine branch (Fig 5.1.2.1.; Moat and Foster 1995).

The pathway to threonine continues with a phosphorylation of homoserine, catalyzed by homoserine kinase (ThrB), leading to homoserine phosphate. The threonine synthase (ThrC) catalyzes the rather complex conversion of homoserine phosphate to threonine (Cohen and Saint-Girons 1987).

In *E. coli*, the first specific step of methionine synthesis is catalyzed by homoserine succinyltransferase (MetA), which transforms homoserine into O-succinylhomoserine in the presence of succinyl-CoA. O-succinylhomoserine is transformed to cystathionine in the presence of cysteine. This reaction is catalyzed by cystathionine-γ-synthase (MetB). Cystathionine is cleaved leading to homocysteine, catalyzed by the β-cystathionase (MetC). The last step in methionine synthesis is effected by homoserine methylation. Two enzymes can catalyze this reaction: a vitamin $B_{12}$-dependent transmethylase (MetH) or a vitamin $B_{12}$-independent transmethylase (MetE; Fig 5.1.2.1.; Cohen and Saint-Girons 1987).

In contrast to *E. coli*, other bacteria (e.g. *Pseudomonas putida* or *Corynebacterium glutamaticum*) are able to directly synthezise homocysteine from acylated homoserine. These organisms bypass cystathionine of the transsulfuration pathway via the direct sulhydrylation pathway. *O*-succinylhomoserine sulfhydrylase (**MetZ**), utilizing sulfide as the sulfur donor, is responsible for catalysis of this pathway (Lee and Hwang 2003). Genes encoding both methionine pathways were assigned in the genome of strain EbN1 (Rabus et al 2005), but only MetZ could be identified in this proteomic study. The usage of the cystathione pathway remains unclear.

## Lysine

Bacteria synthesize lysine by a pathway in which the final step is the decarboxylation of diaminopimelate. This compound is an essential building block for peptidoglycan of the bacterial cell wall. Condensation of aspartate β-semialdehyde with pyruvate yields dihydrodipicolinate, catalyzed by the dihydrodipicolinate synthase (**DapA**). Dihydrodipicolinate is reduced by dihydrodipicolinate reductase (**DapB**) forming tetrahydrodipicolinate. Succinyl diaminopimelate is synthesized via succinyl-ε-keto-α-aminopimelate, catalyzed by the tetrahydrodipiclinate succinylase (DapC) and the succinyl diaminopimelate aminotransferase (**DapD**), respectively. In the following reaction, succinate is released yielding LL-diaminopimelate, catalyzed by the succinyl diaminopimelate desuccinylase. Subsequent epimerisation by diaminopimelate epimerase (**DapF**) leads to meso-diaminipimelate, which is carboxylated by the diaminopimelate decarboxylase (**LysA**), forming lysine (Fig 5.1.2.1.; Cohen and Saint-Girons 1987).

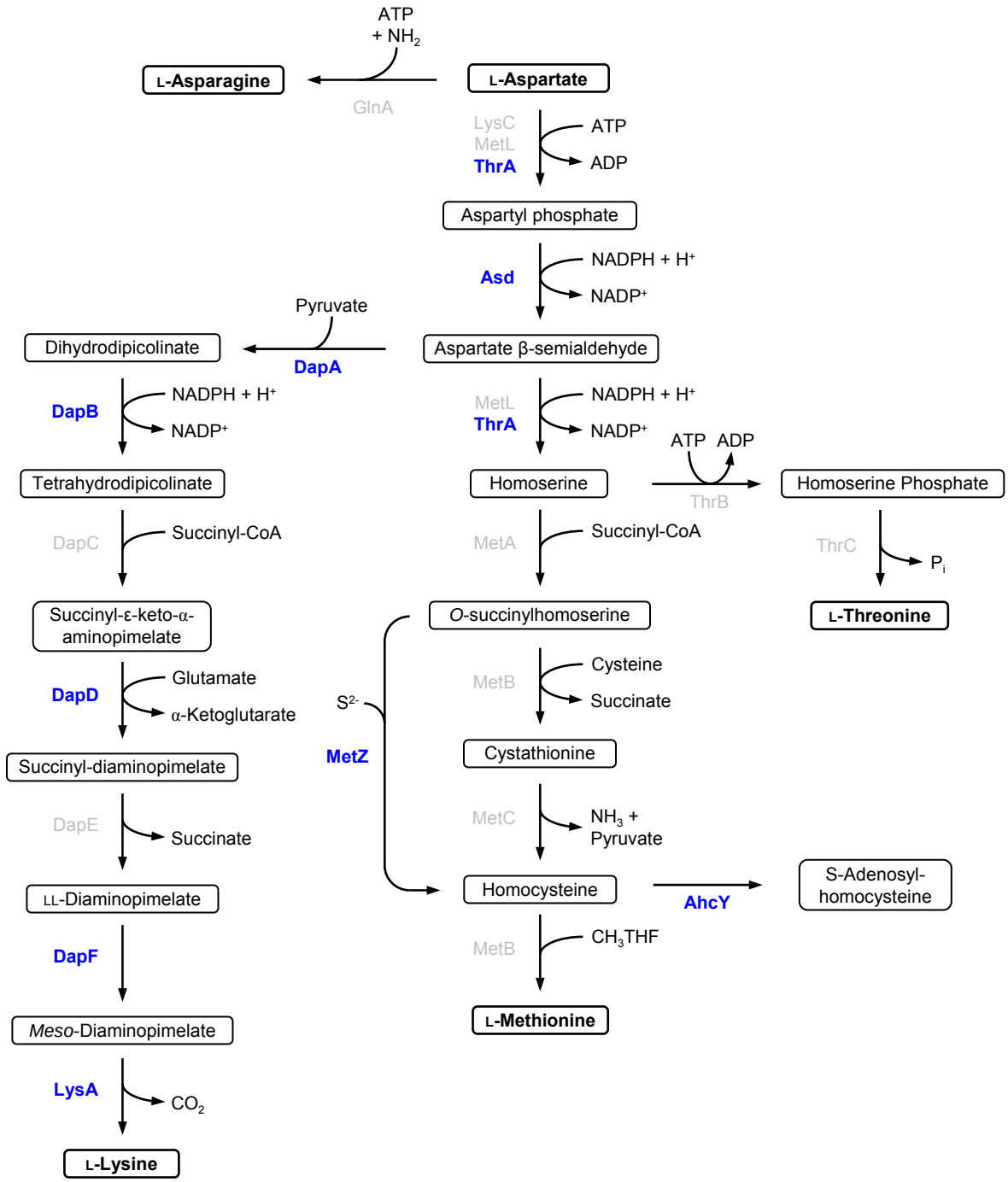


**Fig 5.1.2.1.** Pathway of asparagine, threonine, methionine and lysine biosynthesis. Proteins involved in the different steps are indicated next to the arrows. Substrates and intermediates are framed. Amino acid products are shwon in bold type. Identified proteins are highlighted in blue (modified from Moat and Foster 1995 and Cohen and Saint-Girons 1987).

## 5.1.3. Pyruvate family

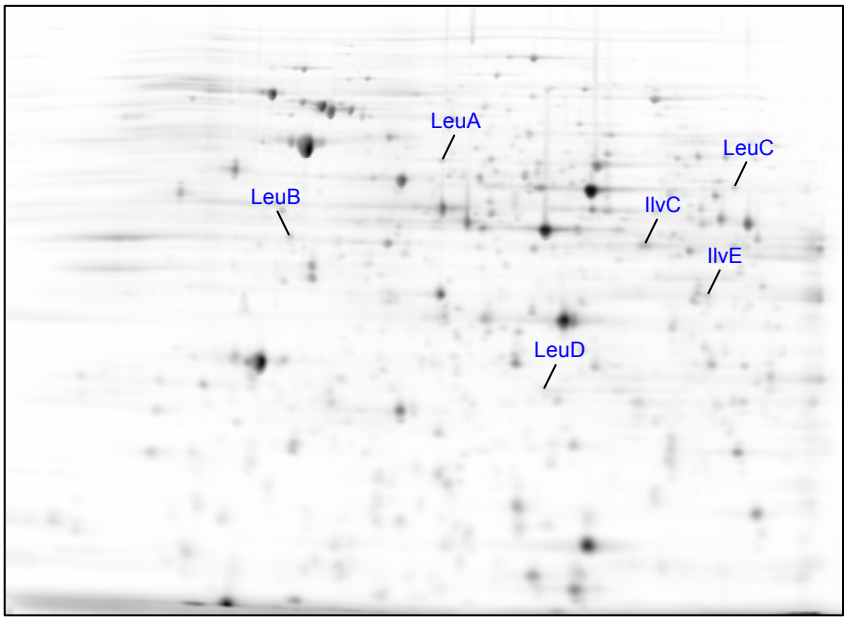


**Fig.5.1.3.** 2DE gel (pH 4-7) of cells grown anaerobically with benzoate. Identified proteins related to amino acid synthesis (pyruvate family) are annotated.

**Table 5.1.3.** Identified proteins related to amino acid synthesis (pyruvate family).

| Orf-No. | Gene | Functional description |
|---|---|---|
| ebA993 | *ilvE* | Branched-chain amino acid aminotransferase |
| ebA4757 | *leuC* | isopropylmalate dehydratase, large subunit |
| ebA4758 | *leuD* | isopropylmalate dehydratase, small subunit |
| ebA4760 | *leuB* | β-isopropylmalate dehydrogenase |
| ebA7134 | *ilvC* | Ketol-acid reductoisomerase |
| ebA7154 | *leuA* | α-isopropylmalate synthase |

### Valine and isoleucine

In the isoleucine-valine pathway, four of the steps in both sequences are catalyzed by the same enzymes. The first common feature in the two pathways is a reaction in which an acetal group, generated by the decarboxylation of pyruvate, is condesed with a second pyruvate or with α-ketobutyrate at the α-carbonyl carbon. The resulting acetohydroxy acid is thus a branched chain acid, but the branch is at the α-carbon rather than at the β-carbon. An intramolecular rearrangement, in which a methyl or ethyl group is transferred from the α-carbon to the β-carbon, yields the carbon sceleton of valine or isoleucine. The ketol-acid reductoisomerase (**IlvC**) catalyzing this rearrangement also catalyzes an NADPH-dependent reduction to yield the α,β-dihydroxy acid intermediates. Removal of a water molecule from these intermediates (IlvD) yields the α-keto acids which undergo transamination by the brached-chain amino acid aminotransferase (**IlvE**) to yield valine and isoleucine (Umbarger 1996).

The intermediate precursor of valine, α-ketoisovalerate, represents a branch point. Condensation with acetyl-CoA initiates the series of reactions leading to leucine synthesis.

## Leucine

The first step in leucine synthesis is the formation of α-isopropylmalate from α-ketoisovalerate and acetyl-CoA, catalyzed by the α-isopropylmalate synthase (**LeuA**). The following reaction, catalyzed by the iopropylmalate dehydratase (**LeuCD**), yields β-isopropylmalate, which is further oxidized by the β-isopropylmalate dehydrogenase (**LeuB**) forming α-ketoisocarproate. A transamination reaction involving glutamate leads to leucine (Moat and Foster 1995).

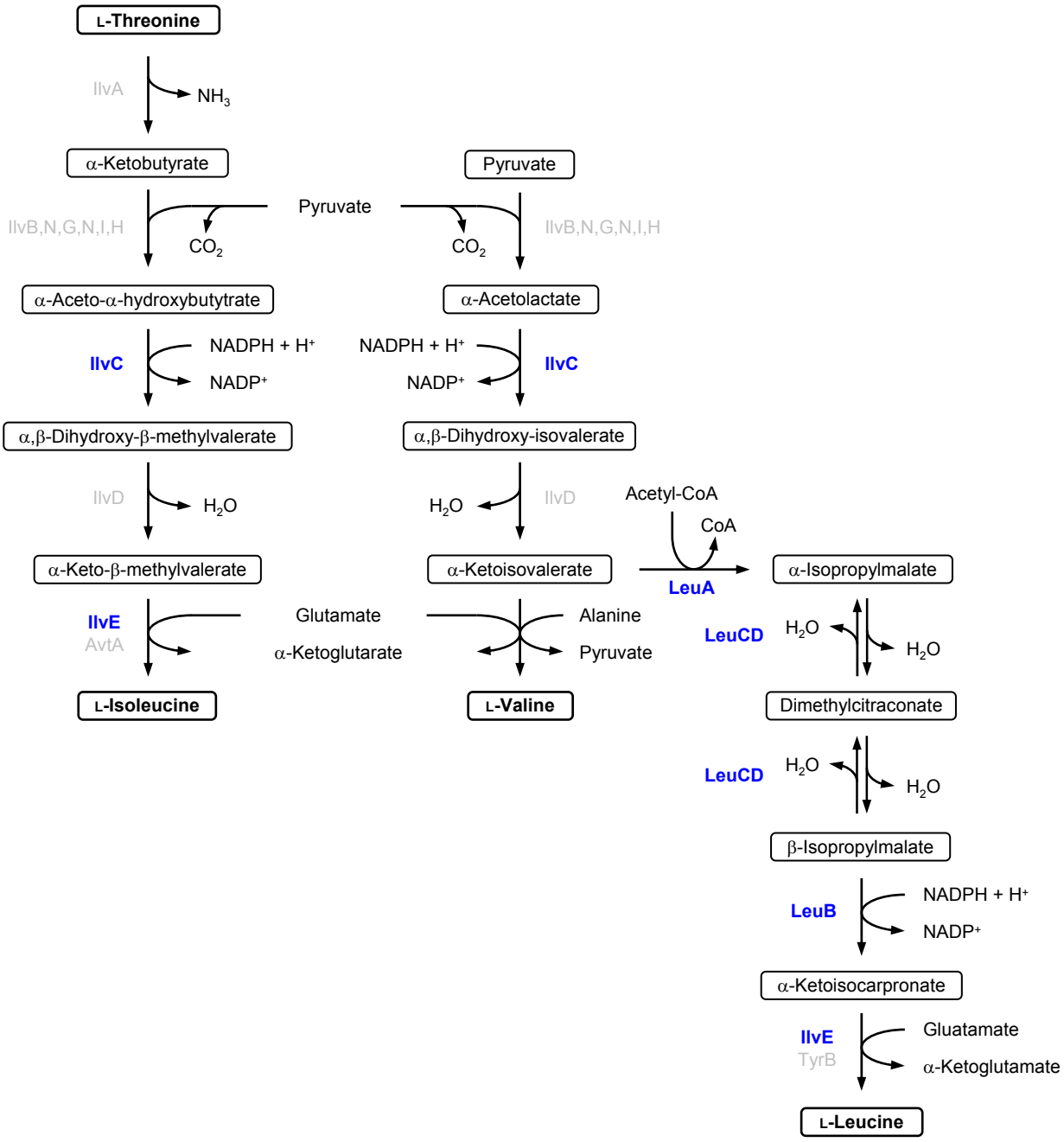


**Fig 5.1.3.1.** Pathway of isoleucine, valine and leucine biosynthesis. Proteins involved in the different steps are indicated next to the arrows. Substrates and intermediates are framed. Amino acid products are shwon in bold type. Identified proteins are highlighted in blue (modified from Umbarger 1996).

## 5.1.4. Triose family

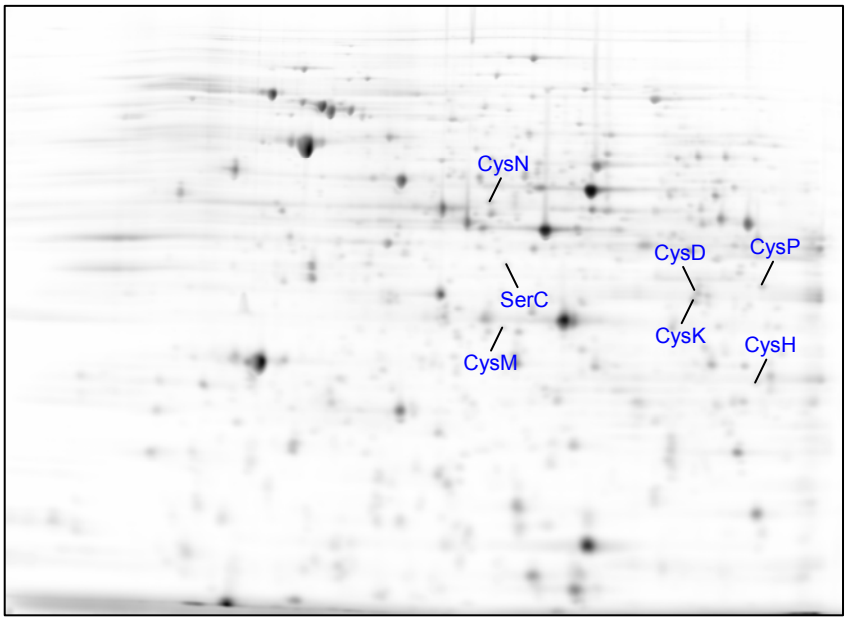


**Fig.5.1.4.** 2DE gel (pH 4-7) of cells grown anaerobically with benzoate. Identified proteins related to amino acid synthesis (triose family) are annotated.

**Table 5.1.4.** Identified proteins related to amino acid synthesis (triose family).

| Orf-No. | Gene | Functional description |
|---|---|---|
| ebA896 | *cysM* | Cysteine synthase B |
| ebA907 | *serC* | Phosphoserine aminotransferase |
| ebA2623 | *cysH* | APS-reductase |
| ebA2625 | *cysD* | ATP sulfurylase, small subunit |
| ebA2628 | *cysN* | ATP sulfurylase, large subunit |
| ebA4678 | *cysK* | Cysteine synthase A |
| ebA6204 | *cysP* | Periplasmatic thiosulfate-binding protein |

The synthesis of serine requires three primary enzymes, 3-phosphoglycerate dehydrogenase (SerA), 3-phosphoserine aminotransferase (**SerC**) and 3-phosphosernie phosphatase (SerB). The initial reaction is the oxidation of 3-phosphoglycerate to 3-phosphohydroxypyruvate, followed by transamination to 3-phosphoserine and dephosphorylation to serine. The interconversion of serine and glycine occurs mainly by a single enzyme, the serine hydroxymethyltransferase (GlyA; Stauffer 1987).

Serine also serves as precursor for cysteine. The acetylation of serine to O-acetylserine, catalyzed by the serine acetyltransferase (CysE), is followed by the formation of cysteine catalyzed by the cysteine synthase (**CysKM**). At this point, the pathway converges with sulfate reduction accounting for the required sulfur. During the assimilatory suflate reduction, adenosine phosphosulfate (APS) is formed by the ATP sulfurylase (**CysDN**) involving consumption of ATP. The addition of another phosphate to APS yields phosphoadenosine phosphosulfate (PAPS), which is reduced by the phosphoadenylyl sulfate reductase (**CysH**) to sulfite. Finally, the sulfite reductase (CysGIJ) reduces sulfite to sulfide, which can be used for cysteine synthesis by the acetylserine sulfurylase (CysDN; Fig 5.1.4.1.; Moat and Foster 1995)

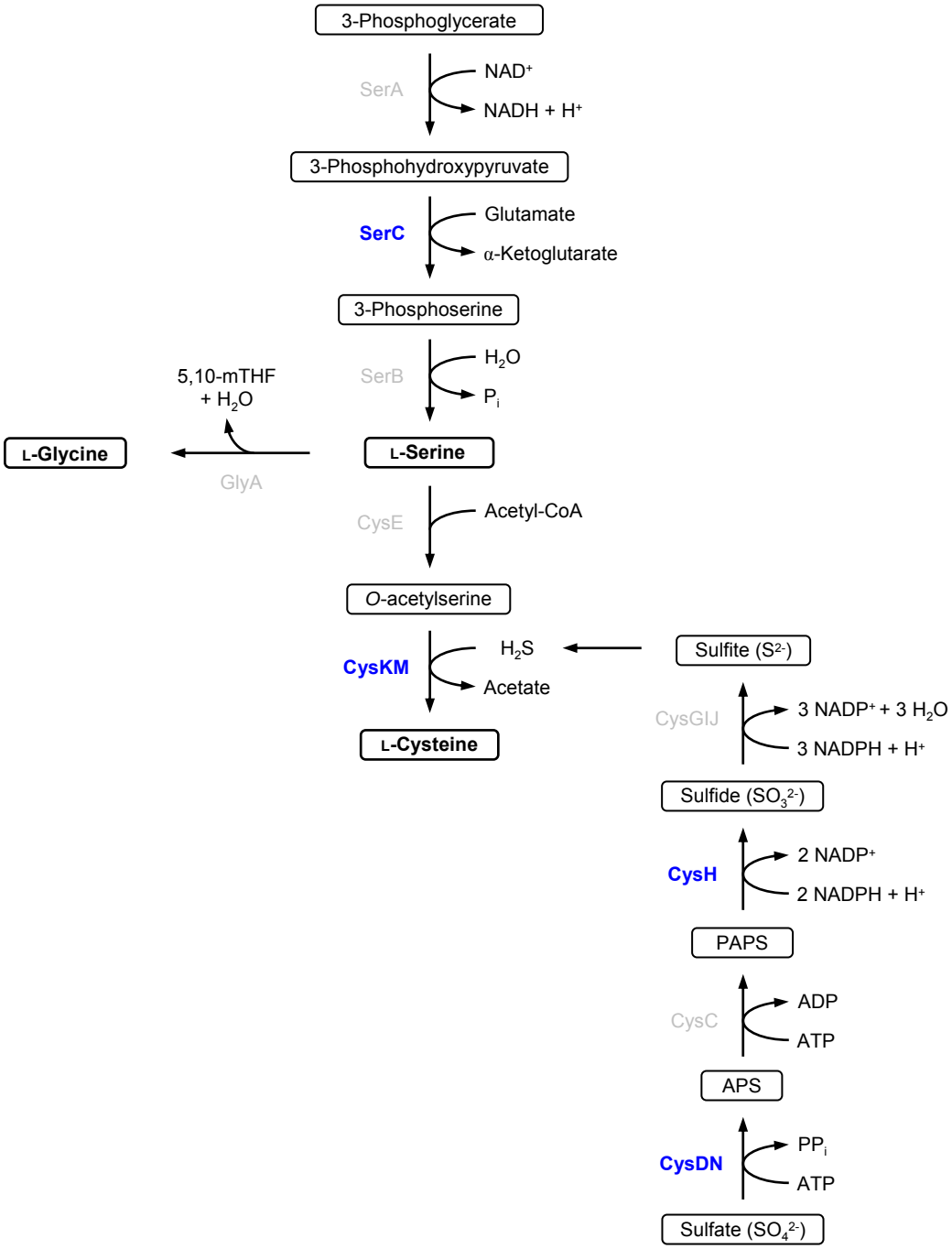


**Fig 5.1.4.1.** Pathway of glycine, serine and cysteine biosynthesis. Proteins involved in the different steps are indicated next to the arrows. Substrates and intermediates are framed. Amino acid products are shwon in bold type. Identified proteins are highlighted in blue. Abbreviations: mTHF: methylene-tetrahydrofolate, APS: adenosine phosphosulfate, PAPS: 3-phosphoadenosine phosphosulfate (modified from Moat and Foster 1995).

## 5.1.5. Aromatic amino acid family

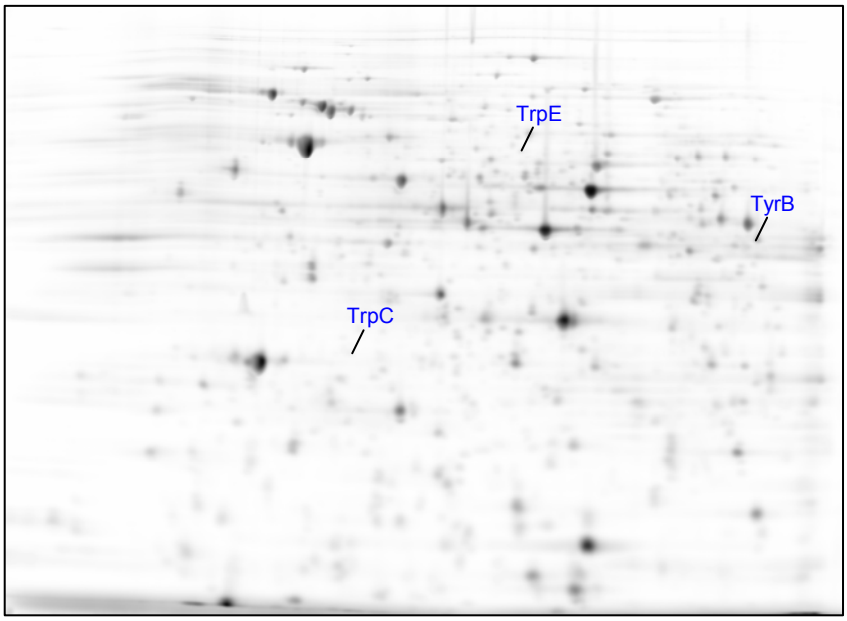


**Fig.5.1.5.** 2DE gel (pH 4-7) of cells grown anaerobically with benzoate. Identified proteins related to amino acid synthesis (aromatic amino acid family) are annotated.

**Table 5.1.5.** Identified proteins related to amino acid synthesis (aromatic amino acid family).

| Orf-No. | Gene | Functional description |
|---|---|---|
| ebA4177 | *trpE* | Anthranilate synthase, component I |
| ebA4201 | *trpC* | Indole-3-glycerol phosphate synthase |
| ebA5437 | *tyrB* | Aromatic-amino-acid transaminase |

The aromatic amino acids phenylalanine, tyrosine and tryptophan are produced via a common pathway that begins with the condensation of erythrose-4-phosphate and phosphoenolpyruvate to form 3-desoxy-D-arabinoheptulosonate 7-phosphate (DAHP). DAHP is converted to shikimate and then to chorismate (Moat and Foster 1995).

The first reaction of the terminal pathway to tryptophan involves the conversion of chorismate and glutamine to anthranilate, glutamate and pyruvate. The enzyme catalizing this reaction is the anthranilate synthase (**Trp**D**E**). Component I (**TrpE**) contains the binding site for chorismate, but cannot catalyze the formation of anthranilate with glutamine as the nitrogen source. The subsequent formation of phosphoribosyl anthranilate (PRA) is catalyzed by the anthranilate phosphoribosyl transferase (TrpD). PRA is converted to 1-(O-carboxyphenylamino) 1-deoxyribulose 5-phosphate (CDRP) and this compound in turn is converted to indoleglycerol phosphate (InGP) by a single enzyme, the PRA isomerase/InGP synthase (**TrpC**). Kinetic studies on the purified enzyme led to the conclusion that the enzyme contained two distinct and nonoverlapping sites for the reaction PRA → CDRP → InGP. The final formation of tryptophan and glyceraldehyde out of InGP and serine is catalyzed by the tryptophan synthase (TrpAB; Fig 5.1.6.1.; Pittard 1987).

The first reaction of both the phenylalanine amnd tyrosine pathways involves the conversion of chorismate to prephenate. The enzymes that carry out the synthesis of prephenate have been referred to as chorismate mutases (PheA or TyrA). Subsequently, prephenate dehydrogenase carries out the second reaction in the tyrosine pathway. It could be demonstrated, that both activities are the product of a single bifunctional enzyme, referred to as chorismate mutase-prephenate dehydrogenase (TyrA). Activity of the latter is inhibited by tyrosine with the most significant inhibition being exerted

on the second activity, causing up to 95 % inhibition. The last reaction involves the transamination of the α-ketoacid 4-hydroxyphenylpyruvate catalyzed by the aromatic aminotransferase (**TyrB**) with glutamate as the amino donor (Pittard 1987).

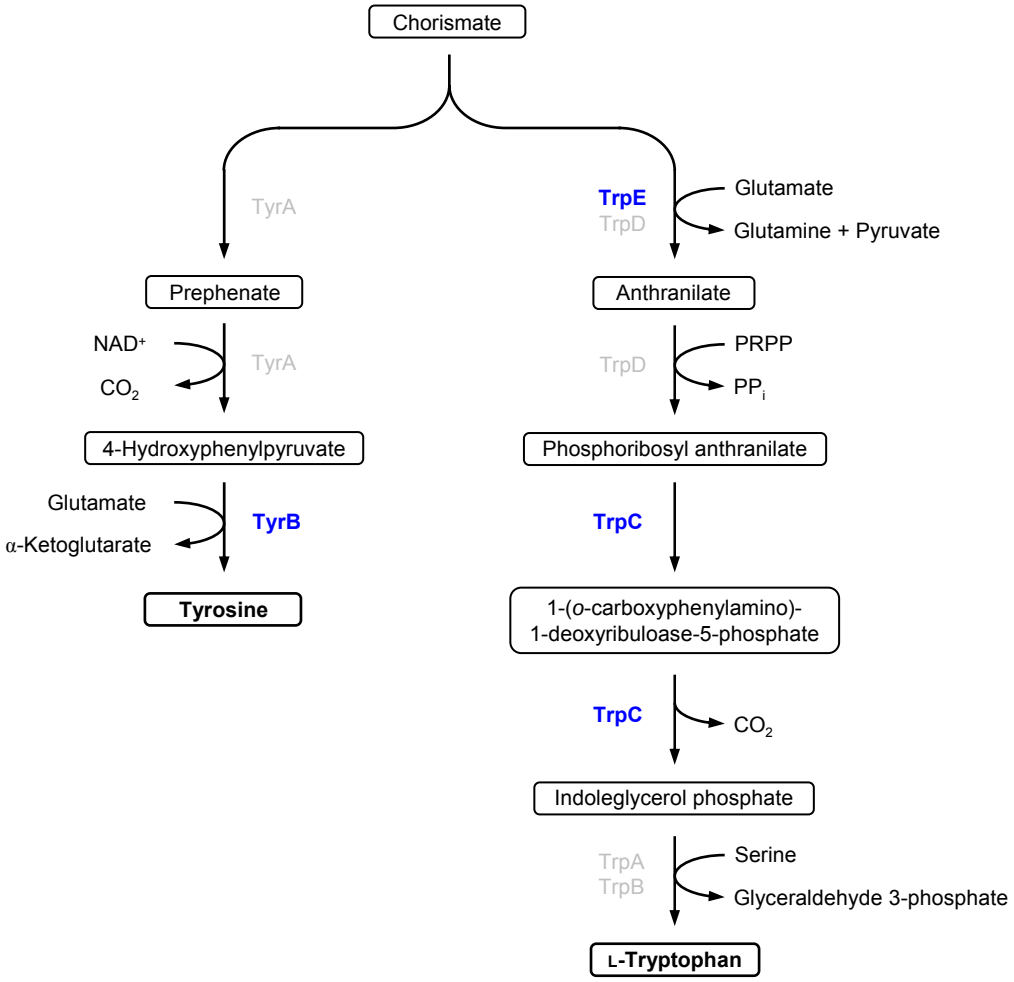


**Fig 5.1.5.1.** Pathway of tyrosine and tryptophan biosynthesis. Proteins involved in the different steps are indicated next to the arrows. Substrates and intermediates are framed. Amino acid products are shwon in bold type. Identified proteins are highlighted in blue. Abbreviations: PRPP: 5-phosphoribosyl 1-pyrophosphate (modified from Pittard 1987).

## 5.1.6. Histidine

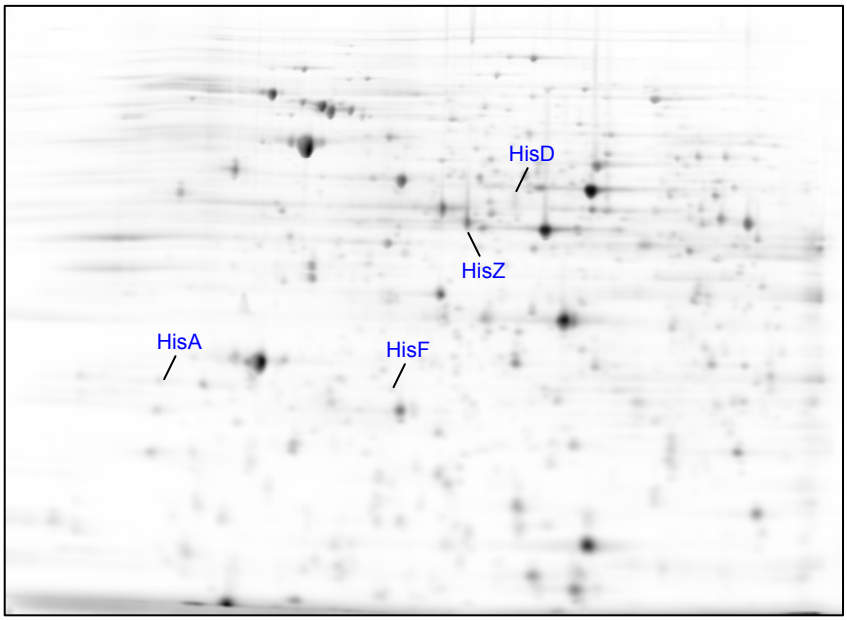


**Fig.5.1.6.** 2DE gel (pH 4-7) of cells grown anaerobically with benzoate. Identified proteins related to amino acid synthesis (histidine) are annotated.

**Table 5.1.6.** Identified proteins related to amino acid synthesis (histidine).

| Orf-No. | Gene | Functional description |
|---|---|---|
| ebA1250 | *hisZ* | ATP phosphoribosyltransferase, regulatory subunit |
| ebA1291 | *hisF* | Imidazoleglycerol phosphate synthase |
| ebA1293 | *hisA* | 1-(5-phosphoribosyl)-5-[(5-phosphoribosyl-amino)methylideneamino]imidazole-4-carboxyamide isomerase |
| ebA1299 | *hisD* | Histidinol dehydrogenase |

The biosynthesis of histidine occours via a unique pathway that is more closely linked to the metabolism of pentoses and purines than to any of the other amino acid families. Furthermore, a considerable amount of energy is required for the synthesis of each histidine molecule.

The first reaction in the pathway is catalyzed by the ATP-phosphoribosylpyrophosphate (PRPP) transferase (HisG) and involves a displacement on C-1 of PRPP by N-1 of the purine ring of ATP, releasing a pyrophosphate molecule. The next steps involve hydrolysis of the N′-5′-phosphoribosyl-ATP to N′-5′-phosphoribosyl-AMP and pyrophosphate catalyzed by the phosphoribosyl-ATP pyrophosphohydrolase (HisE) followed by a ring-opening reaction on the purine ring of the AMP-containing intermediate catalyzed by the phosphoribosyl-AMP cyclohydrolase (HisI). Subsequent, an internal redox reaction known as an Amadori rearrangement is catalyzed by 1-(5-phosphoribosyl)-5-[(5-phosphoribosyl-amino)methylideneamino]imidazole-4-carboxyamide isomerase (**HisA**). The amidocyclase (HisH) catalyzes the addition of a nitrogen atom from glutamine, followed by a ring closure catalyzed by the Imidazoleglycerol phosphate synthase (**HisF**) to form an imidazole group attached to glycerol phosphate. The final steps in histidine biosynthesis include the dehydration catalyzed by one activity of the bifunctional imidazoleglycerolephosphate dehydrase (HisB), followed by a ketonisation of the resulting enol catalyzed by the histidinol phosphate aminotransferase (HisC).

A dephosphorylation of L-histidinol-phosphate catalyzed by the other activity of histidinol phosphate phosphatase (HisB) and and $NAD^+$-dependent oxidation of the promary hydroxyl group of L-histidinol by the histidinol dehydrogenase (**HisD**) to give the amino acid end product, L-histidine (Fig 5.1.6.1.; Winkler 1987).

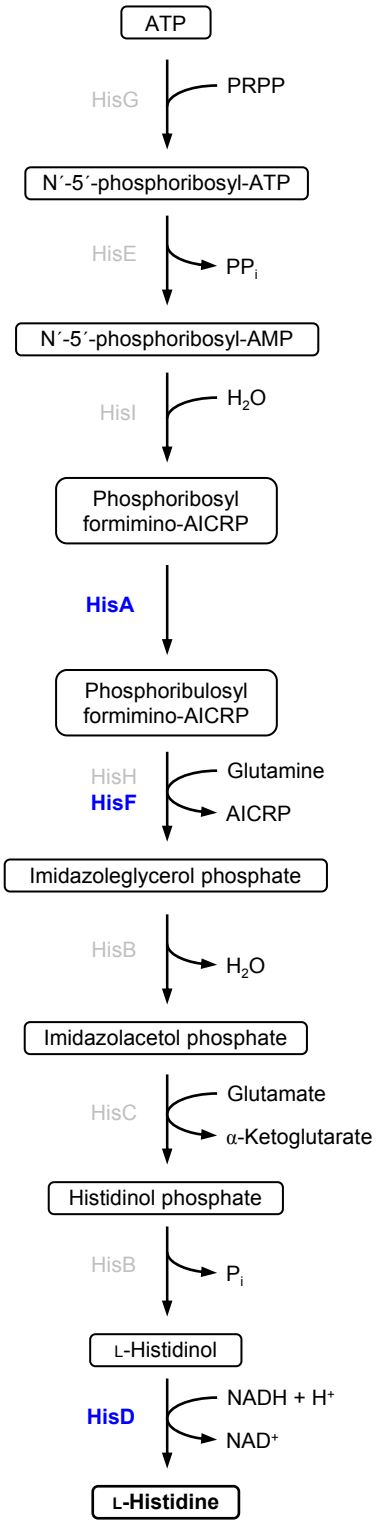


**Fig 5.1.6.1.** Pathway of histidine biosynthesis. Proteins involved in the different steps are indicated next to the arrows. Substrates and intermediates are framed. Amino acid products are shwon in bold type. Identified proteins are highlighted in blue. Abbreviations: AICRP: 5-aminoimidazole-4-carboxyamide ribonucleotide (modified from Winkler 1987).

## 5.3. Purine and pyrimidine synthesis

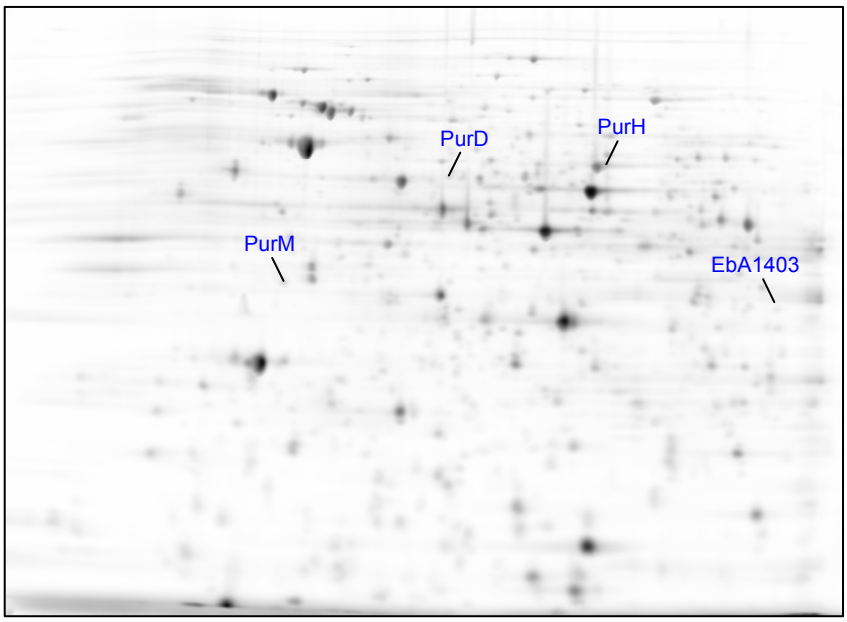


**Fig.5.3.** 2DE gel (pH 4-7) of cells grown anaerobically with benzoate. Identified proteins related to pruine and pyrimidine synthesis are annotated.

**Table 5.3.** Identified protein related to purine and pyrimidine synthesis.

| Orf-No. | Gene | Functional description |
|---|---|---|
| ebA1153 | *purH* | Phosphoribosylaminoimidazolecarboxy-amide formyltransferase |
| ebA1155 | *purD* | Phosphoribosylamine-glycine ligase |
| ebA1406 | | Phosphoribosyl transferase |
| ebA7104 | *purM* | Phosphoribosylglycinamidine cycle-ligase |

### Purine synthesis

In the first step in purine biosynthesis, the amide group of glutamine displaces the pyrophosphate group of 5-phosphoribosyl-1-pyrophosphate (PRPP) to form 5-phosphoribosylamine. This step is catalyzed by PRPP amidotransferase (PurF). In the second step, the amino group of 5-phosphoribosylamine reacts with ATP and the carboxyl group of glycine to form 5´-phoshporibosyl-1-glycinamide and ADP, catalyzed by the phosphoribosylamine-glycine ligase (**PurD**). The free amino group of the glycin residue is formylated by 10-formyltetrahydrofolic acid to give 5´-phosphoribosyl-*N*-formylglycinamide (FGAR). At this point, nitrogen atom 3 of the purine ring is introduced by transfer of the amide group from glutamine catalyzed by FGAR amidotransferase (PurNT). The reaction is energized by ATP, and the product formed is 5´-phosphoribosyl-N-formylglycinamidine. An ATP-dependent ring closure by the Phosphoribosylglycinamidine cycle-ligase (**PurM**) completes the formation of the imidazole ring of 5´-phosphoribosyl-5-aminoimidazole (AIR). Carbon is introduced from bicarbonate by the AIR carboxylase (PurE) to yield 5´-phosphoribosyl-5-aminoimidazole-4-carboxylic acid, followed by a two-step amination in which the amino group of aspartate is transferred to the carboxylic group of 5´-phosphoribosyl-5-aminoimidazole-4-carboxylic acid forming 5´-phosphoribosyl-4-carboxamide-5-aminoimidazole (AICAR). The final carbon atom of the purine ring is introduced by transfer of the formyl group from 10-formyltetrahydrofolate to the 5-amino group of AICAR to yield 5´-phosphoribosyl-4-carboxamnide-5-formamidoimidazole, catalyzed by Phosphoribosylaminoimidazolecarboxy-amide formyltransferase (**PurH**). In the last step the secodn ring is closed by elimination of one molecule of

water to form inosine 5´-monophosphate (IMP), catalyzed by the IMP cyclohydrolase (Fig 5.3.1.; Moat and Foster 1995, Neuhard and Nygaard 1987).

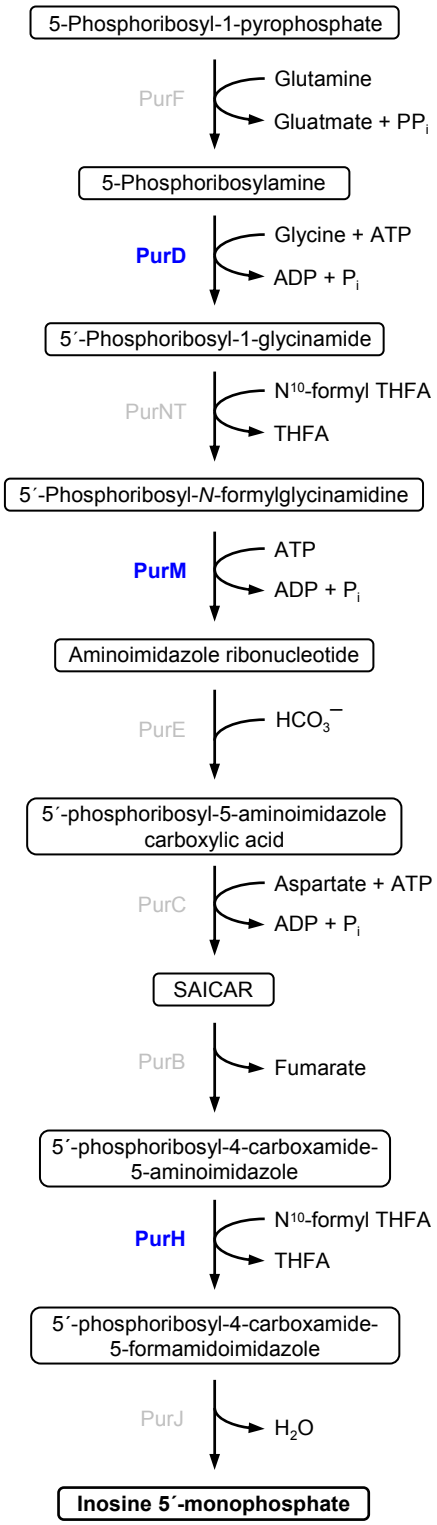


**Fig 5. 3.1.** Pathway of purine biosynthesis. Proteins involved in the different steps are indicated next to the arrows. Substrates and intermediates are framed. The central intermediate of ATP and GTP synthesis, IMP, is shwon in bold type. Identified proteins are highlighted in blue. Abbreviations: THFA: tetrahydrofolic acid; SAICAR: 5´-phosphoribosyl-4-(*N*-succinocarboxamide)-5-aminoimidazole (modified from Moat and Foster 1995; Neuhard and Nygaard 1987).

## 5.4. Lipid synthesis

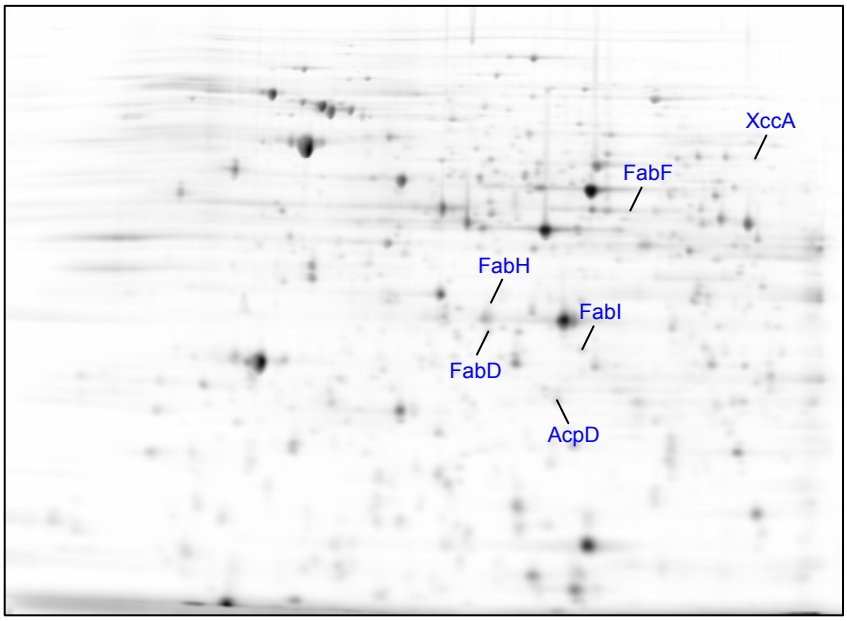


**Fig.5.4.** 2DE gel (pH 4-7) of cells grown anaerobically with benzoate. Identified proteins related to lipid synthesis are annotated.

**Table 5.4.** Identified proteins related to lipid synthesis.

| Orf-No. | Gene | Functional description |
|---|---|---|
| ebA3879 | *acpD* | Acyl-carrier protein phophodiesterase |
| ebA5455 | *fabH* | β-ketoacyl-(acyl-carrier-protein) synthase III |
| ebA5456 | *fabD* | Probable malonyl-CoA (acyl-carrier-protein) transacylase |
| ebA5459 | *fabF* | β-ketoacyl-(acyl-carrier-protein) synthase II |
| ebA6664 | *fabI* | Enoyl-(acyl-carrier-protein) reductase |
| ebB9 | *xccB* | Biotin carboxyl-carrier-protein of unknown carboxylase |

The mechanism of fatty acid synthesis is conserved in prokaryotes and eukaryotes and proceeds in two stages, initiation and cyclic elongation. A unique feature of the pathway is that all of the intermediates are covalently bound to the acyl-carrier protein (ACP), a small and highly soluble protein. The fatty acid is in thioester linkage to the thiol of the 4′-phosphopantetheine prosthetic group. This prosthetic group undergoes metabolic turnover, the apoprotein being inactive in fatty acid synthesis. ACP synthase transfers 4′-phosphopantetheine from CoA to apo-ACP, whereas ACP phosphodiesterase (**AcpD**) cleaves the prosthetic group from ACP (Cronan and Rock 1996).

The first step in fatty acid synthesis is the converson of acetyl-CoA to malonyl-CoA by the acetyl-CoA carboxylase which is composed of four proteins: biotin-carboxyl-carrier-protein (**XccB**), biotin carboxylase (AccC) and the carboxyltransferase (AccAD; DiRusso et al. 1999).

There are three potential mechanisms for the initiation of fatty acid biosynthesis. First, β-ketoacyl-acyl-carrier-protein synthase III (**FabH**) catalyzes the condensation of acetyl-CoA with malonyl-ACP to yield acetoacetyl-ACP. Second, the acetate moiety is first tranferred from acetyl-CoA to acetyl-ACP by either acetyl-CoA:ACP transacylase or synthase III. The acetyl-ACP is then

condensed with malonyl-ACP by synthase I or II (**FabF**). The third pathway involves the decarboxylation of malonyl-ACP by synthase I to form acetyl-ACP followed by subsequent condensation with malonyl-ACP (Cronan and Rock 1996).

The first step of the elongation in fatty acid biosynthesis is the condensation of malonyl-ACP with a growing acyl chain by one of the β-ketoacyl-ACP synthases. The resulting β-ketoester is reduced by an NADPH-dependent β-ketoacyl-ACP reductase (FabG) followed by removal of a water molecule by the β-hydroxyacyl-ACP dehydrase (FabZ). The final reduction is catalyzed by an NADH-dependent enoyl-ACP reductase (**FabI**) to form acyl-ACP which in turn serves as substrate for another round of elongation (Cronan and Rock 1996).

The malonyl-CoA ACP transacylase (**FadD**) prepares malonate for the use in the biosynthesis of fatty acids. The coenzyme A of malonyl-CoA is exchanged by ACP, the energy-rich bonds being identical (DiRusso et al. 1999).

## 5.6. Riboflavin synthesis

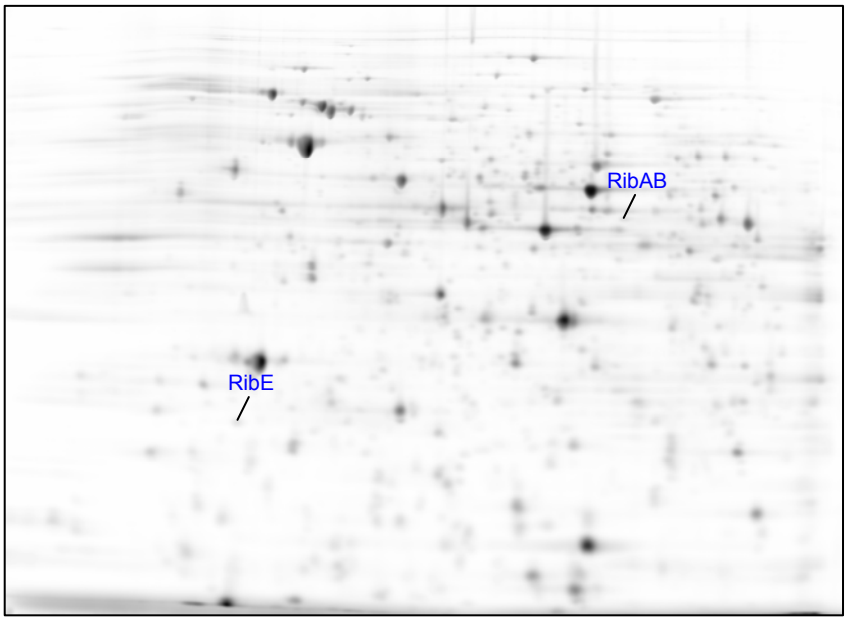


**Fig.5.6.** 2DE gel (pH 4-7) of cells grown anaerobically with benzoate. Identified proteins related to riboflavin synthesis are annotated.

**Table 5.6.** Identified proteins related to riboflavin synthesis.

| Orf-No. | Gene | Functional description |
|---|---|---|
| ebA3567 | *ribAB* | riboflavin biosynthesis bifunctional protein: GTP cyclohydrolase II, 3,4-dihydroxy-2-butanone-4-phosphate synthase |
| ebA3569 | *ribE* | Riboflavin synthase, α-chain |

In the first step of riboflavin biosynthesis, the C8 of GTP is released as formate by the action of GTP cyclohydrolase II (**RibAB**) and the opening of the imidazole ring is accompanied by the release of pyrophosphate, yielding the product 2,5-diamino-6-ribosylamino-4(3H)-pyrimidinone 5´-phosphate. This reaction is followed by hydrolytic deamination of the pyrimidine ring and by reduction of the ribosyl side chain, leading to the formation of 5-amino-6-ribitylamino-2,4(1H,3H)-pyrimidinedione 5´-phosphate. After hydrolysis of the phosphoric ester the condensation of the product (5-amino-6-ribitylamino-2,4(1H,3H)-pyrimidinedione; ARP) with L-3,4-dihydroxy-2-butanone 4-phosphate yields 6,7-dimethyl-8-ribityllumazine. Dismutation of the lumazine by the riboflavin synthase (**RibE**) yields riboflavin and ARP which can be recycled in the pathway. Riboflavin can be converted to FMN and FAD by a bifunctional riboflavin kinase/FAD synthase (Bacher et al. 1996).

The intermediate L-3,4-dihydroxy-2-butanone 4-phosphate can also be formed from ribulose 5-phosphate. This reaction involves the release of C4 of ribulose phosphate as formate, catalyzed by the bifunctional **RibAB** (3,4-dihydroxy-2-butanone 4-phosphate synthase activity; Fig 5.6.1.; Bacher et al. 1996).

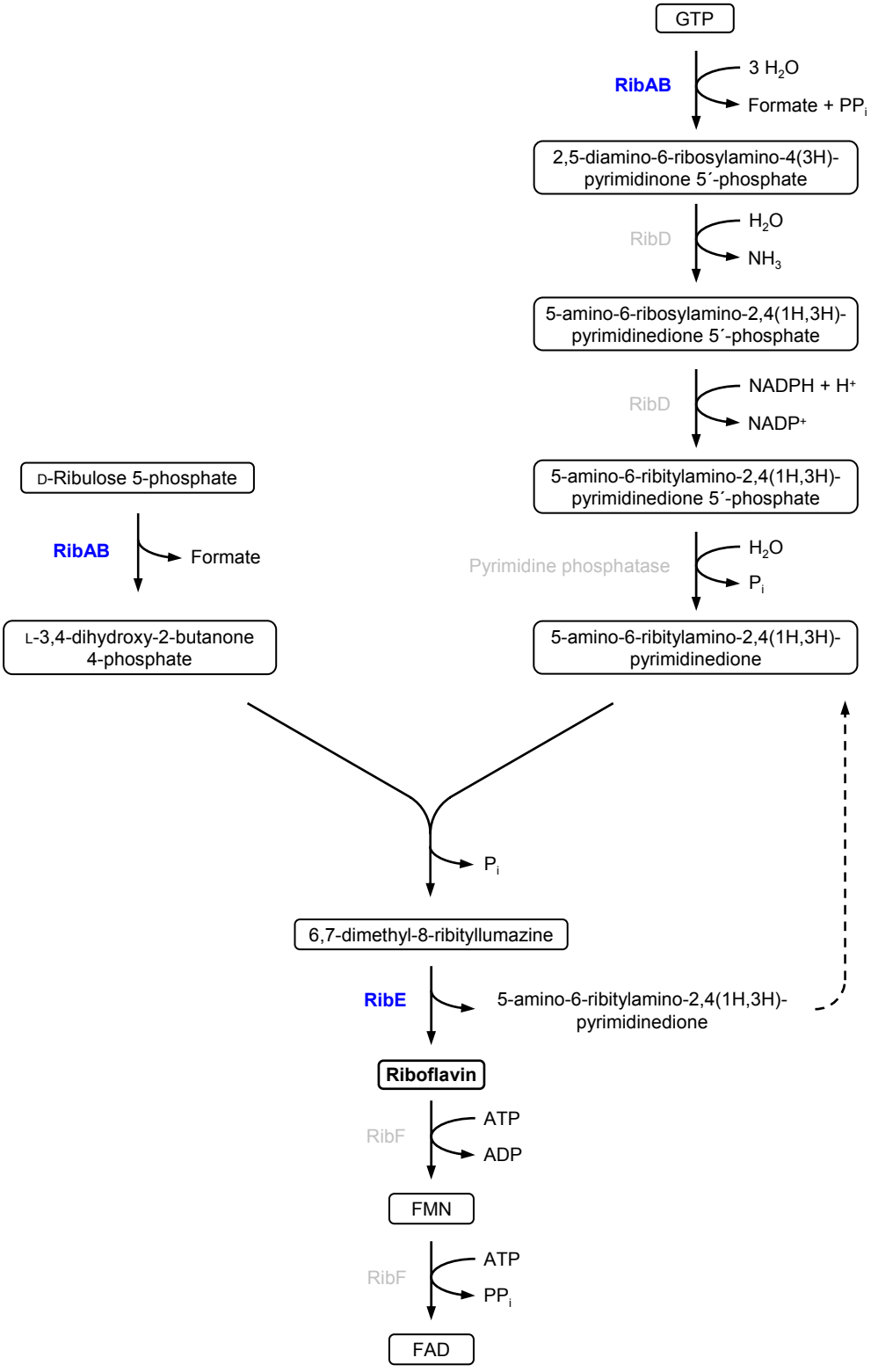


**Fig 5. 6.1.** Pathway of riboflavin biosynthesis. Proteins involved in the different steps are indicated next to the arrows. Substrates and intermediates are framed. Riboflavin is shwon in bold type. Identified proteins are highlighted in blue (modified from Bacher et al. 1996).

## 5.7. Folate synthesis

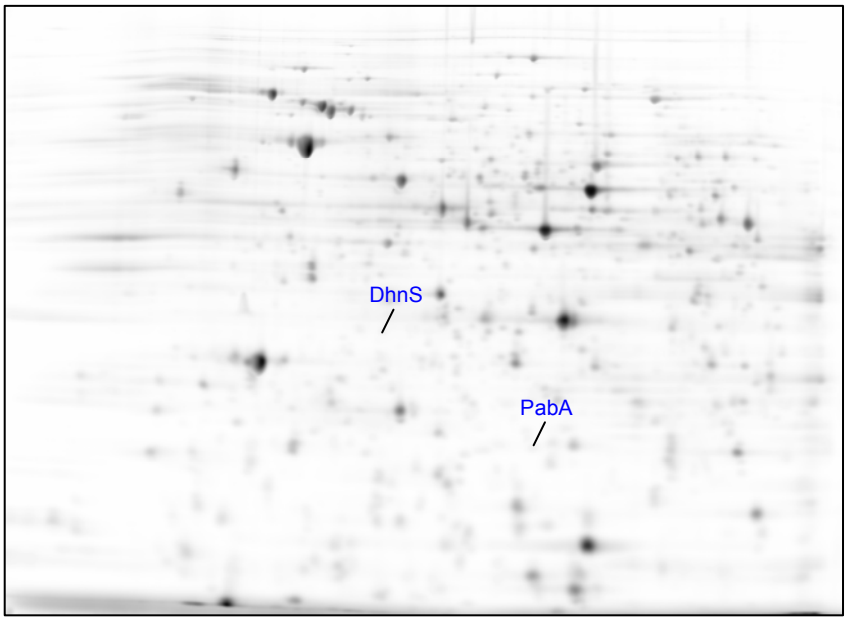


**Fig.5.7.** 2DE gel (pH 4-7) of cells grown anaerobically with benzoate. Identified proteins related to folate synthesis are annotated.

**Table 5.7.** Identified proteins related to folate synthesis.

| Orf-No. | Gene | Functional description |
|---|---|---|
| ebA4199 | *pabA* | Anthranilate synthase, component II |
| ebA4824 | *dhnS* | Dihydropteroate synthase |

*p*-Aminobenzoate (PABA) is a central intermediate in the dihydrofolate synthesis. In a condensation reaction of PABA and 6-hydroxymethyl-$H_2$pterin pyrophosphate, catalyzed by Dihydropteroate synthase (**DhnS**), Dihydropteroate, the precursor of Dihydrofolate, is formed. PABA is synthesized from chorismate in two steps. The 4-amino-4-deoxy-chorismate (ACD) synthase, a heterodimer of **PabA** and PabB converts chorismate and glutamine to ADC and glutamate. ADC lyase aromatizes ADC, releasing pyruvate and generating PABA. PabA acts as a glutaminase that generates ammonia from glutamine, although activation requires equimolar amounts of PabB. PabB then uses the ammonia to aminate chorismate, generating ADC (Green et al. 1996).

## 5.9. Panthothenic acid / CoA synthesis

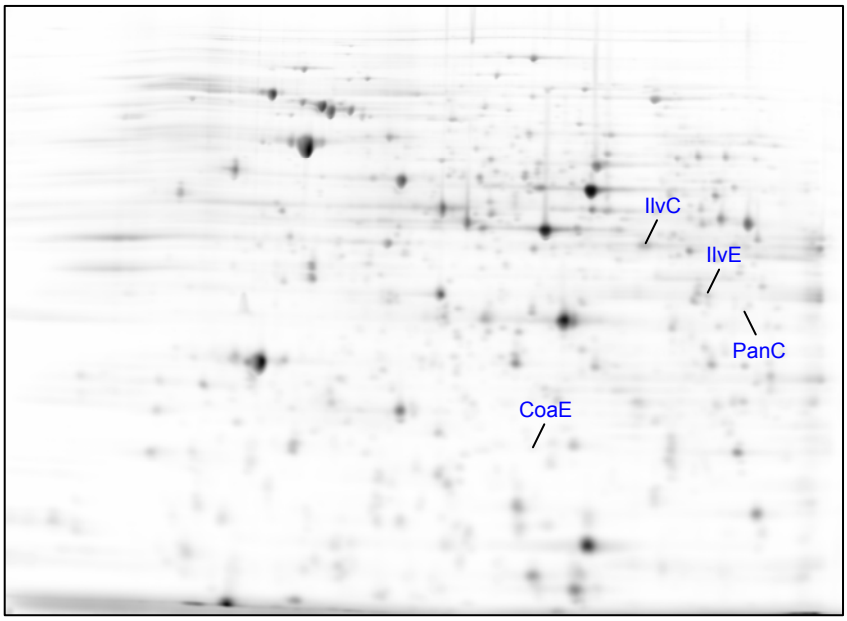


**Fig.5.9.** 2DE gel (pH 4-7) of cells grown anaerobically with benzoate. Identified proteins related to panthothenic acid and CoA synthesis are annotated.

**Table 5.9.** Identified proteins related to panthothenic acid and CoA synthesis.

| Orf-No. | Gene | Functional description |
|---|---|---|
| ebA993 | *ilvE** | Branched-chain amino acid aminotransferase |
| ebA4105 | *coaE* | Predicted dephospho-CoA kinase |
| ebA7120 | *panC* | Pantoate-β-alanine ligase |
| ebA7134 | *ilvC** | Ketol-acid reductoisomerase |

* The protein function is discribed in chapter 5.1.3.

### Panthothenic acid

The first step in the biosynthesis of D-panthoic acid is the transfer of a methyl group from 5,10-methylenetetrahydrofolate to α-ketoisovaleric acid by the α-ketopanthotate hydroxymethyltransferase (PanB) yielding α-ketopanthoate. α-Ketoisovalerate is an intermediate of the valine biosynthesis synthezised from L-valine by the branched-chain amino acid aminatransferase (**IlvE**). The subsequent reduction of α-ketopanthoate to D-panthoate is catalyzed by the α-ketopanthoate reductase (PanE). Studies of mutants lacking PanE have shown, that the ketol-acid-reductoisomerase (**IlvC**), a reductase involved in the biosynthesis of isoleucine and valine, is also capable of catalyzing the reduction of α-ketopanthoate. In the final step panthothenate synthase (**PanC**) catalyzes the ATP-dependent condensation of panthothoate with β-alanine forming panthothenate (Jackowski 1996).

### Coenzyme A

Coenzyme A (CoA) is an essential cofactor in numerous biochemical pathways. It is syntheszised from pantothenate, cysteine and ATP in five enzymatic steps. The final step, the phosphorylation of the 3´-hydroxyl group of dephospho-CoA yielding CoA, is catalyzed by the dephospho-CoA kinase (**CoaE**; O´Toole et al. 2003).

## 5.15. Terpenoid synthesis

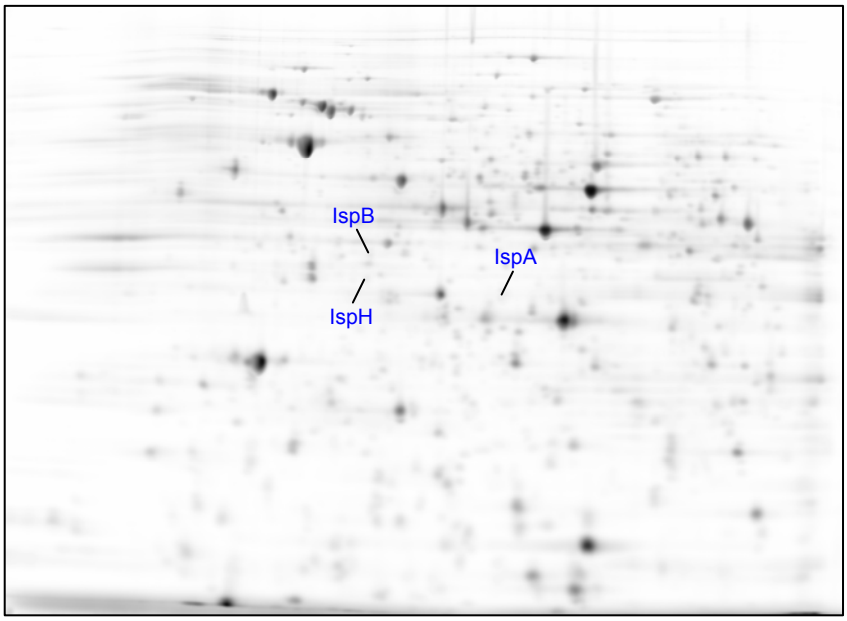


**Fig.5.15.** 2DE gel (pH 4-7) of cells grown anaerobically with benzoate. Identified proteins related to terpenoid synthesis are annotated.

**Table 5.15.** Identified proteins related to terpenoid synthesis.

| Orf-No. | Gene | Functional description |
|---|---|---|
| ebA4440 | *ispA* | Polyprenyl synthetase |
| ebA4444 | *ispH* | 4-Hydroxy-3-methylbut-2-enyl diphosphate reductase |
| ebA4512 | *ispB* | Polyprenyl synthetase |

Isoprenoids are synthesized by a consecutive condensaion of their five-carbon precursor, isopentyl diphosphate (IPP), to its isomer, dimethylallyl diphosphate (DMAPP). The first committed step of the nonmevalonate pathway involves the conversion of 1-deoxy-D-xylulose 5-phosphate into 2-C-methyl-D-erythriol 4-diphosphate. The branched chain polyol derivative is subsequently converted into the cyclic diphosphate 2-C-methyl-D-erythritol 2,4-cyclodiphosphate by a series of three reactions catalyzed by the IspD, IspE and IspF proteins. The cyclic diphosphate is converted into 1-hydroxy-2-methyl-2-(E)-butenyl 4-phosphate (HMBDP) by an iron-sulfur protein, IspG. The HMBDP is finally coverted into a mixture of IPP and DMAPP by the HMBDP reductase (**IspH**; Zepeck et al. 2005).

Four enzymes are involved in isoprenyl biosynthesis: (I) the polyprenyl synthetase (**IspA**) catalyzes the condensation of IPP with DMAPP as well as (II) with geranyl-pyrophosphate to yield farnesyl pyrophosphate (FPP) as the final product. The octaprenyl pyrophosphate synthase (**IspB**) catalyzes the condensation of IPP with FPP yielding octaprenyl pyrophosphate. The reaction is repeated to generate a growing molecule with trans regiochemistry around the double bond for the octaprenyl compound (White 1996).

## 5.16. Polyhydroxybutyrate synthesis and degradation

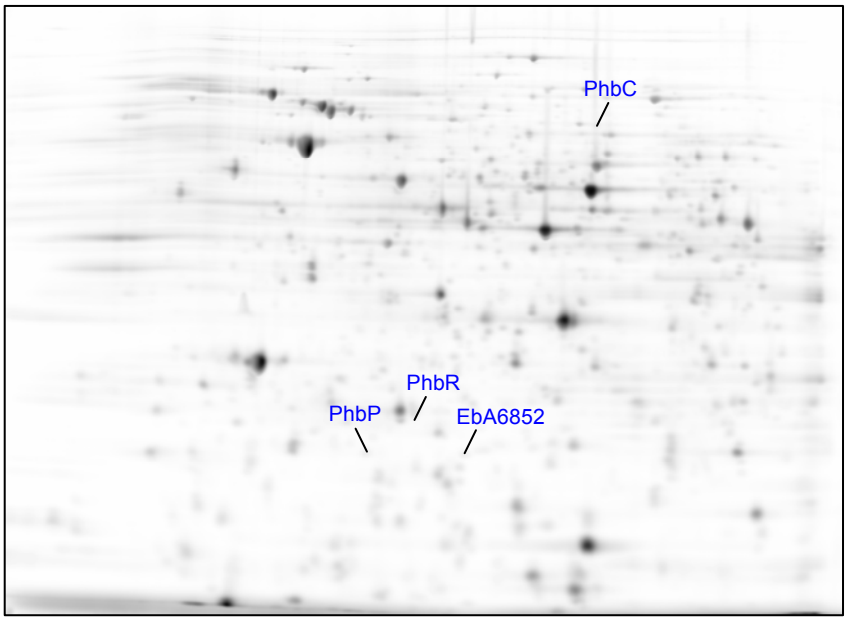


**Fig.5.16.** 2DE gel (pH 4-7) of cells grown anaerobically with benzoate. Identified proteins related to polyhydroxybutyrate synthesis and degradation are annotated.

**Table 5.16.** Identified proteins related to polyhydroxybutyrate synthesis and degradation.

| Orf-No. | Gene | Functional description |
|---|---|---|
| ebA2771 | *phbP* | Related to granule-associated proteins (phasins) |
| ebA3628 | *phbC* | Putative poly-β-hydroxybutyrate synthase |
| ebA4732 | *phbR* | Predicted polyhydroxyalcanoate synthase repressor |
| ebA6852 | | Probable phaisn |

Polyhydroxyalcanoates (PHAs) represent a group of biopolymers that are synthesized by many bacteria as storage compounds and deposited as insoluble cytoplasmatic inclusions. Biosynthesis of the most frequent occuring type of PHA, polyhydroxybutyrate (PHB), proceeds in three steps and starts from the central intermediate acetyl-CoA. Two molecules of acetyl-CoA are condensed to acetoacetyl-CoA, catalyzed by a β-ketothiolase (PhbA); acetoacetyl-CoA is subsequently reduced by a stereospecific acetoacetyl-CoA-reductase (PhbB) to *R*-(-)-3-hydroxybutyryl-CoA. The final step is catalyzed by by the PHB synthase (**PhbC**) and polymerizes the acyl moieties of 3-hydroxybutyryl-CoA to PHB with concominant release of coenzyme A. The PHB-synthase is associated to the surface of the PHB granules. It becomes only PHB-granule-bound during PHB biosynthesis, when the growing hydrophobic polyester molecules confer amphiphilicity to the enzyme-polyester complex (Pötter and Steinbüchel 2004).

Phasins (**EbA6852**) represent a class of most probably noncatalytic proteins consisting of a hydrophobic domain, which associates with the surface of the PHB granules, and of a predominantly hydrophilic/amphiphilic domain exposed to the cytoplasm. This layer of phasins stabalizes the PHB granules and prevents coalescence of separated granules (Pötter and Steinbüchel 2004).

The transcriptional regulator **PhbR** is proposed to be a repressor of PhaP1 expression in *Ralstonia eutropha*. Derepression of PhaR requires biosynthesis and accumulation of PHB (Pötter and Steinbüchel 2004).

# 6. References

Ackrell, B.A.C. (2000) Progress in understanding structure-function relationships in respiratory chain complex II. *FEBS Letters* **466**: 1-5.

Al-Karadaghi, S., Kristensen, O., and Liljas, A. (2000) A decade of progress in understanding the structural basis of protein synthesis. *Progress in Biophysics & Molecular Biology* **73**: 167-193.

Andrews, S.C., Robinson, A.K., and Rodriguez-Quinones, F. (2003) Bacterial iron homeostasis. *FEMS Microbiology Reviews* **27**: 215-237.

Aoki, H., Adams, S.L., Chung, D.G., Yaguchi, M., Chuang, S.E., and Ganoza, M.C. (1991) Cloning, sequencing and overexpression of the gene for prokaryotic factor EF-P involved in peptide bond synthesis. *Nucleic Acids Research* **19**: 6215-6220.

Aravind, L., and Anantharaman, V. (2003) HutC/FarR-like bacterial transcription factors of the GntR family contain a small molecule-binding domain of the chorismate lyase fold. *FEMS Microbiology Letters* **222**: 17-23.

Arca, P., Garcia, P., Hardisson, C., and Suarez, J.E. (1990) Purification and study of a bacterial glutathione S-transferase. *FEBS Letters* **263**: 77-79.

Bacher, A., Eberhardt, S., and Richter, G. (1996) Biosynthesis of riboflavin. In *Escherichia coli and Salmonella thyphimurium*. Neidhardt, F. (ed). Washington D.C:: American Society for Microbiology, pp. 657-665.

Boll, M., Fuchs, G., and Heider, J. (2002) Anaerobic oxidation of aromatic compounds and hydrocarbons. *Current Opinion in Chemical Biology* **6**: 604-611.

Borukhov, S., Lee, J., and Laptenko, O. (2005) Bacterial transcription elongation factors: new insights into molecular mechanism of action. *Molecular Microbiology* **55**: 1315-1324.

Brackmann, R., and Fuchs, G. (1993) Enzymes of anaerobic metabolism of phenolic compounds. 4-hydroxybenzoyl-CoA reductase (dehydroxylating) from a denitrifying *Pseudomonas* species. *Eur J Biochem* **213**: 563-571.

Breese, K., and Fuchs, G. (1998) 4-Hydroxybenzoyl-CoA reductase (dehydroxylating) from the denitrifying bacterium *Thauera aromatica* - prosthetic groups, electron donor, and genes of a member of the molybdenum-flavin-iron-sulfur proteins. *Eur J Biochem* **251**: 916-923.

Breinig, S., Schiltz, E., and Fuchs, G. (2000) Genes involved in anaerobic metabolism of phenol in the bacterium *Thauera aromatica*. *J Bacteriol* **182**: 5849-5863.

Brenot, A., King, K.Y., Janowiak, B., Griffith, O., and Caparon, M.G. (2004) Contribution of glutathione peroxidase to the virulence of *Streptococcus pyogenes*. *Infection & Immunity* **72**: 408-413.

Bycroft, M., Hubbard, T.J.P., Proctor, M., Freund, S.M.V., and Murzin, A.G. (1997) The solution structure of the S1 RNA binding domain - a member of an ancient nucleic acid-binding fold. *Cell* **88**: 235-242.

Cabiscol, E., Tamarit, J., and Ros, J. (2000) Oxidative stress in bacteria and protein damage by reactive oxygen species. *International Microbiology* **3**: 3-8.

Caldovic, L., and Tuchman, M. (2003) N-acetylglutamate and its changing role through evolution. *Biochemical Journal* **372**: 279-290.

Carles, J., and Bourguet, M. (1957) Organic acids of wheat. *Comptes Rendus des Seances de la Societe de Biologie et de Ses Filiales* **151**: 383-387.

Carpousis, A.J. (2002) The *Escherichia coli* RNA degradosome: structure, function and relationship to other ribonucleolytic multienyzme complexes. *Biochemical Society Transactions* **30**: 150-155.

Ceccarelli, E.A., Arakaki, A.K., Cortez, N., and Carrillo, N. (2004) Functional plasticity and catalytic efficiency in plant and bacterial ferredoxin-NADP(H) reductases. *Biochimica et Biophysica Acta-Proteins & Proteomics* **1698**: 155-165.

Cecchini, G., Schroder, I., Gunsalus, R.P., and Maklashina, E. (2002) Succinate dehydrogenase and fumarate reductase from *Escherichia coli*. *Biochimica et Biophysica Acta - Bioenergetics* **1553**: 140-157.

Cha, M.K., Kim, W.C., Lim, C.J., Kim, K., and Kim, I.H. (2004) *Escherichia coli* periplasmic thiol peroxidase acts as lipid hydroperoxide peroxidase and the principal antioxidative function during anaerobic growth. *Journal of Biological Chemistry* **279**: 8769-8778.

Chalmers, R.M., Keen, J.N., and Fewson, C.A. (1991) Comparison of benzyl alcohol dehydrogenases and benzaldehyde dehydrogenases from the benzyl alcohol and mandelate pathways in *Acinetobacter calcoaceticus* and from the TOL-plasmid-encoded toluene pathway in *Pseudomonas putida*. N-terminal amino acid sequences, amino acid compositions and immunological cross-reactions. *Biochemical Journal* **273**: 99-107.

Champion, K.M., Zengler, K., and Rabus, R. (1999) Anaerobic degradation of ethylbenzene and toluene in denitrifying strain EbN1 proceeds via independent substrate-induced pathways. *Journal of Molecular Microbiology & Biotechnology* **1**: 157-164.

Chapman-Smith, A., and Cronan, J.E., Jr. (1999) The enzymatic biotinylation of proteins: a post-translational modification of exceptional specificity. *Trends in Biochemical Sciences* **24**: 359-363.

Cohen, G.N., and Saint-Girons, I. (1987) Biosynthesis of threonine, Lysine and methionine. In *Escherichia coli and Salmonella thyphimurium*. Neidhardt, F. (ed). Washington D.C:: American Society for Microbiology, pp. 429-441.

Compton, L.A., Davis, J.M., Macdonald, J.R., and Bachinger, H.P. (1992) Structural and functional characterization of *Escherichia coli* peptidyl-prolyl cis-trans isomerases. *European Journal of Biochemistry* **206**: 927-934.

Corzett, T.H., Fodor, I.K., Choi, M.W., Walsworth, V.L., Chromy, B.A., Turteltaub, K.W., and McCutchen-Maloney, S.L. (2006) Statistical analysis of the experimental variation in the proteomic characterisation of human plasma by two-dimensional difference gel electrophoresis. *Journal of Proteome Research* **5**: 2611-2619.

Coulombre, B., and Burton, Z.F. (1999) DNA bending and wrapping around RNA polymerase: A "revolutionary" model describing transcriptional mechanisms. *Microbiology & Molecular Biology Reviews* **63**: 457-+.

Coy, M., and Neilands, J.B. (1991) Structural dynamics and functional domains of the fur protein. *Biochemistry* **30**: 8201-8210.

Cronan, J.E., and Rock, C.O. (1996) Biosynthesis of membrane lipids. In *Escherichia coli and Salmonella thyphimurium*. Neidhardt, F. (ed). Washington D.C:: American Society for Microbiology, pp. 612-632.

Cusack, S. (1997) Aminoacyl-tRNA synthetases. *Current Opinion in Structural Biology* **7**: 881-889.

Defeu Soufo, H.J., and Graumann, P.L. (2005) *Bacillus subtilis* actin-like protein MreB influences the positioning of the replication machinery and requires membrane proteins MreC/D and other actin-like proteins for proper localization. *BMC Cell Biology* **6**: 10.

Deuerling, E., Schulze-Specking, A., Tomoyasu, T., Mogk, A., and Bukau, B. (1999) Trigger factor and DnaK cooperate in folding of newly synthesized proteins. *Nature* **400**: 693-696.

Diaz, E., Ferrandez, A., Prieto, M.A., and Garcia, J.L. (2001) Biodegradation of aromatic compounds by *Escherichia coli*. *Microbiology & Molecular Biology Reviews* **65**: 523-+.

DiRusso, C.C., Black, P.N., and Weimar, J.D. (1999) Molecular inroads into the regulation and metabolism of fatty acids, lessons from bacteria. *Progress in Lipid Research* **38**: 129-197.

Dougan, D.A., Mogk, A., and Bukau, B. (2002) Protein folding and degradation in bacteria: To degrade or not to degrade? That is the question. *Cellular and Molecular Life Sciences* **59**: 1607-1616.

Föcking, M., Boersema, P.J., O´Donoghue, N., Lubec, G., Pennington, S.R., Cotter, D.R., and Dunn, M.J. (2006) 2-D DIGE as a quantitative tool for investigating the HUPO Brain Proteome Project mouse series. *Proteomics* **6**: 4914-4931.

Friedrich, T., and Bottcher, B. (2004) The gross structure of the respiratory complex I: A Lego-System. *Biochimica et Biophysica Acta - Bioenergetics* **1657**: 71.

Fu, J.C., Ding, L., and Clarke, S. (1991) Purification, gene cloning, and sequence analysis of an L-isoaspartyl protein carboxyl methyltransferase from *Escherichia coli. Journal of Biological Chemistry* **266**: 14562-14572.

Gade, D., Thiermann, J., Markowsky, D., and Rabus, R. (2003) Evaluation of two-dimensional difference gel electrophoresis for protein profiling. Soluble proteins of the marine bacterium *Pirellula* sp. strain 1. *Journal of Molecular Microbiology & Biotechnology* **5**: 240-251.

Gade, D., Gobom, J., and Rabus, R. (2005a) Proteomic analysis of carbohydrate catabolism and regulation in the marine bacterium *Rhodopirellula baltica*. *Proteomics* **5**: 3672-3683.

Gade, D., Stuhrmann, T., Reinhardt, R., and Rabus, R. (2005b) Growth phase dependent regulation of protein composition in *Rhodopirellula baltica*. *Environmental Microbiology* **7**: 1074-1084.

Gade, D., Theiss, D., Lange, D., Mirgorodskaya, E., Lombardot, T., Glockner, F.O., et al. (2005c) Towards the proteome of the marine bacterium *Rhodopirellula baltica*: Mapping the soluble proteins. *Proteomics* **5**: 3654-3671.

Gerdes, K., Moller-Jensen, J., and Jensen, R.B. (2000) Plasmid and chromosome partitioning: surprises from phylogeny. *Molecular Microbiology* **37**: 455-466.

Gescher, J., Zaar, A., Mohamed, M., Schagger, H., and Fuchs, G. (2002) Genes coding for a new pathway of aerobic benzoate metabolism in *Azoarcus evansii*. *Journal of Bacteriology* **184**: 6301-6315.

Gescher, J., Ismail, W., Olgeschlager, E., Eisenreich, W., Worth, J., and Fuchs, G. (2006) Aerobic benzoyl-coenzyme A (CoA) catabolic pathway in *Azoarcus evansii*: Conversion of ring cleavage product by 3,4-dehydroadipyl-CoA semialdehyde dehydrogenase. *Journal of Bacteriology* **188**: 2919-2927.

Ghisla, S., and Thorpe, C. (2004) Acyl-CoA dehydrogenases - A mechanistic overview. *European Journal of Biochemistry* **271**: 494-508.

Gibson, J., Dispensa, M., Fogg, G.C., Evans, D.T., and Harwood, C.S. (1994) 4-Hydroxybenzoate-coenzyme A ligase from *Rhodopseudomonas palustris* - purification, gene sequence, and role in anaerobic degradation. *Journal of Bacteriology* **176**: 634-641.

Gibson, J., Dispensa, M., and Harwood, C.S. (1997) 4-Hydroxybenzoyl coenzyme A reductase (dehydroxylating) is required for anaerobic degradation of 4-

hydroxybenzoate by *Rhodopseudomonas palustris* and shares features with molybdenum-containing hydroxylases. *Journal of Bacteriology* **179**: 634-642.

Gillooly, D.J., Robertson, A.G.S., and Fewson, C.A. (1998) Molecular characterization of benzyl alcohol dehydrogenase and benzaldehyde dehydrogenase II of *Acinetobacter calcoaceticus*. *Biochemical Journal* **330**: 1375-1381.

Greated, A., Lambertsen, L., Williams, P.A., and Thomas, C.M. (2002) Complete sequence of the IncP-9 TOL plasmid pWW0 from *Pseudomonas putida*. *Environmental Microbiology* **4**: 856-871.

Green, J.M., Nichols, B.P., and Matthews, R.G. (1996) Folate biosynthesis, reduction and polyglutamylation. In *Escherichia coli and Salmonella thyphimurium*. Neidhardt, F. (ed). Washington D.C:: American Society for Microbiology, pp. 665-673.

Grentzmann, G., Kelly, P.J., Laalami, S., Shuda, M., Firpo, M.A., Cenatiempo, Y., and Kaji, A. (1998) Release factor RF-3 GTPase activity acts in disassembly of the ribosome termination complex. *Rna-A Publication of the Rna Society* **4**: 973-983.

Grunden, A.M., and Shanmugam, K.T. (1997) Molybdate transport and regulation in bacteria. *Archives of Microbiology* **168**: 345-354.

Hansen, A.M., Lehnherr, H., Wang, X., Mobley, V., and Jin, D.J. (2003) *Escherichia coli* SspA is a transcription activator for bacteriophage P1 late genes. *Mol Microbiol* **48**: 1621-1631.

Hartl, F.U. (1996) Molecular chaperones in cellular protein folding. *Nature* **381**: 571-580.

Harwood, C.S., Burchhardt, G., Herrmann, H., and Fuchs, G. (1998) Anaerobic metabolism of aromatic compounds via the benzoyl-CoA pathway. *FEMS Microbiology Reviews* **22**: 439-458.

Hase, C.C., and Finkelstein, R.A. (1993) Bacterial extracellular zinc-containing metalloproteases. *Microbiological Reviews* **57**: 823-837.

Hegeman, G.D. (1966) Synthesis of the enzymes of the mandelate pathway by *Pseudomonas putida*. I. Synthesis of enzymes by the wild type. *Journal of Bacteriology* **91**: 1140-1154.

Heider, J., and Fuchs, G. (1997) Microbial anaerobic aromatic metabolism. *Anaerobe* **3**: 1-22.

Henkin, T.M. (2000) Transcription termination control in bacteria. *Current Opinion in Microbiology* **3**: 149-153.

Herendeen, D.R., and Kelly, T.J. (1996) DNA-polymerase III - running rings around the fork. *Cell* **84**: 5-8.

Hoffman, D.W., Davies, C., Gerchman, S.E., Kycia, J.H., Porter, S.J., White, S.W., and Ramakrishnan, V. (1994) Crystal structure of prokaryotic ribosomal protein L9 - a bi-lobed RNA-binding protein. *EMBO Journal* **13**: 205-212.

Hopper, D.J., and Taylor, D.G. (1977) The purification and properties of *p*-cresol-(acceptor) oxidoreductase (hydroxylating), a flavocytochrome from *Pseudomonas putida*. *Biochemical Journal* **167**: 155-162.

Ibba, M., and Soll, D. (2000) Aminoacyl-tRNA synthesis. *Annual Review of Biochemistry* **69**: 617-650.

Ishige, K., and Noguchi, T. (2000) Inorganic polyphosphate kinase and adenylate kinase participate in the polyphosphate : AMP phosphotransferase activity of *Escherichia coli*. *Proceedings of the National Academy of Sciences of the United States of America* **97**: 14168-14171.

Jackowski, S. (1996) Biosynthesis of pantothenic acid and coenzyme A. In *Escherichia coli and Salmonella thyphimurium*. Neidhardt, F. (ed). Washington D.C:: American Society for Microbiology, pp. 687-695.

Jeon, C.O., Park, M., Ro, H.S., Park, W., and Madsen, E.L. (2006) The naphthalene catabolic (nag) genes of *Polaromonas naphthalenivorans* CJ2: Evolutionary implications for two gene clusters and novel regulatory control. *Applied & Environmental Microbiology* **72**: 1086-1095.

Karp, N.A., and Lilley, K.S. (2005) Maximising sensitivity for detecting changes in protein expression: Experimental design using minimal CyDyes. *Proteomics* **5**: 3105-3115.

Kawakami, H., Iwura, T., Takata, M., Sekimizu, K., Hiraga, S., and Katayama, T. (2001) Arrest of cell division and nucleoid partition by genetic alterations in the sliding clamp of the replicase and in DnaA. *Molecular Genetics & Genomics: MGG* **266**: 167-179.

Kennedy, S.I., and Fewson, C.A. (1968) Enzymes of the mandelate pathway in Bacterium N.C.I.B. 8250. *Biochemical Journal* **107**: 497-506.

Kisker, C., Schindelin, H., and Rees, D.C. (1997) Molybdenum-cofactor-containing enzymes - structure and mechanism. *Annual Review of Biochemistry* **66**: 233-267.

Kramer, G., Rauch, T., Rist, W., Vorderwulbecke, S., Patzelt, H., Schulze-Specking, A., et al. (2002) L23 protein functions as a chaperone docking site on the ribosome. *Nature* **419**: 171-174.

Kube, M., Heider, J., Amann, J., Hufnagel, P., Kuhner, S., Beck, A., et al. (2004) Genes involved in the anaerobic degradation of toluene in a denitrifying bacterium, strain EbN1. *Archives of Microbiology* **181**: 182-194.

Kuhner, S., Wohlbrand, L., Fritz, I., Wruck, W., Hultschig, C., Hufnagel, P., et al. (2005) Substrate-dependent regulation of anaerobic degradation pathways for toluene and ethylbenzene in a denitrifying bacterium, strain EbN1. *Journal of Bacteriology* **187**: 1493-1503.

Kunau, W.H., Dommes, V., and Schulz, H. (1995) Beta-oxidation of fatty acids in mitochondria, peroxisomes and bacteria - a century of continued progress. *Progress in Lipid Research* **34**: 267-342.

Laempe, D., Eisenreich, W., Bacher, A., and Fuchs, G. (1998) Cyclohexa-1,5-Diene-1-Carboxyl-Coa Hydratase, an Enzyme Involved in Anaerobic Metabolism of Benzoyl-Coa in the Denitrifying Bacterium Thauera Aromatica (Vol 255, Pg 618, 1998). *European Journal of Biochemistry* **257**: 528.

Laempe, D., Jahn, M., and Fuchs, G. (1999) 6-hydroxycyclohex-1-ene-1-carbonyl-CoA dehydrogenase and 6-oxocycsohex-1-ene-1-carbonyl-CoA hydrolase, enzymes of the benzoyl-CoA pathway of anaerobic aromatic metabolism in the denitrifying bacterium Thauera aromatica. *European Journal of Biochemistry* **263**: 420-429.

Laempe, D., Jahn, M., Breese, K., Schagger, H., and Fuchs, G. (2001) Anaerobic metabolism of 3-hydroxybenzoate by the denitrifying bacterium *Thauera aromatica*. *Journal of Bacteriology* **183**: 968-979.

Lahiri, S.D., Zhang, G.F., Dunaway-Mariano, D., and Allen, K.N. (2002) Caught in the act: The structure of phosphorylated beta-phosphoglucomutase from *Lactococcus lactis*. *Biochemistry* **41**: 8351-8359.

Lambert, P.A. (1988) Enterobacteriaceae: composition, structure and function of the cell envelope. *Society for Applied Bacteriology Symposium Series* **17**: 21S-34S.

Lee, H.S., and Hwang, B.J. (2003) Methionine biosynthesis and its regulation in Corynebacterium glutamicum: parallel pathways of transsulfuration and direct sulfhydrylation. *Applied Microbiology & Biotechnology* **62**: 459-467.

Leinfelder, W., Forchhammer, K., Veprek, B., Zehelein, E., and Bock, A. (1990) In vitro synthesis of selenocysteinyl-tRNA(UCA) from seryl-tRNA(UCA): involvement and characterization of the selD gene product. *Proceedings of the National Academy of Sciences of the United States of America* **87**: 543-547.

Livingstone, A., and Fewson, C.A. (1971) Regulation of enzymes converting L-mandelate into benzoate in bacterium N.C.I.B. 8250. *Biochemical Journal* **121**: 8P-9P.

Lochmeyer, C., Koch, J., and Fuchs, G. (1992) Anaerobic degradation of 2-aminobenzoic acid (anthranilic acid) via benzoyl-coenzyme A (CoA) and cyclohex-1-enecarboxyl-CoA in a denitrifying bacterium. *Journal of Bacteriology* **174**: 3621-3628.

Lopez-Campistrous, A., Semchuk, P., Burke, L., Palmer-Stone, T., Brokx, S.J., Broderick, G., et al. (2005) Localization, annotation, and comparison of the *Escherichia coli* K-12 proteome under two states of growth. *Molecular & Cellular Proteomics* **4**: 1205-1209.

MacKintosh, R.W., and Fewson, C.A. (1988) Benzyl alcohol dehydrogenase and benzaldehyde dehydrogenase II from *Acinetobacter calcoaceticus*. Substrate specificities and inhibition studies. *Biochemical Journal* **255**: 653-661.

Mansy, S.S., and Cowan, J.A. (2004) Iron-sulfur cluster biosynthesis: Toward an understanding of cellular machinery and molecular mechanism ]. *Accounts of Chemical Research* **37**: 719-725.

Marolda, C.L., and Valvano, M.A. (1996) The GalF protein of Escherichia coli Is not a UDP-glucose pyrophosphorylase but interacts with the GalU protein possibly to regulate cellular levels of UDP-glucose. *Molecular Microbiology* **22**: 827-840.

Mattick, J.S. (2002) Type IV pili and twitching motility. *Annual Review of Microbiology* **56**: 289-314.

McLeish, M.J., Kneen, M.M., Gopalakrishna, K.N., Koo, C.W., Babbitt, P.C., Gerlt, J.A., and Kenyon, G.L. (2003) Identification and characterization of a mandelamide hydrolase and an NAD(P)(+)-dependent benzaldehyde dehydrogenase from *Pseudomonas putida* ATCC 12633. *Journal of Bacteriology* **185**: 2451-2456.

Moat, A.G., and Foster, J.W. (1995) *Microbial physiology*. New York: Wiley-Liss, Inc.

Mohamed, M.E.S., Ismail, W., Heider, J., and Fuchs, G. (2002) Aerobic metabolism of phenylacetic acids in *Azoarcus evansii*. *Archives of Microbiology* **178**: 180-192.

Mohamed, M.e.-S., and Fuchs, G. (1993) Purification and characterization of phenylacetate-coenzyme A ligase from a denitrifying *Pseudomonas* sp., an enzyme involved in the anaerobic degradation of phenylacetate. *Archives of Microbiology* **159**: 554-562.

Murakami, K., Kimura, M., Owens, J.T., Meares, C.F., and Ishihama, A. (1997) The two alpha subunits of Escherichia coli RNA polymerase are asymmetrically arranged and contact different halves of the DNA upstream element. *Proceedings of the National Academy of Sciences of the United States of America* **94**: 1709-1714.

Murayama, N., Shimizu, H., Takiguchi, S., Baba, Y., Amino, H., Horiuchi, T., et al. (1996) Evidence for involvement of *Escherichia coli* genes pmbA, csrA and a previously unrecognized gene tldD, in the control of DNA gyrase by LetD(CcdD) of sex factor F. *Journal of Molecular Biology* **259**: 203.

Nakamoto, R.K., Ketchum, C.J., and al-Shawi, M.K. (1999) Rotational coupling in the F0F1 ATP synthase. *Annual Review of Biophysics & Biomolecular Structure* **28**: 205-234.

Neuhard, J., and Nygaard, P. (1987) Purines and pyrimidines. In *Escherichia coli and Salmonella thyphimurium*. Neidhardt, F. (ed). Washington D.C:: American Society for Microbiology, pp. 446-470.

Noda, M., Kawahara, Y., Ichikawa, A., Matoba, Y., Matsuo, H., Lee, D.G., et al. (2004) Self-protection mechanism in D-cycloserine-producing Streptomyces lavendulae - Gene cloning, characterization, and kinetics of its alanine racemase and D-alanyl-D-alanine ligase, which are target enzymes of D-cycloserine. *Journal of Biological Chemistry* **279**: 46143-46152.

Olivera, E.R., Minambres, B., Garcia, B., Muniz, C., Moreno, M.A., Ferrandez, A., et al. (1998) Molecular characterization of the phenylacetic acid catabolic pathway in *Pseudomonas putida* U - the phenylacetyl-CoA catabolon. *Proceedings of the National Academy of Sciences of the United States of America* **95**: 6419-6424.

O'Toole, N., Barbosa, J., Li, Y.G., Hung, L.W., Matte, A., and Cygler, M. (2003) Crystal structure of a trimeric form of dephosphocoenzyme A kinase from *Escherichia coli*. *Protein Science* **12**: 327-336.

Owens, R.M., Pritchard, G., Skipp, P., Hodey, M., Connell, S.R., Nierhaus, K.H., and O'Connor, C.D. (2004) A dedicated translation factor controls the synthesis of the global regulator Fis. *EMBO Journal* **23**: 3375-3385.

Pittard, A.J. (1987) Biosynthesis of aromatic amino acids. In *Escherichia coli and Salmonella thyphimurium*. Neidhardt, F. (ed). Washington D.C:: American Society for Microbiology, pp. 368-390.

Poole, L.B. (2005) Bacterial defenses against oxidants: mechanistic features of cysteine-based peroxidases and their flavoprotein reductases. *Archives of Biochemistry & Biophysics* **433**: 240-254.

Potter, M., and Steinbuchel, A. (2005) Poly(3-hydroxybutyrate) granule-associated proteins: Impacts on poly(3-hydroxybutyrate) synthesis and degradation. *Biomacromolecules* **6**: 552-560.

Rabus, R. (2005) Functional genomics of an anaerobic aromatic-degrading denitrifying bacterium, strain EbN1. *Applied Microbiology & Biotechnology* **68**: 580-587.

Rabus, R., Kube, M., Heider, J., Beck, A., Heitmann, K., Widdel, F., and Reinhardt, R. (2005) The genome sequence of an anaerobic aromatic-degrading denitrifying bacterium, strain EbN1. *Archives of Microbiology* **183**: 27-36.

Rathsam, C., Eaton, R.E., Simpson, C.L., Browne, G.V., Valova, V.A., Harty, D.W.S., and Jacques, N.A. (2005) Two-dimensional fluorescence difference gel electrophoretic analysis of *Streptococcus mutans* biofilms. *Journal of Proteome Research* **4**: 2161-2173.

Read, J.A., Ahmed, R.A., Morrison, J.P., Coleman, W.G., and Tanner, M.E. (2004) The mechanism of the reaction catalyzed by ADP-beta-L-glycero-D-manno-heptose 6-epimerase. *Journal of the American Chemical Society* **126**: 8878-8879.

Rhee, S.K., and Fuchs, G. (1999) Phenylacetyl-CoA:acceptor oxidoreductase, a membrane-bound molybdenum-iron-sulfur enzyme involved in anaerobic metabolism of phenylalanine in the denitrifying bacterium *Thauera aromatica*. *European Journal of Biochemistry* **262**: 507-515.

Rosenberg, S.L. (1971) Regulation of the mandelate pathway in *Pseudomonas aeruginosa*. *Journal of Bacteriology* **108**: 1257-1269.

Rothfield, L., Taghbalout, A., and Shih, Y.L. (2005) Spatial control of bacterial division-site placement. *Nature Reviews* **Microbiology. 3**: 959-968.

Rudolphi, A., Tschech, A., and Fuchs, G. (1991) Anaerobic degradation of cresols by denitrifying bacteria. *Archives of Microbiology* **155**: 238-248.

Sauer, U., Canonaco, F., Heri, S., Perrenoud, A., and Fischer, E. (2004) The soluble and membrane-bound transhydrogenases UdhA and PntAB have divergent functions in NADPH metabolism of *Escherichia coli*. *Journal of Biological Chemistry* **279**: 6613-6619.

Schneider, S., Mohamed, M.E., and Fuchs, G. (1997) Anaerobic metabolism of L-phenylalanine via benzoyl-CoA in the denitrifying bacterium *Thauera aromatica*. *Archives of Microbiology* **168**: 310-320.

Shapleigh, J.P. (2006) The denitrifying prokaryotes. In *The Prokaryotes*. New York: Springer, pp. 769-792.

Sluis, M.K., Larsen, R.A., Krum, J.G., Anderson, R., Metcalf, W.W., and Ensign, S.A. (2002) Biochemical, molecular, and genetic analyses of the acetone carboxylases from *Xanthobacter autotrophicus* strain Py2 and *Rhodobacter capsulatus* strain B10. *Journal of Bacteriology* **184**: 2969-2977.

Stauffer, G.V. (1987) Biosynthesis of serine and glycine. In *Escherichia coli and Salmonella thyphimurium*. Neidhardt, F. (ed). Washington D.C:: American Society for Microbiology, pp. 412-418.

Stevens, J.M., Uchida, T., Daltrop, O., and Ferguson, S.J. (2005) Covalent cofactor attachment to proteins: cytochrome c biogenesis. *Biochemical Society Transactions* **33**: 792-795.

Stojiljkovic, I., and Hantke, K. (1994) Transport of haemin across the cytoplasmic membrane through a haemin-specific periplasmic binding-protein-dependent transport system in *Yersinia enterocolitica*. *Molecular Microbiology* **13**: 719-732.

Stoldt, M., Wohnert, J., Gorlach, M., and Brown, L.R. (1998) The NMR structure of *Escherichia coli* ribosomal protein L25 shows homology to general stress proteins and glutaminyl-tRNA synthetases. *EMBO Journal* **17**: 6377-6384.

Tam, L.T., Antelmann, H., Eymann, C., Albrecht, D., Bernhardt, J., and Hecker, M. (2006) Proteome signatures for stress and starvation in *Bacillus subtilis* as revealed by a 2-D gel image color coding approach. *Proteomics* **6**: 4565-4585.

Tang, Y., Quail, M.A., Artymiuk, P.J., Guest, J.R., and Green, J. (2002) *Escherichia coli* aconitases and oxidative stress: post-transcriptional regulation of sodA expression. *Microbiology* **148**: 1027-1037.

Thonymeyer, L. (1997) Biogenesis of respiratory cytochromes in bacteria. *Microbiology & Molecular Biology Reviews* **61**: 337 ff.

Tsou, A.Y., Ransom, S.C., Gerlt, J.A., Buechter, D.D., Babbitt, P.C., and Kenyon, G.L. (1990) Mandelate pathway of *Pseudomonas putida:* sequence relationships involving mandelate racemase, (S)-mandelate dehydrogenase, and benzoylformate decarboxylase and expression of benzoylformate decarboxylase in *Escherichia coli*. *Biochemistry* **29**: 9856-9862.

Umbarger, H.E. (1987) Biosynthesis of the branched-chain amino acids. In *Escherichia coli and Salmonella thyphimurium*. Neidhardt, F. (ed). Washington D.C:: American Society for Microbiology, pp. 442-456.

Umitsuki, G., Wachi, M., Takada, A., Hikichi, T., and Nagai, K. (2001) Involvement of RNase G in in vivo mRNA metabolism in *Escherichia coli*. *Genes to Cells* **6**: 403-410.

Vipond, C., Suker, J., Jones, C., Tang, C., Feavers, I.M., and Wheeler, J.X. (2006) Proteomic analysis of a meningococcal outer membrane vesicle vaccine prepared from the group B strain NZ98/254. *Proteomics* **6**: 3400-3413.

Walter, S., and Buchner, J. (2002) Molecular chaperones - Cellular machines for protein folding. *Angewandte Chemie-International Edition* **41**: 1098-1113.

Weiss, D.S. (2004) Bacterial cell division and the septal ring. *Molecular Microbiology* **54**: 588-597.

Weissborn, A.C., Liu, Q.Y., Rumley, M.K., and Kennedy, E.P. (1994) UTP-alpha-D-glucose-1-phosphate uridylyltransferase of *Escherichia coli* - isolation and DNA sequence of the galU gene and purification of the enzyme. *Journal of Bacteriology* **176**: 2611-2618.

Wheelis, M.L., Palleroni, N.J., and Stanier, R.Y. (1967) The metabolism of aromatic acids by *Pseudomonas testosteroni* and *P. acidovorans*. *Archiv fur Mikrobiologie* **59**: 302-314.

Winkler, M.E. (1987) Biosynthesis of histidine. In *Escherichia coli and Salmonella thyphimurium*. Neidhardt, F. (ed). Washington D.C:: American Society for Microbiology, pp. 395-411.

Yeo, C.C., Wong, M.V.M., Feng, Y.M., Song, K.P., and Poh, C.L. (2003) Molecular characterization of an inducible gentisate 1,2-dioxygenase gene, xlnE, from *Pseudomonas alcaligenes* NCIMB 9867. *Gene* **312**: 239-248.

Zepeck, F., Grawert, T., Kaiser, J., Schramek, N., Eisenreich, W., Bacher, A., and Rohdich, F. (2005) Biosynthesis of isoprenoids. Purification and properties of IspG protein from *Escherichia coli*. *Journal of Organic Chemistry* **70**: 9168-9174.

Zhou, J.H., and Xu, Z.H. (2005) The structural view of bacterial translocation-specific chaperone SecB: implications for function. *Molecular Microbiology* **58**: 349-357.